N-3 POLYUNSATURATED FATTY ACIDS DIFFERENTIALLY ENHANCE B-CELL MEDIATED IMMUNITY IN LEAN AND OBESE MICE

By

Heather L. Teague

July, 2014

Director of Dissertation: Saame R. Shaikh

Major Department: Biochemistry

Docosahexaenoic acid (DHA) and eicosapentaenoic acid (EPA) are bioactive n-3 polyunsaturated fatty acids (PUFAs) in fish oil that exert immunomodulatory effects. The general paradigm suggests n-3 PUFAs exert immunosuppressive effects, however, the role of n-3 PUFAs on B-cell mediated immunity is understudied. We first tested the hypothesis that n-3 PUFAs would suppress B-cell activation and antigen presentation. The functional changes n-3 PUFAs exert on B cells were determined and compared to dendritic cells (DC). Initially, we established n-3 PUFAs increased cytokine production from lipopolysaccharide (LPS) stimulated B cells *ex vivo* relative to the control. In contrast, n-3 PUFAs decreased DC activation with LPS by reducing cytokine secretion and decreasing surface expression of costimulatory molecules. The antigen presentation assays revealed n-3 PUFAs decreased IL-2 secretion from $CD4^+$ T cells when B cells presented antigen compared to the control. In comparison, only CD69 surface expression on $CD4^+$ T cells decreased when n-3 PUFA treated DCs presented the antigen compared to the control. Mechanistically, we investigated changes in lipid microdomain clustering on B cells and DCs induced by n-3 PUFAs to determine if the observed functional changes correlated with membrane changes. N-3 PUFAs

diminished lipid microdomain clustering on the B-cell surface, but had no effect on DCs. We then relied on a lean and obese murine model to determine if the functional enhancement of B cells observed *ex vivo* were recapitulated *in vivo.* N-3 PUFAs increased serum IgM levels compared to controls when stimulated by a T-independent antigen. Additionally, n-3 PUFAs supplemented to an obesogenic diet rescued the decrement in serum IgM levels observed with the obesogenic diet compared to the lean control. Considering the limitations of fish oil, we investigated the effects of the clinically relevant EPA and DHA ethyl esters on antibody production in an obese murine model. EPA and DHA differentially increased *ex vivo* B-cell activation, *in vivo* natural serum IgM and cecal IgA compared to controls. Altogether, the data show n-3 PUFAs boost immune responses from B cells, which challenges the current notion about n-3 PUFAs, and has clinical implications for immunocompromised populations, such as the obese.

N-3 POLYUNSATURATED FATTY ACIDS DIFFERENTIALLY ENHANCE B-CELL MEDIATED IMMUNITY IN LEAN AND OBESE MICE

A Dissertation

Presented To the Faculty of the Department of Biochemistry

East Carolina University

In Partial Fulfillment of the Requirements for the Degree

Doctor of Philosophy

By

Heather L. Teague

July, 2014

N-3 POLYUNSATURATED FATTY ACIDS DIFFERENTIALLY ENHANCE B-CELL MEDIATED IMMUNITY IN LEAN AND OBESE MICE

By

Heather L. Teague

APPROVED BY:

DIRECTOR OF DISSERTATION: _____
Saame R. Shaikh, Ph.D.

COMMITTEE MEMBER: _____
Lance Bridges, Ph.D.

COMMITTEE MEMBER: _____
Mark Mannie, Ph.D.

CHAIR OF THE DEPARTMENT OF BIOCHEMISTRY: _____
Phillip Pekala, Ph.D.

DEAN OF THE GRADUATE SCHOOL: _____
Paul J. Gemperline, Ph.D.

DEDICATION

I dedicate this dissertation to Rylee Faith, my courageous daughter who is always smiling and is a constant source of joy and inspiration. Her words will forever echo in my ear, “You can do it Momma.”

ACKNOWLEGEMENTS

I would like to thank God for the incredible people He placed in my life, providing me a network of support that helped me succeed. I would like to thank Robert and Cindy Teague, my parents, for their continuous support and encouragement. You are the rock that stands behind me, a fortress I can depend on no matter what the circumstance. I would like to thank my incredible sister Lynsey Haman for both her moral support and scientific contribution. In addition to being a never-ending source of encouragement, she designed the cover image for our JLR, November 2013, publication. I would like to thank Dan and Janie Petrole, your love and encouragement are always with me. I would like to thank Michelle Robinson, Kaitlyn Morrison, Beth Rasberry, Mary Moldt and Andrew Friday. Your friendship and support mean more to me than words can describe and I could not have completed this program without each of you.

I would like to thank my advisor Dr. Shaikh for allowing me to be a part of his lab and for everything he has taught me the last 5 years. Dr. Shaikh stretched me beyond my own limits, challenging me daily, and guiding me to become a better scientist and person. His constant guidance, rapid feedback and enthusiasm about science created an environment that allowed me to flourish. I would like to thank Dr. Gemperline for believing in me when I didn't believe in myself. If it wasn't for all the time and effort Dr. Gemperline invested in me during a critical period of my life, I would not be here today.

I would like to thank the members of the Shaikh lab, Drew Rockett, Mitch Harris, Jarrett Whelan, Madison Sullivan, and Perrine Lallemand for all of your contributions to my project and for creating an enjoyable work environment. Especially Mitch and Drew

for taking the time to teach and train me. I would like to thank my committee, Dr. Pekala, Dr. Bridges and Dr. Mannie for all of your contributions to my work. Each of you challenged me in a different way, making me an all-around better scientist. I would also like to thank the Biochemistry Department for investing in my scientific endeavors, and taking the time to prepare me for what is to come.

TABLE OF CONTENTS

LIST OF TABLES

LIST OF FIGURES

LIST OF ABBREVIATIONS

PUFA	Polyunsaturated Fatty Acid
DHA	Docosahexaenoic Acid
EPA	Eicosapentaenoic Acid
ALA	α-Linolenic Acid
AA	Arachidonic Acid
OA	Oleic Acid
VLDL	Very Low-Density Lipoproteins
PE	Phosphatidylethanolamine
PC	Phosphatidylcholine
SREBP-1c	Sterol Regulatory Element Binding Protein-1c
STED	Stimulated Emission Depletion Microscopy
PALM	Fluorescence Photoactivation Localization Microscopy
STORM	Stochastic Optical Reconstruction Microscopy
PKC	Protein Kinase C
LAT	Linker for Activation of T cells
DC	Dendritic Cell
TNF- α	Tumor Necrosis Factor- α
GPR120	G-Protein Coupled Receptor 120
GPR40	G-Protein Coupled Receptor 40
PPAR	Peroxisome Proliferator-Activated Receptors
NF-κB	Nuclear Factor-Kappa B
IL	Interleukin

LTB4	Leukotriene B4
V	Variable
D	Diversity
J	Joining
BCR	B-cell Receptor
Ig	Immunoglobulin
TLR	Toll-like Receptors
MHC	Major Histocompatibility Complex
AID	Activation-Induced Cytidine Deaminase
CD	Cluster of Differentiation
TLR4	Toll-like Receptor 4
LPS	Lipopolysaccharide
PBS	Phosphate Buffered Solution
HBSS	Hanks' Balanced Salt Solution
GM-CSF	Granulocyte-Macrophage Colony-Stimulating Factor
HLA	Human Leukocyte Antigen
APC	Antigen Presenting Cell
POPC	1-Palmitoyl-2-Oleoyl-Phosphatidylcholine
SDPC	1-Stearoyl-2-Docosahexaenoyl-Phosphatidylcholine
Chol	Cholesterol
DHA-Bodipy	4,4-Difluoro-5,7-Dimethyl-4-Bora-3a,4a-Diaza-Sindacene-3-Docosahexaenoic Acid
ROI	Region of Interest

RFU	Relative Fluorescence Units
PA-Bodipy	Palmitic Acid-Labeled Bodipy
ABCA1	ATP-Binding Cassette Transporter 1
LCPUFA	Long Chain Polyunsaturated Fatty Acid
IFN	Interferon
GP	Generalized Polarization
MFI	Mean Fluorescence Intensity
TGF	Transforming Growth Factor
SFA	Saturated Fatty Acid
MUFA	Mono-Unsaturated Fatty Acid
MD-2	Myeloid Differentiation Factor 2
TNP-LPS	Trinitrophenylated-Lipopolysaccharide
HF	High Fat Diet
HF-OA	High Fat Diet Enriched with Oleic Acid
HF-EPA	High Fat Diet Enriched with Eicosapentaenoic Acid
HF-DHA	High Fat Diet Enriched with Docosahexaenoic Acid
BSA	Bovine Serum Albumin
GFP	Green Fluorescent Protein
CREB	cAMP Response Element-Binding Protein
RvD1	Resolvin D1
17-HDHA	17(R)-Hydroxy Docosahexaenoic Acid
HA	Hemagglutinin

CHAPTER 1 : INTRODUCTION

History of n-3 Polyunsaturated Fatty Acids

Investigations of n-3 polyunsaturated fatty acids (PUFA) for clinical utilization originated in the 1970s when Bang and Dyerburg began studying a small population of Greenland Eskimos with a low incidence of ischemic heart disease (*1*). The observation unique to this population was that Greenland Eskimos consumed large amounts of animal fat, typically associated with a high incidence of ischemic heart disease; however, only 3 cases of heart disease out of 1350 inhabitants were reported from the years of 1963 to 1967 (*1*). Even more surprising, diabetes mellitus was nonexistent within this population (*1*). Bang and Dyerburg were intrigued; they began studying the Greenland Eskimos in search of the source limiting the development of cardiovascular disease (*1*). The one characteristic distinguishing this population of Eskimos from the surrounding villages was their reliance on hunting and fishing for food (*1*). Bang and Dyerburg measured the total lipids, cholesterol and triglyceride concentrations in the plasma of the Greenland Eskimos, due to the associations between high cholesterol and atherosclerotic disease, and compared the values to the Danish population, a population consuming a more civilized western diet (*1*). The Greenland Eskimos had reduced total lipids, decreased cholesterol, triglycerides and phospholipids, and less β-lipoprotein and pre-β-lipoprotein particles (*1*). Bang and Dyerburg credited this difference to be a result of the Greenland Eskimos consuming almost five times as much n-3 PUFAs as the Danish from large amounts of fish intake, concomitant with a decrease in saturated fatty acid consumption (*2*). These findings opened the door to investigations focused on the benefits of n-3 PUFAs on overall human health, their

impact on disease, and the detailed mechanisms associated with their multifaceted effects (*3, 4*).

N-3 PUFA Sources

The two bioactive n-3 PUFAs highly concentrated in the oils of fish are docosahexaenoic acid (DHA) and eicosapentaenoic acid (EPA). DHA and EPA are characterized by their long fatty acid chains containing multiple double bonds, with the first double bond occurring at the third carbon from the methyl end. Increasing DHA and EPA intake can be accomplished via marine fish oil or dietary supplements; however, there are several factors to consider. Marine sources notably differ in the amount of DHA and EPA, in addition to the ratio of DHA to EPA. For example, a 3 oz. serving of wild Atlantic salmon contains about 0.9-1.56 g of EPA + DHA compared to sockeye salmon, containing 0.68 g EPA + DHA (*5*). Additionally, mackerel contains a range from 0.34 to 1.57 g of EPA + DHA in a 3 oz. serving (*5*). The type of fish consumed will determine the amount of DHA or EPA ingested.

When relying on dietary supplements to increase DHA and EPA intake, factors such as chemical form and purity should be considered. DHA and EPA purified from fish oil are linked to a glycerol backbone, with other saturated and monounsaturated fatty acyl chains, to form triglycerides. EPA and DHA purified from krill oil are conjugated to phospholipids and contain anti-oxidants. Highly purified EPA and DHA ethyl esters are available clinically and are marketed under the name Lovaza, originally known as Omacor (*5, 6*). The highly purified EPA and DHA ethyl esters are the only chemical form that are synthetic compounds which are free of environmental toxins, such as dioxins, polychlorinated biphenyls and proteins bound to methyl mercury (*7*). Although EPA and

DHA ethyl esters are toxin free, there is debate regarding which chemical form of EPA and DHA is more readily absorbed (*8*). Schuchardt et al. investigated the bioavailability of each chemical form of EPA and DHA by measuring the changes in fatty acid composition of plasma phospholipids from 12 healthy young men at 72 hours following ingestion of 1.7 g of krill oil, fish oil or EPA + DHA ethyl esters (*9*). Although significance was not established, the study showed a trend for the highest incorporation of EPA and DHA into plasma phospholipids from krill oil, followed by EPA and DHA in triglyceride form from fish oil and then EPA and DHA in the ethyl ester chemical form (*9*). Neurbronner et al. utilized the same dose of 1.7 g of EPA + DHA for a longer intervention period of 6 months administered to 150 volunteers and determined EPA and DHA as triglycerides led to a faster and increased uptake by red blood cells compared to ethyl esters (*8*). Even though differences in n-3 PUFA uptake exist between triglycerides and ethyl esters, significant increases in EPA and DHA in the plasma are observed from both chemical forms, suggesting either supplement form is sufficient.

Biochemistry of EPA and DHA

Dietary intake of DHA and EPA is the most efficient way to increase DHA and EPA levels, however, *de novo* synthesis of DHA and EPA does occur. DHA and EPA *de novo* synthesis transpires in the endoplasmic reticulum of the liver, and a limited amount in the brain, from α-linolenic acid (ALA), albeit an inefficient process in humans (*3, 10-12*). ALA is an 18-carbon n-3 PUFA containing three double bonds and is an essential fatty acid, meaning it must be consumed in the diet. Humans do not possess the desaturase required to add double bonds to form ALA (*4*). One limiting factor for DHA

and EPA synthesis is the pathway is in constant competition with arachidonic acid (AA) synthesis, an n-6 PUFA synthesized from linoleic acid, due to both pathways utilizing the same enzymes, Δ6-desaturase and Δ5-desaturase (Fig. 1.1) (*11, 13*). Conversion of ALA to EPA and DHA is reduced by 40% in humans consuming large quantities of n-6 PUFAs (*14*). Additionally, nutritional status, hormones and feedback inhibition by end products regulate Δ5 and Δ6-desaturase activity (*15*). Δ5 and Δ6-desaturase activity requires insulin and thyroxin, whereas glucagon, epinephrine, adrenocorticotropic hormone and glucocorticoids downregulate desaturation (*12, 15*).

The pathway for EPA and DHA biosynthesis is illustrated in Figure 1 where ALA is converted to stearidonic acid (18:4, n-3) by Δ6-desaturase, an enzyme responsible for the addition of a double bond. Stearidonic acid is then elongated by an elongase to eicosatetraenoic acid (20:4, n-3) (*11, 13*). Δ5-desaturase then adds a double bond to eicosatetraenoic acid producing EPA (*11, 13*). The steps required to produce DHA from EPA are lengthier due to the lack of the appropriate desaturases. EPA undergoes two elongation steps to form a 24:5, n-3 long chain fatty acid (*11, 13*). This very long chain fatty acid is translocated to the peroxisome to remove two carbons by β-oxidation producing DHA (*11, 13*). EPA is also produced from DHA through a process termed retroconversion, a β-oxidation reaction occurring in the peroxisome that is hormonally regulated by estrogen (*16*).

Dietary n-3 PUFAs undergo digestion in the small intestine where they are hydrolyzed by pancreatic lipases in the intestinal lumen and absorbed into the enterocytes via fatty acid translocase (CD36) (*17*). In the enterocytes, n-3 PUFAs are incorporated into chylomicrons, which bypass the liver and migrate through the

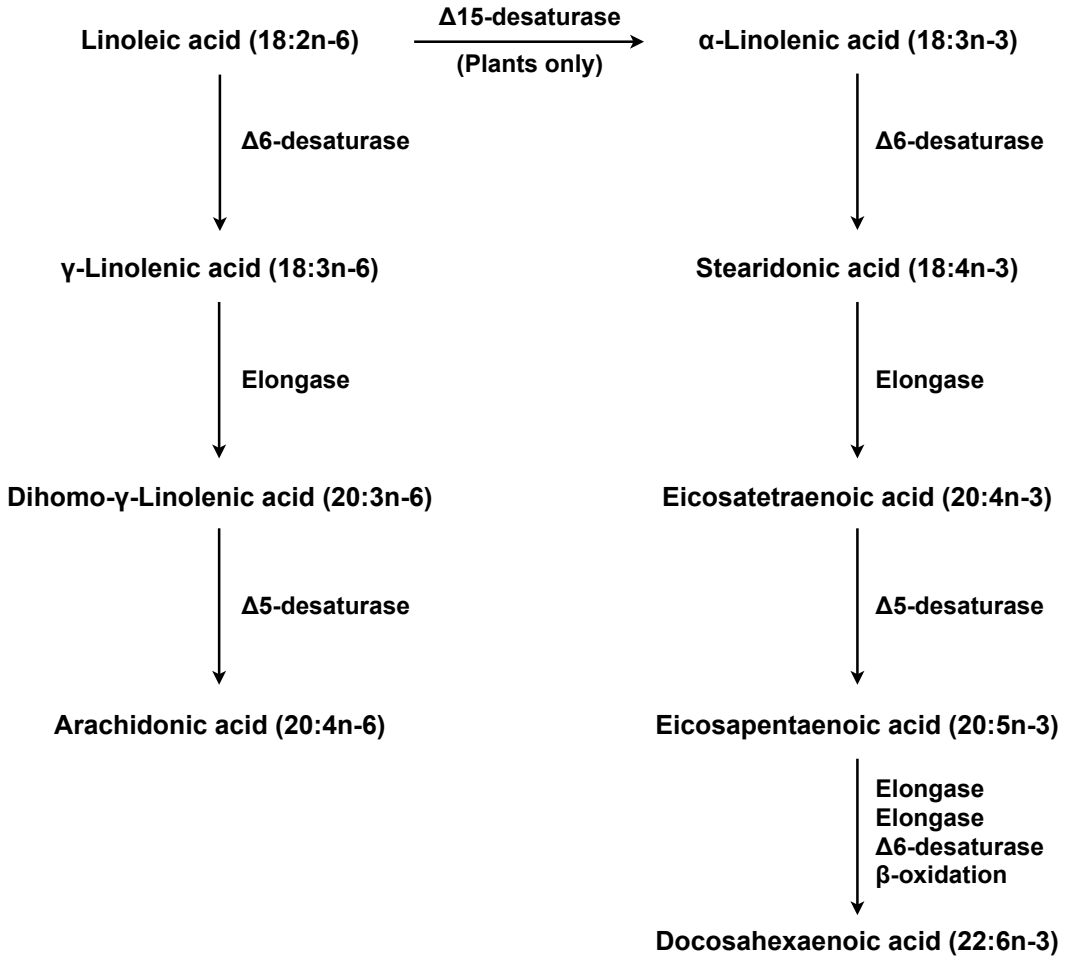

Figure 1.1: EPA and DHA Biosynthesis.
The *de novo* synthesis of n-3 and n-6 PUFAs from the essential fatty acids linoleic (18:2) and ALA acid (18:3). Both pathways are in constant competition due to utilization of the same enzymes for AA, EPA and DHA acids synthesis. The Δ15-desaturase is only present in plants, therefore linoleic and ALA acids must be consumed in the diet.

lymphatic system for distribution to the peripheral tissues (*7*). Remnant particles then return to the liver and the remaining n-3 PUFAs are released as either very low-density lipoproteins (VLDL) or bound to albumin for assimilation throughout most tissues (*7, 15, 18*). Upon lipoprotein lipase cleavage, the n-3 PUFAs are either stored as triglycerides, or esterified into cholesterol esters and phospholipids, where they are incorporated into the cellular plasma membrane (*19*). N-3 PUFAs primarily incorporate into

phosphatidylethanolamine (PE) followed by phosphatidylcholine (PC), however this is tissue specific (*20*). In heart tissue n-3 PUFAs incorporate into PE and PC, compared to the outer cone rod cells of the retina and neural tissues, where n-3 PUFAs incorporate into phosphatidylserine and PE, with a small amount in PC (*20-22*). In macrophages, human plasma and erythrocytes, n-3 PUFAs primarily incorporate into PC and PE, competing with n-6 PUFAs for the Sn2 position (*3, 11, 23, 24*). EPA and DHA supplementation therefore increases their levels in phospholipids at the expense of AA, which becomes important when considering the inflammatory response (*25*).

N-3 PUFAs and Disease

Over the last four decades, studies focused on the potential benefits of consuming n-3 PUFAs in various disease states have increased (*26-31*). However, the development of n-3 PUFAs for clinical use is limited to the reduction of serum triglyceride levels, in which multiple mechanisms are identified (*6, 13*). EPA and DHA inhibit secretion of VLDL by increasing degradation of B-100 containing lipoproteins, resulting in reduce plasma triglyceride levels (*7, 32*). Diacylglycerol acyltransferase inhibition by EPA reduces triglyceride biosynthesis (*7, 33*). EPA and DHA also lower sterol regulatory element binding protein-1c (SREBP-1c) levels, thereby reducing hepatic lipogenesis (*7, 34*). Studies on the efficacy of n-3 PUFAs for the treatment of cardiovascular disease and rheumatoid arthritis are ongoing. Although the data suggest n-3 PUFAs potentially exert positive effects, the results are inconclusive (*27, 35-37*). While a meta-analyses investigating fish intake and coronary heart disease mortality demonstrated those consuming fish up to 5 times a week had a reduction in risk of coronary heart disease by 38%, more recent studies conclude n-3 PUFAs have no

effect on the outcome of cardiovascular disease (*27, 35, 36*). Galan et al. conducted a 4.7 year investigation of 2501 subjects taking B vitamins and/or 600 mg EPA + DHA per day and reported no significant improvements were observed (*27*).

The benefits of n-3 PUFA supplementation to rheumatoid arthritis patients have been modest, lowering the need for non-steroidal anti-inflammatory drugs and reducing morning stiffness, although pain and swelling are unaffected (*38-40*). One rational for the conflicting results may be due to inconsistencies between studies. Experimental designs for clinical trials lack consistency in critical factors such as intervention timing and dose, due to a lack of mechanistic understanding (*41-43*). The following paragraphs will address the mechanisms that are characterized, including the effects of n-3 PUFAs on membrane organization, eicosanoid metabolism, gene expression and cellular signaling (*44-46*).

The Cell Membrane, Lipid Microdomains and N-3 PUFAs

The cellular plasma membrane is a highly organized structure critical for cell function (*47*). An understanding of membrane organization has increased significantly since the fluid mosaic model from Singer and Nicholson in 1972 that described the plasma membrane as a fluid lipid bilayer containing diffuse monomeric and amphiphilic proteins (*48*). Identification of specialized membrane domains, such as lipid microdomains, challenged the notion that the plasma membrane lipids were simply a passive fluid solvent, moving the field into a new area of investigation (*49*). Since then it was established that lipid microdomains (i.e. lipid rafts), estimating to be 10-200 nm in size, are highly ordered membrane domains defined as dynamic, nanoscale, ordered assemblies of proteins and lipids that can coalesce into larger, more stable domains

(*49*). Lipid microdomains are composed primarily of glycosphingolipids, cholesterol and GPI-anchored proteins on the outer leaflet, and saturated phospholipids in the inner leaflet (*50-52*). Within these liquid-ordered domains, receptors are recruited to activate intracellular processes, signaling complexes are assembled and ion channels stabilized for current conduction (*52-54*). Additionally, crosslinking of raft-associated receptors induces formation of a larger domain where more sustained signaling can occur (*47, 55*).

The existence of lipid microdomains is highly controversial (*56*). Initially, the controversy was attributed to the techniques employed for lipid microdomain isolation. The crude extraction of lipid microdomains with low doses of non-ionic detergent, a method prone to artifacts, defined the detergent resistant membrane fraction as the lipid microdomain component versus the detergent soluble membrane (*49, 57*). Additionally, this process results in homogenized lipids, providing no information on how they are dispersed in the cellular plasma membrane. (*58*). However, advances in super resolution microscopy like stimulated emission depletion (STED), fluorescence photoactivation localization microscopy (PALM) and stochastic optical reconstruction microscopy (STORM) have supported the existence of lipid microdomains, revealing dynamic, nanoscale domains in living cells (*49, 59-61*). A new model by Owen et al. also supports the existence of ordered domains; however, Owen proposed that the majority of the plasma membrane is a series of connected cholesterol-dependent lipid domains (*62*).

In relation to immunity, which is the focus of this thesis, the cellular plasma membrane houses transmembrane proteins and lipidated proteins that act as receptors

to foreign pathogens or cytokines, which regulate immune processes in an autocrine, endocrine and paracrine fashion (*47, 63*). Interactions between immune cells through antigen presentation, integrin recognition, and adhesion molecules are dependent on the cellular plasma membrane integrity and often rely on the formation of lipid microdomains for sustained signaling (*4, 47*). N-3 PUFAs readily incorporate into plasma membrane phospholipids, altering the lipid composition, and effecting cell signaling through changes in membrane lipid-protein lateral organization (*4*). For example, Fan et al. established n-3 PUFAs incorporate into the lipid microdomains of splenic T cells, reducing recruitment of protein kinase Cθ (PKC), an intracellular signaling protein, into the immunological synapse thereby decreasing signaling (*64*). Additionally, n-3 PUFAs displace linker for activation of T cells (LAT), blocking phosphorylation and therefore signal transduction (*65*). One proposed mechanism is the S-acylation of proteins by n-3 PUFAs displaces the proteins from lipid microdomains, down regulating signaling (*66*). N-3 PUFAs also populate non-lipid microdomains, effecting protein organization (*67*). These findings combined demonstrate the critical role n-3 PUFAs play in immune cell signaling by altering the cellular membrane composition (*20, 67-69*). Furthermore, these findings warrant a thorough investigation on how altering the plasma membrane lipid content affects the function of other immune cell types such as B cells and dendritic cells (DC), an area of research with insufficient information.

N-3 PUFAs and the Inflammatory Response

One major component of immunity is the inflammatory response, a defense mechanism intimately linked to dietary n-3 and n-6 PUFAs (*3*). Inflammation is a

response initiated by a host challenge from pathogens, tissue injury or surgical trauma, protecting the tissue from damage and ultimately restoring physiological homeostasis (*3, 70*). The inability to resolve inflammation produces a state of chronic inflammation, a problematic tendency underlying many disease states (*71*). Two critical processes describe inflammation, the onset of acute inflammation and inflammation resolution. At the onset of acute inflammation a series of eicosanoids, leukotrienes and prostaglandins synthesized from the n-6 PUFA AA, drive the inflammatory response (*72-74*) Leukotriene B_4 (LTB4) recruits neutrophils, which migrate via diapedesis. Vasoconstriction is induced by thromboxane A_2, vasodilation by prostaglandins and vascular permeability by cysteinyl leukotrienes (*70, 75*). Although n-6 PUFA derived metabolites predominately contribute to inflammation, lipoxins A_4 and prostaglandin E_2 exert both pro-inflammatory and resolving effects (*30, 76*). Furthermore, dihomo-γ-linolenic acid, a product of γ-linolenic acids elongation, exerts some anti-inflammatory effects (*77*).

N-3 PUFAs contribute to the resolution of inflammation by several identified mechanisms. DHA and EPA are precursors for specialized proresolving mediators responsible for driving inflammation resolution termed resolvins, protections, lipoxins and maresins (*76*). For example, EPA is a precursor for leukotriene B_5 and is thought to be a 10-30 times less potent neutrophil chemoattractant than LTB4, therefore reducing neutrophil recruitment (*3, 78*). Prostaglandin D_3, synthesized from EPA, antagonizes the prostaglandin D_2 receptor, inhibiting neutrophil migration (*3*). In addition, the pro-resolving mediators recruit monocytes to phagocytose apoptotic neutrophils and debris (*76*). Even though elucidation of the mechanisms by which n-3 PUFAs aid in

inflammation resolution is ongoing, it is clear these pro-resolving mediators promote tissue homeostasis by inhibiting neutrophil recruitment, blocking the production of pro-inflammatory cytokines and inducing macrophage phagocytosis of apoptotic cells (*3, 19, 79*).

Additional mechanisms by which n-3 PUFAs modulate inflammation include interactions with membrane-bound and cytosolic receptors (*80*). G-protein coupled receptor 120 (GPR120), a G-coupled membrane bound receptor expressed on adipose tissue and macrophages, directly binds EPA and DHA, inhibiting tumor necrosis factor (TNF)-α production, a pro-inflammatory cytokine (*81-83*). DHA and EPA also act as ligands for G-protein coupled receptor 40 (GPR40), a G-coupled receptor abundantly expressed in the brain and pancreas, decreasing inflammation through the inhibition of inflammasomes (*84, 85*). Peroxisome proliferator-activated receptors (PPARs) also respond to interactions with n-3 PUFAs by inhibiting pro-inflammatory gene transcription due to the inhibition of nuclear factor-kappa B (NF-κB) activation (*86*).

Immune Cell Targets of N-3 PUFAs

Some of the identified immune cell targets of dietary n-3 PUFAs are T cells, macrophages and neutrophils, with most of the effects of n-3 PUFAs being characterized as immunosuppressive. As previously discussed, n-3 PUFAs suppress interleukin (IL)-2 production from activated T cells through membrane modifications (*64*). In murine activated macrophage-like J774A.1 cells, DHA treatment reduced cytokine secretion, reduced costimulatory molecule surface expression, impaired oxidative metabolism and decreased phagolysosome maturation (*87*). In addition, Chiu et al. showed DHA treatment of the murine macrophage cell line RAW 264.7 promoted

macrophage polarization to an anti-inflammatory M2 phenotype (*88*). N-3 PUFA treatment of human neutrophils resulted in decreased expression of TNF receptors, receptors upregulated by n-6 PUFAs (*89*). Healthy volunteers consuming dietary fish oil showed EPA targets neutrophils, suppressing LTB4 synthesis and inhibiting neutrophil chemotaxis by inhibiting signal transduction (*90*). On the contrary, some studies show the phagocytosis mechanism in both macrophages and neutrophils is enhanced by n-3 PUFAs (*91, 92*). Although there is sufficient data discussing the immune cell targets of n-3 PUFAs, investigations focused on the affects n-3 PUFAs exert on B cells and DCs are limited. B cells play a critical role in the immune response, especially when combating pathogens the innate immune system failed to eliminate. B cells involvement in the adaptive or secondary immune response largely determines the pathological outcome. DCs are the front line of defense when combating antigen and are responsible for activating the adaptive immune response. Therefore, this thesis focused on understanding how n-3 PUFAs affect B-cell and DC function, which is a key component to the big picture of understanding how n-3 PUFAs modulate immunity.

B-Cell Development

B cells are unique, multifaceted immune cells possessing functional responsibilities for both the innate and adaptive immune response. B cells not only produce antibody, they secrete cytokines and serve as antigen presenting cells (*93*). Proper B-cell development is critical for a functional immune system and in the prevention of autoreactive disease states. The development of B cells occurs in the bone marrow from haematopoietic stem cells (Fig. 1.2) (*94*). Once the haematopoietic

stem cells have differentiated into common lymphoid progenitor cells, either a T-cell or B-cell will be generated from this point (*47*). Cells destined to become B cells progress

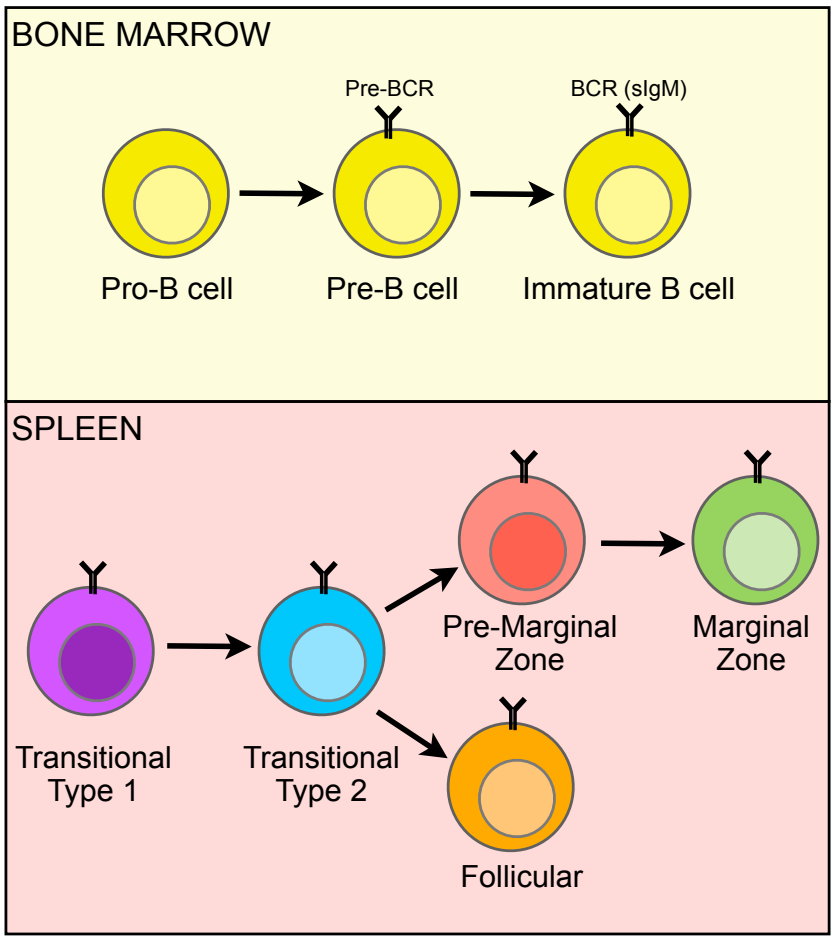

Figure 1.2: B-cell Development.
B- cell development originates in the bone marrow. Once a functional BCR is expressed on the B-cell surface, migration to the secondary lymphoid organs occurs. B cells then develop into either marginal zone or follicular B cells.

to the pro-pre B-cell stage (*47*). During the pro-phase of B-cell development, B cells must produce a μ heavy chain through the variable (V), diversity (D) and joining (J) gene segment rearrangement process known as somatic recombination (*47*). The successfully rearranged μ heavy chain then combines with a non-polymorphic surrogate light chain to form a pre-B-cell receptor (BCR) on the B-cell surface (*95*). Pre-BCR surface expression arrests the heavy chain rearrangement process and proliferation of

the pro-B-cell is initiated, a process driven by IL-7 (*95-97*). Inefficiency in rearranging the μ heavy chain would result in elimination of the B-cell (*47*). Thus, a species with a mutation resulting in the inability to generate the μ heavy chain would be completely void of B cells. The large population of newly generated pre-B cells begins rearranging the light chain through a similar process, only involving the V and J gene segments (*47*). Once successful light chain rearrangement has occurred, the immunoglobulin (Ig) M BCR is assembled and expressed on the surface, therefore qualifying the B-cell as a naïve immature B-cell (*47*).

Subsequent to exiting the bone marrow, immature B cells home to the secondary lymphoid tissues for further development (Fig. 1.2). B cells are in the transitional type 1 B-cell phase, characterized by low surface IgD, upon arrival to the spleen (*94*). Transitional type 1 B cells can be present in both the spleen and bone marrow and do not possess the ability to recirculate (*94*). Upregulation of IgD surface expression designates the B-cell as a transitional type 2 B-cell that is now equipped with the ability to recirculate (*98*). From the transitional type 2 B-cell stage, B cells become either a marginal zone B-cell or a follicular B-cell, two functionally distinct cell types (Fig. 1.2) (*94*).

Naive follicular B cells are phenotypically characterized by high IgD and low IgM surface expression and are the largest population of B cells (*94, 99*). Follicular B cells are strategically localized adjacent to the T-cell zones in the spleen ensuring optimal

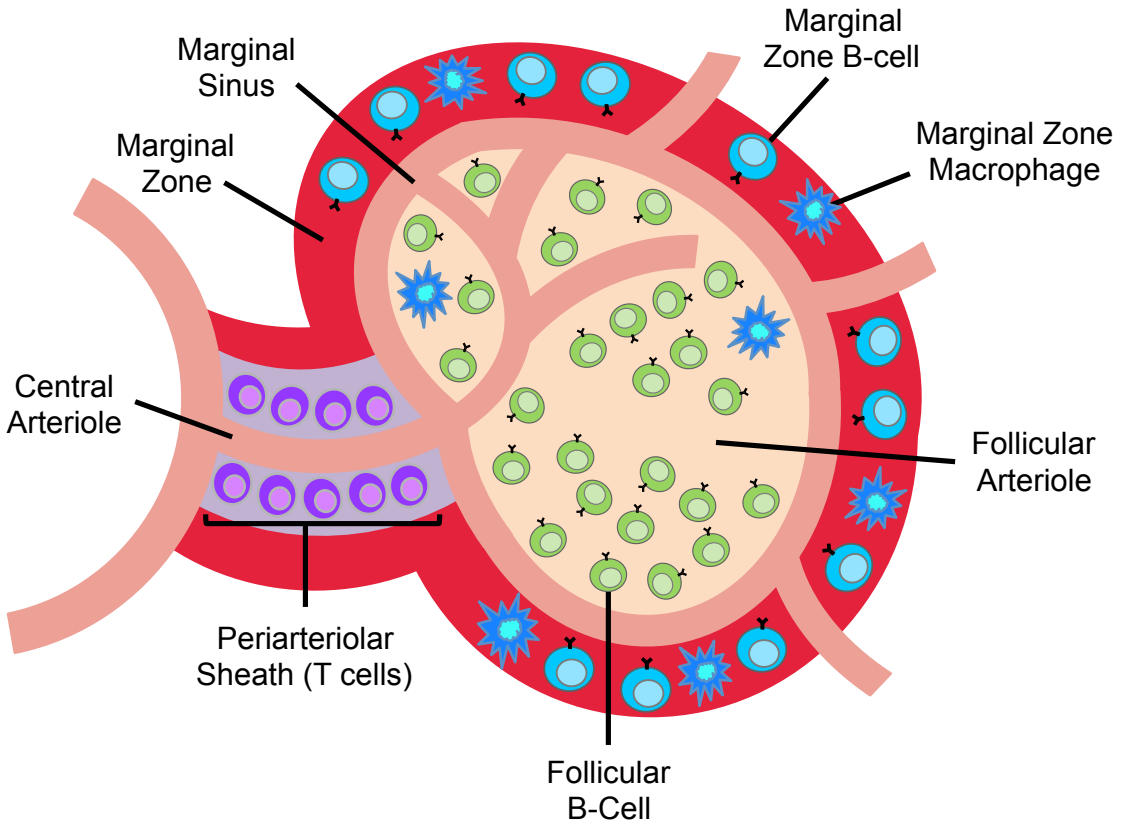

Figure 1.3: Schematic of the Spleen.
The marginal zone (MZ) B cells are strategically localized next to the marginal sinus, allowing the MZ B cells to constantly survey the blood for the presence of pathogens.

conditions for B-cell and T-cell interaction (*94*). Follicular B cells are the B-cell subset most likely to respond to T-dependent protein antigens, a process discussed in the following paragraphs (*94*). Activation of follicular B cells produces long-lived memory cells or short-lived plasma cells, both with monoreactive BCRs (*94, 100*).

Marginal zone B cells are a subset of B cells possessing innate like properties. Marginal zone B cells express high levels of toll-like receptors (TLR) capable of recognizing microbial ligands, in addition to expressing polyreactive BCRs (*100-103*). Marginal zone B cells have been strategically placed at the interface between the circulation and secondary lymphoid tissues, allowing them to survey the blood for the

presence of blood-borne antigens and shuttle antigens to the follicular DCs upon engagement (Fig 1.3) (*94, 95*). One clear distinction between marginal zone B cells and follicular B cells are their self-renewing capabilities with an unlimited lifespan, compared to the lifespan of follicular B cells, which is as little as a few weeks (*94*). Marginal zone B cells typically respond to blood borne pathogens in a T-cell independent manner by engaging both TLR and BCR (*100*). This results in rapid production of antibody and differentiation into a plasmablast, although this process is incapable of inducing memory (*104*).

In addition to marginal zone B cells, B-1 cells are innate like cells residing in the peritoneal and pleural cavities, with small amounts found in the spleen (*99*). B-1 simply delineates B cells that developed earlier during ontogeny than conventional B-2 cells (*99*). B-1 B cells and marginal zone B cells primarily express germline-encoded antigen receptors specific for microbial and self antigens, exhibiting limited diversity (*99*). They are also the primary producers of natural IgM antibodies, a set of antibodies recognized for their immunoregulatory properties and ability to enhance phagocytic clearance of apoptotic cells (*99*). In contrast to the continuous development of B-2 cells *de novo*, B-1 cells undergo limited proliferation to replace dying cells (*99*). Antibody production from B-1 cells comprises the natural antibody repertoire, which are antibodies generated in the absence of antigenic exposure (*99, 105-107*). The natural antibody repertoire may exhibit low affinity and broad crossreactivity, however they directly neutralize and inhibit early pathogen replication (*99, 108-111*). B-1 cells are capable of undergoing class–switch recombination to all isotypes, but prefer switching to IgA by signals distinct from B-2 cells (*99, 112, 113*).

IL-10 secreting regulatory B cells encompasses a newly identified B-cell subset that displays similar phenotypic characteristics as B-1 cells, and may be a member of the “innate-like” B-cell population (*99, 114, 115*). IL-10 producing B cells are a type of regulatory B-cell that suppresses the inflammatory response (*114, 116*). The frequency of IL-10 producing B cells is heightened at the climax of inflammation and inhibits progression of Th-2 driven diseases, making them critical cells for restraining autoimmunity (*93, 114*). IL-10 producing B cells inhibit Th1/Th17 cells during acute inflammation and induce T-regulatory cells (*93, 117*). IL-10 producing B cells also work in parallel to the newly discovered IL-35 producing B cells (*118*). Similar to IL-10 producing B cells; IL-35 producing B cells are negative regulators of immunity, decreasing susceptibility to the development of autoimmune diseases (*118*).

T-cell Dependent Activation

DCs presenting protein antigens to B cells via major histocompatibility complex (MHC) class II initiates a T-cell dependent response (*119*). Upregulation of chemokine receptors recruits B cells to the T-cell zone of the lymphoid tissues where they become fully activated by forming an immunological synapse with T cells (*119*). The activated B cell has one of two fates, they either develop into antibody secreting plasma cells, or they move to the primary follicle and mature into germinal center precursor B cells (*119*). The rapidly proliferating B cells form a mantle zone around the germinal center known as the secondary follicle. The germinal center is made up of two zones, a light zone and a dark zone. Centroblasts, the proliferating B cells, are tightly packed in the dark zone (*119*). Centroblasts undergo somatic hypermutation to increase BCR specificity and affinity for the antigen (*119*). Somatic hypermutation is an activation-

induced cytidine deaminase (AID) driven process that introduces point mutations in the variable gene segment of both the heavy and light chain (*119*). The centroblasts then differentiate into centrocytes; smaller non-diving B cells, and migrates into the light zone where they are tested by follicular DCs and T cells for improved antigen specificity (*119*). The B cells exhibiting strong antigen affinity undergo class-switch recombination, a process replacing the IgM heavy chain with IgG, IgA or IgE, and the remaining B cells undergo apoptosis (*119*).

T-cell Independent Activation

As previously stated, B-1 and marginal zone B cells are the key players in a T-independent immune response (*100*). Upon initiation of a T-independent response through TLRs, B-1 cells and marginal zone B cells downregulate integrin expression, enabling them to redistribute to the blood, lymph nodes or spleen. These B cells then begin proliferating and secreting large amounts of IgA (B-1 B cells) or IgM (marginal zone B cells), consistent with their *in vivo* specificity against mucosal versus blood borne pathogens (*120, 121*). Marginal zone and B-1 B cells also secrete IL-10, a regulatory cytokine that drives the Th2 response (*122*). Interestingly, there is a marked increase in the expression of co-stimulatory molecules, enabling these cells to act as antigen presenting cells, connecting the gap between T-independent and T-dependent immune responses (*123*). The synergy between TLRs and BCRs yields an efficacious T-independent immune response from B-1 and marginal zone B cells (*123*).

Studies investigating the effects of n-3 PUFAs on B cells are limited, especially their impact on antibody production (*124*). The few studies focused on n-3 PUFAs and antibody production exhibit discrepant results (*124*). DHA decreased IgE production

from human B cells activated with IL-4 and anti-CD40 compared to controls (*125*). In contrast, n-3 PUFA consumption enhanced antibody production in broiler birds compared to n-6 PUFAs (*126*). Furthermore, Beli et al. demonstrated n-3 PUFAs had no effect on IgA antibody levels compared to controls in response to respiratory enteric orphan virus in mice (*127*). The lack of consistency in results is most likely attributed to the variation in model systems utilized, and warrants further investigations on how n-3 PUFAs effect antibody production.

Antigen Presenting DCs

DCs are an essential link between innate and adaptive immunity. The key role of DCs is to recognize danger signals or pathogen invasion, capture antigen for processing via the endosomal MHC class II pathway, and present the antigen to naïve B and T cells thereby activating adaptive immunity. DCs are derived from either bone-marrow progenitor cells or monocytes and differentiate into Langerhans cells, interstitial DCs or plasmacytoid DCs (*128, 129*). DC migration from the bone marrow occurs in an immature state followed by localization within a tissue, or continual surveying of the blood (*129*). Phenotypic maturation is induced once an antigen has been encountered and the surface markers required for antigen presentation, such as CD80, CD86, CD40 and MHC class II, are upregulated.

Studies investigating the effects of n-3 PUFAs on DC function demonstrate n-3 PUFAs decrease function by preventing phenotypic maturation (*130, 131*). Kong et al. showed murine bone marrow-derived DCs treated with 50 μM DHA followed by lipopolysaccharide (LPS) stimulation for 24 hours failed to up-regulate MHC class II, CD40, CD80 and CD86 expression while maintaining high levels of endocytic activity,

keeping DCs in the immature phenotype (*132*). Additionally DHA reduced expression of IL-12p70, IL-27 and IL-23 in a dose dependent manner (*132*). Similar results were observed in DCs generated from human peripheral blood monocytes in the presence of granulocyte-macrophage colony stimulating factors (GM-CSF) and IL-4 (*133*). EPA or DHA treatment at 50 μM decreased expression of CD80, CD86 and major histocompatibility class human leukocyte antigen (HLA)-DR on LPS stimulated DCs concomitant with decreased IL-12 and TNFα secretion (*133*).

T-cell activation requires engagement through the TCR via MHC class II molecules and CD80 or CD86 costimulatory molecules through CD28 forming the immunological synapse. A decrease in the expression of MHC class II, CD80 or CD86 would result in decreased T cell activation. Wang et al. measured T cell proliferation after 3 days of stimulation from EPA or DHA treated DCs and found proliferation to be decreased (*133*). One limitation of these studies is they rely on an *in vitro* model system utilizing high doses of DHA or EPA. Studies conducted with pharmacologically relevant doses of n-3 PUFAs on DC function at the *ex vivo* level are required to move the field forward and add to the understanding of the effects of n-3 PUFAs on immune cell function.

Significance

Both DHA and EPA are known to exert immunomodulatory effects on the immune response *in vitro* and *in vivo*. Intriguingly, preliminary data from our lab demonstrated activation of B cells with LPS through toll-like receptor 4 (TLR4) significantly enhanced cytokine production. This result was unexpected as most studies demonstrate n-3 PUFAs exert immunosuppressive effects. Currently, there are limited

data available on the effects of n-3 PUFAs on B cells, with most reported studies utilizing an *in vitro* model system. Additionally, the effects of physiologically relevant doses of n-3 PUFAs on DC activation and antigen presentation at the *ex vivo* level are minimal. In this dissertation I sought to determine the effects of n-3 PUFAs on B-cell activation and antigen presentation, and compare the outcome to the effects of n-3 PUFAs on DCs. I determined if the observed effects were associated with changes in lipid microdomain clustering and membrane order on the B-cell and DC cell surface. I then took advantage of the clinically relevant model of obesity, compared to a lean murine model, to determine if n-3 PUFAs possess immune boosting properties *in vivo*. In addition to cardiovascular disease and diabetes, immunosuppression is associated with obesity (*134-136*). Furthermore, obesity is recognized as an independent risk factor for increased morbidity and mortality to infections, such as influenza (*137, 138*). One aspect of immunosuppression in obesity is due to a poor humoral immune response (*139*). Boosting humoral immunity in immunocompromised populations such as the obese has clinical implications and opens the door to new areas of research (*139*).

Specific Aims

Overview

N-3 PUFAs, specifically DHA and EPA found in fish oil, exert immunomodulatory effects. N-3 PUFAs have utility for resolving inflammation; therefore these molecules may have potential for clinical use. However, the effect of n-3 PUFAs on the function of specific immune cells remains in question. Specifically, few studies have determined the functional and mechanistic consequences of n-3 PUFAs on antigen presenting cells (APCs). For this study, we will test the effects of n-3 PUFAs on the antigen presenting B

cells and DCs. The rationale for studying B cells is data from our lab revealed n-3 PUFA supplementation induced an enhanced response through TLR4, contradictory to the expected results. Therefore, we hypothesize n-3 PUFAs are not globally immunosuppressive and exert cell specific effects. To determine if the effects are cell-specific, we will compare the effects of n-3 PUFAs on B-cell activation and antigen presentation to their effects on DCs, and ascertain if the observed effects are correlated with changes in membrane organization. We will then determine if n-3 PUFAs boost B-cell activation and antibody production in a lean and obese murine model accompanied by studies on select B-cell phenotypes in the bone marrow and spleen. Deducing the effects of n-3 PUFAs on B cells will lead to a more lucid understanding of n-3 PUFAs role in curtailing chronic inflammation and boosting humoral immunity.

Aim 1: To test the hypothesis that n-3 PUFAs exert cell specific effects by enhancing B-cell activation and suppressing DC activation ex vivo.

This aim investigates the functional consequences associated with n-3 PUFA treatment on both B cells and DCs. Data from our lab, contrary to literature, shows B-cell activation (i.e. cytokine secretion) is enhanced when activated by LPS through TLR4 following n-3 PUFA treatment. Initially, we will compare B-cell activation through TLR4 to DC activation. We will examine subsequent events of APC activation such as CD80, CD86, CD69 and MHC class II surface expression in conjunction with cytokine secretion. Then we will concentrate on the impact of n-3 PUFAs on antigen presentation. Several labs have shown in vitro that n-3 PUFAs exert immunosuppressive effects on DC function but little is known about the influence of n-3 PUFAs in DCs *ex vivo*. We will investigate if n-3 PUFAs upregulate B-cell and DC

function by measuring their ability to activate naïve $CD4^+$ T cells. Specifically, we will analyze the MHC class II antigen-processing pathway, an exogenous pathway that activates $CD4^+$ T cells. We will measure surface expression of T-cell activation markers and cytokine secretion to determine the degree of activation.

Aim 2: To test the hypothesis that the enhancement in B-cell function is correlated with changes in membrane organization.

This aim is a mechanistic study determining if n-3 PUFAs target B-cell membrane lateral organization. Initially, we will utilize a custom designed DHA-Bodipy probe to compare plasma membrane versus intracellular localization of DHA in B cells. We will then determine if membrane order effects DHA uptake by B cells. We will use live cell microscopy to measure the amount of DHA-bodipy taken up by B cells at low and high temperatures, which represent a less and more ordered environment. We will then determine if the observed enhancement of B-cell function is associated with changes in lipid microdomain clustering and membrane order. We will take advantage of receptor crosslinking on the cell surface, combined with confocal microscopy, to visualize formation of lipid microdomains on B cells.

Aim 3: To test the hypothesis n-3 PUFAs enhance antibody production in vivo.

This aim will utilize an *in vivo* model system to determine if n-3 PUFAs possess immune boosting properties targeting B-cell function. To the best of our knowledge, changes in how n-3 PUFAs effects splenic B-cell subsets *in vivo* are not investigated. We will target B-cell function by eliciting an immune response against the T-independent antigen, trinitrophenylated-LPS, compared to a saline control. We will compare antigen specific serum IgM levels between n-3 PUFA fed mice and controls.

We will measure phenotypic changes in splenic B-cell subsets according to IgM, IgD, CD21 and CD23 surface expression. Additionally, we will measure changes in bone marrow B-cell subsets according to B220, IgM and IgD surface expression. We will then repeat these measurements in a more physiologically relevant model of murine obesity, an population exhibiting suppressed antibody production. Lastly, we will determine if the comparative efficacy of EPA and DHA ethyl esters, the pharmacologically relevant chemical form.

Impact

Completion of the proposal will: 1) lead to a more comprehensive understanding of the effects of n-3 PUFAs on B-cell and DC activation and antigen presentation; 2) contribute to the current knowledge regarding membrane-associated changes from n-3 PUFA incorporation; 3) provide insight into the immune boosting properties of n-3 PUFAs as both triglycerides and the clinically relevant ethyl esters on humoral immunity *in vivo*; 4) and open the door to clinical investigations utilizing n-3 PUFAs to boost immunity in immunocompromised individuals such as the obese.

CHAPTER 2 : DHA-FLUORESCENT PROBE IS SENSITIVE TO MEMBRANE ORDER AND REVEALS MOLECULAR ADAPTATION OF DHA IN ORDERED LIPID MICRODOMAINS[1]

Introduction

The translation of n-3 PUFAs into clinical trials for the treatment of chronic inflammation requires a basic understanding of their molecular mechanisms (*140*). The mechanisms of n-3 PUFAs are complex and pleiotropic. One mode of action, central to regulating most downstream mechanisms, is the ability of n-3 PUFA acyl chains to disrupt the biophysical properties of the plasma membrane (*141*). Many studies show DHA, in particular, can manipulate the formation of membrane signaling microdomains (i.e. signalosomes, caveolae and rafts) (*141*). The mechanism by which DHA, either upon transport as a fatty acid through the membrane or upon esterification into phospholipids, disrupts membrane microdomain properties remains incomplete (*142, 143*). Specifically, it is unknown how DHA, a highly flexible structure, is capable of exerting an ordering effect upon formation of highly packed lipid microdomains (*144*).

Several methodological issues have prevented a comprehensive understanding of how DHA targets membrane microdomain organization. One major limitation is the lack of appropriate fluorescence tools to study DHA, especially as it relates to determining the physical properties of membranes containing DHA. A few fluorescently labeled fatty acid probes have been used for successfully studying some aspects of n-3 fatty acid biology (*145, 146*). For instance, such probes have been employed in binding

[1] This research was originally published in The Journal of Nutritional Biochemistry. Teague, H., Ross, R., Harris, M., Mitchell, D.C., & Shaikh, S.R. DHA-fluorescent probe is sensitive to membrane order and reveals molecular adaptation of DHA in ordered lipid microdomains. *J Nutr Biochem*. 2013; 24; 188-195.

assays to show low K_d values for unsaturated fatty acids binding with PPARα compared to saturated fatty acids (*147*). However, the use of PUFAs labeled with fluorescent probes to study membrane microdomain organization has remained elusive.

We have established in vitro with EL4 cells and in vivo with B cells that DHA disrupts lipid microdomain size and exerts an ordering effect upon cross-linking GM1 molecules relative to no-crosslinking (*144, 148*). Unexpectedly, while studying membrane organization of B cells, we discovered an n-3 PUFA diet lowered the uptake of a Bodipy fluorophore (*149*). This finding prompted the current study to determine the potential utility of a Bodipy labeled fluorophore as a probe for addressing several unresolved mechanistic questions on how DHA's flexible structure adapts to the formation of ordered lipid microdomains.

The goals of this study were to address the following questions: Does DHA-Bodipy localize to the plasma membrane? Could DHA-Bodipy detect changes in membrane order in cells and in model membranes? If so, could the probe be utilized to provide a potential mechanism by which DHA physically reorients itself within ordered microdomains to increase order? The approach relied on live and fixed cell imaging and time-resolved fluorescence anisotropy methods applied to model membranes (lipid vesicles of controlled composition). The rationale for selecting model membranes was that it is very difficult to study DHA's molecular behavior in ordered and disordered microdomains in cells. The data revealed a mechanistic explanation on how DHA's rotational diffusion and molecular ordering behavior conforms to the ordered lipid microdomain environment.

Materials and Methods

Materials

1-palmitoyl-2-oleoyl-phosphatidylcholine (POPC) and 1-stearoyl-2-docosahexaenoyl-phosphatidylcholine (SDPC) were purchased from Avanti Polar Lipids. Cholesterol (Chol) was purchased from Sigma. 4,4-difluoro-5,7-dimethyl-4-bora-3a,4a-diaza-sindacene-3-docosahexaenoic acid (DHA-Bodipy), Mitotracker, and ER-Tracker were purchased from Invitrogen. DHA-Bodipy was custom synthesized by Invitrogen under stringent conditions to prevent oxidation of the fatty acid. Spectral properties of the probe were determined by adding 1 µL of DHA-Bodipy to 50 µL of phenol-free media in a 96-well flat bottom plate. The excitation and emission peaks were measured using a SpectraMax Gemini (Molecular Devices) and acquired using Softmax Pro software. The collected data were then imported into GraphPad Prism followed by 2-point smoothing analysis.

Cells

EL4 cells were maintained in RPMI 1640 1X media supplemented with 10% heat-inactivated defined fetal bovine serum (Hyclone), 2 mM L-glutamine, and 1% penicillin/streptomycin at 37°C in a 5% CO_2 incubator. Primary $B220^+$ B cells were isolated from the spleens of C57BL/6 mice using methods established previously (*149*).

Imaging

The concentration of DHA-Bodipy was optimized for each cell type and experiment. Splenic B cells were treated with 1.5 µM of DHA-Bodipy in phenol-free RPMI supplemented with 2 mM L-glutamine at 37°C for 1, 10 and 20 minutes. B cells were fixed for 1 hour with 4% paraformaldehyde, washed 3 times with 1X PBS,

mounted on slides in Vitrotubes (Fiber Optic Center, Inc), and imaged using a Zeiss LSM510 confocal microscope (*148*). Live cell imaging experiments were also conducted using a Zeiss LSM510 confocal microscope using stage/objective heaters set at 37°C or 23°C. For co-localization studies, 2.0 x 10^6 EL4 cells at 1.0 x 10^6 cells/mL were treated with 1.3 μM DHA-Bodipy for 24 hours. EL4 cells were counted, washed twice with either Hanks Balanced Salt Solution (HBSS, plus calcium chloride and magnesium chloride) for ER-Tracker staining or RPMI 1640 1X media supplemented with 10% heat-inactivated defined fetal bovine serum (Hyclone), 2 mM L-glutamine, and 1% penicillin/streptomycin (for MitoTracker staining) to remove excess probe. Cells were then re-suspended at 1.0 x 10^6 cells/mL and stained with either 150 nM MitoTracker in RPMI 1640 1X media supplemented with 10% heat-inactivated defined fetal bovine serum (Hyclone), 2 mM L-glutamine, and 1% penicillin/streptomycin, or 2 μM ER-Tracker in HBSS, at 37°C for 30 minutes. Cells were washed twice with phenol-free RPMI with L-glutamine and then placed in a pre-heated petri dish on the stage heater, followed by image acquisition.

The rate of DHA-Bodipy uptake was measured in EL4 cells adhered to Poly-D-lysine coated Delta T dishes (Bioptechs). Delta T dishes were coated with Poly-D-lysine (Sigma) for 15 minutes, rinsed with water and air dried overnight. 1.0 x 10^6 EL4 cells were washed twice with phenol-free RPMI supplemented with 0.5% FBS, 2 mM L-glutamine and resuspended. 1.0 x 10^6 EL4 cells were added to Poly-D-lysine coated dishes and incubated for 30 minutes at 37°C to achieve maximum adherence. Imaging was initiated at 1 minute following addition of 1.5 μM of DHA-Bodipy to Delta T dishes.

Image Analysis

For the plasma membrane and intracellular intensity analysis, following background subtraction, a region of interest (ROI) was drawn around either the plasma membrane or the intracellular region and the intensity was measured for each individual cell. For co-localization analysis, each image was background subtracted and then cropped to a 150 x 150 pixel ROI to analyze each cell individually. Images were then loaded into the NIH ImageJ JACoP plugin, the proper threshold was determined, and Manders coefficients (M1 and M2) were calculated based on the thresholded region (*148, 150*). The rate of DHA-Bodipy uptake was determined by measuring the fluorescence intensity increase over a 25 minute time period at 37°C or 23°C. Fluorescence values were normalized relative to maximal fluorescence intensity.

Preparation of Large Unilamellar Vesicles

Lipid stock solutions with and without added cholesterol were dried from chloroform under a stream of Argon gas, and the resulting phospholipid film was dissolved in cyclohexane. The cyclohexane solution was frozen, then lyophilized for 4 to 5 hours. The resulting powder was dispersed in buffer (10 mM PIPES, 60 mM NaCl, 30 mM KCl, 50 mM DTPA, pH 7.3) and put through 8 to 10 freeze-thaw cycles to form multilamellar vesicles. Large unilamellar vesicles were formed by extrusion 10x through a pair of 0.2 μm membranes using a Lipex extruder (Vancouver, B.C.). All buffers were heavily flushed with argon immediately prior to use, and all preparative procedures involving unsaturated phospholipids were carried out in an argon-filled glove box. Samples for fluorescence measurements were made immediately prior to use by diluting a concentrated vesicle stock solution to 150 μM phospholipid. Total optical

density (vesicle scatter plus absorption) at the wavelength of fluorescence excitation was less than 0.1.

Time-resolved Fluorescence Measurements

Fluorescence lifetime and differential polarization measurements were performed with a Chronos multifrequency cross-correlation phase fluorometer (ISS, Urbana, IL). Excitation at 473 nm was provided by a diode laser. Lifetime and differential polarization data were acquired using decay acquisition software from ISS at 10, 23 and 37°C. Both lifetime and differential polarization measurements were acquired at 15 modulation frequencies logarithmically spaced from 5 to 250 MHz. All lifetime measurements were made with the emission polarizer at an angle of 54.7° relative to the vertically polarized excitation beam and with fluorescein in pH 8.0 buffer in the reference cuvette. For each differential polarization measurement, the instrumental polarization factors were measured, found to be between 1 and 1.05, and the appropriate correction factor applied. Scattered excitation light was removed from the emission beam by a 510 nm highpass filter in the emission beam. At each frequency, data were accumulated until the standard deviations of the phase and modulation ratio were below 0.2° and 0.004, respectively, and these values were used as the standard deviation for the measured phase and modulation ratio in all analysis. Both total intensity decay and differential polarization measurements were repeated at each temperature, with each membrane composition, a minimum of three times.

Analysis of Time Resolved Fluorescence Data

Fluorescence lifetimes were analyzed in terms of a sum of two exponential decays of the form: $I(t) = \alpha 1 \times e^{-t/\tau 1} + \alpha 2 \times e^{-t/\tau 2}$, where a1 and a2 are the fractional

contributions to the intensity decay and t1 and t2 are time constants. To facilitate comparison of fluorescence lifetimes, the intensity-weighted average fluorescence lifetime, <t>, was determined for each sample.

$$< \tau > = \sum_i \frac{\alpha_i \tau_i^2}{\alpha_i \tau_i}$$

Measured polarization-dependent differential phases and modulation ratios for each sample were combined with the measured total intensity decay to yield the anisotropy decay, r(t). Anisotropy decays were analyzed using a sum of two discrete exponential decays of the form:

$$r(t) = (r_o - r_\infty)(\beta_1 \exp(-t/\phi_1) + \beta_2 \exp(-t/\phi_2)) + r_\infty$$

where r_o is the initial fluorescence anisotropy at t=0, r_∞ is the non-decaying anisotropy remaining at the longest time measured in the experiment, φ_i is the ith rotational correlation time and β_i is fractional contribution of the ith component. In order to compare fluorescent probe rotational motion and orientational order we report the average rotational correlation time <φ> and the order parameter S, respectively (*151*).

$$< \phi > = \sum_i \beta_i \phi_i$$

$$S = \sqrt{\frac{r}{r_0}}$$

Statistical Analyses

The reported data are 3-4 independent experiments. Data were analyzed using NIH ImageJ, GraphPad Prism and Excel. All of the data were distributed normally. For analysis of probe organization in model membranes, data were analyzed using a one-

way ANOVA followed by a Bonferroni t test.

Results

Spectral Properties of DHA-Bodipy

The structure of DHA-Bodipy is shown in Figure 2.1A. The fluorophore was not attached on the terminal methyl end of the fatty acid in order to avoid potential artifacts of the fluorophore on the dynamics of the acyl chain. The excitation maximum for the probe was 501 nm and the emission was measured at 515 nm (Fig. 2.1B). The excitation and emission wavelengths were in agreement with the manufacture's reported values and with reported values for other Bodipy fluorophores (*152, 153*).

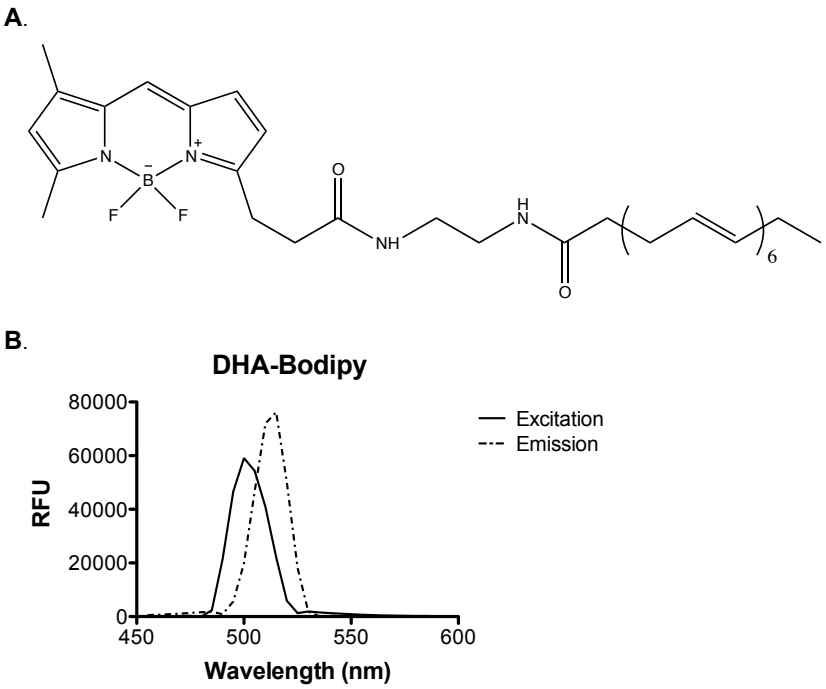

Figure 2.1: Structure and spectral properties of DHA-Bodipy.
(A) Structure of DHA-Bodipy used in this study. (B) Spectral properties of the probe in terms of relative fluorescence units (RFU). The probe was custom synthesized with the fluorophore away from the terminal methyl end in order to avoid any potential effects of the bulky group on the dynamics of the acyl chain, which was the focus of this study. Data in B are representative of 3 individual measurements.

DHA-Bodipy Incorporated into the Plasma Membrane of Primary B cells More Efficiently than EL4 Cells

We first determined if DHA-Bodipy localized into the plasma membrane of primary naïve B cells. This was essential to establish in order to use the probe for addressing questions related to how DHA adapts to ordered lipid microdomains. Cells were treated with DHA-Bodipy for 1, 10, and 20 minutes at 37°C (Fig. 2.2A). Quantitative analysis of fluorescence intensities revealed that DHA-Bodipy incorporated into the plasma membrane (Fig. 2.2B). Over time, the fluorescence intensity increased in the plasma membrane and inside the cell (Fig. 2.2B). However, the ratio of plasma membrane fluorescence intensity to intracellular intensity was relatively constant between 1, 10, and 20 minutes (Fig. 2.2C). Therefore, the cells took up more DHA-Bodipy over time but relatively equal amounts into the plasma membrane and inside the cell.

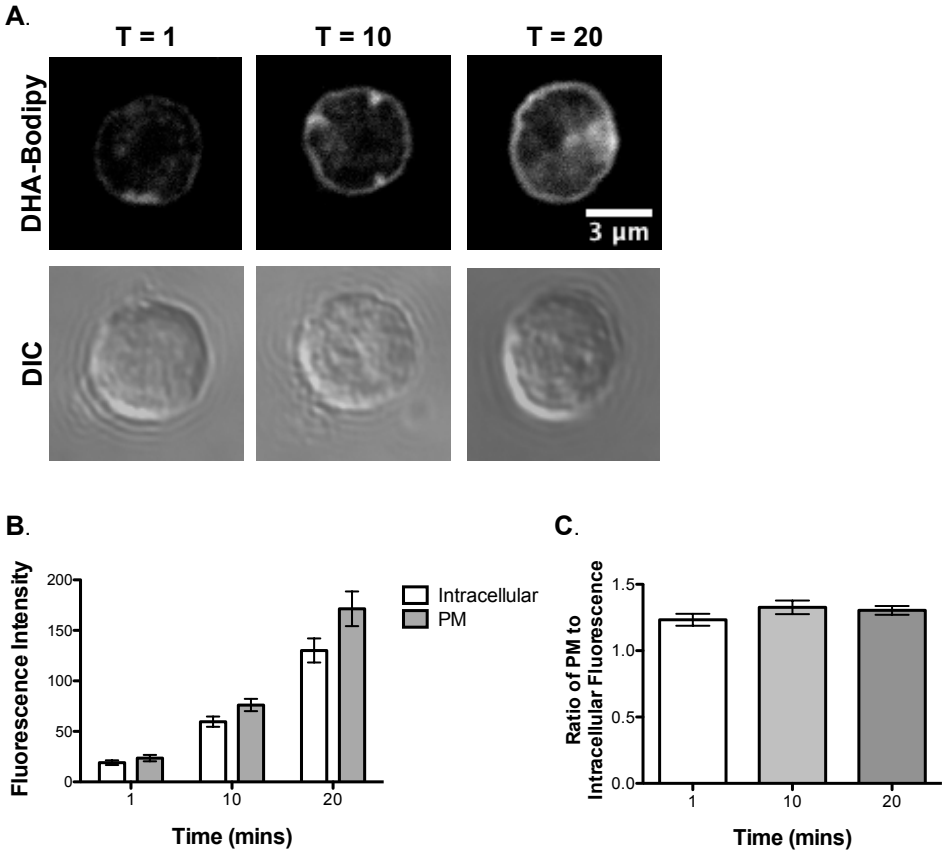

Figure 2.2: DHA-Bodipy incorporates into the plasma membrane of primary B cells.
(A) Sample fluorescent and DIC images of DHA-Bodipy localizing to the plasma membrane (PM) of primary B cells as a function of time at 37°C. (B) Quantification of PM and intracellular DHA-Bodipy total fluorescence intensity as a function of time. (C) Ratio of PM to intracellular DHA-Bodipy fluorescence as a function of time. B cells were stained at 37°C. Data are average ± S.E. from 3 independent experiments.

We next determined if EL4 cells also took up DHA-Bodipy into the plasma membrane. The rationale for selecting EL4 cells was that we have previously used this cell type in several studies to compare our results with B cells (*144, 149*). DHA-Bodipy was rapidly internalized into the cell and showed less staining in the plasma membrane compared to B cells (Supplemental Fig. 1A). We conducted co-localization image analysis to determine where DHA-Bodipy localized to inside the cell after long-term treatment. Co-localization analysis revealed DHA-Bodipy co-localized with the ER

(Supplemental Fig. 1B), with ~ 70% of total DHA-Bodipy co-localizing with the ER according to M2 (Supplemental Fig. 1D), which is the amount of co-localized DHA-Bodipy relative to total DHA-Bodipy present. M1 showed ~80% of ER-Tracker co-localized with DHA-Bodipy compared to the total amount of ER-Tracker staining (Supplemental Fig. 1D). Co-localization between DHA-Bodipy and the MitoTracker were also observed (Supplemental Fig. 1C), revealing ~ 40% of DHA-Bodipy (M2) relative to total DHA-Bodipy exhibiting co-localization (Supplemental Fig. 1E). M1 showed ~70% of MitoTracker co-localized with DHA-Bodipy compared to total MitoTracker present (Supplemental Fig. 1E).

DHA-Bodipy was Sensitive to Membrane Order in Cells and Model Membranes

The subsequent set of experiments addressed if DHA-Bodipy was sensitive to membrane order. Therefore, the rate of DHA-Bodipy uptake was measured in real time at 37°C and 23°C using EL4 cells. EL4 cells were used since they showed rapid uptake of DHA-Bodipy into the cell. The two temperatures were selected since the plasma membrane is highly fluid at 37°C whereas at 23°C the membrane is more ordered (*141*). Figure 2.3A shows the uptake of DHA-Bodipy over time into the cell. Kinetic fitting of fluorescence intensity values revealed the rate of DHA-Bodipy uptake was the same at 37°C and 23°C (data not shown). However, the magnitude of probe uptake was much lower at 23°C relative to 37°C, demonstrating the probe was sensitive to plasma membrane molecular order (Fig. 2.3B).

The DHA-Bodipy was subsequently used to determine if the probe was sensitive to order in model membranes (Fig. 2.3C). The rationale for using model membranes was that we wanted to determine if the probe could provide novel mechanistic

information about DHA in highly disordered and ordered microdomains, which respectively model non-raft and raft-like membranes. Therefore, we used three different types of lipid vesicles that represented highly ordered (POPC/Chol), disordered (POPC) and highly disordered (SDPC) microdomains (*154, 155*). To verify that the probe was sensitive to membrane phase behavior, we measured the stead-state anisotropy in the fluid (37°C) and ordered (23°C) environments, similar to the cell culture studies (Fig. 2.3A,B). Analysis of steady state anisotropies showed that in POPC and POPC/Chol vesicles, anisotropy values were lower at 37°C than 23°C, consistent with more disorder at a higher temperature (Fig. 2.3C). SDPC vesicles showed a similar trend as POPC and POPC/Chol, but the differences between temperatures were smaller. This was probably due to high molecular disorder in SDPC.

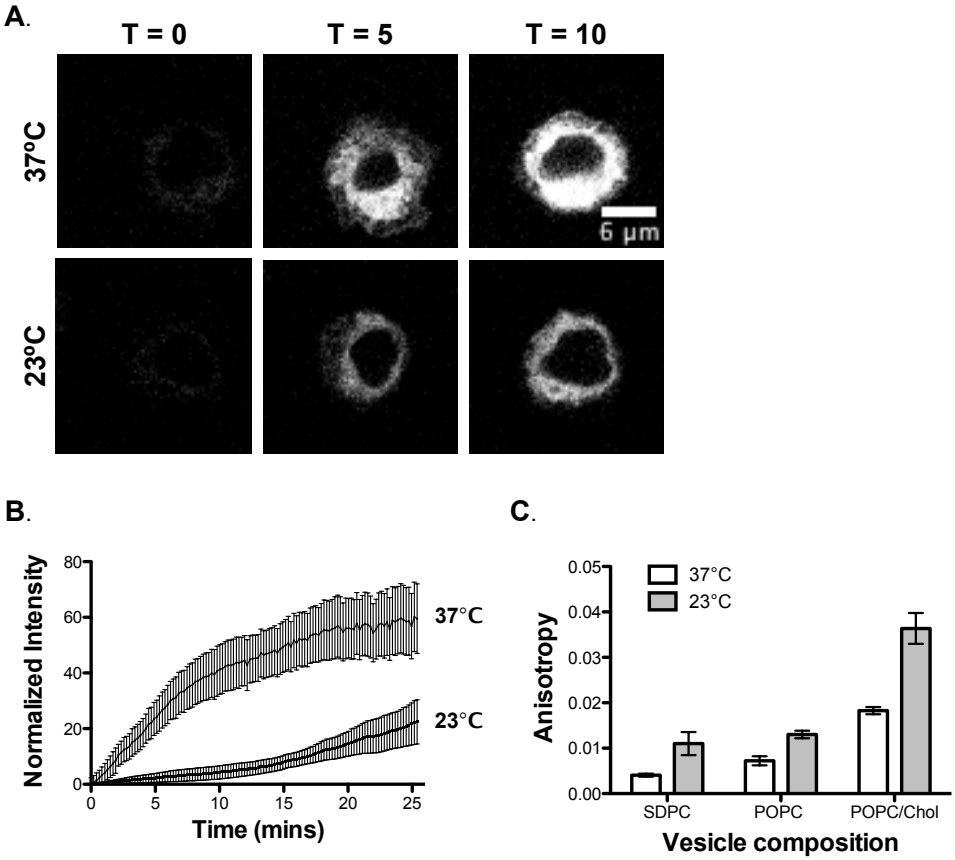

Figure 2.3: DHA-Bodipy is sensitive to membrane order in cells and lipid vesicles. (A) Sample time-lapse images showing uptake of DHA-Bodipy into EL4 cells at 37°C and 23°C upon addition of the probe. (B) Quantification of fluorescent probe uptake as a function of time at 37°C and 23°C. Fluorescence values were normalized to maximal fluorescence. (C) Steady state anisotropy values for SDPC, POPC, and POPC/Chol vesicles at 37°C and 23°C. Data are average ± S.E. from 3-4 independent experiments.

DHA-Bodipy Revealed Novel Molecular Organization in Ordered Lipid Domains

Finally, we used DHA-Bodipy to measure its molecular order and rotational motion in ordered and disordered domains at 37°C, 23°C and 10°C. This question was highly relevant since the mechanism by which the flexible structure of DHA increases the order of lipid microdomains has not been investigated and has remained controversial (*142, 156*). We used SDPC as the control for these studies since this represented the disordered microdomain that contained a PC with DHA.

Fluorescence lifetimes were lowered at all temperatures in POPC vesicles but were higher in POPC/Chol relative to SDPC (Fig. 2.4). This suggested that in the most ordered membrane the DHA-Bodipy had the least interaction with the surrounding water environment. This would be consistent with the DHA fatty acid being lower in the membrane.

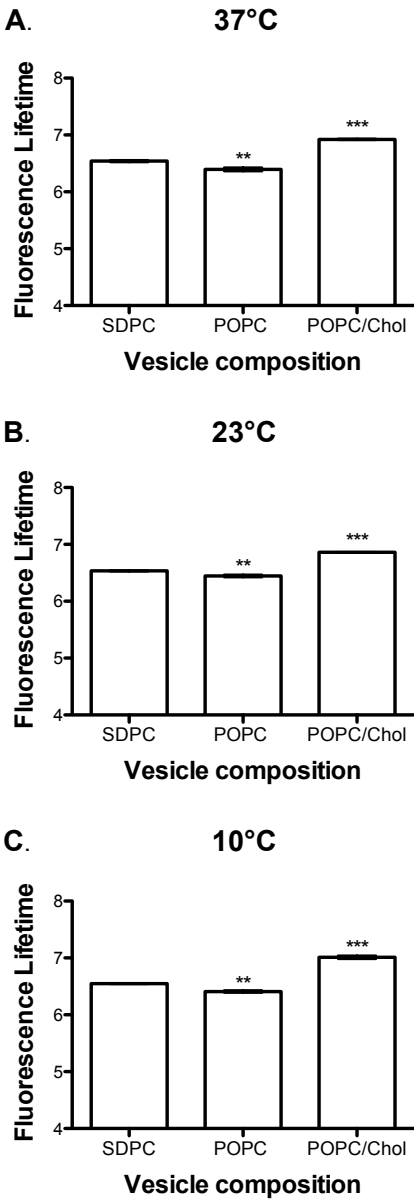

Figure 2.4: DHA-Bodipy has higher fluorescence lifetimes in ordered domains compared to disordered domains.
Fluorescence lifetime of the DHA-Bodipy probe were measured using time-resolved fluorescence anisotropy in lipid vesicles of defined composition at (A) 37°C, (B) 23°C, and (C) 10°C. POPC/Chol, POPC, and SDPC respectively represent highly ordered, disordered, and highly disordered membrane domains. Data are average ± S.E from 3 independent experiments. Asterisks indicate significance from SDPC: **p<0.01, ***p<0.001.

We also measured fluorescence order parameters and rotational correlation times (Fig. 2.5). As the temperature was lowered from 37°C to 10°C, both the order parameters and rotational correlation times increased (Fig. 2.5A-C). The changes in temperature provided an internal control by demonstrating that a decrease in temperature increased the average orientational order and decreased its rate of rotational motion in all three lipid compositions (SDPC, POPC, and POPC/Chol). For most of the temperatures, order parameters and rotational correlation times were increased in POPC vesicles relative to SDPC (Fig. 2.5A-C). For all temperatures, order parameters and rotational correlation times were increased relative to SDPC (Fig. 2.5A-C). The two most robust differences were the high values of the order parameter in POPC/Chol and the fast rotational motion (low rotational correlation time) found in SDPC. This demonstrated that DHA-Bodipy displayed increased order and slower rotational motion in more ordered POPC and highly ordered POPC/Chol membranes relative to SDPC.

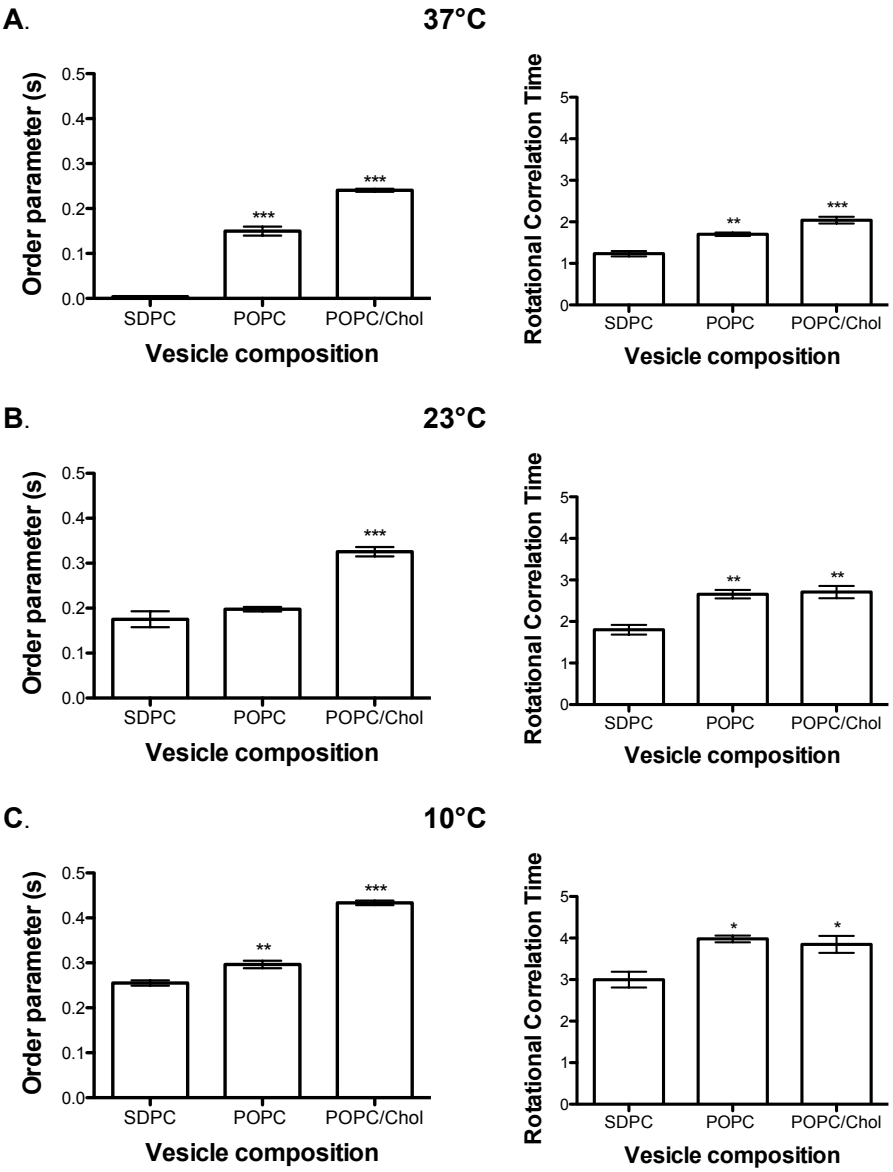

Figure 2.5: DHA-Bodipy displays increased order and decreased rotational diffusion in ordered lipid microdomains.

Order parameters and rotational correlation times for the DHA-Bodipy probe were determined using time-resolved fluorescence anisotropy in lipid vesicles of defined composition at (A) 37°C, (B) 23°C, and (C) 10°C. POPC/Chol, POPC, and SDPC respectively represent highly ordered, disordered, and highly disordered membrane domains. Data are average ± S.E from 3 independent experiments. Asterisks indicate significance from SDPC: *$p<0.05$, **$p<0.01$, $p<0.001$.

Discussion

In this study, we relied on a new DHA-labeled fluorophore to measure uptake into the plasma membrane, sensitivity to membrane order in cells and model membranes, and dynamic organization in model lipid microdomains. The data revealed DHA lowered its rotational diffusion and increased its molecular ordering in an ordered lipid microdomain environment. The results provide novel mechanistic insight on how DHA acyl chains, despite their high degree of conformational flexibility, can increase the molecular order upon the formation of lipid microdomains in vivo.

DHA Incorporation into Naïve B and EL4 Cells

The first set of studies established that DHA-Bodipy, upon short-term treatment, incorporated into the plasma membrane of primary B cells. We ensured the probe was localizing into the plasma membrane and remained in the plasma membrane in primary B cells. We also observed similar effects in experiments with splenocytes (data not shown). Given the structure of the probe, we did not anticipate DHA-Bodipy to become esterified into phospholipids since the fluorophore was located in the headgroup region. We intentionally designed the fluorophore to be localized to the headgroup region rather than the terminal methyl end since we aimed to investigate the molecular motions of the acyl chains. One alternative possibility was to place the Bodipy on a PE headgroup; however, this probe could have been difficult to study since DHA-containing PEs can form inverted hexagonal phase (*154*). Overall, our results were consistent with our previous study in which we showed another Bodipy probe could localize to the plasma membrane (*157*).

In EL4 cells, the DHA-Bodipy probe did not show efficient localization into the plasma membrane upon short-term treatment. This showed that the probe's behavior was cell type dependent. This is consistent with studies, including our own, that have demonstrated differences between primary and immortal cell types (*149*). The finding that DHA-Bodipy, upon long-term treatment, localized into endomembranes was consistent with previous studies with palmitic acid-labeled Bodipy (PA-Bodipy). For instance, Thumser and Storch showed that PA-Bodipy did not esterify into membrane phospholipids in Caco-2 cells but the probe did report identically to an endogenous palmitic acid (*152*). Furthermore, they also showed the probe co-localized with endomembranes and the fatty acid-binding protein (*152*). To ensure our methods did not confound our results, we also conducted select studies with PA-Bodipy and indeed found very similar results to those reported by Thumser and Storch (data not shown). It is important to note that our study was the first, to the best of our knowledge, to study a DHA-labeled Bodipy fluorophore.

The long-term treatment studies with DHA-Bodipy highlighted a potential new area of investigation, that is, the ability of DHA to target intracellular membrane organization. The data raised the possibility that some fraction of DHA localizes in some cell types into the ER and mitochondrial membranes, where it is plausible that the fatty acid exerts it effects on membrane organization and function (*158*). Some studies do show that DHA can manipulate membrane viscosity of the mitochondrial membrane but have not provided mechanistic details (*159*). It is conceivable that DHA could be targeting mitochondrial membrane protein clustering and thereby bioenergetics, which

has consequences for ATP production via the electron transport chain (*158*). We aim to pursue how DHA targets endomembrane organization in the future.

DHA's Flexible Structure Adapts to the Ordered Nature of Lipid Microdomains

The next set of experiments specifically addressed if DHA-Bodipy was sensitive to membrane order in cells and model membranes. These experiments were essential in order to determine if DHA-Bodipy could be used to study its dynamics within ordered lipid microdomains. Indeed, DHA-Bodipy was sensitive to membrane order as uptake of the probe into EL4 cells was lowered in an ordered environment, created by lowering the temperature to 23°C. Several models of fatty acid uptake, which are not entirely in agreement, have been proposed for long chain fatty acids (*160, 161*). These models include free diffusion of fatty acids or uptake mediated by specific proteins such as fatty acid binding proteins. In the future, we aim to use this probe to study the transport of DHA into varying cell types.

The data on membrane order provided novel insight about our previous studies. We previously reported that a high dose of n-3 PUFAs administered to mice prevented the short-term uptake of PA-Bodipy into B cells, relative to a control diet (*149*). Our data here implied that a reduction in uptake could take place in response to an increase in membrane molecular order. Thus, we speculate that n-3 PUFAs in vivo, upon formation of lipid microdomains, may be increasing their molecular order, perhaps by some interactions with cholesterol (*144, 162-164*). This would be highly consistent with data to show that n-3 PUFAs increased the molecular order of rafts on the $CD4^+$ T cell side of the immunological synapse (*165*) or increased membrane order, as we demonstrated, upon cross-linking GM1 microdomains of B cells (*144*).

Lipid vesicles of defined composition were employed to further study if the probe was sensitive to highly ordered (POPC/Chol), disordered (POPC) and highly disordered (SDPC) domains (*154, 155, 166, 167*). These studies demonstrated that the probe was indeed sensitive to molecular order in model membranes, which was evident from changes in temperature and changes in lipid composition.

The time-resolved anisotropy results revealed new mechanistic insight into how DHA behaved when interacting with ordered microdomains. Specifically, we discovered that DHA-Bodipy became ordered in POPC and POPC/Chol vesicles relative to SDPC. This provided evidence that DHA acyl chains, albeit highly disordered, can adapt and interact with ordered lipid microdomains and in fact, can undergo an increase in molecular order inside an ordered domain (*142*). While some biochemical and biophysical studies show that DHA prefers to avoid interactions with cholesterol (*143*), our data suggest that when forced into a raft-like ordered environment, the acyl chain surprisingly is capable of adapting to this environment, which will impact the clustering and activity of surrounding proteins (*142*). Our data are also consistent with a recent study to show that cholesterol could increase the order of DHA esterified to PCs (*164*). This helps explain how n-3 PUFAs in vivo appear to make rafts larger and more ordered (*149, 165*).

There are many important questions that remain unanswered about the mechanistic relationship between DHA and ordered domains that could be addressed in the future with this DHA-labeled fluorophore. For simplicity, we present two examples. One, it is conceivable that DHA's initial uptake through the membrane as a fatty acid could selectively manipulate the organization of membrane microdomains, clustering of

proteins, and/or lateral diffusion of membrane molecules. Second, the existing environment itself could influence the uptake of DHA into the membrane. For example, macrophages that are deficient in the cholesterol transporter ATP-binding cassette transporter 1 (ABCA1) have larger lipid rafts due to increased accumulation of cholesterol (*168, 169*). This increase in molecular order of the plasma membrane would then have an impact on the uptake of fatty acids into the cell including DHA. Thus, the order of the membrane itself would influence the uptake kinetics of DHA and could limit bioavailability of the fatty acid for the cell.

Summary

We have demonstrated for the first time that a new DHA-Bodipy was sensitive to membrane order in both cells and lipid vesicles of defined composition. We then discovered that the highly flexible structure of DHA adapted within ordered lipid microdomains by increasing its molecular order and lowering its rotational diffusion. This now explains mechanistically how DHA can increase lipid microdomain molecular order in vivo.

CHAPTER 3 : DENDRITIC CELL ACTIVATION, PHAGOCYTOSIS, AND CD69 EXPRESSION ON COGNATE T CELLS ARE SUPPRESSED BY N-3 LONG CHAIN POLYUNSATURATED FATTY ACIDS[2]

Introduction

The n-3 long chain polyunsaturated fatty acids (LCPUFAs) EPA and DHA are bioactive molecules found in fish oil, which can suppress some symptoms associated with acute and chronic inflammation (*83, 170-172*). Given that a variety of disease states are characterized by inflammation, n-3 LCPUFAs may have clinical applications for either supplementing or even replacing current pharmacological treatments (*173*). In order to effectively develop n-3 LCPUFAs for clinical use, it is essential to determine the cell specific effects of these fatty acids.

Currently, we know that n-3 LCPUFAs regulate T lymphocyte function in animal models(*174-179*). For example, murine *ex vivo* $CD4^+$ T lymphocyte activation into a classically defined Th1 phenotype by hybridomas or CD3/CD28 antibodies is robustly suppressed by n-3 LCPUFAs, as measured by cytokine secretion and proliferation (*165, 180*). Recently, we demonstrated that n-3 LCPUFAs in fish oil suppressed *ex vivo* murine B lymphocyte stimulation of cognate naïve $CD4^+$ T cells (*144*). We also showed that n-3 LCPUFAs were not globally immunosuppressive, as murine B lymphocyte activation was enhanced at several doses in response to the T-independent antigen LPS (*144, 181*). Our results demonstrated that n-3 LCPUFAs could exhibit differential effects within a single cell type depending on the antigen and the functional endpoint

[2] This research was originally published in Immunology. Teague, H., Rockett, B.D., Harris, M., Brown, D.A., & Shaikh, S.R. Dendritic cell activation, phagocytosis and CD69 expression on cognate T cells are suppressed by n-3 long-chain polyunsaturated fatty acids. *Immunology* 2013; 139; 386-394. © 2013 John Wiley & Sons Ltd.

(*144, 181*). Less is known about the effects of fish oil on other cell types. In this study, we addressed the effects of n-3 LCPUFAs on DCs, a cell type not well studied at the animal level with fish oil.

DCs are the most potent antigen presenting cells and responsible for activating T lymphocytes (*182*). In addition, DCs are scavenger cells, constantly surveying tissues for the presence of a pathogen. Compared to T lymphocytes, DCs are directly activated upon pathogen recognition. However, data addressing how pharmacologically relevant doses of fish oil regulate DC function are limited. The majority of studies with n-3 LCPUFAs and DCs have relied on bone marrow derived cells, which require an *in vitro* model system for experimentation with a lengthy culture period for maturation (*130-132, 183*). Generally, these studies have revealed that EPA and DHA administration robustly suppresses DC maturation and T cell stimulation. In this study, we focused on splenic $CD11c^+$ DCs, which circumvented the need for long-term cell culture.

The first goal of this study was to test the hypothesis that n-3 LCPUFAs would suppress DC function, as predicted by *in vitro* studies.(*130-132, 183*) We investigated three major components of DC function: DC activation upon LPS stimulation, phagocytosis of *E. coli* bioparticles and stimulation of naïve $CD4^+$ T cells. Each assay revealed an element of DC function was suppressed. The second goal was to determine if the immunosuppressive effects of fish oil were mechanistically associated with a re-organization in plasma membrane lipid microdomain spatial distribution and membrane microviscosity (i.e. order) as shown for T and B lymphocytes by our laboratory and others (*144, 148, 149, 184, 185*). We addressed this objective by utilizing quantitative imaging to assay for select changes in membrane microdomain

organization and membrane order. Unlike studies in lymphocytes, we show DC GM1 lipid microdomain clustering and membrane microviscosity were not changed with n-3 LCPUFA intervention.

Materials and Methods

Mice

Male C57BL/6 mice (Charles River) were fed a purified control diet or a fish oil diet (Harlan-Teklad) for 3 weeks, as described previously (*144*). Both diets contained identical ingredients with the exception of the fatty acid source (soybean oil vs. fish oil). The fish oil diet contained approximately 2% of the total kcal from EPA and 1.3% from DHA, which translates to approximately 4 grams of fish oil of high purity consumed by a human on a daily basis (*186*). This pharmacological dose is currently used clinically (e.g. Lovaza) for the treatment of elevated triglycerides and in clinical trials (*187, 188*). Mice immolation was carried out via CO_2 inhalation followed by cervical dislocation. All experiments with mice received prior approval from the Institutional Animal Care and Use Committee at East Carolina University.

Cell Isolation

$CD11c^+$ DCs were purified from splenocytes with a positive selection microbead kit (Miltenyi Biotec). Briefly, isolated spleens were incubated in collagenase D solution (1.4 mg/ml) for 30 minutes at 37°C in a 5% CO_2 incubator. Spleens were then homogenized and red blood cells lysed. DCs were labeled with $CD11c^+$ microbeads following the manufacturer's recommended protocol and >90% DC purity was obtained by sequentially separating cells through two LS columns (*189-191*). $CD4^+$ T cells (> 85% purity) were purified from B6.Cg-Tg(TcraTcrb)425Cbn/J mice (OT-II) (Jackson

Laboratory) via negative selection following the manufacturer's suggested protocol with minor modifications (Miltenyi Biotec). The splenocytes were incubated on a rotator in the $CD4^+$ Biotin cocktail for 30 minutes at 4°C. The anti-Biotin incubation step was also completed on a rotator and separations through two LS columns were required to achieve maximum purity. OT-II transgenic mice were chosen for this assay due to an increased ratio of $CD4^+$ T cells to $CD8^+$ T cells and the ability of the T cell receptor to specifically recognize chicken ovalbumin (OVA 323-339, Genscript) presented by H-2 IA^b molecules.

LPS Stimulation

DCs were stimulated with 2 µg/mL of LPS and incubated for 24 hours in RPMI 1640 1X media (Mediatech) supplemented with 5% heat-inactivated defined fetal bovine serum (FBS) (Hyclone), 2 mM L-glutamine, and 1% penicillin/streptomycin at 37°C in a 5% CO_2 incubator. The concentration of LPS utilized to stimulate splenic DCs was optimized to ensure high expression of costimulatory molecules. The supernatants were collected and the secreted cytokine profiles were measured utilizing an ELISA MAX kit (BioLegend) following the manufacturer's suggested protocol. DC activation was determined by measuring the surface expression of activation markers using fluorescently labeled anti-CD80 16-10A1 (Bio X Cell), anti-MHC class II M5/114.15 (Bio X Cell), and anti-CD11c (Miltenyi Biotec) via a BD LSR II flow cytometer (BD Biosciences). MHC class II and CD80 antibodies were conjugated to fluorophores utilizing an antibody conjugation kit (GE Healthcare).

Phagocytosis Assay

5×10^5 cells were transferred to FACS tubes and washed once in HBSS at 4°C.

DCs were treated with fluorescein conjugated *E. coli* Bioparticles (Invitrogen) for 2 hours at a 1:9-1:11 DC to *E. coli* bioparticle ratio at 37°C and 4°C as the control. Following the 2 hour incubation period, DCs were placed at 4°C to terminate phagocytosis. DCs were washed once with 1X PBS and treated with 1 mg/ml of trypan blue (Invitrogen) for 2 minutes at 4°C to quench extracellular fluorescence (*192*). DCs were then washed 2 times with 1X PBS and phagocytosis was determined by mean fluorescence intensity (MFI) via flow cytometry. The number of bioparticles per experiment was held constant; however, there was some variation in the number of bioparticles between experiments. Therefore, the data required normalized to account for the variation between experiments.

Antigen Presentation

DCs were combined with T cells at a 1:3 ratio (1 x 10^5 DCs to 3 x 10^5 $CD4^+$ T cells) in a 96 well plate. DCs were treated with 10^{-5} M OVA 323-339 (Genscript) as previously described (*144*). The concentration of OVA was optimized for maximum $CD4^+$ T cell activation. Cells were incubated for 24 hours in RPMI 1640 1X media. The supernatants were collected for IL-2 and interferon (IFN) γ analysis via a Multi-Analyte ELISArray kit (SABiosciences) according to manufacturer's protocol. The reported absorbance values for IL-2 and IFNγ correspond respectively to ~ 420 and ~ 60 pg/ml. $CD4^+$ T cell activation was determined by gating on $CD4^+$ cells and measuring the surface expression of CD69 and CD25. Cells were labeled with anti-CD4-PE (Miltenyi Biotech), anti-CD69-FITC (BD Biosciences), and anti-CD25-APC (BD Biosciences) and assayed via flow cytometry on a BD LSR II (BD Biosciences). SYTOX Blue (Invitrogen) was utilized in all flow cytometry experiments to differentiate between live and dead cells.

Control experiments were conducted with DCs and T cells alone to ensure $CD4^+$ T cell activation was due to interactions between the two cell types.

Lipid Microdomain Staining and Image Analysis

DCs were labeled with cholera-toxin subunit B-FITC (Invitrogen) for GM1 molecules and then cross-linked with anti-cholera-toxin to induce clustering. The cells were fixed in 4% paraformaldehyde. Imaging of lipid microdomains was conducted with a Zeiss LSM510 confocal microscope and analyzed as previously described (*148*).

Microviscosity Studies and Analysis

DCs were incubated with 4 μM di-4-ANEPPDHQ (Invitrogen) for 30 minutes at 4°C followed by fixation for 1 hour in 4% paraformaldehyde on ice. DCs were washed 3 times in 1X PBS and loaded into vitrotubes for imaging. Images were acquired on an Olympus Fluoview FV1000 with an excitation at 488 nm with an argon laser. Instrument settings entailed a SM560 beam splitter equipped with two bandwidth filters between 535-565 nm in channel 1 and 565-675 nm in channel 2. Generalized polarization (GP) values were calculated by measuring the fluorescence intensity (MFI) in each channel as previously reported (*144, 193*).

Fatty Acid Analysis

Total fatty acids were extracted utilizing the Folch method (*194*). The rationale for isolating total fatty acids, as opposed to plasma membrane fatty acids, was that very large quantities of DCs ($>1x10^8$) were required, which was not feasible given the low abundance of DCs in the spleen. Fatty acids were separated on a capillary gas chromatography (GC, Shimadzu Scientific Instruments) with a Restek RT-2560 column as previously described (*181*). Peaks were identified by their retention times relative to

standards (Restek) and are expressed as the percent of total peak area for a given treatment.

Statistical Analysis

Data are presented as mean ± SEM. All data are from several independent experiments. Statistical significance was established using a two-tailed unpaired student's t test with the exception of the phagocytosis assay. MFI normalization required a paired student's t test. *P* values < 0.05 were considered significant.

Results

CD80 Surface Expression and TNFα Production from LPS Stimulated DCs is Lowered by n-3 LCPUFAs

In order to determine the effects of n-3 LCPUFA enriched fish oil on DC activation, splenic DCs were purified and stimulated with the T-independent antigen LPS for 24 hours. The surface expression of co-stimulatory CD80 and MHC class II molecules were measured in both the unstimulated (- LPS) and stimulated (+LPS) states (Fig. 3.1A). MHC class II surface expression did not change with n-3 LCPUFA relative to the control (Fig. 3.1A). In the absence of LPS stimulation, n-3 LCPUFA lowered CD80 surface expression by 28% (Fig. 3.1B); in addition, LPS stimulation showed a decrease in CD80 surface expression by 14% (Fig. 3.1B) with fish oil. The levels of TNFα, IL-10, IL-6, IL12p40 and transforming growth factor (TGF) β were also measured (Fig. 3.1C). Quantification of cytokine secretion revealed TNFα production was decreased by 29% with n-3 LCPUFA (Fig. 3.1D). IL-10, IL-12p40, IL-6 and TGFβ secretion were unaffected by n-3 LCPUFA (Fig. 3.1D).

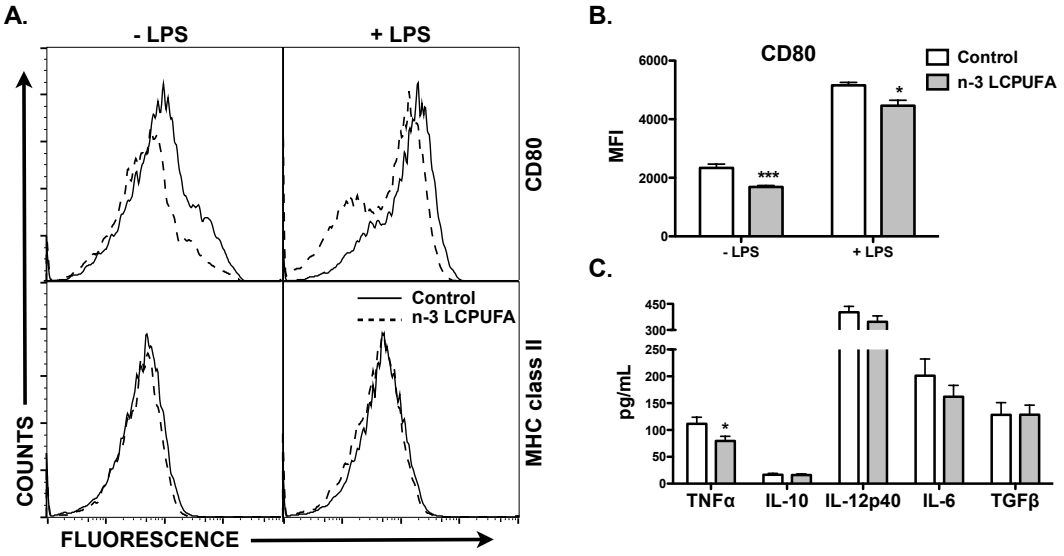

Figure 3.1: CD80 surface expression and TNFα secretion from LPS stimulated DCs is lowered with n-3 LCPUFAs.
DCs were isolated from C57BL/6 mice consuming a control or n-3 LCPUFA diet and stimulated for 24 hours with LPS. (A) Sample flow cytometry histograms of CD80 and MHC class II. (B) The mean fluorescence intensity (MFI) of CD80 in the absence and presence of LPS stimulation (C) TNFα, IL-10, IL-12p40, IL-6 and TGFβ cytokine secretion was measured after 24 hours of LPS stimulation. Data are from 6-10 independent experiments. Asterisks indicate significance from control: *p<0.05, ***p<0.001.

CD11c$^+$ Surface Expression and Uptake of *E. coli* Bioparticles by DCs is Suppressed with n-3 LCPUFAs

Immediately following DC purification, we measured a 12% decrease in the surface expression of CD11c, a key marker involved in phagocytosis, with the n-3 LCPUFA diet (Fig. 3.2A) (*195, 196*). Therefore, we assessed if phagocytosis was reduced by quantifying DC uptake of fluorescently labeled opsonized *E. coli* bioparticles at 37°C and 4°C (Fig. 3.2B). The 4°C control was required to ensure measured fluorescence was a result of phagocytized bioparticles as opposed to *E. coli* bioparticles bound to the cell surface. We discovered the percentage of DCs engulfing *E. coil* bioparticles did not change (data not shown); however, the amount of *E. coli* bioparticles taken up was lowered by 12% (Fig. 3.2C). The data in Figure 3.2C were normalized to

account for slight variations in the number of bioparticles used between experiments. Raw MFI values ranged from ~3200-4200 but showed a consistent decrease with fish oil in each experiment.

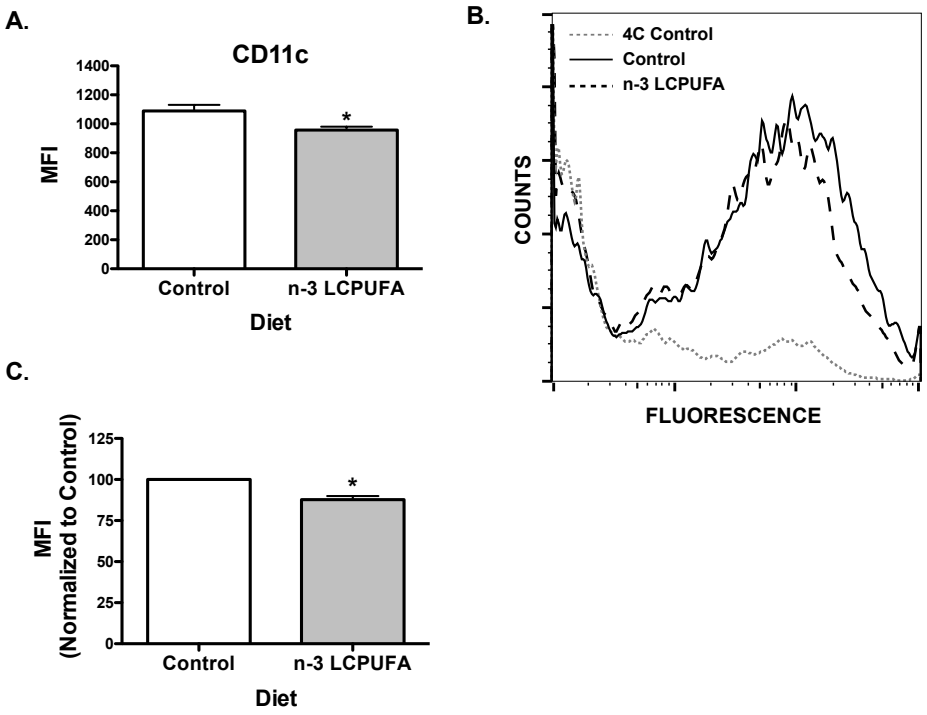

Figure 3.2: DC CD11c$^+$ surface expression and phagocytosis are suppressed by n-3 LCPUFAs.
(A) The surface expression of CD11c on DCs isolated from C57BL/6 mice consuming a control or n-3 LCPUFA diet. (B) Sample flow cytometry histograms of fluorescence uptake of *E. coli* bioparticles. (C) The amount of *E. coli* bioparticles taken up as indicated by the mean fluorescence intensity (MFI). MFI was normalized due to a slight variation in the number of bioparticles administered to the cells between experiments. Data are from 6-8 independent experiments in A and 4 for B-C. Asterisk indicates significance from control: *$p<0.05$.

CD69 Surface Expression on the Surface of CD4$^+$ T cells Was Lowered with n-3 LCPUFAs Upon DC Stimulation

DCs are the most potent antigen presenting cells, which activate naïve T cells. Therefore, we determined if n-3 LCPUFAs suppressed the ability of DCs to present antigen to CD4$^+$ T cells. We first optimized activation of naïve T cells as a function of peptide dose and discovered that 10^{-5} M peptide provided the most robust response

(data not shown). We measured the surface expression of CD69 and CD25 on the surface of activated $CD4^+$ T cells after 24 hours of stimulation (Fig. 3.3A). The percentage of $CD69^+$ T cells remained unchanged (data not shown); however, CD69 surface expression was decreased by 22% with n-3 LCPUFAs relative to the control diet (Fig. 3.3B). No change was observed in CD25 surface expression (Fig. 3.3B). IL-2 and IFNγ cytokine secretion between the control and experimental diet were equivalent (Fig. 3.3C). We also conducted select experiments at 48 hours of T cell stimulation and measured no differences in the Th2 cytokines IL-4 and IL-5 in response to n-3 LCPUFA (data not shown).

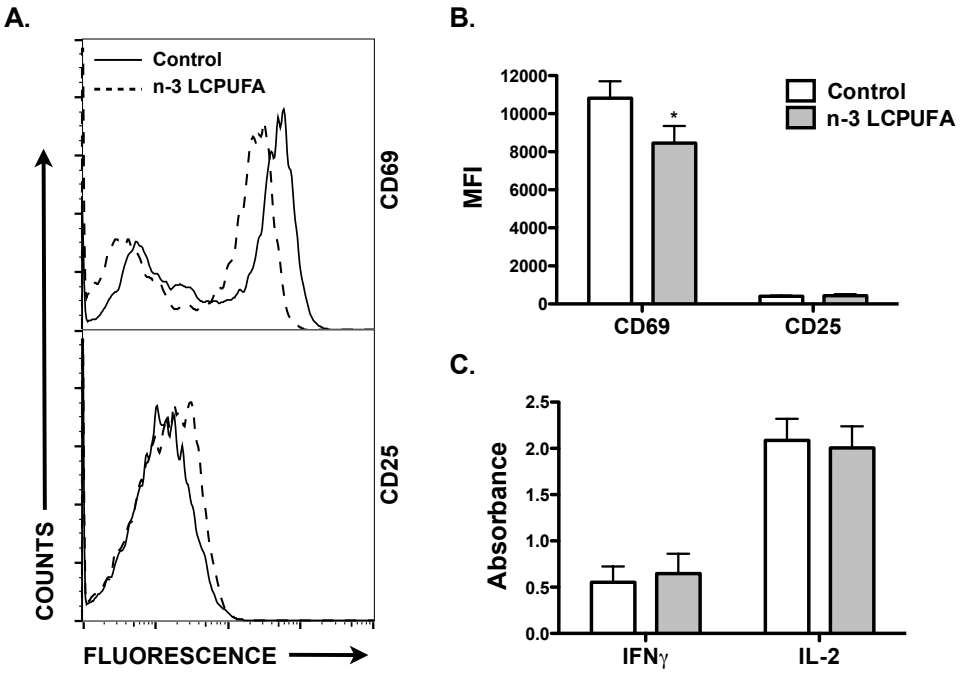

Figure 3.3: CD69 expression on $CD4^+$ T cells is lowered upon stimulation with DCs isolated from mice fed n-3 LCPUFAs.
DCs were isolated from C57BL/6mice consuming a control or n-3 LCPUFA diet and incubated with naïve $CD4^+$ T cells isolated from transgenic mice for 24 hours. T cell activation was measured by (A) CD69 and CD25 surface expression and (B) quantitated in terms of mean fluorescence intensities (MFI). (C) IL-2 and IFNγ secretion were measured with ELISAs. Data are from 7 independent experiments. Asterisk indicates significance from control: *$p<0.05$.

Lipid Microdomain GM1 Clustering and Membrane Microviscosity on the Surface of DCs is not Influenced by n-3 LCPUFAs Despite Increased Levels of EPA and DHA.

We and others have previously reported that fish oil mechanistically targets B and T lymphocyte activation and/or antigen presentation by disrupting the clustering of lipid microdomains (*144, 174-176*). To investigate if the changes in DC function were dependent on the underlying lipid microdomain organization, we measured changes in GM1 microdomain clustering with n-3 LCPUFA intervention (Fig. 3.4A). Image analysis revealed there were no differences in the distribution of size of the lipid microdomains between control and n-3 LCPUFA diets (Fig. 3.4B). In addition, when analyzing the percentage of cells exhibiting clustered lipid microdomains, we observed no distinction between control and n-3 LCPUFA (data not shown).

We next determined if there was a decrease in DC microviscosity (i.e. increase in fluidity) with n-3 LCPUFAs. Imaging studies with the polarity sensitive membrane dye di-4-ANEPPDHQ revealed there was an increase in di-4-ANEPPDHQ uptake with fish oil intervention as indicated by increased fluorescence intensity in both channel 1 (535-565 nm) by 23% and channel 2 (565-675 nm) by ~21% (Fig. 3.4C). However, the calculated GP values showed no change between the control and n-3 LCPUFA diets (Fig. 3.4D).

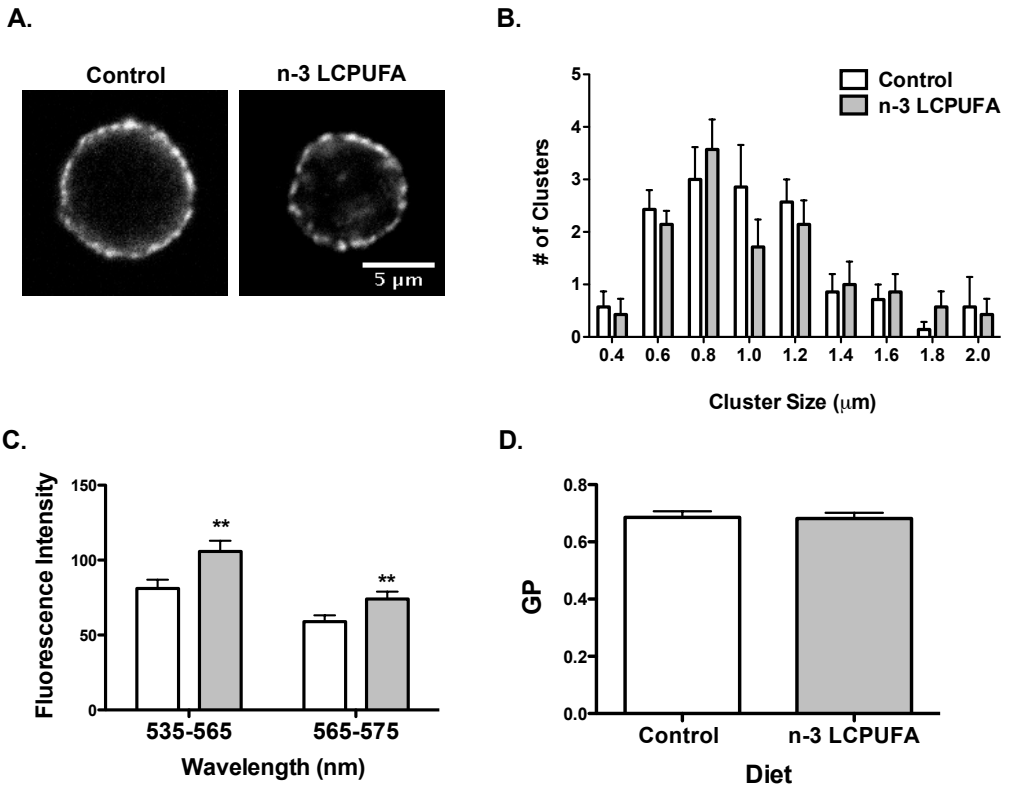

Figure 3.4: DC GM1 lipid microdomain clustering and membrane microviscosity are not influenced by n-3 LCPUFAs.
DCs were isolated from C57BL/6 mice consuming either a control or n-3 LCPUFA diet. (A) Confocal images of cholera toxin-induced lipid microdomains and the (B) distribution of microdomain size measured in terms of Feret's diameter. (C) Fluorescence intensity of di-4-ANEPPDHQ measured in the 535-565 nm and 565-675 nm channels. (D) Generalized polarization (GP) of di-4-ANEPPDHQ. Data are from 6-8 independent experiments. Asterisks indicate significance from control: **p<0.01.

Finally, we measured the total fatty acid content of DCs to determine if there was an increase in the amount of EPA and DHA with the fish oil diet (Fig. 3.5A). Palmitoleic (16:1), EPA (20:5), docosapentaenoic acid (22:5 n-3) and DHA (22:6) all increased with n-3 LCPUFA enriched diet (Fig. 3.5A). Interestingly, we did not observe a change in palmitic acid (16:0) between control and fish oil, as seen previously with B lymphocytes (Figure 5A)(*144*). We observed a decrease in oleic acid (OA,18:1), linoleic acid (18:2) and AA (20:4) (Fig. 3.5A) with n-3 LCPUFA relative to the control. There was no change

in the total levels of saturated (SFA) and monounsaturated (MUFA) fatty acids (Fig. 3.5B). A decrease in total n-6 PUFAs concomitant with an increase in total n-3 PUFAs were measured with DCs from the n-3 LCPUFA diet relative to controls, lowering the n-6/n-3 ratio (Fig. 3.5B).

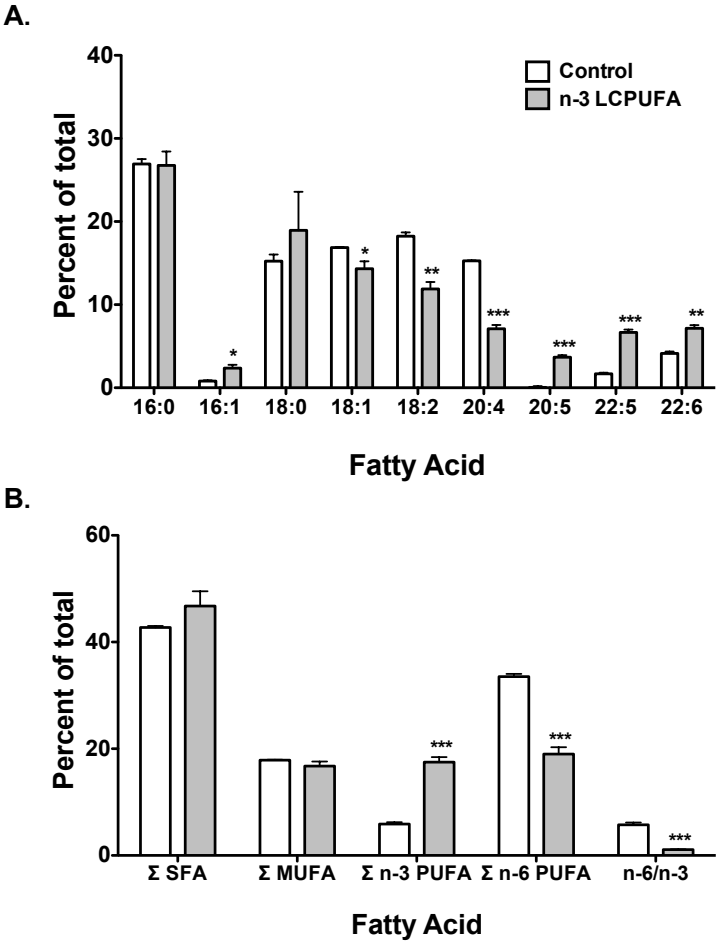

Figure 3.5: DC EPA and DHA levels are increased in response to a diet enriched in n-3 LCPUFAs.
(A) Fatty acid composition of DCs isolated from mice fed control and n-3 LCPUFA diets. (B) The total saturated fatty acid (SFA), monounsaturated fatty acid (MUFA), n-3 PUFA, n-6 PUFA and n-6:n-3 ratio. Data are from 3 independent experiments. Asterisks indicate significance from control: *p<0.05, **p<0.01, ***p<0.001.

Discussion

This study tested the hypothesis that n-3 LCPUFA-enriched fish oil would suppress DC function, as reported with *in vitro* studies. First, the data showed select costimulatory molecule and cytokine secretion was reduced with fish oil supplementation. Second, n-3 LCPUFA lowered CD11c expression and phagocytosis. Third, n-3 LCPUFAs lowered surface expression of a T cell activation marker. Finally, we demonstrated the observed changes were independent of GM1 microdomain clustering and membrane microviscosity.

N-3 LCPUFAs and DC Activation

CD80 is a costimulatory molecule on the surface of DCs involved in T cell activation. CD80 upregulation serves as a measure of DC maturation subsequent to antigen stimulation. In this study, n-3 LCPUFAs decreased the surface expression of CD80 in both the un-stimulated and LPS stimulated states. In addition, n-3 LCPUFAs lowered the amount of TNFα produced by the DCs. Overall, these findings are in agreement with several *in vitro* studies. For example, Wang et al. showed treatment of DCs, produced from culturing peripheral blood human monocytes, with 50 μM EPA or DHA resulted in decreased CD80 and HLA-DR expression, as well as TNFα and IL-12p70 production, following LPS stimulation (*133*). We did not measure a change in MHC class II surface expression. A few differences exist between our work and that of Wang et al (*133*). First, the DCs between the studies were derived from different tissues. Second, with the *in vitro* study, the cells were treated with the single fatty acids, EPA or DHA, compared to our study where fish oil contained a mixture of fatty acids including EPA and DHA.

An investigation by Zeyda et al. also reported similar findings, where 20 μM EPA treatment decreased CD80 expression and TNFα and IL-12p40 production from DCs differentiated from human peripheral blood monocytes after 48 hours of LPS stimulation (*183*). We utilized a 24-hour incubation period to ensure the effects of n-3 LCPUFA supplementation were not lost in the culture conditions, as previously reported (*181*). An additional study with LDL receptor knockout mice by Nakajima et al. also showed EPA suppressed DC maturation, lowering CD80, CD86 and CD40 surface expression on DCs (*197*). A study by Monk et al. compared cytokine secretion from LPS stimulated DCs isolated from *Fat-1* transgenic to wild type mice (*177*). Our data were not in complete agreement with Monk et al. They reported that following 24 hours of LPS stimulation, they observed an increase in IL-10, a decrease in TGF-β1 and IL-12p40 and no change in TNFα or IL-6 secretion. The differences between our study and their could be due to the concentration of LPS used (we relied on 2 μg/ml vs. 10 μg/ml) or the different mouse strains. Additional studies on bone marrow derived DCs from Zapata-Gonzalez et al. showed a down regulation of costimulatory molecules, decreased cytokine secretion and an upregulation of PPARγ expression in a DHA concentration dependent manner (*198*). Together, these studies suggest n-3 LCPUFAs exert immunosuppressive effects on LPS stimulated DCs in both *in vitro* and *ex vivo* studies, albeit at different magnitudes.

One major limitation of the aforementioned studies, including our own work, is that the studies have relied on *ex vivo* measurements. To address the impact of fish oil on inflammatory responses, future studies will require *in vivo* measurements with appropriate doses of LPS and several rodent models of acute and chronic inflammation.

These are highly relevant given that fish oil's immunosuppressive effects may be beneficial for select inflammatory conditions; yet, pose a significant risk in response to bacterial and/or viral infections. Indeed, Schwerbrock et al., demonstrated that administration of fish oil can decrease mouse survival in response to influenza infection (*199*).

N-3 LCPUFAs and Phagocytosis

CD11c expressed on DCs acts as a receptor for the complement component iC3b and is involved in cell adhesion (*195, 200, 201*). For the first time, we showed CD11c surface expression was reduced with n-3 LCPUFA supplementation. Given that CD11c has been shown to be involved in phagocytosis, we also discovered a reduction in phagocytosis (*195, 196*). These results are not in agreement with an *in vitro* study by Kong et al (*132*). They reported that 50 μM DHA treatment resulted in decreased expression of costimulatory surface markers and cytokine production from bone marrow derived DCs but observed no change in FITC-dextran uptake.

DC Antigen Presentation

Blockage of CD80 on DCs leads to a 24% decrease in naïve $CD4^+$ T lymphocyte activation (*202*). Concomitant with the CD80 reduction, we anticipated antigen presentation to naïve $CD4^+$ T lymphocytes with n-3 LCPUFA modified DCs would also be reduced as reported for rat DCs (*203*). Although we did not observe a change in IL-2 or IFNγ production from the $CD4^+$ T lymphocytes, we did measure a decrease in CD69 surface expression. It is unclear why DCs from fish oil fed mice displayed CD69 surface expression, yet had no impact on CD25 expression or cytokine secretion. Interestingly,

we have made the exact same observation with a lower dose of n-3 LCPUFAs modeling human intake at 2 grams per day (data not shown).

Our data were consistent with a human study by Kew et al. that showed a reduction in CD69 expression on T cells isolated from humans consuming DHA and activated with concanavalin A for 24 hours (*204*). Similar to our study, Kew et al., measured no change in IL-2 or IFNγ secretion. In addition, the data were consistent with recent work from our lab that showed B lymphocytes isolated from fish oil fed mice exhibited lowered antigen presentation as measured by decreased IL-2 secretion from $CD4^+$ T lymphocytes (*144*). Suppressing aspects of T cell stimulation with both DCs and B lymphocytes could have an additive effect. This would then contribute toward suppression in $CD4^+$ T lymphocyte activation, likely suppressing Th1 and promoting Th2 immunity.

Membrane Microdomain Organization of DCs

Although we confirmed an increase in EPA and DHA uptake by DCs, we did not observe a change in membrane reorganization based on induced GM1 microdomain formation and microviscosity. Some studies have previously shown that increased levels of EPA and DHA are not always associated with a decrease in membrane order (*141*). Interestingly, we did discover that the uptake of the polarity sensitive dye was increased suggesting that n-3 LCPUFAs could be increasing membrane permeability. Overall, these findings suggest the immunosuppressive effects are occurring independent of changes in lipid microdomain clustering and are possibly a result of events occurring further downstream in the signaling cascade. Our data do not rule out the possibility that fish oil is targeting other key aspects of membrane organization such

as lipid-protein spatio-temporal distribution. For example, it is possible, that fish oil could be targeting TLR4 lateral distribution, as demonstrated *in vitro* (*205*). We did measure TLR4 surface expression and found no difference between the control and n-3 LCPUFA diets (data not shown). DHA could also be preventing the aggregation of TLR4 with its regulatory proteins such as myeloid differentiation factor (MD)-2 or NADH oxidase, which would contribute toward a decrease in downstream gene activation and cytokine secretion (*205*). Our rationale for focusing on GM1 microdomains was to compare the data to recent studies by our group and others showing that fish oil targets lipid microdomain clustering in B and T lymphocytes (*144, 165, 174*).

The data suggest the effects of n-3 LCPUFAs are dependent on the cell type and function. Comparing DCs to B lymphocytes, LPS stimulation leads to opposite effects *ex vivo*. In addition, the effect of n-3 LCPUFAs on lipid microdomain organization and molecular order were vastly different between the cell types. One key difference is that B and T lymphocytes are developed from a common lymphoid progenitor where DCs are developed from a common myeloid progenitor. Both cell types are also morphologically different due to differing functional requirements. DCs are irregularly shaped with protruding dendrites, while B and T lymphocytes are spherical in nature. We speculate that inherit morphological differences could explain how n-3 LCPUFA incorporation into the plasma membrane results in different effects on membrane organization.

Summary

Overall, we show that n-3 LCPUFAs, at a pharmacologically relevant dose, suppress key aspects of splenic DC function. The imaging studies reveal that n-3

LCPUFAs have no effect on DC plasma membrane microdomain clustering and microviscosity. Future studies will be required to understand how n-3 LCPUFAs exert functional effects on varying subsets of DCs, especially *in vivo*, and the underlying mechanisms of action.

CHAPTER 4 : N-3 PUFAS ENHANCE THE FREQUENCY OF MURINE B-CELL SUBSETS AND RESTORE THE IMPAIRMENT OF ANTIBODY PRODUCTION TO A T-INDEPENDENT ANTIGEN IN OBESITY[3]

Introduction

Long chain n-3 PUFAs found in fish oil generally exert immunosuppressive effects and aid in the resolution of inflammation (*206, 207*). Pre-clinical studies show the immunomodulatory properties of n-3 PUFAs have clinical applications (*208*). For instance, n-3 PUFAs can suppress murine adipose inflammation, which has positive effects on the development of insulin resistance (*83*). In comparison, studies in humans remain inconclusive with some reports of potential benefits of n-3 PUFAs in prevention and/or treatment of rheumatoid arthritis (*209*).

One limitation in the clinical implementation of n-3 PUFAs for treating various disease symptoms is that the underlying cellular targets of the fatty acids remain uncertain. Marine n-3 PUFAs are increasingly accepted to suppress cell-mediated immunity in rodent models of health and disease (*210*). In contrast, there is a paucity of data on the immumodulatory effects of n-3 PUFAs on the humoral arm of the immune system. In particular, B cells are key players in generating a humoral immune response. B cells also serve as antigen presenting cells and express pattern recognition receptors to elicit responses in innate immunity (*211, 212*). B cells are broadly categorized as B1 cells, which are predominant in peritoneal cavities, and B2 cells, which are abundant in

[3] This research was originally published in The Journal of Lipid Research. Teague, H., Fhaner, C.J., Harris, M., Duriancik, D.M., Reid, G.E., & Shaikh, S.R. N-3 PUFAs enhance the frequency of murine B-cell subsets and restore the impairment of antibody production to a T-independent antigen. *J Lipid Res*. 2013; 54; 3130-3138. © the American Society for Biochemistry and Molecular Biology.

secondary lymphoid tissues including the spleen and lymph nodes (*213*). B1 and B2 cells can be further categorized into various subsets including, but not limited to B1a, B1b, transitional, pre-marginal zone, marginal zone, pre-follicular, follicular, regulatory B10, and newly identified GM-CSF secreting innate response activator B cells (*212-214*). To date, no laboratory has tested the role of n-3 PUFAs in impacting the phenotype of differing B-cell subsets and antibody production to a T-independent antigen, particularly *in vivo*.

We previously reported that n-3 PUFA administration to C57BL/6 mice at high doses enhanced B-cell activation upon *ex vivo* stimulation with LPS, a T-independent antigen (*215*). While these findings challenged the dogma that n-3 PUFAs were immunosuppressive, we attributed these results to the use of a high dose of n-3 PUFAs (*216*). Subsequent studies in C57BL/6 and SMAD3$^{-/-}$ mice consuming lower doses of n-3 PUFAs showed the same effect; that is, n-3 PUFAs exerted an immune enhancing effect on *ex vivo* B-cell activation with LPS stimulation (*217, 218*). Therefore, the goal of this study was to test the hypothesis that n-3 PUFAs could exert an immune enhancing effect on B cells upon *in vivo* stimulation with a T-independent antigen.

We first tested the impact of n-3 PUFAs in the absence and presence of antigen stimulation on murine B-cell subsets in the bone marrow and spleen, in addition to surface and circulating antibody levels. We then tested the potential immune enhancing properties of n-3 PUFAs in a model of diet-induced obesity. The rationale for studying B-cell phenotypes and antibody production with mice consuming high fat diets was that obese individuals respond poorly to vaccinations and infections (*219-222*). Supporting studies in rodents show obesity is associated with impaired antibody production upon

viral infection, although the impact of obesity on B-cell phenotypes is far less known (*134, 223*). Therefore, this clinical population could benefit is n-3 PUFAs can boost humoral immunity. Our data reveal that n-3 PUFAs, upon antigen stimulation, enhance the frequency of select B-cell phenotypes accompanied by an increase in surface and/or circulating IgM antibody production in lean and obese mice relative to controls.

Materials and Methods

Mice and Diets

Male C57BL/6 mice were fed a purified control low fat diet enriched in soybean oil (Harlan-Teklad) or a diet enriched in menhaden fish oil as previously described for 4 weeks (*217, 224, 225*). Briefly, 1.3% of the total kcal from the fish oil was from DHA and 2% from EPA. For diet-induced obesity studies, mice were fed for 10 weeks the control and low fat n-3 PUFA diets described above in addition to a high fat diet and a high fat diet + fish oil providing 1.3% and 2% of total kcal from DHA and EPA respectively. The dose of n-3 PUFAs corresponded to the equivalent of pharmacological levels in humans (~4-5 grams of n-3 PUFAs per day), which is used in clinical trials and in the treatment of elevated triglycerides (*209, 226*). Both of the high fat diets were 45% of total kcal from fat, which is an adequate representation of high fat consumption in humans in the Western population (*227*). The composition of the diets is shown in Supplemental Table 1. Mice were sacrificed via CO_2 inhalation followed by cervical dislocation. All of the experiments with mice fulfilled the guidelines established by the East Carolina University Brody School of Medicine for euthanasia and humane treatment.

Shotgun Lipidomics

Cells lyophilized in PBS were first subjected to monophasic chloroform

extraction, then the extracts were dried under a stream of nitrogen, washed twice using 10 mM ammonium bicarbonate and dried completely under a stream of nitrogen prior to dissolving in 250 µL of 4:2:1 isopropanol/methanol/chloroform and stored at -80^{o}C. Prior to mass spectrometry analysis, 10 µL of each extract and 2 µL of 10mM $PC_{(14:0/14:0)}$ internal standard were placed into a Whatman Multichem 96 well plate (Sigma Aldrich, St. Louis, MO) and dried under nitrogen, then subjected to sequential derivatization of aminophospholipids with $^{13}C_1$-S,S'-dimethylthiobutanoylhydroxysuccinimide ester ($^{13}C_1$-DMBNHS) and plasmalogen containing lipids with iodine and methanol, as previously described (*228, 229*). After washing twice with 10 mM ammonium bicarbonate and dried, samples were resuspended in 40 µL 4:2:1 isopropanol/methanol/chloroform + 20 mM ammonium formate and introduced to a high resolution/accurate mass Thermo LTQ Orbitrap Velos (Thermo Scientific, San Jose, CA) mass spectrometer using an Advion Nanomate Triversa (Advion, Ithaca, NY) nano electrospray source. Mass spectra (MS) were acquired for 2 minutes at 100,000 mass resolving power in positive ionization mode. Identification and relative quantification of individual lipid ions (i.e., assignment of the head group identity and acyl/alkyl chain linkage type and total carbons:double bonds) from the MS spectra was performed using LIMSA (*230*), as previously described (*228*). HCD-MS/MS of polyunsaturated lipid ions containing at least 4 degrees of unsaturation were acquired for 30 seconds, each in negative ionization mode at 100,000 mass resolving power. The relative fatty acid content within individual PC and PE polyunsaturated lipids was then assigned using the relative abundances of the fatty acid anions formed by HCD-MS/MS.

In vivo Injections and Serum Collection

Mice were fed the control and experimental diets for 3 or 9 weeks, injected i.p. with saline or 1 μg trinitrophenylated-LPS (TNP-LPS, Biosearch Technologies). The dose of TNP-LPS was selected to elicit a mild immune response (*231, 232*). Mice continued to consume the diets for an additional 7 days when blood was collected using a capiject tube (Fisher) coated with a serum separator. The blood was centrifuged at 1300 rpm for 15 minutes at room temperature and the serum was collected and frozen for subsequent analyses.

Isolation of Splenic B Cells

$B220^+$ B cells were purified from splenocytes with a negative selection microbead kit (Miltenyi Biotec) as previously described (*217, 224*). 0.5×10^6 splenic B cells were transferred to a 96 well plate and stained with a combination of B220-FITC (Miltenyi Biotec), IgM-PE (Southern Biotech), CD40-PerCP/Cy5.5 (Biolegend), IgD-APC (Biolegend), CD21-APC/Cy7 (Biolegend), MHC class II-PE (Bio X Cell) and CD19-PerCP/Cy5.5 (Biolegend) in 1X PBS supplemented with 0.1% BSA for 20 minutes on ice. The major splenic B-cell populations analyzed were $IgM^+IgD^-CD21^-$ (transitional 1), $IgM^+IgD^+CD21^-$ (transitional 2/follicular), $IgM^+IgD^+CD21^+$ (pre-marginal zone) and $IgM^+IgD^-CD21^+$ (marginal zone) (*213, 233-235*).

Isolation of Bone Marrow Cells

Bone marrow was obtained from the mouse tibia and femur. Each leg was removed from the mouse, degloved and placed in RPMI 1640 1X media (Mediatech) supplemented with 5% heat-inactivated defined fetal bovine serum (FBS) (Hyclone), 2 mM L-glutamine, and 1% penicillin/streptomycin. Muscle tissue was removed with a

razor. Once the bones were completely cleaned, the bone marrow was flushed into 20 mL of media. Cells were then filtered through a 70 μm filter, red blood cells were lysed, and filtered once more through a 40 μm filter. 0.5 x 10^6 cells were transferred to a 96 well plate, washed once with 100 μL 1X PBS supplemented with 0.1% BSA. Bone marrow cells were stained with FcR Block (Miltenyi Biotec) for 10 minutes on ice followed by B220-FITC (Miltenyi Biotec), IgM-PE (Southern Biotech), CD19-PerCP/Cy5.5 (Biolegend) or CD19-APC (Biolegend), IgD-APC (Biolegend) and CD21-APC/Cy7 (Biolegend). Dead cells were stained with Sytox Blue (Invitrogen).

Flow Cytometry

Splenic and bone marrow cells were stained with fluorophore labeled antibodies as described above and analyzed with a BD LSRII flow cytometer. Surface marker analysis relied on measurements of mean fluorescence intensity (MFI) and splenic and bone marrow phenotypes were analyzed in terms of percentage of the live cells and also converted to frequencies based on the number of isolated B cells.

ELISAs

TNP specific IgM levels in serum were measured with an ELISA. 96-well plates were coated with 5 μg/ml of TNP-BSA (Biosearch Technologies) for 24 hours at 4ºC, then blocked for an additional 24 hours with 5% milk in 1X PBS at 4ºC. Following four washes with 0.05% tween in 1X PBS, the serum was diluted in 1% milk in 1X PBS and 100 μl added to each well. The plate was incubated at 37ºC for 1 hour. HRP-conjugated goat-anti-mouse IgM (Southern Biotech) was diluted 1:5000 in 1% milk in 1X PBS, 100 μl added to each well and incubated at 37ºC for 1 hour. Following 6 washes, 100 μl of TMB SureBlue (KPL) were added to each well for 2 minutes and 30 seconds at room

temperature for plate development. 100 µl of TMB Stop Solution (KPL) were added to stop the reaction and fluorescence was measured at 450 nm.

Statistical Analysis

All of data are from 6-8 independent experiments (i.e. 6-8 mice per diet). The data sets were ensured to be parametric distributions using a Kolmogorov-Smirnov test. Statistical significance was then established using an unpaired two-tailed t test or a one-way ANOVA followed by a Tukeys multiple comparison t test. P values less than 0.05 were considered to be significant.

Results

N-3 PUFAs Remodeled the B-cell Lipidome

We first ensured the uptake of n-3 PUFAs into the B cells using a lipidomics strategy (Supplemental Fig. 2). The data revealed significant remodeling of polyunsaturated phospholipid PC and PE species between the control and n-3 PUFA samples, most notably corresponding to decreased PC(36:4), PC(38:4), PC(o-38:5) PE(36:4), PE(p-36:4), PE(38:4), PE(p-38:4) and PE(40:4) ions, each containing abundant AA fatty acyl chains, and increased PC(36:5), PC(38:5), PC(38:6), PE(38:5), PE(38:6), PE(p-38:6) and PE(40:6) ions, containing abundant EPA, docosapentaenoic acid (DPA) or DHA fatty acyl chains, with only minimal changes observed in the relative amounts of total polyunsaturated species between control and n-3 PUFA samples. Also consistent with these results was an increase in EPA, DPA and DHA content of other lipid classes (e.g., esterified cholesterol).

N-3 PUFAs Increased the Percentage and Frequency of B-cell Subsets in the Absence and Presence of Antigen in Lean Mice

We first studied the impact of n-3 PUFAs on B-cell phenotypes in the absence of antigen upon 4 weeks of feeding. The n-3 PUFA diet had a tendency to elevate the number of splenocytes and the number of isolated B cells compared to the control diet (Fig. 4.1A). We next phenotyped the major splenic B-cell subsets in terms of the percentage of cells and frequency (Supplemental Fig. 3A). The n-3 PUFA diet increased the percentage by 25% (Fig. 4.1B) and the frequency (Fig. 4.1C) by 49% of $IgM^+IgD^-CD21^-$ (transitional 1) B cells. There was no significant effect on the percentage or frequency of $IgM^+IgD^+CD21^-$ (transitional 2/follicular), $IgM^+IgD^+CD21^+$ (pre-marginal zone) and $IgM^+IgD^-CD21^+$ marginal zone cells (Fig. 4.1B,C).

Upon antigen stimulation, n-3 PUFAs significantly elevated the number of splenocytes by 30% and B cells by 39% (Fig. 4.1D). N-3 PUFAs increased the percentage of $IgM^+IgD^-CD21^-$ (transitional 1) by 55% and $IgM^+IgD^-CD21^+$ (marginal zone) cells by 31%, but slightly decreased the percentage of $IgM^+IgD^+CD21^+$ (pre-marginal zone) cells by 7% (Fig. 4.1E). Frequency analysis revealed that $IgM^+IgD^-CD21^-$ (transitional 1), $IgM^+IgD^+CD21^-$ (transitional 2/follicular), $IgM^+IgD^+CD21^+$ (pre-marginal zone) and $IgM^+IgD^-CD21^-$ (marginal zone) cells were all elevated by 71%, 56% 37% and 55% respectively with n-3 PUFAs relative to the control diet (Fig. 4.1F).

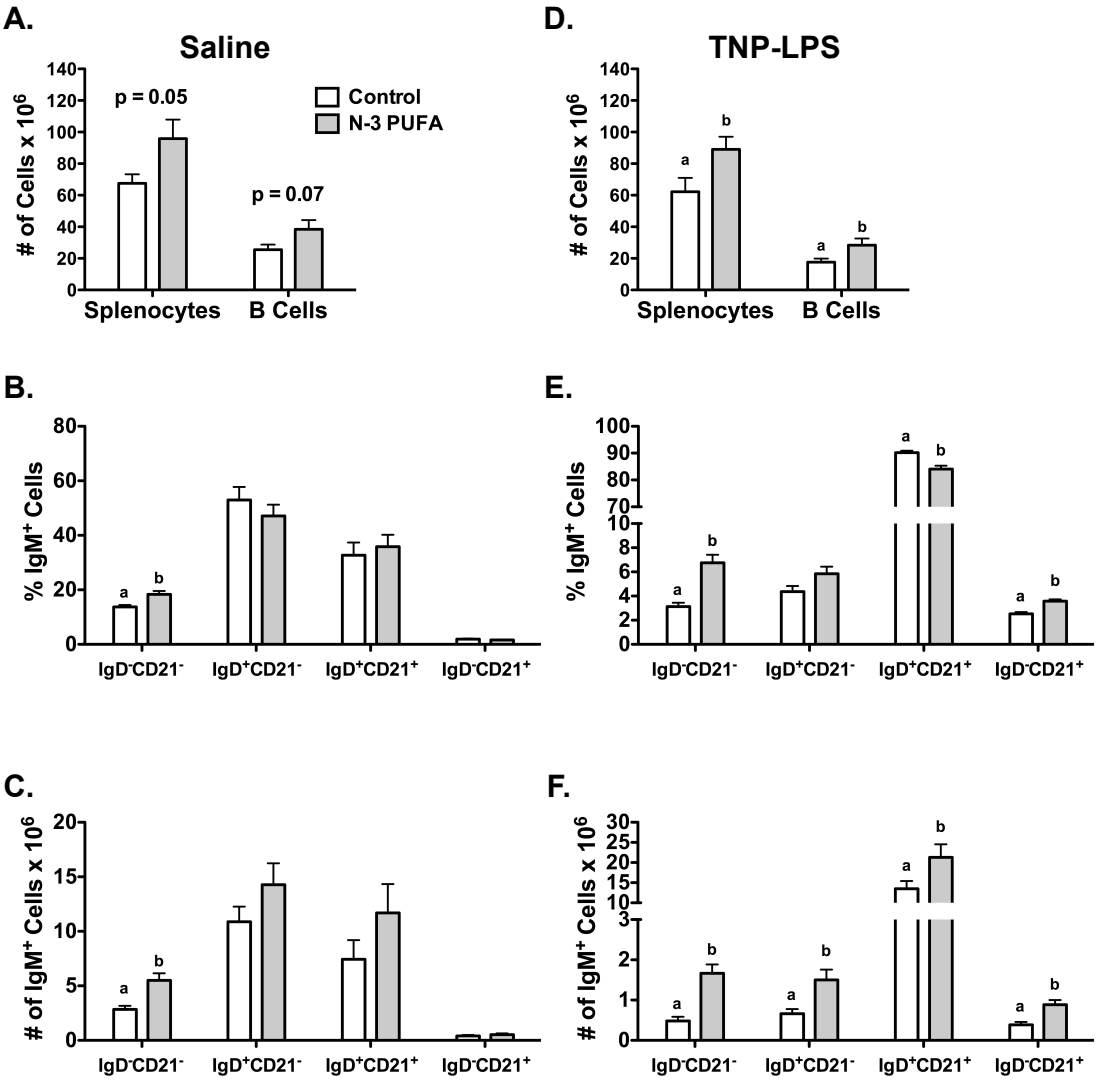

Figure 4.1: N-3 PUFAs differentially enhance the percentage and frequency of B cells in the absence and presence of antigen stimulation.
(A) Number of splenocytes and B cells from mice fed control and n-3 PUFA diets for 4 weeks in the absence of antigen stimulation. Corresponding (B) percentage and (C) frequency of $IgM^+IgD^-CD21^-$ (transition 1) $IgM^+IgD^+CD21^-$ (transitional 2/follicular) $IgM^+IgD^+CD21^+$ (pre-marginal zone) and $IgM^+IgD^-CD21^+$ (marginal zone) subsets. (D) Number of splenocytes and B cells, (E) percentage and (F) frequency of IgM^+ B-cell subsets upon antigen stimulation. Data are from 8 independent experiments. Letters that do not match indicate statistical significance ($p<0.05$).

N-3 PUFAs Exerted Differential Effects on the Percentage of Bone Barrow B cells in the Absence and Presence of Antigen

We next tested the effects of n-3 PUFAs on the percentage of B cells in the bone

marrow (Fig. 4.2A, Supplemental Fig. 3B). Compared to the control diet, n-3 PUFAs decreased the percentage of naïve $B220^{lo}IgM^{+}$ by 22% and mature $B220^{hi}IgM^{+}$ cells by 13%, but had no effect on pre/pro $B220^{lo}IgM^{-}$ B cells (Fig. 4.2A). Upon antigen stimulation, n-3 PUFAs decreased the percentage of naïve $B220^{lo}IgM^{+}$ cells by 24% with no effect on pre/pro $B220^{lo}IgM^{-}$ and mature $B220^{hi}IgM^{+}$ cells (Fig. 4.2B).

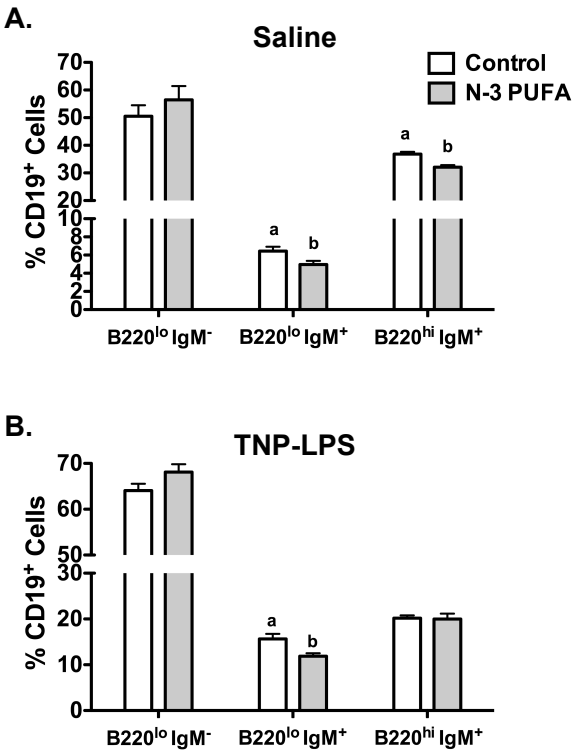

Figure 4.2: N-3 PUFAs modify the proportion of B cells in the bone marrow. Percentage of $B220^{lo}IgM^{-}$ (pre-pro), $B220^{lo}IgM^{+}$ (immature) and $B220^{hi}IgM^{+}$ (mature) B cells in the bone marrow of mice injected with (A) saline or (B) or antigen. Mice were fed control and n-3 PUFA diets for 4 weeks. Data are from 8 independent experiments. Letters that do not match indicate statistical significance ($p<0.05$).

N-3 PUFAs Increased Surface IgM

Flow cytometry analysis of the MFI showed that surface IgM, IgD and CD19 expression were unchanged with n-3 PUFA intervention (Fig. 4.3A). Upon antigen stimulation, surface IgM (Fig. 4.3B) was elevated by 13% and CD19 decreased by 9% on splenic B cells with n-3 PUFAs. IgD surface expression was not influenced by n-3 PUFAs (Fig. 4.3B). Circulating levels of serum TNP-LPS specific IgM were not modified in response to n-3 PUFAs relative to the control diet (Fig. 4.3C).

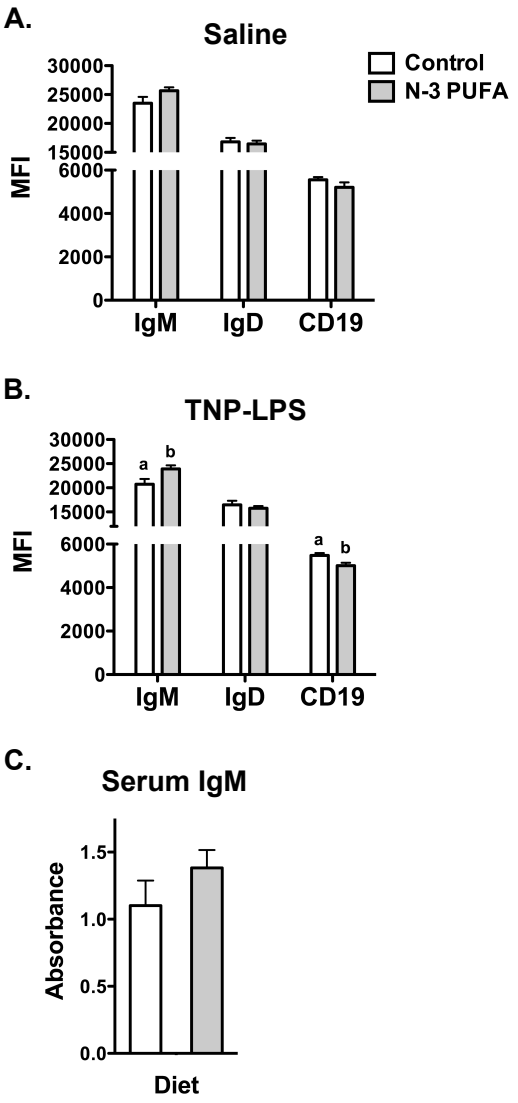

Figure 4.3: N-3 PUFAs increase surface IgM levels.
Mean fluorescence intensity (MFI) of surface IgM, IgD and CD19 expression in the (A) absence and (B) presence of antigen stimulation. (C) Circulating levels of IgM upon TNP-LPS stimulation. Mice were fed control and n-3 PUFA diets for 4 weeks. Data are from 6-8 independent experiments. Letters that do not match indicate statistical significance ($p<0.05$).

N-3 PUFAs Enhanced Transitional and Marginal Zone B-cell Subsets in Lean and Obese Mice Upon Long-term n-3 PUFA Intervention

The next goal of this study was to determine if n-3 PUFAs could exert immune enhancing effects in the context of diet-induced obesity. To promote obesity, mice were fed various diets for 10 weeks. This promoted a 22% weight gain in mice fed a high fat diet relative to the control diet (Supplemental Fig. 4). Incorporation of n-3 PUFAs into the high fat diet also resulted in significant weight gain by 30% relative to the control

(Supplemental Fig. 4). Furthermore, Echo-MRI measurements on a few animals revealed an increase in the percentage of fat mass of mice consuming the high fat and high fat + fish oil diets compared to the low-fat control and low-fat n-3 PUFA diets (data not shown). To be consistent with our aforementioned short-term n-3 PUFA intervention studies, we also measured the effects of the low fat n-3 PUFA diet, which had no impact on body weight gain relative to the control diet (Supplemental Fig. 4).

The number of splenocytes was not increased with any of the experimental diets (Fig. 4.4A). The high fat diet + n-3 PUFAs increased the number of B cells by 47% relative to the control diet (Fig. 4.4A). Phenotype analysis revealed that the n-3 PUFA and the high fat diet + n-3 PUFAs increased the percentage of $IgM^+IgD^-CD21^-$ (transitional 1) B cells by 43% and 57% respectively (Fig. 4.4B). The high fat diet also increased the percentage of transitional 1 B cells by 33% (Fig. 4.4B). The high fat + n-3 PUFA diet lowered the percentage of $IgM^+IgD^+CD21^+$ (pre-marginal zone) cells by 10% (Fig. 4.4B) relative to the control. The frequency of the $IgM^+IgD^-CD21^-$ (transitional 1) and $IgM^+IgD^-CD21^+$ (marginal zone) B cells was elevated respectively by 69% and 55% with the high fat + n-3 PUFA diet relative to the control (Fig. 4.4C). When analyzing the percentage of bone marrow populations with n-3 PUFA intervention in the context of obesity, we observed no change in the percentage of pre/pro, naïve, and mature B cells (Fig. 4.5).

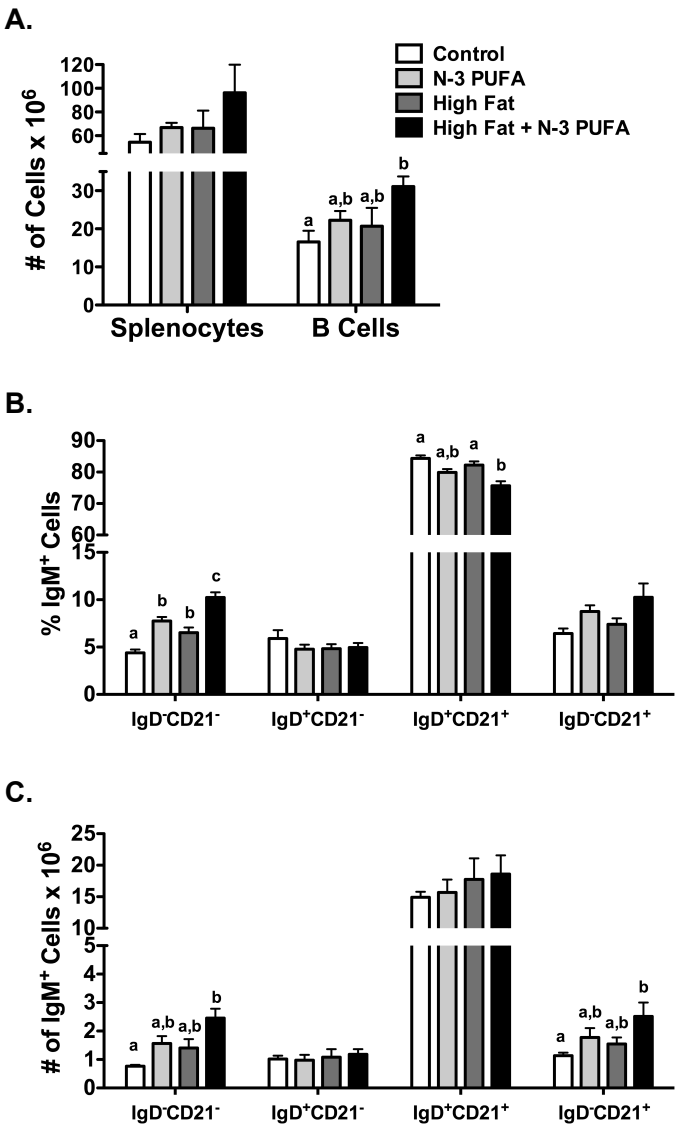

Figure 4.4: High fat diet supplemented with n-3 PUFAs enhances the frequency of transitional 1 and marginal zone B cells.

(A) Number of splenocytes and B cells from mice fed control, n-3 PUFA, high fat, and high fat + n-3 PUFA diets for 10 weeks. Corresponding (B) percentage and (C) frequency of $IgM^+IgD^-CD21^-$ (transitional 1) $IgM^+IgD^+CD21^-$ (transitional 2/follicular) $IgM^+IgD^+CD21^+$ (pre-marginal zone) and $IgM^+IgD^-CD21^+$ (marginal zone) subsets upon antigen stimulation. Data are from 6 independent experiments. Letters that do not match indicate statistical significance ($p<0.05$).

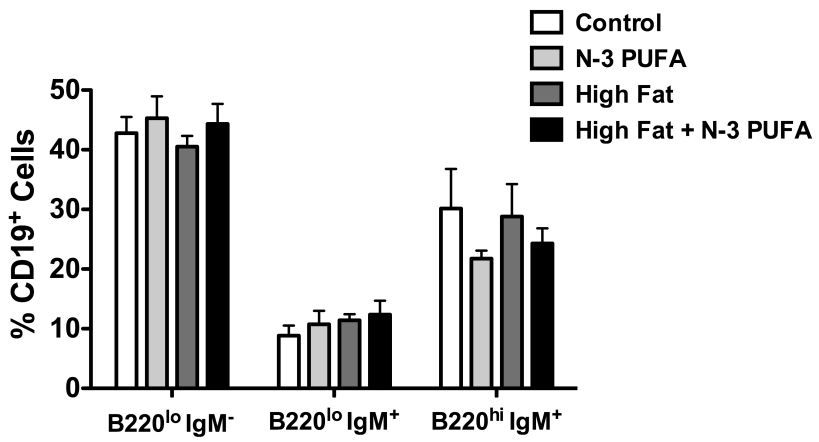

Figure 4.5: N-3 PUFAs in lean and obese mice have no impact on the proportion of B cells in the bone marrow.
Percentage of $B220^{lo}IgM^{-}$ (pre-pro), $B220^{lo}IgM^{+}$ (immature) and $B220^{hi}IgM^{+}$ (mature) B cells in the bone marrow of mice injected with antigen. Mice were fed control, n-3 PUFA, high fat, and high fat + n-3 PUFA diets for 10 weeks. Data are from 6 independent experiments.

N-3 PUFAs Increased Circulating IgM in Lean Mice and Rescued the Decrement in Antibody Production in Obese Mice

Surface IgM levels of splenic B cells were unchanged with the n-3 PUFA, high fat, and high fat + n-3 PUFA diets compared to the control (Fig. 4.6A). The n-3 PUFA diet and the high fat + n-3 PUFA diet lowered IgD expression by 13% and 15% respectively (Fig. 4.6A). In addition, the n-3 PUFA diet and high fat + n-3 PUFA diet lowered CD19 expression respectively by 11% and 9% (Fig. 4.6B). The CD19 data required normalization since two different fluorophores were used during the study. Relative to the control diet, a 17% increase in circulating TNP-specific IgM levels was measured with n-3 PUFAs (Fig. 4.6C). The high fat diet lowered TNP-specific IgM levels by 20% compared to the lean control (Fig. 4.6C). Addition of n-3 PUFAs to the high fat diet elevated IgM levels by 21% relative to the high fat diet (Fig. 4.6C).

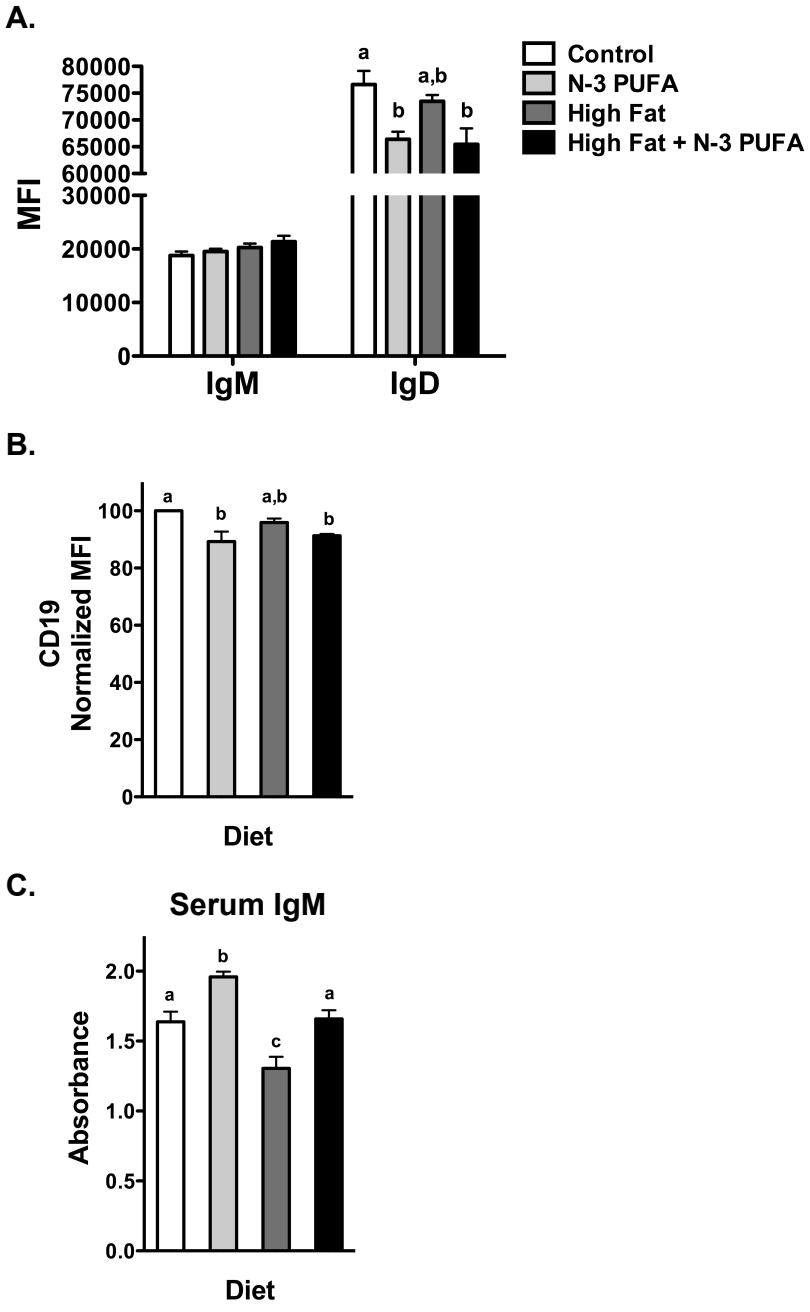

Figure 4.6: N-3 PUFAs increase IgM levels in lean and obese mice.

Mean fluorescence intensity (MFI) of (A) IgM, IgD and (B) CD19 expression. (C) Circulating levels of IgM upon antigen stimulation. Mice were fed control, n-3 PUFA, high fat, and high fat + n-3 PUFA diets for 10 weeks. Data are from 6 independent experiments. Letters that do not match indicate statistical significance ($p<0.05$).

Discussion

The purpose of this study was to determine the functional role of n-3 PUFAs on *in vivo* B-cell phenotypes and antibody production. The field has focused heavily on the impact of dietary n-3 fatty acids on cell-mediated immunity (*210*). This study opens a new avenue of research by demonstrating that n-3 PUFAs can target B cells *in vivo* and specifically improve murine antibody production to a T-independent antigen in the context of an obesogenic diet. B cells have recently emerged as major players in the etiology of several diseases (*214, 236, 237*). Thus, it is vital to determine how long chain n-3 PUFAs regulate B-cell phenotypes and thereby their function, given that individuals are increasingly consuming marine n-3 PUFAs as over-the-counter or prescription supplements.

Implications of Enhancing Transitional and Marginal Zone B cells

A significant advancement from this study is that n-3 PUFAs increased the frequency of transitional 1 B cells in the absence of antigen. Transitional 1 B cells are either eliminated through negative selection in response to strong BCR signals or with appropriate signals will progress to transitional 2 B cells and ultimately become mature follicular B cells (*238*). Since the data show that n-3 PUFAs are promoting the formation of this subset in the absence of antigen, these cells may be poised to become T2 or mature B cells, which could have potential benefits in boosting B-cell-mediated responses to various T-independent and T-dependent antigens that are of relevance for humans. However, increased T1 cells with long chain n-3 PUFAs could also be detrimental for some diseases. For instance, lupus erythematosus and Sjögren's syndrome are characterized by an increased number of transitional B cells (*239*).

Consumption of long chain n-3 PUFAs for these select individuals could exacerbate their disease.

Upon antigen stimulation, we measured an increase in the number of all B-cell subsets. Select studies with CD23 as a marker showed that the majority of cells in the $IgM^{+}IgD^{+}CD21^{-}$ subset were follicular (data not shown). We focused on marginal zone B cells in particular, since these cells are innate-like B lymphocytes equipped with toll-like receptors capable of responding to T-independent antigens (*240*). Our data show that post-antigen stimulation, marginal zone B lymphocyte numbers were increased after 4 weeks of consuming n-3 PUFAs. Again, enhancing the number of marginal zone B cells could have negative consequences for some diseases (*241*). Marginal zone B lymphocytes are significant autoantigen presenting cells in the pancreatic lymph nodes due to their ability to process and present insulin (*242*). On the other hand, subsets of marginal zone B cells can secrete IL-10, which has utility for treatment of autoimmune and inflammatory disease (*243, 244*).

The Role of n-3 PUFAs in Enhancing IgM in Lean and Obese Mice

B cells from mice fed n-3 PUFAs for 4 weeks displayed increased surface but not circulating IgM levels. The lack of an increase in circulating IgM levels could be due to several reasons. We assayed IgM levels a week after immunization and perhaps n-3 PUFAs were increasing IgM levels at other time points after immunization. The rationale for selecting one week after immunization was that TNP specific IgM levels are highest at this time point (*234*). Furthermore, n-3 PUFAs may be better at promoting immune enhancing effects in response to secondary immunizations. We did not conduct

secondary immunizations since TNP-LPS does not promote a robust secondary response.

In some studies, n-3 PUFAs modulate the antibody response, which appears to vary between model systems. One study demonstrated DHA treatment of human B cells suppressed IgE when activated with IL-4/anti-CD40 (*245*). Similarly, another study showed consumption of long chain n-3 PUFAs by female mice lowered the antibody response for pups in response to ovalbumin (*246*). Some recent studies suggest n-3 fatty acids may have a role in enhancing humoral immunity. Gurzell et al., showed that administration of a DHA enriched diet to mice on a 129 background increased fecal IgA in the absence of antigen (*218*). In another study, Ramon et al. showed that *in vitro* treatment of human B cells with select resolvins enhanced IgM and IgG production (*247*).

We tested the role of n-3 PUFAs in obesity since obesity is associated with poor immune responses and in particular, obese individuals respond poorly to vaccinations and infections (*219, 220, 222*). Beck and co-workers have shown that obesity impairs the immune response to influenza vaccination in humans (*219*). To the best of our knowledge, no lab has shown a decrement in the antibody response to a T-independent antigen with a high fat diet. The data here show that obese mice had diminished antibody production to TNP-LPS. One concern may be that administration of our high fat diet did not completely model obesity, which is a multi-faceted disease that manifests in response to dietary, genetic, and/or environmental factors (*248*). We defined obesity in the context of excess nutrition leading to increased fat mass, which was ensured via Echo-MRI and total body weight measurements relative to a lean control diet.

Nevertheless, future studies will need to address the extent of the obesity phenotype including adipocyte hyperplasia, the degree of adipose inflammation and possible impairment in insulin sensitivity. This will aid in determining whether the high fat diet itself or obesity is driving the reduction in IgM levels.

The reduction in IgM levels in response to the high fat diet were consistent with a recent study by Winer et.al (*237*). In their study, they report a reduction in IgM levels from obese mice that consumed a high fat diet for ~8 weeks in the absence of antigen stimulation (*237*). In addition, the decrement in IgM levels were shown to be a ramification of increased class-switched mature B cells resulting in elevated IgG2 autoantibodies. In our study we did not measure class-switched autoantibodies. Interestingly, B-cell phenotypes from the obesity model in our study remained unchanged compared to the control with the exception of an increased percentage of transitional 1 B cells. This aspect of our study did not agree with the study by Winer et. al. which showed a decrease in the percentage of transition 1 B cells in the spleen but an increase in the adipose (*237*). The differences between studies could be due to the levels of fat used and the duration of administration of the high fat diets. It is possible that phenotypic changes were occurring in the adipose and even other B cells subsets including B1a and B1b B cells with the high fat diets in our model system, which we aim to investigate in the future.

The n-3 PUFA diet restored antibody production in the context of obesity compared to the high fat diet alone and elevated IgM levels in lean mice relative to lean controls. These data raise the exciting possibility that n-3 PUFAs may have potential clinical applications in not only suppressing inflammation, as many studies suggest, but

also boosting immunity by targeting B cells (*142*). It is interesting to note that the elevation in IgM in the lean condition was time dependent (i.e. we measured an effect at 10 weeks but only a trend at 4 weeks of feeding). Similarly, we observed a decrease in IgD surface expression subsequent to the 10-week feeding period that was not observed at 4 weeks. We also observed a reduction in naïve and mature B cells in the absence of antigen stimulation but only a reduction in naïve B cells in bone marrow after 4 weeks of n-3 PUFA feeding. The effects on the bone marrow were abolished after 10 weeks of feeding. Thus, these finding suggest that the effects of n-3 PUFAs are time and antigen dependent. In the case of the bone marrow, n-3 PUFAs could be targeting BCR signaling and/or factors such as IL-7 that regulate B-cell development (*249*). Alternatively, n-3 PUFAs may be targeting the recirculating pool of B cells in the bone marrow.

One possible explanation of increased circulating IgM could be due to decreased CD19 surface expression, a marker shown to regulate B-cell development (*250*). Indeed, we observed decreased CD19 expression in the bone marrow as well (data not shown). Tsitsikov et al. reported decreased CD19 signaling resulted in increased circulating IgM, suggesting the observed decrease in surface expression may be correlated with increased circulating antibody (*251*).

Finally, enhanced IgM production with n-3 PUFAs may also have clinical benefits for atherosclerosis. Natural IgM antibodies have been shown to bind oxidized low-density lipoprotein and protect against atherosclerosis (*252, 253*). N-3 PUFAs could be developed as adjuvant therapy to boost IgM levels. Therefore, it will be of utility to test

the impact of n-3 PUFAs on B1a derived IgM antibodies to determine if similar effects are measured as observed in this study.

Summary

In summary, we show that n-3 PUFAs increased the frequency of B cells upon short-term intervention and in the context of high fat feeding upon antigen stimulation. Moreover, n-3 PUFAs increased IgM levels in lean mice and rescued the decrement in antibody production of obese mice. These findings open the possibility of testing various n-3 PUFAs for boosting B-cell meditated immune responses. This may have significant beneficial effects for select clinical populations such as the obese.

CHAPTER 5 : EICOSAPENTAENOIC AND DOCOSAHEXAENOIC ACID ETHYL ESTERS DIFFERENTIALLY ENHANCE B-CELL ACTIVITY IN MURINE OBESITY[4]

Introduction

Numerous studies in pre-clinical and clinical models suggest that dietary supplementation with marine long chain n-3 PUFAs, EPA and DHA, has potential for alleviating some of the complications associated with obesity (*254-256*). For example, prescription n-3 PUFA supplements are effective in treating moderate to severe hypertriglyceridemia that is prevalent in obese individuals (*6, 257*). Furthermore, extensive experiments in rodents demonstrate that n-3 PUFAs suppress cell-mediated immunity and inflammation (*124*). N-3 PUFAs diminish the activation of Th1/Th17 cells and promote an M2 over an M1 macrophage phenotype in adipose tissue, which contributes toward improved insulin sensitivity (*83, 258*). In contrast, much less is known about the role of n-3 PUFAs on B-cell driven humoral immunity, which is central in establishing host immune responses. This is essential to determine given that obese individuals generally display suppressed humoral immunity (*139*).

Our lab has reported that n-3 PUFAs from fish oil enhance B-cell activity (*144, 259*). Our initial studies in lean C57BL/6 mice showed that dietary administration of n-3 PUFAs as menhaden fish oil enhanced B-cell cytokine secretion (*144, 181*). Subsequent experiments demonstrated that menhaden fish oil elevated the frequency of B cells and antibody production in lean mice and rescued the decrement in antibody

[4] This research was originally published in The Journal of Lipid Research. Teague, H., Harris, M., Fenton, J., Lallemand, P., Shewchuk, B., & Shaikh, S.R. Eicosapentaenoic and docosahexaenoic acid ethyl esters differentially enhance B-cell activity in murine obesity. *J Lipid Res*. 2014 pii: jlr.M049809. [Epub ahead of print] © the American Society for Biochemistry and Molecular Biology.

production in mice consuming obesogenic diets in response to antigen stimulation (*259*). These results were consistent with recent studies. For instance, Gurzell et al. demonstrated DHA-enriched fish oil boosted B-cell antibody production of Smad3$^{-/-}$ mice and Tomasdottir et al. showed fish oil enhanced the B-cell responses in a model of murine peritonitis (*260, 261*).

A major limitation of the aforementioned studies on n-3 PUFAs and B cells is that fish oil has various components and its composition varies dramatically depending on the marine source (*262*). Therefore, in order to effectively develop n-3 PUFAs for clinical trials, here we focused on the individual activity of EPA and DHA. We first determined if EPA and DHA ethyl esters, modeling prescription supplements, had any benefits on the obese phenotype. This was essential to determine since there is discrepancy in the literature on how n-3 PUFAs impact key aspects of obesity (*263*). We then determined if EPA and DHA ethyl esters enhanced the frequency of select B-cell subsets, which led to studies on antibody production. Finally, we determined if EPA and DHA exerted equivalent immune enhancing effects on B-cell activation and potential membrane-mediated mechanisms. The studies also addressed the impact of time of intervention, which is a key variable to elucidate in order to develop future clinical trials on n-3 PUFAs.

Materials and Methods

Mice and Diets

Male C57BL/6 mice, about 5 weeks old, were fed experimental diets for 5 or 10 weeks. Mice were fed a low fat control diet, a high fat diet (HF), or a high fat diet enriched with oleic acid (HF-OA), eicosapentaenoic acid (HF-EPA), or docosahexaenoic

acid (HF-DHA) ethyl esters (Harlan Teklad). Ethyl esters were greater than 90% purity. The control diet was a 5% fat by weight diet and high fat diets contained 45% of total kcal from fat. The ethyl esters of OA, EPA, or DHA accounted for 2% of total energy. This corresponded to levels of EPA and DHA that are achievable with dietary supplementation and used in clinical trials (*6, 188*). Supplemental Table 2 shows the composition of the diets. At the end of the feeding period, mice were euthanized with CO_2 inhalation followed by cervical dislocation. Epididymal adipose tissue, cecum, and spleen were harvested following euthanasia. Mice were euthanized in accordance with the guidelines set forth by East Carolina University Brody School of Medicine for euthanasia and humane treatment.

Measurements of Fat Mass

Lean and fat mass were determined with EchoMRI (Active Field Resources, LLC, Houston, TX). In order to measure the size of adipocytes, epididymal adipose tissue was harvested and immediately fixed in 4% paraformaldehyde overnight, then dehydrated, and embedded in paraffin. Sections were cut at 5 μm and stained with hematoxylin and eosin. Images were acquired with a confocal microscope (Olympus, FV1000) using a 20X objective. Fluorescent microscopy images were digitized to 8-bits and the area was measured using NIH ImageJ. For each mouse, 120 adipocytes were measured in 4 independent microscopic fields.

Glucose Clearance and Fasting Insulin

Subsequent to a 6-hour fast, baseline glucose levels were measured with a glucometer. Mice were then injected i.p. with 2.5 g dextrose (Hospira, Inc., Lake Forest, IL) per kg lean mass and glucose measurements were made from the tail vein.

Following a 6-hour fasting period, serum insulin was measured according to manufacturer's protocol via an ELISA (Crystal Chem, Inc., Downers Grove, IL). Briefly, 5 µl of sample combined with 95 µl of sample diluent were added to an antibody-coated microplate. Following a 2-hour incubation, anti-insulin enzyme conjugate was added and incubated for 40 minutes. Stop solution was then added and absorbance measured at 450 nm.

Adipose Inflammatory Profile

RNA was extracted from 100 mg of adipose tissue with the RNeasy Mini Kit (Qiagen, Hilden, Germany). cDNA was made following the manufactures protocol using the RT^2 First Strand Kit (Qiagen, Hilden, Germany). A custom RT^2 PCR Array plate (Qiagen, Hilden, Germany), coated with the primers for the genes of interest and formulated for use on the Biorad IQ5 Real Time PCR machine, was combined with RT^2 SYBR Green qPCR Mastermix (Qiagen, Hilden, Germany) that contained buffer, HotStart DNA Taq polymerase, and SYBR Green dye. The genes measured were TNFα, IL-6, IL-10, IL-4, GAPDH, and β2m. GAPDH and β2m were chosen as reference genes because the copy number was constitutively expressed in all diets. ΔC_t was calculated using the equation $\Delta C_{t=} C_t^{GOI} - C_t^{HSK}$, where GOI is the gene of interest and HSK is the average of both housekeeping genes. $\Delta\Delta C_t$ was determined by subtracting the ΔC_t of the control from the ΔC_t of the experimental diets. The fold change from the control was calculated by the $2^{-\Delta\Delta Ct}$ method.

Splenic B-cell Isolation and Phenotyping

Splenocytes were subjected to a negative selection microbead kit (Miltenyi Biotec, Auburn, CA) to purify $B220^+$ B cells as previously described (*144*). Red blood

cells were lysed with ACK lysis buffer (Life Technologies, Grand Island, NY). 0.5 x 10^6 B cells were transferred to a 96 well plate and blocked with FcR block (Miltenyi Biotec, San Diego, CA). Splenic B Cells were then stained with an antibody cocktail containing B220-FITC (Miltenyi Biotec, San Diego, CA), IgM-PE (Southern Biotech, Birmingham, AL), IgD-APC (Biolegend, San Diego, CA), CD23-PE/Cy7 (Biolegend, San Diego, CA) and CD21-PerCp/Cy5.5 (Biolegend, San Diego, CA) in 1X PBS supplemented with 0.1% BSA. Dead cells were gated out with Sytox Blue (Invitrogen, Carlsbad, CA). The major splenic B-cell populations analyzed were $IgM^+IgD^-CD21^{low}CD23^-$ (transitional 1), $IgM^+IgD^+CD21^{mid}CD23^+$ (transitional 2), $IgM^+IgD^+CD21^{hi}CD23^+$ (pre-marginal zone), $IgM^+IgD^-CD21^{hi}CD23^-$ (marginal zone) and $IgD^+IgM^-CD21^{mid}CD23^+$ (follicular) (*94, 264*). The gating strategy is depicted in Supplemental Fig. 5.

Fatty Acid Analysis of B cells

Total lipids were extracted as previously described using the Folch method (*181, 194*). Isolated lipids from splenic $B220^+$ B cells were methylated using 1 ml boron trifluoride-methanol solution (Sigma, St. Louis, MO) for 90 minutes at 100°C. The resulting methyl esters were extracted again with hexane and water and separated based on retention times by gas chromatography (Shimadzu GC-2010, Columbia, MD). Peaks were analyzed by area as shown previously (*181*).

IgM and IgA Analyses

Serum was collected as previously described and analyzed for natural IgM. Natural IgM levels in serum were measured with an ELISA. 5 µg/ml of anti-IgM (Southern Biotech, Birmingham, AL) was used to coat 96-well plates at 4ºC. The plate was blocked with 5% milk in 1X PBS for 24 hours at 4ºC. The serum was then diluted

1:400 in 1% milk in 1X PBS, 100 µl added to each well, and incubated at 37ºC for 1 hour. A 1:5000 dilution of HRP-conjugated goat-anti-mouse IgM (Southern Biotech, Birmingham, AL) in 1% milk in 1X PBS was added to each well and incubated at 37ºC for 1 hour. TMB SureBlue (KPL, Gaithersburg, MD) was utilized to develop the plate followed by the addition of TMB stop solution (KPL, Gaithersburg, MD). Absorbance was measured at 450 nm and a calibration curve was generated to convert absorbance values to absolute levels of IgM.

The cecum was harvested and cecal contents were collected in a pre-weighed microcentrifuge tube. Cecal contents were processed as previously described (*260*). Briefly, contents were frozen at -80°C until analysis. Once thawed, the cecal contents were placed in a 25% w/v solution of protease inhibitors in PBS. Samples were vortexed 10 minutes and then centrifuged at 16,000 g for 10 minutes. Supernatants were collected, centrifuged once more and collected for protein analysis. IgA was determined via an ELISA according to manufacturer.

B-cell Activation

1 x 10^6 B cells were plated in 1 ml of RPMI-1640 1X media (Corning Cellgro, Manassas, VA) supplemented with 5% heat-inactivated, defined fetal bovine serum (FBS) (Thermo Scientific, Waltham, MA), 2 mM L-glutamine (Corning Cellgro, Manassas, VA), 1% penicillin/streptomycin (Corning Cellgro, Manassas, VA), and 50 µM β-mercaptoethanol (Sigma, St. Louis, MO) in a 24-well plate (Becton Dickinson, Franklin Lakes, NJ). B cells were stimulated with LPS (Sigma, St. Louis, MO) at a concentration of 1 µg/ml and incubated at 37°C in 5% CO_2 for 24 hours. Supernatants

were collected after pelleting the cells by centrifugation at 300 g for 5 minutes and TNFα, IL-6, and IL-10 were measured with an ELISA (Biolegend, San Diego, CA).

Two-photon Polarization Imaging

1 x 10^6 purified B cells were washed twice with 1X PBS and stained with 1 μM Laurdan (Life Technologies, Grand Island, NY) for 15 minutes at 4°C and then washed twice with 1X PBS. The staining was conducted at 4°C to induce the formation of an ordered plasma membrane. 1 ml of 4% paraformaldehyde (Electron Microscopy Sciences, Hatfield, PA) was used to fix the cells for 30 minutes on ice. The stained B cells were washed three times with 1X PBS and loaded into capillary tubes (Fiber Optic Center, New Bedford, MA). Multi-photon fluorescent imaging was conducted using an Olympus FV-1000 confocal microscope. Emission was measured at 400-460 nm and 495-540 nm. For each diet sample, a minimum of 10 cells were imaged in order to calculate the GP. GP was calculated using $GP = \frac{I^{(400-460)} - (Gfactor \times I^{(495-540)})}{(400-460) + (Gfactor \times (495-540))}$ where I is the fluorescence intensity. The G factor was calculated using a control sample with a known GP (*265*).

Ba/F3 Cell Culture and Fatty Acid Treatment

Ba/F3 cells, an IL-3-dependent murine pro-B-cell line expressing green fluorescent protein (GFP)-tagged TLR4, and Chinese hamster ovary cells were obtained from Dr. Daniel H. Hwang (UC Davis). Ba/F3 cells were maintained in RPMI 1640 (Corning Cellgro, Manassas, VA) supplemented with 70 U/mL recombinant murine IL-3, 10% heat-inactivated defined FBS (Hyclone), 2 mM L-glutamine (Corning Cellgro, Manassas, VA), 1% penicillin/streptomycin (Corning Cellgro, Manassas, VA), 100 μM β-mercaptoethanol and 2 μg/mL puromycin at 37°C in a 5% CO_2 incubator. The source of

recombinant murine IL-3 was medium conditioned by Chinese hamster ovary cells that were genetically engineered to produce up to 70,000 U/ mL of murine IL-3. 2.5 x 10^5 Ba/F3 cells were treated for 24 hours with fatty acid free bovine serum albumin (BSA) or 25 μM of oleic acid (OA), EPA or DHA in complete medium. Fatty acid free BSA and OA served as controls to ensure specificity of EPA and DHA.

Fluorescence Recovery After Photobleaching (FRAP) Microscopy

2.5 x 10^5 Ba/F3 cells were washed twice, added to poly-D-lysine-coated glass-bottom dishes, and washed twice to remove non-adhering cells. Adherent cells were immersed in phenol red-free RPMI supplemented with 10% FBS and stimulated with 1μg/mL LPS (Sigma, St. Louis, MO) for 20 minutes at 37°C. FRAP measurements were made using an Olympus FV-1000 confocal microscope. An attenuated laser beam was focused through a 60X objective on the cell surface. For bleaching, a ROI was defined as a circle of a 1 μm radius. Initial fluorescence was recorded followed by a 175 ms bleach with 50% laser power, then fluorescence recovery was measured for 50 s. For each experimental condition, 40 recovery curves were collected in 4 independent experiments. TLR4 mobile fraction and diffusion coefficients were calculated as previously described (*266, 267*).

Statistical Analyses

The data sets were ensured to be parametric distributions using a Kolmogorov-Smirnov test. Statistical significance was then established using a one-way or two-way ANOVA followed by a Bonferroni multiple comparison t tests. The two-photon and FRAP microscopy data displayed non-parametric distributions and were therefore

analyzed with a Kruskal-Wallis test followed by a Dunn's multiple comparison test. For all data sets, p values less than 0.05 were considered to be significant.

Results

EPA and DHA Ethyl Esters Maintained the Obesogenic Phenotype

Given that we were studying the effects of EPA and DHA on B-cell activity in obesity, it was essential to establish the effects of the ethyl esters on fat mass, adipose inflammation, and glucose/insulin levels. After 5 weeks of feeding, the final body weight of the mice consuming control and high fat diets remained the same (Fig. 5.1A). Obesity, defined here as an increase in body weight beyond that seen in the control group, was not observed until 10 weeks of feeding. The HF, HF-EPA and HF-DHA diets increased body weight respectively by 22%, 34% and 27% compared to the lean control (Fig. 5.1A). The HF-OA diet modestly increased the final weight by 14% ($p = 0.07$) (Fig. 5.1A).The HF-EPA diet elevated body weight by 17% compared to the HF-OA diet (Fig. 5.1A).

The increase in body weight was driven by fat mass. Echo-MRI measurements showed the HF diet elevated fat mass by 89% compared to the control (Fig. 5.1B). The fat mass of mice consuming the HF-OA, HF-EPA and HF-DHA diets were elevated 120%, 100% and 112% compared to the lean control (Fig. 5.1C). There were no detectable differences in fat mass between mice fed the high fat diets. Compared to the lean control, adipocyte size was increased respectively by 46%, 55%, 78%, and 58% with the HF, HF-OA, HF-EPA and HF-DHA diets (Fig. 5.1C,D). HF-EPA increased adipocyte size by 23% compared to the HF diet and 15% compared to the HF-OA diet (Fig. 5.1D). Furthermore, we analyzed the inflammatory profile of the adipose tissue.

The relative gene expression of pro-inflammatory (TNFα, IL-6) and anti-inflammatory (IL-10, IL-4) cytokines was not significantly elevated with any of the high fat diets relative to the lean control (Fig. 5.1E).

Glucose tolerance tests revealed that all of the HF diets suppressed fasting glucose clearance compared to the lean control (Fig. 5.1F). The area under the curve (AUC) for glucose clearance was increased respectively by 34-61% for all of the HF diets compared to the control (Fig. 5.1G). Fasting insulin was not significantly elevated for mice consuming HF diets compared to the control (Fig. 5.1H). However, the HF-OA and HF-DHA showed a trend in elevated fasting insulin (Fig. 5.1H). Altogether, these studies established the mice consuming HF diets had elevated fat mass with poor glucose clearance.

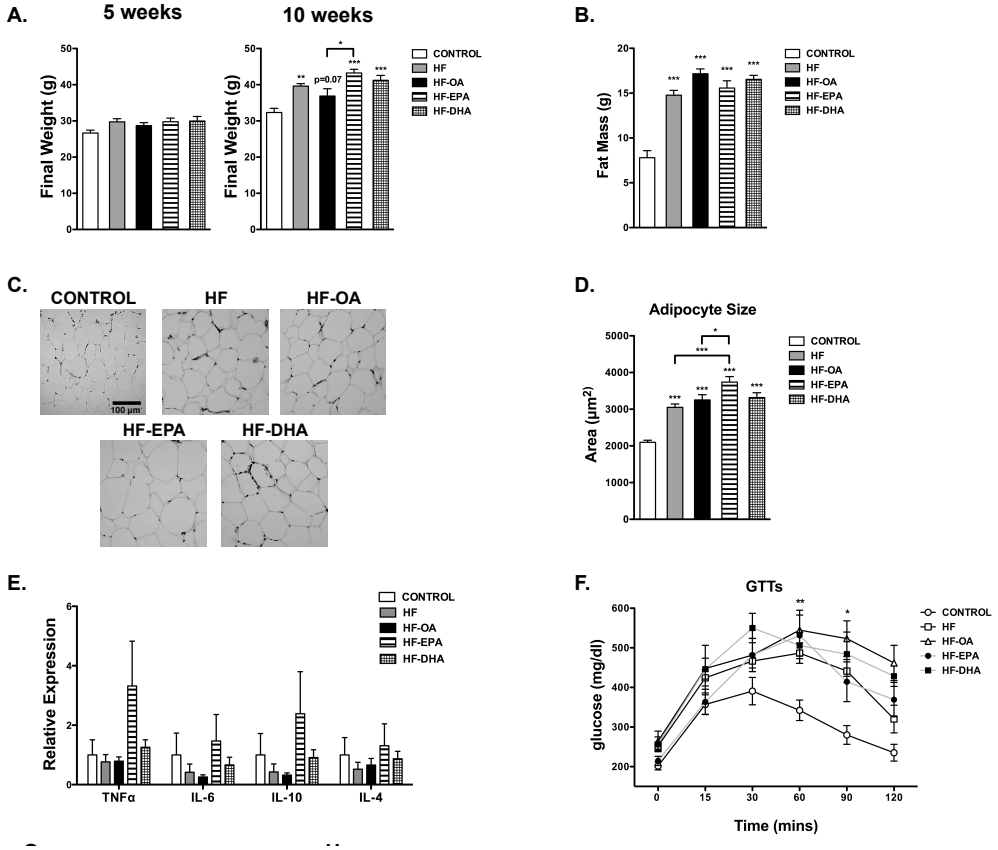

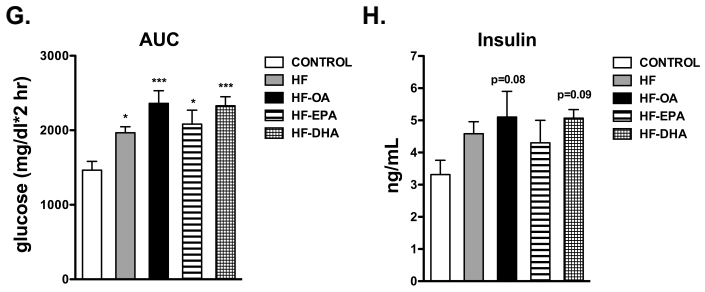

Figure 5.1: The obese phenotype is maintained with EPA and DHA ethyl esters.
Mice were fed control, HF, HF-OA, HF-EPA or HF-DHA for 5 or 10 weeks. (A) Final body weights after 5 and 10 weeks of feeding. (B) Fat mass, (C) paraffin-embedded sections of epididymal adipose tissue and (D) average adipocyte size following 10 weeks of feeding. (E) Relative gene expression of epididymal adipose tissue after 10 weeks of feeding. (F) Glucose tolerance tests were used to calculate the (F) area under the curve (G) and fasting insulin were measured after 6 hours of fasting for the 10-week feeding period. Data are average ± S.E. from 6-12 animals per diet except D, which were 3 animals per diet. Asterisks indicate significance from lean control unless indicated by a bracket: *p<0.05, **p<0.01, ***p<0.001.

EPA and DHA Ethyl Esters Increased B-cell Levels of EPA and DHA at the Expense of Linoleic and Arachidonic Acid

The uptake of EPA and DHA ethyl esters has never been tested on B cells; thus, we measured the total B-cell fatty acid content after dietary intervention. After 5 weeks of feeding, linoleic acid (18:2) was respectively decreased 36%, 39%, and 43% with the HF, HF-OA and HF-EPA diets compared to the control (Table 5.1). HF-EPA decreased AA (20:4) by 40% concomitant with a 46-fold increase in EPA (20:5) and a 6-fold increase in docosapentaenoic acid (22:5, n-3) compared to the control (Table 5.1). Compared to the control, HF-DHA decreased AA by 51% and DHA constituted 17.3% of the total fatty acids. EPA, due to retroconversion from DHA, was also slightly elevated (Table 5.1). Total n-6 PUFAs decreased with the HF-EPA and HF-DHA diet by 37-41%

accompanied by an increase in total n-3 PUFAs with the HF-EPA and HF-DHA diet by 3-fold (Table 5.1).

Table 5.1: Fatty acid composition of B cells after 5 weeks of treatment.[1]

Fatty Acid	Control	HF	HF-OA	HF-EPA	HF-DHA
C14:0	0.6 ± 0.3	2.4 ± 0.7	2.8 ± 0.6*	1.7 ± 0.4	1.6 ± 0.3
C16:0	25.1 ± 1.8	23.2 ± 1.5	25.1 ± 1.2	24.8 ± 0.5	24.1 ± 1.2
C16:1	1.4 ± 0.2	1.4 ± 0.2	1.5 ± 0.3	1.5 ± 0.0	1.4 ± 0.1
C18:0	22.4 ± 0.8	21.1 ± 0.5	21.7 ± 0.6	20.3 ± 0.2	20.2 ± 0.3
C18:1 trans	0.1 ± 0.0	0.1 ± 0.0	0.1 ± 0.0	0.1 ± 0.0	0.1 ± 0.0
C18:1 cis	10.1 ± 0.3	10.9 ± 0.8	12.4 ± 1.6	9.4 ± 0.3	9.7 ± 0.2
C18:2 (n-6)	11.2 ± 0.2	7.2 ± 0.2[a]	6.8 ± 0.1[a]	6.4 ± 0.2[a]	10.2 ± 0.5
C20:4 (n-6)	21.0 ± 1.0	25.3 ± 0.5	21.4 ± 2.4	12.7 ± 0.3[a]	10.2 ± 0.2[a]
C20:5 (n-3)	0.2 ± 0.0	0.2 ± 0.0	0.3 ± 0.0	9.2 ± 0.4[a]	3.6 ± 0.1[a]
C22:5 (n-3)	1.7 ± 0.2	2.5 ± 0.2	2.4 ± 0.3	10.2 ± 0.4[a]	1.8 ± 0.1
C22:6 (n-3)	6.2 ± 0.5	5.7 ± 0.3	5.4 ± 0.7	3.7 ± 0.2	17.3 ± 0.7[a]
∑ SFA	48.1 ± 1.5	46.7 ± 1.6	49.6 ± 1.9	46.8 ± 0.5	45.8 ± 1.3
∑ MUFA	11.6 ± 0.3	12.3 ± 0.9	14.0 ± 1.6	11.0 ± 0.4	11.1 ± 0.1
∑ PUFA (n-3)	8.1 ± 0.6	8.5 ± 0.5	8.1 ± 1.1	23.2 ± 0.6[a]	22.6 ± 0.8[a]
∑ PUFA (n-6)	32.2 ± 1.0	32.5 ± 0.4	28.3 ± 2.4	19.1 ± 0.4[a]	20.4 ± 0.7[a]

[a]Data are average ± S.E. from 4-5 animals per diet. Asterisks indicate significance from control: [a] $p<0.001$.

After 10 weeks of feeding, HF-OA decreased LA by 40% relative to the control (Table 5.2). HF increased AA levels by 33% compared to the control (Table 5.2). HF-EPA decreased LA and AA by 49% and 39%, respectively, compared to the control diet in addition to a 28-fold increase in EPA and a 5-fold increase in DPA (Table 5.2). HF-DHA decreased AA by 43% and 4.6% of total fatty acids were from EPA, and 19.1% from DHA (Table 5.2). HF-EPA and HF-DHA respectively increased the total n-3 PUFAs by 120% and 166% compared to the control (Table 5.2). Total n-6 PUFAs decreased by 43% and 27% with the HF-EPA and HF-DHA diet, respectively, compared to the control (Table 5.2). Overall, the data showed that EPA and DHA ethyl esters were effectively taken up by the B cells at the expense of n-6 PUFAs.

Table 5.2: Fatty acid composition of B cells after 10 weeks of treatment.[2]

Fatty Acid	Control	HF	HF-OA	HF-EPA	HF-DHA
C14:0	0.7 ± 0.3	1.1 ± 0.6	0.3 ± 0.2	1.3 ± 0.6	0.7 ± 0.3
C16:0	26.9 ± 3.0	20.6 ± 2.7	18.9 ± 1.7	19.1 ± 2.0	17.4 ± 3.2
C16:1	1.7 ± 0.4	1.0 ± 0.2	1.0 ± 0.2	1.0 ± 0.3	1.1 ± 0.3
C18:0	18.4 ± 2.1	22.7 ± 0.7	22.4 ± 0.6	29.2 ± 7.7	20.6 ± 0.6
C18:1 trans	0.1 ± 0.0	0.1 ± 0.0	0.1 ± 0.0	0.1 ± 0.0	0.0 ± 0.0
C18:1 cis	10.7 ± 0.5	10.8 ± 0.4	12.1 ± 0.6	9.2 ± 1.1	10.5 ± 0.5
C18:2 (n-6)	10.9 ± 1.0	7.1 ± 0.4	6.5 ± 0.3	5.6 ± 0.7[a]	11.3 ± 2.5
C20:4 (n-6)	20.6 ± 0.7	27.3 ± 1.2[a]	25.8 ± 0.3	12.5 ± 1.7[b]	11.8 ± 2.0[b]
C20:5 (n-3)	0.3 ± 0.1	0.2 ± 0.0	0.7 ± 0.3	8.3 ± 1.2[c]	4.6 ± 0.1[c]
C22:5 (n-3)	2.1 ± 0.2	2.8 ± 0.3	3.2 ± 0.3	9.7 ± 1.2[c]	2.9 ± 0.6
C22:6 (n-3)	7.6 ± 0.9	6.3 ± 0.8	9.1 ± 1.2	4.0 ± 0.8	19.1 ± 1.2[c]
∑ SFA	45.9 ± 1.2	44.4 ± 2.1	41.6 ± 1.6	49.7 ± 6.4	38.6 ± 3.0
∑ MUFA	12.5 ± 0.5	11.9 ± 0.4	13.1 ± 0.7	10.3 ± 1.1	11.6 ± 0.5
∑ PUFA (n-3)	10.0 ± 1.1	9.3 ± 0.9	12.9 ± 1.6	22.0 ± 3.0[b]	26.6 ± 1.8[c]
∑ PUFA (n-6)	31.6 ± 1.2	34.4 ± 1.5	32.3 ± 0.3	18.0 ± 2.4[c]	23.1 ± 2.2[a]

[2]Data are average ± S.E. from 4-5 animals per diet. Asterisks indicate significance from control: [a] $p<0.05$, [b] $p<0.01$, [c] $p<0.001$.

EPA and DHA Differentially Increased the Percentage and/or Frequency of Select Transitional 1 B Cells

Here we determined if EPA and DHA ethyl esters also enhanced the frequency of B-cell subsets. After 5 weeks of feeding, HF-EPA increased spleen weight by 33% compared to the lean control, HF, and HF-OA diets (Fig. 5.2A). HF-DHA increased spleen weight by 17% compared to the HF diet (Fig. 5.2A) No change was observed in the number of splenocytes or B cells at 5 weeks with the HF-EPA or HF-DHA diets compared to the control (Fig. 5.2B). We then quantified the percentage and frequency of splenic B-cell subsets. At 5 weeks, HF-EPA and HF-DHA increased the percentage of transitional 1 B cells by 54% and 63%, respectively, compared to the lean control (Fig. 5.2C). HF-DHA increased the percentage of transitional 1 B cells by 41% compared to HF-OA (Fig. 5.2C). HF-EPA increased the frequency of transitional type 1 B cells by 63% compared

to the control and by 66% compared to HF-OA (Fig. 5.2D). HF and HF-OA had no effect on the percentage or frequency of B cells relative to the control (Fig. 5.2C,D).

Following 10 weeks of feeding, the HF diet increased spleen weight by 60% compared to the control (Fig. 5.2E). The HF-EPA and HF-DHA diets increased spleen weight by 96% and 89% respectively compared to the control and 47% and 41% respectively compared to HF-OA (Fig. 5.2E). HF-EPA had a tendency to increase the number of splenocytes ($p = 0.05$) and B cells ($p = 0.06$) compared to the lean control (Fig. 5.2F). The percentage of transitional 1 B cells increased with HF-EPA and HF-DHA by 43% and 39%, respectively, compared to the control (Fig. 5.2G). Compared to HF, HF-EPA and HF-DHA increased the percentage of transitional 1 B cells by 35% and 31% respectively (Fig. 5.2G). Compared to HF-OA, HF-EPA and HF-DHA increased the percentage of transitional 1 B cells by 52% and 47% respectively (Fig. 5.2G). The percentage of transitional 2 B cells was elevated by 34% with the HF-OA diet relative to the lean control (Fig. 5.2G). HF-DHA increased the percentage of pre-marginal zone B cells by 41% compared to the lean control (Fig. 5.2G). The percentage of follicular B cells was decreased by HF-OA and HF-EPA by 9% relative to the control and by 11% with the HF-DHA relative to the control (Fig. 5.2G).

Transitional type 1 B cells increased in frequency by 103% with HF-EPA compared to the control and 113% compared to HF-OA (Fig. 5.2H). Compared to HF, HF-EPA increased the frequency of transitional 1 B cells by 51% (Fig. 5.2H). HF-EPA also increased the frequency of transitional 2 B cells by 73% compared to the control (Fig. 5.2H). The frequency of B cells did not change in the remaining subsets with the high fat diets compared to the control (Fig. 5.2H). Overall, the data showed that EPA

and DHA had the most robust effect on the frequency and/or the percentage of transitional 1 B cells.

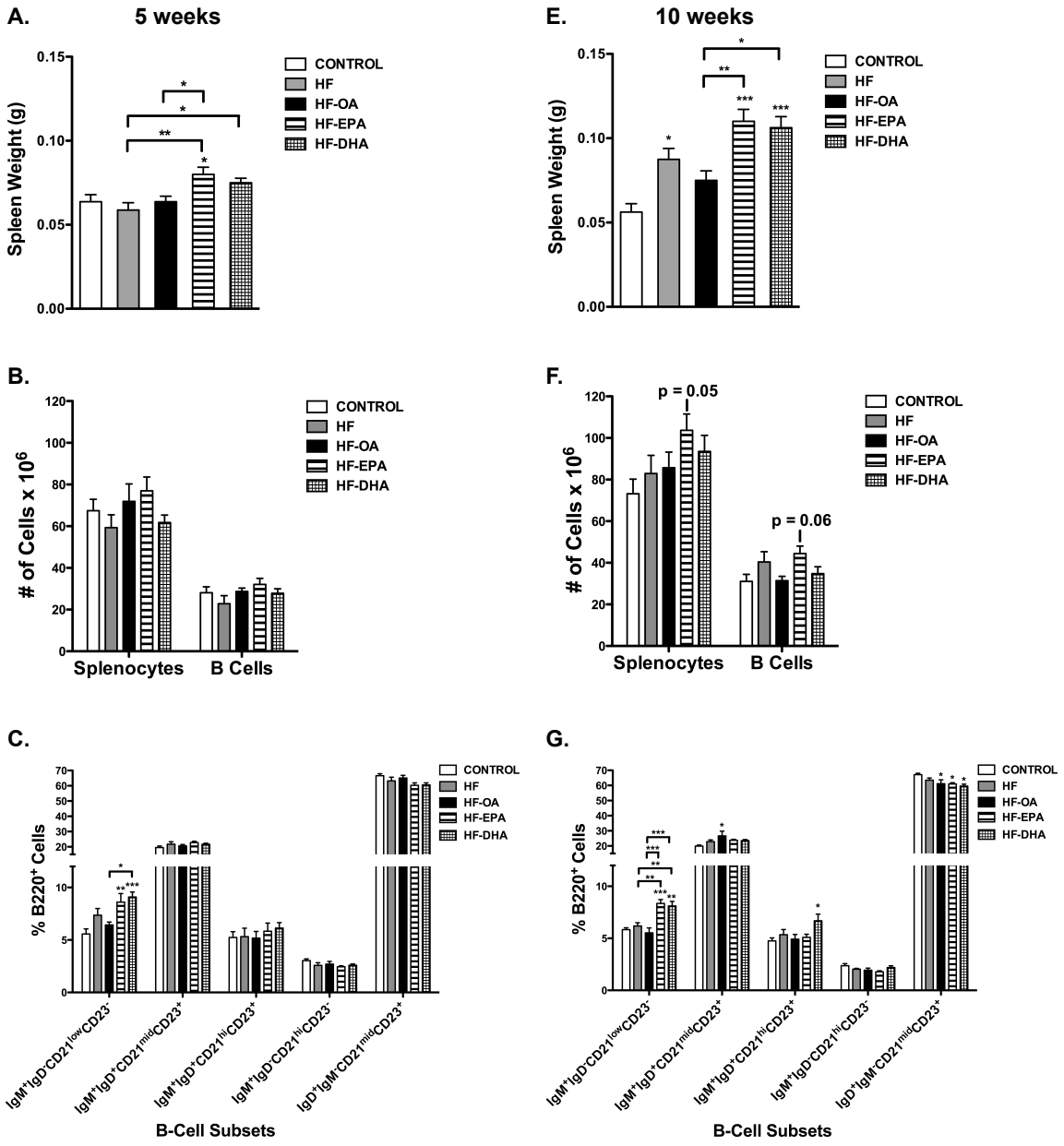

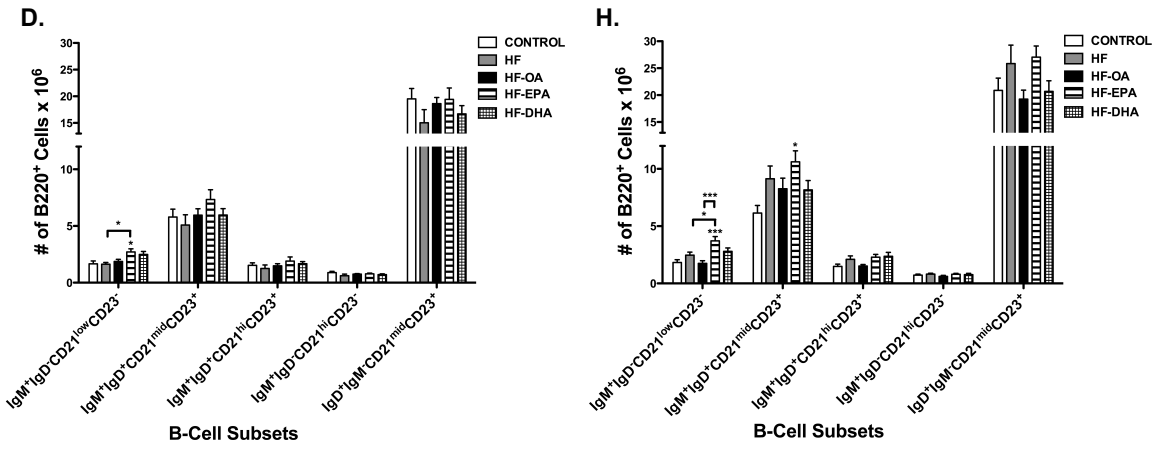

Figure 5.2: The percentage and frequency of select B-cell subsets is differentially enhanced with EPA and DHA.
(A) Spleen weight and (B) number of splenocytes and B cells from mice fed control, HF, HF-OA, HF-EPA and HF-DHA diets for 5 weeks. Corresponding (C) percentage and (D) frequency of $IgM^+IgD^-CD21^{low}CD23^-$ (transitional 1), $IgM^+IgD^+CD21^{mid}CD23^+$ (transitional 2), $IgM^+IgD^+CD21^{hi}CD23^+$ (pre-marginal zone), $IgM^+IgD^-CD21^{hi}CD23^-$ (marginal zone) and $IgD^+IgM^-CD21^{mid}CD23^+$ (follicular) B-cell subsets at 5 weeks. (E) Spleen weight, (F) number of splenocytes and B cells and corresponding (G) percentage and (H) frequency of transitional 1, transitional 2, pre-marginal zone, marginal zone and follicular B-cell subsets from mice fed various diets for 10 weeks. Data are average ± S.E. from 8 animals per diet. Asterisks indicate significance from control unless indicated by a bracket: *p<0.05, **p<0.01, ***p<0.001.

Surface IgM is Elevated with DHA, but not EPA

We also analyzed the total surface levels of IgM, IgD, CD23 and CD21, the markers used to phenotype the B cells. After 5 weeks of feeding, only EPA increased CD23 surface expression by 20% compared to the lean control, whereas EPA and DHA had no effect on IgM, IgD, and CD21 (Fig. 5.3A). After 10 weeks, DHA increased IgM surface expression by 16% relative to the lean control (Fig. 5.3B). EPA and DHA had no effect on IgD (Fig. 5.3B) but both increased CD23 surface expression by 20% and 15% respectively (Fig. 5.3B). EPA and DHA did not influence CD21 surface expression (Fig. 5.3B). The HF and HF-OA diets had no effect on IgM, IgD, CD23, and CD21 expression at 5 and 10 weeks.

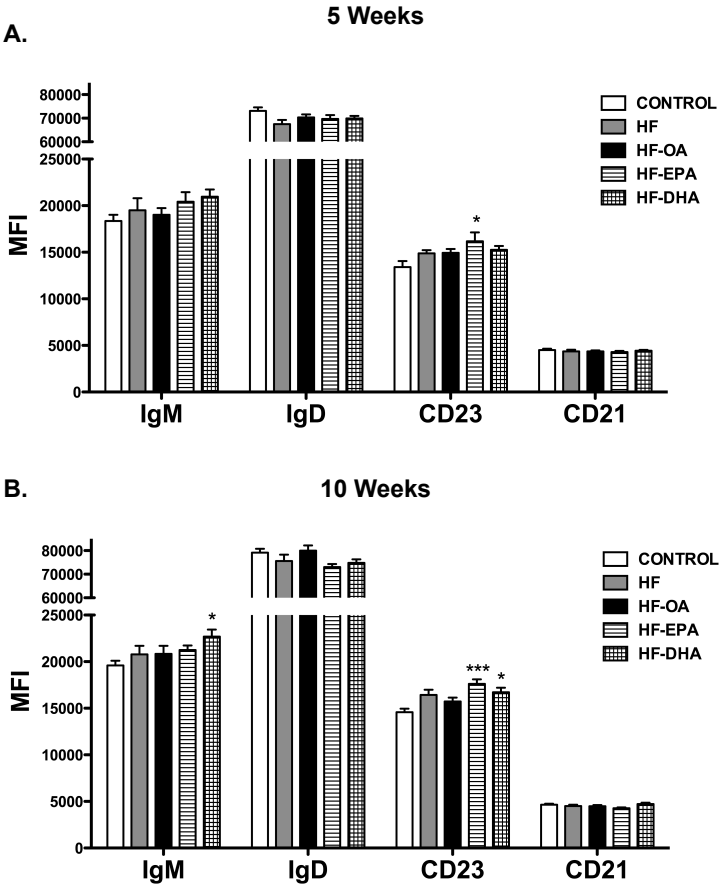

Figure 5.3: Surface IgM and CD23 expression are differentially enhanced with EPA and DHA.
Splenic B220^{+} B cells were isolated from mice consuming a control, HF, HF-OA, HF-EPA or HF-DHA diet for 5 weeks or 10 weeks. Surface expression of IgM, IgD, CD23 and CD21 at (A) 5 and (B) 10 weeks were measured via flow cytometry. Data are average ± S.E. from 7-8 animals per diet. Asterisks indicate significance from lean control: *p<0.05, ***p<0.001.

EPA and DHA Differentially Increased Natural IgM and IgA

Splenic B-1 cells, which are found in the transitional 1 population, produce the majority of circulating natural IgM (*268*). Therefore, we sought to determine if EPA and DHA increased circulating levels of IgM. After 5 weeks of dietary intervention, HF-EPA modestly increased total IgM in the serum by 19% (p=0.05) compared to the control (Fig. 5.4A). After 10 weeks, the HF-EPA and HF-DHA diets modestly elevated total IgM

by 20% and 15%, respectively, compared to the control (Fig. 5.4B). Compared to HF-OA, HF-EPA increased total IgM at 10 weeks by 20% (Fig. 5.4B). The HF and HF-OA diets had no effect on IgM levels relative to the lean control.

We also measured cecal IgA given that it is produced from B1 cells. The levels of cecal IgA were not influenced by any of the HF diets after 5 weeks of dietary intervention (Fig. 5.4C). After 10 weeks, HF-EPA increased IgA by 63% relative to the control (Fig. 5.4D). The other HF diets had no statistically significant effect on IgA levels compared to the control. In general, IgA levels were higher with all of the diets at 10 weeks compared to 5 weeks.

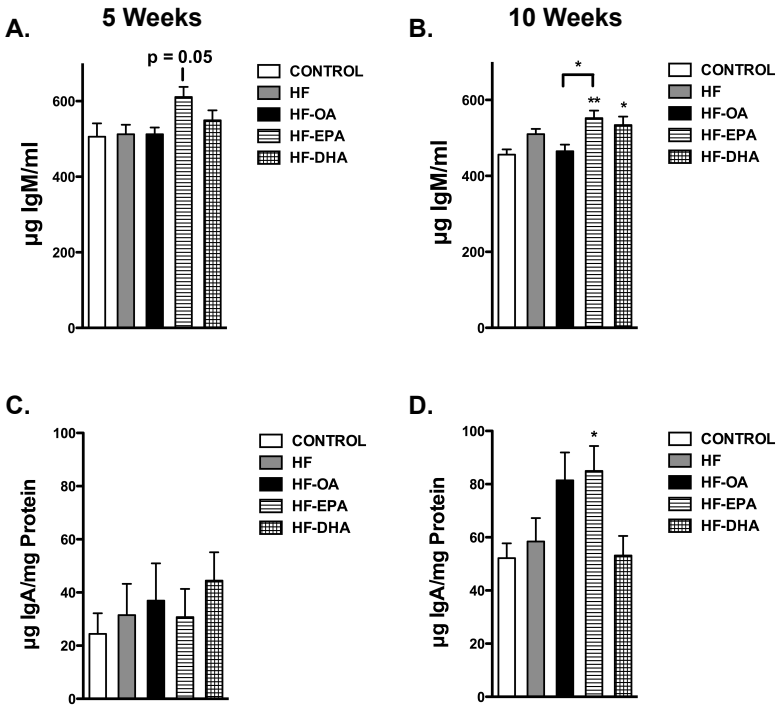

Figure 5.4: Antibody production is differentially enhanced with EPA and DHA.
Natural IgM levels at (A) 5 and (B) 10 weeks and cecal IgA levels at (C) 5 and (D) 10 of consuming a control, HF, HF-OA, HF-EPA or HF-DHA diet. Data are average ± S.E. from 8 animals per diet. Asterisks indicate significance from control unless indicated by a bracket: *p<0.05, **p<0.01.

EPA and DHA Differentially Enhanced B-cell Cytokine Secretion *Ex Vivo*

We next conducted *ex vivo* experiments on B-cell cytokine secretion. The rationale was to directly compare to previous *ex vivo* studies in lean mice using fish oil. HF, HF-OA, HF-EPA and HF-DHA did not effect cytokine production relative to the lean control after 5 weeks of feeding (Fig. 5.5A). After 10 weeks, TNFα secretion increased with HF-EPA and HF-DHA 186% and 188% respectively compared to the control (Fig. 5.5B). HF-EPA and HF-DHA respectively increased IL-6 by 142% and 182% compared to the control at 10 weeks (Fig. 5.5B). Compared to HF-OA, HF-DHA increased IL-6 production by 127% (Fig. 5.5B). HF-DHA increased the production of IL-10 by 75% compared to the lean control (Fig. 5.5B). These results established that EPA and DHA differentially boost B-cell cytokine secretion.

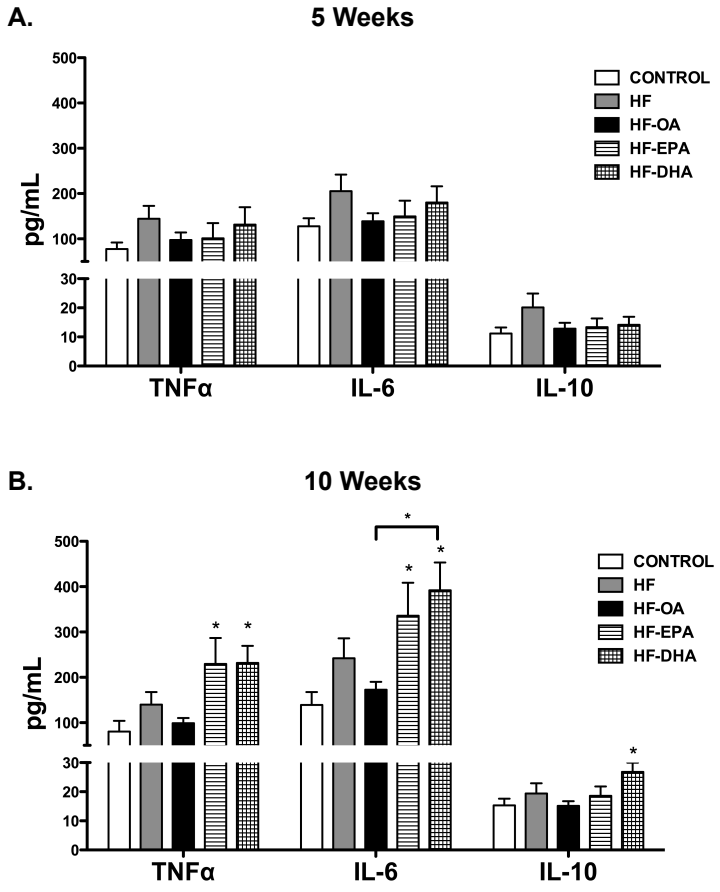

Figure 5.5: B-cell cytokine secretion is differentially enhanced with EPA and DHA.
Splenic B220^{+} B cells were isolated from C57BL/6 mice consuming control, HF, HF-OA, HF-EPA or HF-DHA diets for 5 or 10 weeks and stimulated for 24 hours with LPS. (A) TNFα, (B) IL-6, and (C) IL-10 cytokine levels from supernatants. Data are average ± S.E. from 8 animals per diet. Asterisks indicate significance from control unless indicated by a bracket: *p<0.05, **p<0.01, ***p<0.001.

EPA and DHA Ethyl Esters Differentially Promote the Molecular Order of Lipid Microdomains Without an Effect on TLR4 Lateral Mobility

The mechanisms of EPA and DHA are pleiotropic and we focused on the potential effects of EPA and DHA on *ex vivo* B-cell membrane organization. The studies relied first on Laurdan, a fluorescent membrane probe that detects changes in membrane polarity, to quantify changes in B-cell plasma membrane order upon the

formation of ordered membrane microdomains (Fig. 5.6A). After 5 weeks of feeding, there was no change in fluorescence intensity of Laurdan in the ordered and disordered fluorescence channels (Fig. 5.6B). GP values between all of the high fat diets relative to the control were unchanged. However, the GP value for HF-EPA was elevated relative to DHA by 39% (Fig. 5.6C).

After 10 weeks of feeding, HF-EPA significantly increased the fluorescence intensity in the ordered channel by 68% relative to the control (Fig. 5.6D). There was no effect of the HF diets on fluorescence intensity in the disordered channel (Fig. 5.6D). HF-EPA and HF-DHA, relative to the lean control, increased GP values by 20-21% (Fig. 5.6E). GP values were generally higher at 10 weeks of feeding compared to 5 weeks for all of the diets.

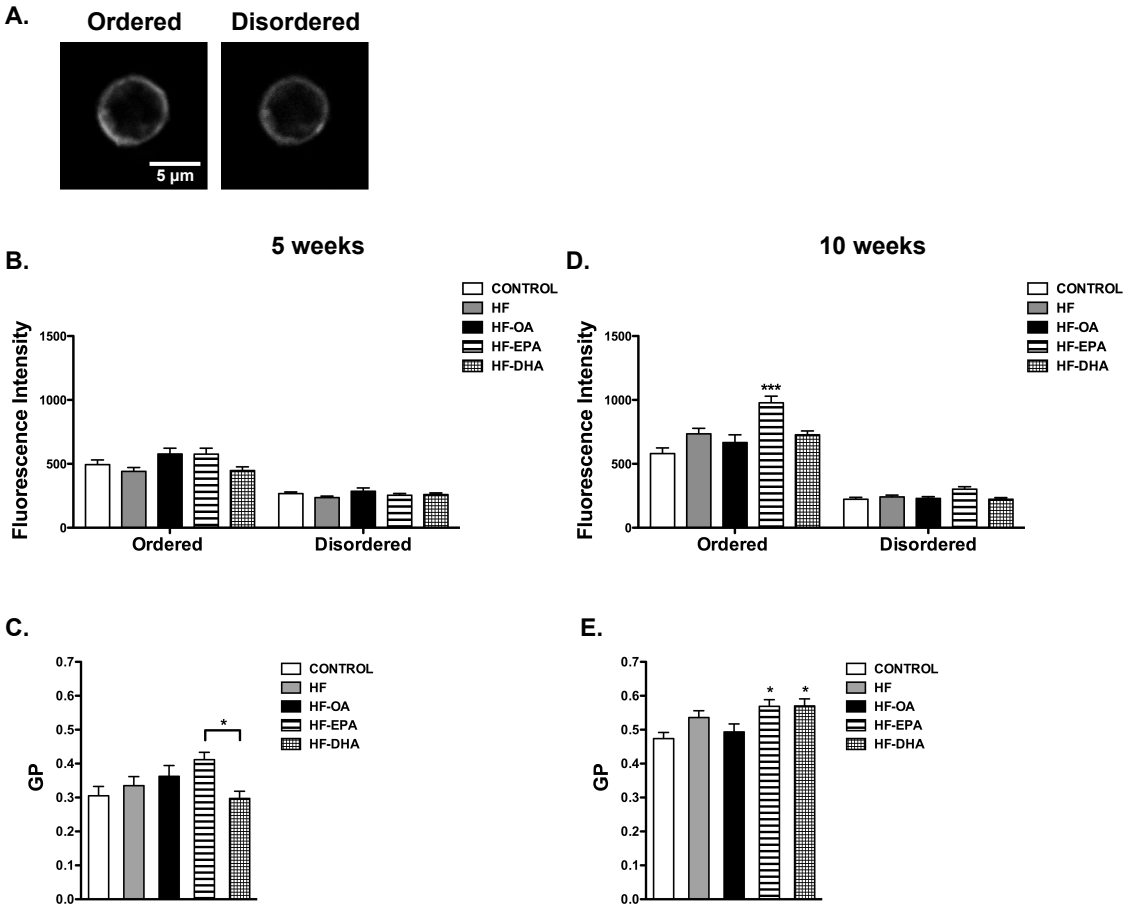

Figure 5.6: B-cell plasma membrane molecular organization is differentially elevated with EPA and DHA.
Splenic B220^{+} B cells were isolated from C57BL/6 mice consuming control, HF, HF-OA, HF-EPA or HF-DHA diets for 5 or 10 weeks and stained with Laurdan. (A) Sample images of Laurdan used to measure fluorescence intensities in the ordered (400-460 nm) and disordered (495-540 nm) channels and to calculate generalized polarization (GP). (B) Fluorescence intensities in the ordered and disordered channels and (C) GP values after 5 weeks of intervention. (D) Fluorescence intensities in the ordered and disordered channels and (E) the associated GP values after 10 weeks of intervention. Data are average ± S.E. from 4-5 animals per diet. Asterisks indicate significance from control unless indicated by a bracket: *p<0.05.

The increase in molecular order suggested that EPA and DHA may serve to lower the long-range diffusion of TLR4 molecules as a mechanism by which LPS stimulation

could enhance downstream B-cell activation. We therefore conducted FRAP microscopy of GFP-TLR4 upon LPS addition using an *in vitro* model system to calculate the fraction of mobile molecules and diffusion coefficients (Fig. 5.7A). We relied on treatment with fatty acids at 25 μM, which closely models the levels achieved *in vivo* (*156, 181*). TLR4 mobile fractions were not affected by treatment with OA, EPA, or DHA relative to the BSA control (Fig. 5.7B). Similarly, diffusion coefficients remained constant with OA, EPA, and DHA treatment compared to the BSA control (Fig. 5.7C).

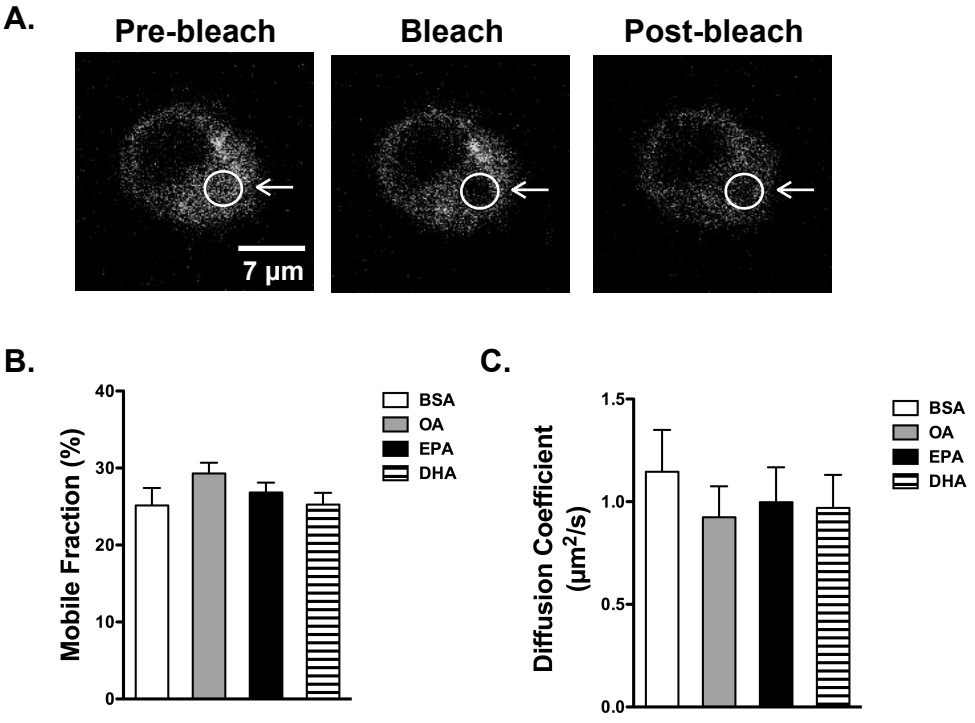

Figure 5.7: TLR4 lateral mobility is not lowered by EPA and DHA.
Ba/F3 stably transfected with GFP-TLR4 were treated for 24 hours with BSA or 25 μM OA, EPA, or DHA complexed to BSA. (A) Sample FRAP images for measuring the mobile fraction and diffusion coefficients. (B) Mobile fractions and (C) diffusion coefficients of GFP-TLR4. Data are average ± S.E. from 4 independent experiments.

Discussion

The field of immunity and diet has not addressed how EPA and DHA individually impact B-cell activity. This study advances the discipline by demonstrating that EPA and DHA ethyl esters, modeling human pharmacological intake, are not equivalent on enhancing B-cell activity in a murine model of diet-induced obesity. Furthermore, the data reveal that the effects of EPA and DHA are time-dependent and the underlying mechanism of action with B-cell cytokine secretion is independent of changes in TLR4 lateral diffusion.

EPA vs. DHA Ethyl Esters on B-cell Activity

The initial experiments on the obese phenotype established that we are studying mice with increased fat mass and poor glucose clearance and no excessive adipose tissue inflammation. Fasting insulin levels tended to be elevated but were not statistically significant. The lack of improvement in glucose clearance or fasting insulin with EPA and DHA was consistent with some clinical studies that reveal no benefits of n-3 PUFA consumption on glucose and insulin sensitivity (*269*).

The general paradigm is that EPA and DHA are immunosuppressive, anti-inflammatory, or inflammation-resolving molecules based on studies with macrophages, neutrophils, dendritic cells, and T cells in varying model systems (*83, 177, 183, 225, 270, 271*). Our lab initially identified immune enhancing properties of n-3 PUFA enriched fish oil on B-cell activity in lean mice, which was recently confirmed by others (*144, 260*). Here we tested the effects of EPA and DHA ethyl esters since they are used in clinical trials and for the treatment of elevated triglycerides (*6*). Elucidating the differences between EPA and DHA is of significance given that numerous studies at the

pre-clinical and clinical levels, focused mostly on inflammation, have relied on fish oils (e.g. menhaden, tuna oil) and prescription ethyl ester supplements (Lovaza) that are mixtures of EPA and DHA or more recently just one fatty acid (Vascepa) (*6, 272*). This contributes toward conflicting results in the field since the individual activity of EPA compared to DHA is much less studied. Our data establish that EPA and DHA are not biologically equivalent on several aspects of B-cell activity.

B1 B cells, in addition to marginal zone B cells, are the subtypes that readily produce IgM and class switch to IgA (*268, 273*). We measured an increase in the percentage and/or frequency of transitional 1 B cells, which contain B1 cells, with EPA and DHA after 10 weeks of feeding. This led us to measure natural IgM, which is generated predominately from splenic B1 cells (*268*). IgM levels were modestly elevated with EPA and DHA, which correlated with an increase in the percentage of transitional 1 B cells at 10 weeks of feeding. Similarly, EPA significantly increased cecal IgA, which correlated with the increase in the frequency of transitional 1 B cells. These studies suggest that changes in the frequency and/or percentage of B cells may be contributing toward enhanced antibody production and moreover, the effects of EPA and DHA are not equivalent. Future studies will need to address if the increase in the T1 compartment with EPA or DHA reflects an increase in B1 cells in addition to determining if B1a and B1b cells are elevated particularly in peritoneal cavities.

The *ex vivo* B-cell activation studies also revealed differences between EPA and DHA at 10 weeks. EPA and DHA increased TNFα and IL-6 secretion; however, only DHA increased IL-10 secretion. We did not measure upregulation of cell surface molecules given that our past studies with mice have consistently shown no effect of n-3

PUFAs on B-cell activation markers (*144, 181*). Interestingly, DHA, but not EPA, increased surface IgM, consistent with our previous studies with fish oil (*259*). The results with DHA increasing IL-10 secretion were consistent with a study by Olson et al., which showed that DHA increased *ex vivo* secretion of IL-10 from LPS-stimulated splenocytes (*273*). The results open the door to the possibility that DHA may increase IL-10 secretion from B cells *in vivo*, which could be driven by natural IgM. Natural IgM increases phagocytosis of apoptotic cells in the marginal zone to increase IL-10 secreting B cells (*268, 274*). Furthermore, improving IL-10 secretion in the adipose is of particular significance since IL-10 secreting B cells improve insulin sensitivity in obesity (*275*).

The studies also reveal that timing of intervention had an effect on the measured outcomes. Administration of EPA and/or DHA for 5 weeks during the early stages of weight gain did not have a robust effect on B-cell frequency, antibody production, and *ex vivo* cytokine secretion. On the other hand, prolonged exposure for 10 weeks significantly increased the functional outcomes of EPA and DHA. These results may explain some of the inconsistencies in the literature on the efficacy of EPA and DHA. For instance, some clinical studies have relied on short-term intervention while others have used long-term intervention (*276-278*). The differences in time may also reflect the age and the metabolic profile of the animals. Some studies have focused on moderately overweight individuals while others on more obese people (*269, 279*). Thus, the data suggest that future clinical trials targeting humoral immunity and likely other aspects of immunity with n-3 PUFAs will have to account for timing of intervention and the cohort of individuals that are being targeted.

An unexpected finding was that the two high fat diets in the absence of EPA and DHA had no influence on B-cell activity. Several studies report that high fat diets dysregulate B-cell driven humoral immunity (*280, 281*). Winer et al. demonstrated that high fat diets promote the accumulation of B cells in the adipose tissue that secrete pathogenic autoantibodies (*281*). We measured CD19 mRNA expression in the adipose and did not find an increase in its expression (data not shown). DeFuria et al. demonstrated that high fat diets increase *ex vivo* B-cell cytokine secretion (*282*). The data from our lab are not in complete agreement with the studies by Winer et al. and DeFuria et al. The discrepancy between our findings and the two aforementioned studies may be due to differences between the composition and the levels of the fat source (*281, 282*). This study relied on a moderate dose of milkfat (45% of total kcal), modeling human consumption, whereas others have used high fat diets (60% of total kcal from fat) enriched in lard (*283*). The unexpected results open a new area of investigation; that is, the possibility that dietary fat composition and content have differential effects on B-cell function.

Implications for the General Public and Clinical Trials

The general public is increasingly consuming n-3 PUFA supplements of varying composition (*6, 284*). The pre-clinical data show that EPA and DHA are not biologically equivalent and may have potential benefits for boosting IgM and IgA levels in select clinical populations. Several diseases are associated with altered humoral immunity (*285, 286*). In particular, the data suggest that EPA and DHA may have benefits for modestly elevating antibody levels in obesity, which is associated with increased susceptibility to infections and poor responses to vaccinations (*134, 139*). Given that the

majority of total IgM is natural IgM derived from B1 cells, we speculate that EPA and DHA could be developed for boosting IgM levels in atherosclerosis (*287*). Natural IgM suppresses the progression of atherosclerosis by clearance of oxidized low-density lipoprotein and apoptotic cells (*288*). This is of value in select clinical populations such as those with lupus that have increased susceptibility to cardiovascular disease which is associated with low levels of IgM antibodies against phosphorylcholine (*289, 290*). Similarly, enhancing IgA levels with EPA likely has potential benefits for boosting immunity. IgA, some of which is derived from B1 cells, has been shown to contribute toward clearing microbes from the gut (*268, 291*).

Potential Mechanisms

We previously proposed a model, based on studies with lean mice, in which n-3 PUFAs promote the formation of ordered lipid microdomains, which we suggested would lower the lateral diffusion of B-cell antigen receptors. Therefore, we first tested the effects of EPA and DHA on the molecular packing of ordered lipid microdomains. EPA and DHA ethyl esters increased the molecular packing of lipid microdomains, consistent with data to show n-3 PUFAs increase molecular order of lipid microdomains on the T-cell side of the immunological synapse (*165*). Furthermore, EPA and DHA ethyl esters exerted differential effects on the intensity of Laurdan in the ordered channel. EPA, but not DHA, selectively increased the fluorescence intensity of Laurdan in the ordered channel at 10 weeks, suggesting that EPA may have a stronger effect on ordered domains. Our results validate recent NMR studies in model membranes that show EPA and DHA are not structurally equivalent (*292, 293*).

Although paradoxical to the general notion that EPA and DHA simply decrease membrane packing, the data suggest that when these fatty acids interact with ordered domains, they increase their molecular order and can adapt to the ordered environment (*143, 294*). This may be driven by several variables, which include the loss of arachidonic acid, a highly disordered fatty acid, and a displacement of cholesterol from disordered to ordered domains (*143, 295*).

We next tested the effects of EPA and DHA on TLR4 diffusion. We relied on an *in vitro* model system with GFP-transfected TLR4 that would promote a high degree of TRL4 expression given that surface TLR4 expression is low on primary B cells. Contrary to our prediction, FRAP imaging showed that EPA and DHA did not lower TLR4 diffusion, as measured by the diffusion coefficient and mobile fraction. Thus, the data suggest EPA and DHA are not impacting long-range protein diffusion and may be influencing other aspects of protein lateral organization, likely on a nanometer scale. It is possible that EPA and DHA may also exert differential effects on B-cell activation downstream of the plasma membrane. One possibility is that EPA and DHA may differentially target downstream transcription factors, which would explain why DHA, but not EPA, enhances IL-10 secretion. For instance, in T cells, TNFα and IL-6 transcription proceeds through the NF-κB pathway, compared to IL-10 production regulated by the transcription factor CREB (*296*). Thus, it is possible that EPA and DHA target the membrane in different ways that eventually differentially impact downstream production of TNFα, IL-6 and IL-10.

Summary

In summary, this study showed that B-cell activity was differentially enhanced with EPA and DHA ethyl esters, modeling human pharmacological intake, in a time-dependent manner in diet-induced obesity. Furthermore, we demonstrated the effects of EPA and DHA were accompanied by significant changes in membrane packing independent of an effect on TLR4 diffusion. Our results show that EPA and DHA are not biologically equivalent on a key aspect of immunity, which has broad implications for the general public and select clinical populations that are increasingly consuming n-3 PUFAs.

CHAPTER 6 : DISCUSSION

Overview

A significant amount of literature addresses the immunosuppressive effects of n-3 PUFAs. In this study we tested the immune enhancing properties of n-3 PUFAs. We demonstrate n-3 PUFAs target B-cell mediated immunity and that EPA and DHA are not biologically equivalent. We began with mechanistic studies and determined DHA targets B-cell membrane organization and possesses the ability to adapt to the surrounding lipid microdomain environment. We then compared the effects of n-3 PUFAs between two antigen-presenting cells, DCs and B cells, and found that n-3 PUFAs exert cell-specific effects on the plasma membrane and functional outcomes. N-3 PUFAs enhanced B-cell cytokine production subsequent to LPS stimulation accompanied by a change in lipid microdomain organization while suppressing DC cytokine production with no effect on membrane microdomain organization.

We then established n-3 PUFAs enhance B-cell function at the *in vivo* level, boosting antibody production in a lean and obese model system. Finally, we utilized EPA and DHA ethyl esters and determined that EPA and DHA differentially enhance B-cell cytokine secretion and antibody production. Altogether, we provide novel insight into the *in vivo* effects of n-3 PUFAs on B-cell function and move the field forward in understanding the pleiotropic effects associated with these complex lipids.

N-3 PUFAs Differentially Target Lipid Microdomain Organization

N-3 PUFAs target immune cells on multiple levels from modifying lipid microdomain organization and membrane molecular order to serving as precursors for specialized proresolving lipid mediators, modifying intracellular signaling, regulating

gene expression, mediating transcriptional expression through histone modifications and acting as ligands for receptors such as GRP120 (*83, 297-299*). At the membrane level, it is known that DHA influences microviscosity, curvature stress, permeability, lipid microdomain formation, elasticity, protein conformation and phospholipid flip-flop; however the impact of the surrounding membrane environment on DHA molecular order is understudied (*141, 293*). It was timely to address how differential states of membrane order in artificial vesicles altered the molecular order of n-3 PUFAs. This allowed us to gain insight into how these highly disordered fatty acyl chains incorporated into the tightly packed lipid microdomains (*144, 300*). We determined, utilizing model membranes, that in an ordered environment, DHA adapted to its surroundings and became ordered (*294*). This finding was intriguing and provided insight as to how the exceptionally disordered DHA could infiltrate an ordered lipid microdomain. Studies by Mihailescu et al. also demonstrated the sensitivity of DHA to the surrounding environment (*164*). Mihailescu et al. showed that cholesterol increased the order of PC-containing DHA, therefore allowing DHA to favorably incorporate into lipid microdomains (*164*). Rockett et al. produced similar findings at the *ex vivo* level, demonstrating that in an un-stimulated environment n-3 PUFA treated B cells exhibited a decrease in membrane molecular order compared to the controls; however upon crosslinking of GM1, the membrane molecular order of the n-3 PUFA treated B cells became equivalent with the molecular order of the control cells (*144*). N-3 PUFAs also increased the molecular order of lipid microdomains on the $CD4^+$ T-cell side of the immunological synapse (*165*). NMR studies reveal the ability of DHA to infiltrate lipid microdomains is dependent on the phospholipid headgroup, proving that a larger headgroup like PC

allows for localization within the ordered lipid microdomain, compared to a PE-containing DHA that remains in the non-raft and more disordered region of the membrane (*300, 301*). One explanation recently proposed is that n-3 PUFAs exert ordering effects on the membrane by incorporating into lipid microdomains, resulting in a redistribution of cholesterol into to the disordered region, therefore creating an ordering effect on the more fluid regions of the membrane (*301*).

N-3 PUFAs Exert Distinct Functional Effects on Immune Cells

Lipid microdomains are the platforms assembled to stabilize receptors during receptor-mediated signaling. In T cells and macrophages, raft disruption by n-3 PUFAs suppresses cellular function (*87, 144, 165, 302*). Therefore we sought to determine if n-3 PUFAs altered lipid microdomain organization on the surface of two critical and understudied immune cells, B cells and DCs, and correlated our findings with changes in cellular activation. We determined the effects of n-3 PUFAs on lipid microdomain organization are specific to B cells, with no change observed on the DC surface. Furthermore, the observed changes in lipid microdomain organization on the B-cell surface were dose-dependent and attributed to DHA but not EPA (*293*). One explanation may be ascribed to the functional differences between the cell types. DCs are phagocytic cells with dendrites that protrude from the membrane, compared to B cells that are spherical in nature. The differing functions between the cell types may require unique lipid compositions.

N-3 PUFAs target B-cell function, suppressing antigen presentation concomitant with enhancing B-cell activation. We previously established n-3 PUFAs exert an ordering effect on the membrane and localize within lipid microdomains, modifications

that may differentially impact B-cell activation and antigen presentation. In the context of B-cell activation, a more ordered membrane may further stabilize the TLR4/MD-2 complex and therefore enhance signaling upon binding of LPS, leading to increased cytokine production. Mechanistically, one difference between B-cell activation and antigen presentation is B-cell activation is independent of T-cell interaction, compared to antigen presentation that requires formation of an immunological synapse with T cells within a lipid microdomain. It is known n-3 PUFAs affect the lateral displacement of proteins within lipid microdomains required for antigen presentation, thereby reducing the interaction between B and T cells and decreasing signaling (*224*). Furthermore, Rockett et al. demonstrated n-3 PUFAs suppressed MHC class II accumulation at the immunological synapse (*224, 260*). This resulted in decreased PKCθ recruitment in $CD4^+$ T cells and lowered IL-2 secretion (*224*). The lateral displacement of proteins from the immunological synapse also occurs in n-3 PUFA treated EL4 cells (*148, 149, 165*). Altogether, an increase in membrane order from n-3 PUFAs may enhance T-independent activation of B cells through TLR4, concomitant with suppressing antigen presentation from B cells by disrupting MHC class II lateral organization and decreasing T-cell signaling (*224*).

Although n-3 PUFAs did not effect lipid microdomain organization on the DC surface, n-3 PUFAs suppressed DC activation, phagocytosis and CD69 expression on CD4+ T cells. These findings are consistent with the current literature suggesting lipids play a key role in DC function. Weatherill et al. reported that DHA antagonized the upregulation of costimulatory molecules and pro-inflammatory cytokine secretion observed when DCs were stimulated through TLR4 by either saturated fatty acids or

bacterial LPS (*303, 304*). In addition, Zeyda et al. demonstrated both EPA and AA inhibited upregulation of costimulatory molecules and pro-inflammatory cytokine production from LPS stimulated DCs (*183, 303*). Similar effects were observed when treating human monocyte derived DCs with EPA, linoleic acid and OA, however the effects were not as robust as DHA (*198*). Two significant studies contribute to the possible mechanistic explanation behind the actions of n-3 PUFAs on DCs. Zapata-Gonzalez et al. revealed that DHA acts as a PPARγ agonist and showed the effects of DHA on DC activation are prevented by a PPARγ inhibitor (*198, 303*). More recent studies support a role for glycolysis and lipogenesis in TLR-mediated DC activation (*305, 306*). Glycolysis is rapidly induced upon TLR ligation, generating NADPH and TCA intermediates to support lipogenesis (*305, 306*). The fatty acids then enhance ER and Golgi membrane synthesis allowing them to fulfill the cellular activation requirements such as the production of pro-inflammatory cytokines (*305*). In hepatocytes, n-3 PUFAs enhance fatty acid oxidation and inhibit fatty acid synthesis by regulating key transcription factors such as PPARα, which could also occur in DCs (*307*). Combined, if n-3 PUFAs decrease lipogenesis in DCs, this may down-regulate ER and Golgi membrane synthesis, leading to decreased cytokine production. Future studies are required to determine the effects of n-3 PUFAs on the biochemical reactions required to sustain an innate immune response from DCs, and if altering DC lipogenesis plays a role in the suppression of DC activation.

N-3 PUFAs Boost Humoral Immunity

The ability to enhance B-cell function in an *ex vivo* model opened the door to developing n-3 PUFAs to boost humoral immunity clinically. Boosting humoral immunity

is efficacious to multiple immunosuppressed populations including cancer patients and the obese. Obesity is not only linked to the metabolic syndrome, it is now emerging that obese individuals have increased susceptibility to infections as a result of decreased levels of antibodies (*134, 139*). Therefore, we sought to determine if n-3 PUFAs could boost humoral immunity in a lean and obese model system *in vivo*. In two separate studies, we measured the n-3 PUFA-induced changes in TNP-specific and natural IgM levels in the serum. Interestingly, n-3 PUFAs elevated TNP-specific IgM production in lean mice compared to lean controls and recovered the decrement in TNP-specific IgM levels observed in mice consuming a high fat diet. Natural IgM and fecal IgA were also differentially increased following EPA or DHA ethyl ester supplementation to high fat diets. Concomitant with increased serum antibody levels, specific B-cell subsets showed an increase in frequency. These findings are of great significance due to the critical role of IgM in the immune response.

IgM is a unique antibody in that it has a low specificity for antigens; however, it neutralizes a wide range of pathogens due to its high avidity (*268, 308*). IgM is essential for the clearance of apoptotic cells, a fundamental process of the immune system and a requirement for the resolution of inflammation (*268, 309-312*). Recent studies suggest IgM has a central role in preventing an uncontrolled inflammatory response, and serum levels may predict influenza outcome (*313*). In the context of autoimmune diseases, the inability of IgM deficient mice to clear apoptotic debris results in the development of a lupus-like syndrome (*268*). In addition, IgM deficient mice produce IgG autoantibodies (*109, 314*). Furthermore, in hyperlipidemic mice, IgM deficiency increased their susceptibility to developing atherosclerosis (*252*). Therefore, boosting both antigen-

specific and natural IgM levels in obese individuals may protect against the development of atherosclerosis, decrease chronic inflammation by aiding in the clearance of apoptotic cells and debris, and may improve the outcome to common infections.

The immunoglobulin responsible for maintaining host-commensal mutualism in the intestinal lumen is IgA (*315*). When secreted, this polymeric antibody coats commensal bacteria and soluble antigens to inhibit their binding to the host epithelium, preventing penetration into the lamina propria (*315, 316*). IgA deficiency results in alterations in the composition of the gut microbiota, which is proving to be a crucial factor in disease development (*315*). The balance in gut microbiota has been studied in multiple prevalent diseases including multiple sclerosis, rheumatoid arthritis and type 1 diabetes (*315, 317-321*). In both multiple sclerosis and rheumatoid arthritis, symptoms are reduced in mouse models housed in germ-free conditions (*318-320*). However, in type 1 diabetes, certain bacterial populations may provide protection against disease development (*315*). In our studies, EPA ethyl esters supplemented to a high fat diet elevated IgA levels in the gut. Due to the critical nature of IgA maintaining host-commensal mutualism, it is imperative to understand how this increase in IgA impacts the microbiota populations in order to avoid n-3 PUFA administration to populations that may experience negative outcomes. In addition, this finding warrants studies on the possible improvement of conditions such as multiple sclerosis and rheumatoid arthritis due to increased IgA production.

Mice consuming an n-3 PUFA diet exhibited an elevated number of splenic B cells and altered B-cell subsets, which may mechanistically contribute to increased

levels of circulating IgM. B-1 B cells residing in the spleen are responsible for a large amount of IgM production (*99*). Additionally, n-3 PUFAs, specifically DHA, elevated the surface expression of membrane bound IgM, the BCR, which could also lead to increased signaling. The specialized proresolving mediators resolvin D1 (RvD1) and 17(R)-hydroxy docosahexaenoic acid (17-HDHA) may be responsible for the elevation in IgM production (*322*). Recent *in vitro* studies demonstrate that RvD1 and 17-HDHA increased antigen specific IgM from human $CD19^+$ B cells when stimulated with CpG ODN 2395 and anti-IgM (*322*). 17-HDHA increased both IgM and IgG levels in the supernatants after 7 days of incubation in a dose-dependent manner (*322*). B-cell proliferation assays revealed 17-HDHA did not influence the number of B cells, however increased the number of B cells secreting IgM and IgG in a dose-dependent manner (*322*). RvD1 and 17-HDHA are both found in the spleen and synthesized from DHA (*322*). Future *in vivo* investigations are required to determine if these lipid metabolites are driving the increase in circulating IgM. Future studies are also needed to further understand how n-3 PUFAs impact the function and frequency of select B-cell subsets in mouse (Table 6.1) and human. It will be of interest to determine if EPA and DHA specifically target B1 B cells and regulatory B cells, key immune cells in obesity (*281, 323*).

Table 6.1: A comprehensive list of murine B-cell subsets and their corresponding phenotypes and functions.

B-Cell Subset	Phenotype	Characteristics and Functional Role	Ref.
Pre-Pro	$B220^{+}CD19^{-}$ $CD24^{lo}CD43^{+}$ IgM^{-}	B-cell precursors in the bone marrow lacking heavy-chain DJ rearrangements.	(*324, 325*)
Pre	$B220^{+}CD19^{+}$ $CD24^{+}CD43^{-}$ IgM^{-}	Express a pre-BCR, a checkpoint in B-cell development, in which signaling induces proliferation and recombination of the immunoglobulin light chain.	(*97, 324*)
Immature	$B220^{+}CD19^{+}$ $CD24^{+}CD43^{-}$ IgM^{+}	Express a functional BCR and then exit the bone marrow and home to the secondary lymphoid organs for further development. Immature B cells undergo a negative selection process before maturing to B cells in which BCR cross-linking results in activation.	(*324, 326*)
Transitional 1	$B220^{+}CD19^{+}$ $CD22^{hi}CD23^{-}$ $CD21^{lo}IgM^{hi}IgD^{lo}$	Newly generated non-circulating B cells found in bone marrow and spleen. Survival is dependent upon BCR signals. Give rise to follicular and marginal zone B cells.	(*94, 327*)
Transitional 2	$B220^{+}CD19^{+}$ $CD22^{hi}CD23^{+}$ $CD21^{mid}IgM^{hi}IgD^{+}$	Earliest B cells to express CD23, persisting in all B-cell follicles. Attain the ability to re-circulate and represent clones that were not eliminated by self-tolerance.	(*94, 327*)
Marginal Zone	$B220^{+}IgM^{hi}IgD^{lo}$ $CD21^{hi}CD43^{-}$ $CD23^{-}CD1d^{hi}$	Localized to the marginal sinus where they respond rapidly to blood-borne pathogens. Express high levels of CD1d for lipid antigen presentation. Elevated CD21 levels facilitate transport of immune complexes from the circulation to the splenic follicles. Equipped to elicit T-independent immune responses.	(*94, 99, 327*)
Follicular	$B220^{hi}CD19^{+}$ $CD23^{hi}CD1d^{mid}$ $CD21^{mid}IgM^{lo}IgD^{hi}$	Recirculating conventional B cells equipped to elicit T-cell dependent responses to protein antigens.	(*94, 99, 327*)
B-1	$CD19^{+}IgM^{hi}$ $CD5^{+/-}CD43^{+}$ $CD23^{-}IgD^{lo}$ $Cd1d^{mid}$	Generated before birth and the fetal liver is an efficient source. B-1a cells are poorly reconstituted by adult bone marrow. B-1a cells secrete polyreactive IgM in an antigen-independent manner. B-1b cells produce antibodies after encountering T cell independent antigens.	(*99*)
IL-35 Producing	$IgM^{+}CD138^{hi}$ $CD43^{+}TACI^{+}$ $CXCR4^{+}CD1d^{mid}$ $Tim1^{mid}$	Express anti-inflammatory cytokines, excluding IL-6, and are critical regulators of T-cell mediated immunity.	(*118*)
Regulatory	$CD5^{+}CD19^{hi}$ $CD1d^{+/hi}CD21^{+}$	Depend upon CD19 for development. Regulate inflammatory responses with IL-10 production.	(*99, 114*)

	$CD23^{+/-}CD43^{+/-}$ $IgM^{hi}IgD^{lo/mid}$	Variable cell-surface phenotype.	
Plasma Cells	$CD138^{+}$Surface Ig^{neg}	Terminally differentiated, non-dividing B cells that secrete substantial amounts of clonospecific antibodies. They rapidly respond to microbial pathogens.	(*118, 328*)
Memory	$B220^{+}$ $CD80^{+/-}$\PD-$L2^{+/-}$ $CD73^{+/-}$	Quiescent, non-antibody secreting B cells that have previously encountered antigen. These cells are poised to rapidly participate in secondary antibody responses.	(*329, 330*)
Innate Response Activator	$IgM^{hi}CD23^{lo}$ $CD43^{+}CD93^{+}$	An inflammatory B-cell subset derived from transitional B-1a B cells. They control IgM production via autocrine granulocyte/macrophage colony-stimulating factor signaling.	(*331, 332*)

N-3 PUFAs Exert Time-dependent Effects

The timing of n-3 PUFA intervention impacts the observed functional changes. In chapter 4 we sought to determine if n-3 PUFAs enhanced B-cell function. We injected a T-independent antigen at 3 weeks, due to the maximum uptake of n-3 PUFAs by B cells occurring at 3 weeks, and allowed 7 days for an immune response to be elicited. Serum IgM showed an increasing trend in the n-3 PUFA fed mice compared to the control, however failed to establish significance. We extended the following study to 10 weeks in order to develop a diet-induced obesity model, characterized by elevated body weight, and injected the T-independent antigen at week 9. Surprisingly, serum IgM levels were elevated in the mice consuming the lean n-3 PUFA diet compared to the lean controls.

We subsequently designed a 5-week and 10-week study investigating the effects of EPA and DHA ethyl esters on natural IgM and fecal IgA. Minimal changes from EPA and DHA ethyl esters were observed subsequent to the 5-week feeding period. At 10 weeks, EPA and DHA ethyl esters differentially increased antibody production,

differentially elevated select surface markers, altered B-cell subsets, increased membrane molecular order and differentially increased cytokine secretion from LPS stimulated B cells. These studies demonstrate that intervention timing is a critical factor when designing clinical trials and present more questions to be addressed. For example, at what time period do the effects of n-3 PUFAs plateau? Is long-term n-3 PUFA consumption safe or should the time frame be limited? Addressing these questions will determine the maximum change n-3 PUFAs exert over time and move the field forward in developing n-3 PUFAs for clinical utilization.

The Implications of N-3 PUFAs on B-cell Function in Disease States

Overall, the data presented highlight the immune enhancing effects of n-3 PUFAs on B-cell mediated immunity and suggest n-3 PUFA supplementation may modestly improve the pathological outcome of chronic inflammatory diseases associated with obesity. The role of B cells in insulin resistance gained negative attention when Winer et al. demonstrated a high fat diet increased B-cell infiltration into adipose tissue and resulted in the secretion of pathogenic IgG antibodies ultimately resulting in insulin resistance (*281*). In these studies, B-cell elimination abrogated adipose tissue inflammation and insulin/glucose sensitivity (*281*). One key detail in the study by Winer et al. is the high fat-fed mice exhibit decreased levels of IgM (*281*). As previously discussed, a deficiency in IgM in hyperlipidemic mice results in autoantibody IgG production concomitant with increased susceptibility to the development of atherosclerotic lesions (*252, 268, 314*). It is possible the development of insulin resistance was a result of the impaired ability of B cells to produce natural IgM, leading to the production of pathogenic IgG antibodies, decreased apoptosis and increased

inflammation (*268, 281*). Enhancing natural IgM production via n-3 PUFA supplementation rather than eliminating B cells may prevent the development of pathogenic IgG antibodies, improve the clearance of necrotic adipocytes and decrease chronic inflammation. Similarly, in atherosclerosis the continual recruitment of leukocytes combined with the failure to remove apoptotic polymorphonuclear neutrophils contributes to the development of atherosclerotic lesions, a condition typically associated with obesity (*333*). It is possible increased IgM levels combined with increased biosynthesis of specialized proresolving mediators, may prevent the generation of pathogenic IgG antibodies and prevent polymorphonuclear neutrophil accumulation in atherosclerotic lesions by enhancing clearance of apoptotic cells (*334*). Further investigations are warranted to determine if n-3 PUFAs improve the response to infections in an obese state, however the increase in antibody production to a T-independent antigen provides evidence this may be the case.

As the rate of obesity continues to escalate, the negative consequences associated with obesity are continually being elucidated. Most recently, obesity was identified as an independent risk factor for influenza morbidity (*137, 139, 335*). One explanation for the increased risk is a higher BMI is associated with a decline in influenza antibody titers post vaccination, suggesting obesity patients exhibit in suppressed humoral immune response (*139*). In our obesity model, we observed an increase in both natural and antigen-specific antibody production subsequent to n-3 PUFA consumption. Furthermore, the decrement in antibody production observed in the diet-induced obesity model was recovered upon n-3 PUFA supplementation. This opens the door to the possibility of utilizing n-3 PUFAs as a method to boost antibody

production in obese individuals to improve influenza survival rates. As previously mentioned, elevating natural IgM levels alone could improve the outcome of influenza infection (*313*). Several studies have identified n-3 PUFA-derived lipid mediators as a source of improvement to influenza infection (*336*). Ramon et al. demonstrated mice immunized with influenza derived-HA coupled with 17-HDHA resulted in increased hemagglutinin (HA)-specific IgM and IgG levels compared to those immunized with HA alone (*337*). Morita et al. determined protectin D1, a DHA-derived lipid mediator, suppresses influenza virus replication and protects against lethal influenza infection (*336*). Although treatment with pro-resolving lipid mediators reveals promising results, determining if n-3 PUFA dietary supplementation boosts humoral immunity in an infection model is critical.

Negative Outcomes and Future Explorations

Although n-3 PUFAs prove to have immune boosting properties, the possible negative consequences associated with n-3 PUFA consumption need to be considered. For example, patients with systemic and discoid lupus erythematosus exhibit elevated IgM, IgA and IgG antibody levels (*338*). Further increasing antibody production may exacerbate the disease. In obese patients, n-3 PUFAs could increase insulin (*83*) resistance by enhancing pathogenic IgG production rather than reducing IgG through increased IgM (*281*). Deciphering the mechanisms n-3 PUFAs boost B-cell mediated immunity will aid in the assessment of which populations benefit most from n-3 PUFA supplementation and which populations should not consume high levels of n-3 PUFAs.

The role GPR120 receptors, G-protein-coupled receptors for long chain n-3 PUFAs, play in the inflammatory response has become a topic of great interest (*83, 85,*

339). Current studies are focused on the expression of GPR120 on macrophages and adipocytes, revealing ligation of GPR120 with DHA inhibits TGF-β activated kinase 1 (TAB1)-mediated inflammation (*83*). Furthermore, Ichimura et al. demonstrated GPR120 deficient mice exhibit glucose intolerance, fatty liver, decreased adipocyte differentiation and lipogenesis, and enhanced liver lipogenesis (*339*). Ichimura et al. then investigated adipose tissue from obese subjects and found they expressed a non-responsive GPR120 receptor due to a deleterious non-synonymous mutation that inhibits signaling (*339*). Altogether, the data highlight the critical role GPR120 receptors play in regulating inflammation and reveal a mutation in obese subjects, which may be linked to the development of obesity (*339*). Although these findings reveal novel concepts regarding the inflammatory response and n-3 PUFAs, the data are confined to macrophages and adipocytes. The expression of GPR120 on other cells types, specifically B cells, remains un-investigated and presents and entire area for examination.

Conclusion

All together, this work highlights the functional enhancement n-3 PUFAs exert on B cells, increasing the possibilities for clinical utilization. It emphasizes that intervention timing is a critical step for designing experiments investigating n-3 PUFAs, and establishes that EPA and DHA differentially target B-cell function. Lastly, these studies establish pharmacologically relevant doses of n-3 PUFA may provide beneficial outcomes in immunosuppressed individuals such as the obese. The data also warrant future mechanistic studies on how EPA and DHA boost B-cell activity.

REFERENCES

1. Bang, H. O., Dyerberg, J., and Nielsen, A. B. (1971) Plasma lipid and lipoprotein pattern in Greenlandic West-coast Eskimos, *Lancet 1*, 1143-1145.

2. Bang, H. O., Dyerberg, J., and Sinclair, H. M. (1980) The composition of the Eskimo food in north western Greenland, *Am J Clin Nutr 33*, 2657-2661.

3. Yates, C. M., Calder, P. C., and Ed Rainger, G. (2014) Pharmacology and therapeutics of omega-3 polyunsaturated fatty acids in chronic inflammatory disease, *Pharmacol Ther 141*, 272-282.

4. Shaikh, S. R., and Edidin, M. (2006) Polyunsaturated fatty acids, membrane organization, T cells, and antigen presentation, *Am J Clin Nutr 84*, 1277-1289.

5. Kris-Etherton, P. M., Harris, W. S., and Appel, L. J. (2002) Fish consumption, fish oil, omega-3 fatty acids, and cardiovascular disease, *Circulation 106*, 2747-2757.

6. Maki, K. C., Lawless, A. L., Kelley, K. M., Dicklin, M. R., Kaden, V. N., Schild, A. L., Rains, T. M., and Marshall, J. W. (2011) Effects of prescription omega-3-acid ethyl esters on fasting lipid profile in subjects with primary hypercholesterolemia, *J Cardiovasc Pharmacol 57*, 489-494.

7. Rupp, H. (2009) Omacor (prescription omega-3-acid ethyl esters 90): From severe rhythm disorders to hypertriglyceridemia, *Adv Ther 26*, 675-690.

8. Neubronner, J., Schuchardt, J. P., Kressel, G., Merkel, M., von Schacky, C., and Hahn, A. (2011) Enhanced increase of omega-3 index in response to long-term n-3 fatty acid supplementation from triacylglycerides versus ethyl esters, *Eur J Clin Nutr 65*, 247-254.

9. Schuchardt, J. P., Schneider, I., Meyer, H., Neubronner, J., von Schacky, C., and Hahn, A. (2011) Incorporation of EPA and DHA into plasma phospholipids in response to different omega-3 fatty acid formulations--a comparative bioavailability study of fish oil vs. krill oil, *Lipids Health Dis 10*, 145.

10. de Gomez Dumm, I. N., and Brenner, R. R. (1975) Oxidative desaturation of alpha-linoleic, linoleic, and stearic acids by human liver microsomes, *Lipids 10*, 315-317.

11. Arterburn, L. M., Hall, E. B., and Oken, H. (2006) Distribution, interconversion, and dose response of n-3 fatty acids in humans, *Am J Clin Nutr 83*, 1467S-1476S.

12. Bezard, J., Blond, J. P., Bernard, A., and Clouet, P. (1994) The metabolism and availability of essential fatty acids in animal and human tissues, *Reprod Nutr Dev 34*, 539-568.

13. Jump, D. B. (2008) N-3 polyunsaturated fatty acid regulation of hepatic gene transcription, *Curr Opin Lipidol 19*, 242-247.

14. Emken, E. A., Adlof, R. O., and Gulley, R. M. (1994) Dietary linoleic acid influences desaturation and acylation of deuterium-labeled linoleic and linolenic acids in young adult males, *Biochim Biophys Acta 1213*, 277-288.

15. Farooqui, A. A., and SpringerLink (Online service). (2009) Beneficial Effects of Fish Oil on Human Brain, 1. ed., Springer-Verlag New York, New York, NY.

16. Djouadi, F., Weinheimer, C. J., Saffitz, J. E., Pitchford, C., Bastin, J., Gonzalez, F. J., and Kelly, D. P. (1998) A gender-related defect in lipid metabolism and glucose homeostasis in peroxisome proliferator- activated receptor alpha- deficient mice, *J Clin Invest 102*, 1083-1091.

17. Abumrad, N. A., and Davidson, N. O. (2012) Role of the gut in lipid homeostasis, *Physiol Rev 92*, 1061-1085.

18. Jump, D. B. (2002) The biochemistry of n-3 polyunsaturated fatty acids, *J Biol Chem 277*, 8755-8758.

19. Stulnig, T. M. (2003) Immunomodulation by polyunsaturated fatty acids: mechanisms and effects, *Int Arch Allergy Immunol 132*, 310-321.

20. Stillwell, W., Shaikh, S. R., Zerouga, M., Siddiqui, R., and Wassall, S. R. (2005) Docosahexaenoic acid affects cell signaling by altering lipid rafts, *Reprod Nutr Dev 45*, 559-579.

21. Fliesler, S. J., and Anderson, R. E. (1983) Chemistry and metabolism of lipids in the vertebrate retina, *Prog Lipid Res 22*, 79-131.

22. Stubbs, C. D., and Smith, A. D. (1984) The modification of mammalian membrane polyunsaturated fatty acid composition in relation to membrane fluidity and function, *Biochim Biophys Acta 779*, 89-137.

23. Quehenberger, O., Armando, A. M., Brown, A. H., Milne, S. B., Myers, D. S., Merrill, A. H., Bandyopadhyay, S., Jones, K. N., Kelly, S., Shaner, R. L., Sullards, C. M., Wang, E.,

Murphy, R. C., Barkley, R. M., Leiker, T. J., Raetz, C. R., Guan, Z., Laird, G. M., Six, D. A., Russell, D. W., McDonald, J. G., Subramaniam, S., Fahy, E., and Dennis, E. A. (2010) Lipidomics reveals a remarkable diversity of lipids in human plasma, *J Lipid Res 51*, 3299-3305.

24. Andreyev, A. Y., Fahy, E., Guan, Z., Kelly, S., Li, X., McDonald, J. G., Milne, S., Myers, D., Park, H., Ryan, A., Thompson, B. M., Wang, E., Zhao, Y., Brown, H. A., Merrill, A. H., Raetz, C. R., Russell, D. W., Subramaniam, S., and Dennis, E. A. (2010) Subcellular organelle lipidomics in TLR-4-activated macrophages, *J Lipid Res 51*, 2785-2797.

25. Healy, D. A., Wallace, F. A., Miles, E. A., Calder, P. C., and Newsholm, P. (2000) Effect of low-to-moderate amounts of dietary fish oil on neutrophil lipid composition and function, *Lipids 35*, 763-768.

26. Georas, S. N., Guo, J., De Fanis, U., and Casolaro, V. (2005) T-helper cell type-2 regulation in allergic disease, *Eur Respir J 26*, 1119-1137.

27. Galan, P., Kesse-Guyot, E., Czernichow, S., Briancon, S., Blacher, J., and Hercberg, S. (2010) Effects of B vitamins and omega 3 fatty acids on cardiovascular diseases: a randomised placebo controlled trial, *Bmj 341*, c6273.

28. Cawood, A. L., Ding, R., Napper, F. L., Young, R. H., Williams, J. A., Ward, M. J., Gudmundsen, O., Vige, R., Payne, S. P., Ye, S., Shearman, C. P., Gallagher, P. J., Grimble, R. F., and Calder, P. C. (2010) Eicosapentaenoic acid (EPA) from highly concentrated n-3 fatty acid ethyl esters is incorporated into advanced atherosclerotic plaques and higher plaque EPA is associated with decreased plaque inflammation and increased stability, *Atherosclerosis 212*, 252-259.

29. Kremer, J. M., Bigauoette, J., Michalek, A. V., Timchalk, M. A., Lininger, L., Rynes, R. I., Huyck, C., Zieminski, J., and Bartholomew, L. E. (1985) Effects of manipulation of dietary fatty acids on clinical manifestations of rheumatoid arthritis, *Lancet 1*, 184-187.

30. Calder, P. C. (2006) n-3 polyunsaturated fatty acids, inflammation, and inflammatory diseases, *Am J Clin Nutr 83*, 1505S-1519S.

31. Remans, P. H., Sont, J. K., Wagenaar, L. W., Wouters-Wesseling, W., Zuijderduin, W. M., Jongma, A., Breedveld, F. C., and Van Laar, J. M. (2004) Nutrient supplementation with polyunsaturated fatty acids and micronutrients in rheumatoid arthritis: clinical and biochemical effects, *Eur J Clin Nutr 58*, 839-845.

32. Robinson, J. G., and Stone, N. J. (2006) Antiatherosclerotic and antithrombotic effects of omega-3 fatty acids, *Am J Cardiol 98*, 39i-49i.

33. Berge, R. K., Madsen, L., Vaagenes, H., Tronstad, K. J., Gottlicher, M., and Rustan, A. C. (1999) In contrast with docosahexaenoic acid, eicosapentaenoic acid and hypolipidaemic derivatives decrease hepatic synthesis and secretion of triacylglycerol by decreased diacylglycerol acyltransferase activity and stimulation of fatty acid oxidation, *Biochem J 343 Pt 1*, 191-197.

34. Davidson, M. H. (2006) Mechanisms for the hypotriglyceridemic effect of marine omega-3 fatty acids, *Am J Cardiol 98*, 27i-33i.

35. He, K., Song, Y., Daviglus, M. L., Liu, K., Van Horn, L., Dyer, A. R., and Greenland, P. (2004) Accumulated evidence on fish consumption and coronary heart disease mortality: a meta-analysis of cohort studies, *Circulation 109*, 2705-2711.

36. Kromhout, D., Giltay, E. J., and Geleijnse, J. M. (2010) n-3 fatty acids and cardiovascular events after myocardial infarction, *N Engl J Med 363*, 2015-2026.

37. Yokoyama, M., Origasa, H., Matsuzaki, M., Matsuzawa, Y., Saito, Y., Ishikawa, Y., Oikawa, S., Sasaki, J., Hishida, H., Itakura, H., Kita, T., Kitabatake, A., Nakaya, N., Sakata, T., Shimada, K., and Shirato, K. (2007) Effects of eicosapentaenoic acid on major coronary events in hypercholesterolaemic patients (JELIS): a randomised open-label, blinded endpoint analysis, *Lancet 369*, 1090-1098.

38. Stamp, L. K., James, M. J., and Cleland, L. G. (2005) Diet and rheumatoid arthritis: a review of the literature, *Semin Arthritis Rheum 35*, 77-94.

39. James, M. J., and Cleland, L. G. (1997) Dietary n-3 fatty acids and therapy for rheumatoid arthritis, *Semin Arthritis Rheum 27*, 85-97.

40. Fritsche, K. (2006) Fatty acids as modulators of the immune response, *Annu Rev Nutr 26*, 45-73.

41. Sorensen, L. S., Thorlacius-Ussing, O., Schmidt, E. B., Rasmussen, H. H., Lundbye-Christensen, S., Calder, P. C., and Lindorff-Larsen, K. (2014) Randomized clinical trial of perioperative omega-3 fatty acid supplements in elective colorectal cancer surgery, *Br J Surg 101*, 33-42.

42. Hlais, S., El-Bistami, D., El Rahi, B., Mattar, M. A., and Obeid, O. A. (2013) Combined fish oil and high oleic sunflower oil supplements neutralize their individual effects on the lipid profile of healthy men, *Lipids 48*, 853-861.

43. Mocellin, M. C., Pastore e Silva Jde, A., Camargo Cde, Q., Fabre, M. E., Gevaerd, S., Naliwaiko, K., Moreno, Y. M., Nunes, E. A., and Trindade, E. B. (2013) Fish oil

decreases C-reactive protein/albumin ratio improving nutritional prognosis and plasma fatty acid profile in colorectal cancer patients, *Lipids 48*, 879-888.

44. Nakamura, M. T., Cheon, Y., Li, Y., and Nara, T. Y. (2004) Mechanisms of regulation of gene expression by fatty acids, *Lipids 39*, 1077-1083.

45. Benatti, P., Peluso, G., Nicolai, R., and Calvani, M. (2004) Polyunsaturated fatty acids: biochemical, nutritional and epigenetic properties, *J Am Coll Nutr 23*, 281-302.

46. Yaqoob, P. (2003) Fatty acids as gatekeepers of immune cell regulation, *Trends Immunol 24*, 639-645.

47. Zuidscherwoude, M., de Winde, C. M., Cambi, A., and van Spriel, A. B. (2014) Microdomains in the membrane landscape shape antigen-presenting cell function, *J Leukoc Biol 95*, 251-263.

48. Singer, S. J., and Nicolson, G. L. (1972) The fluid mosaic model of the structure of cell membranes, *Science 175*, 720-731.

49. Simons, K., and Gerl, M. J. (2010) Revitalizing membrane rafts: new tools and insights, *Nat Rev Mol Cell Biol 11*, 688-699.

50. Pike, L. J. (2006) Rafts defined: a report on the Keystone Symposium on Lipid Rafts and Cell Function, *J Lipid Res 47*, 1597-1598.

51. Simons, K., and Ikonen, E. (1997) Functional rafts in cell membranes, *Nature 387*, 569-572.

52. Jacobson, K., Sheets, E. D., and Simson, R. (1995) Revisiting the fluid mosaic model of membranes, *Science 268*, 1441-1442.

53. Triantafilou, M., Morath, S., Mackie, A., Hartung, T., and Triantafilou, K. (2004) Lateral diffusion of Toll-like receptors reveals that they are transiently confined within lipid rafts on the plasma membrane, *J Cell Sci 117*, 4007-4014.

54. Wong, W., and Schlichter, L. C. (2004) Differential recruitment of Kv1.4 and Kv4.2 to lipid rafts by PSD-95, *J Biol Chem 279*, 444-452.

55. Lingwood, D., and Simons, K. (2010) Lipid rafts as a membrane-organizing principle, *Science 327*, 46-50.

56. Leslie, M. (2011) Mysteries of the cell. Do lipid rafts exist?, *Science 334*, 1046-1047.

57. Lingwood, D., and Simons, K. (2007) Detergent resistance as a tool in membrane research, *Nat Protoc 2*, 2159-2165.

58. Macdonald, J. L., and Pike, L. J. (2005) A simplified method for the preparation of detergent-free lipid rafts, *J Lipid Res 46*, 1061-1067.

59. Hell, S. W. (2007) Far-field optical nanoscopy, *Science 316*, 1153-1158.

60. Schermelleh, L., Heintzmann, R., and Leonhardt, H. (2010) A guide to super-resolution fluorescence microscopy, *J Cell Biol 190*, 165-175.

61. Rust, M. J., Bates, M., and Zhuang, X. (2006) Sub-diffraction-limit imaging by stochastic optical reconstruction microscopy (STORM), *Nat Methods 3*, 793-795.

62. Owen, D. M., Williamson, D. J., Magenau, A., and Gaus, K. (2012) Sub-resolution lipid domains exist in the plasma membrane and regulate protein diffusion and distribution, *Nat Commun 3*, 1256.

63. Edidin, M. (2003) The state of lipid rafts: from model membranes to cells, *Annu Rev Biophys Biomol Struct 32*, 257-283.

64. Fan, Y. Y., Ly, L. H., Barhoumi, R., McMurray, D. N., and Chapkin, R. S. (2004) Dietary docosahexaenoic acid suppresses T cell protein kinase C theta lipid raft recruitment and IL-2 production, *J Immunol 173*, 6151-6160.

65. Zeyda, M., Staffler, G., Horejsi, V., Waldhausl, W., and Stulnig, T. M. (2002) LAT displacement from lipid rafts as a molecular mechanism for the inhibition of T cell signaling by polyunsaturated fatty acids, *J Biol Chem 277*, 28418-28423.

66. Liang, X., Nazarian, A., Erdjument-Bromage, H., Bornmann, W., Tempst, P., and Resh, M. D. (2001) Heterogeneous fatty acylation of Src family kinases with polyunsaturated fatty acids regulates raft localization and signal transduction, *J Biol Chem 276*, 30987-30994.

67. Wassall, S. R., and Stillwell, W. (2008) Docosahexaenoic acid domains: the ultimate non-raft membrane domain, *Chem Phys Lipids 153*, 57-63.

68. Stulnig, T. M., Berger, M., Sigmund, T., Raederstorff, D., Stockinger, H., and Waldhausl, W. (1998) Polyunsaturated fatty acids inhibit T cell signal transduction by modification of detergent-insoluble membrane domains, *J Cell Biol 143*, 637-644.

69. Stulnig, T. M., Huber, J., Leitinger, N., Imre, E. M., Angelisova, P., Nowotny, P., and Waldhausl, W. (2001) Polyunsaturated eicosapentaenoic acid displaces proteins from membrane rafts by altering raft lipid composition, *J Biol Chem 276*, 37335-37340.

70. Serhan, C. N., Chiang, N., and Van Dyke, T. E. (2008) Resolving inflammation: dual anti-inflammatory and pro-resolution lipid mediators, *Nat Rev Immunol 8*, 349-361.

71. Calder, P. C. (2013) Omega-3 polyunsaturated fatty acids and inflammatory processes: nutrition or pharmacology?, *Br J Clin Pharmacol 75*, 645-662.

72. Lewis, R. A., Austen, K. F., and Soberman, R. J. (1990) Leukotrienes and other products of the 5-lipoxygenase pathway. Biochemistry and relation to pathobiology in human diseases, *N Engl J Med 323*, 645-655.

73. Tilley, S. L., Coffman, T. M., and Koller, B. H. (2001) Mixed messages: modulation of inflammation and immune responses by prostaglandins and thromboxanes, *J Clin Invest 108*, 15-23.

74. Kroetz, D. L., and Zeldin, D. C. (2002) Cytochrome P450 pathways of arachidonic acid metabolism, *Curr Opin Lipidol 13*, 273-283.

75. Lawrence, T., Willoughby, D. A., and Gilroy, D. W. (2002) Anti-inflammatory lipid mediators and insights into the resolution of inflammation, *Nat Rev Immunol 2*, 787-795.

76. Serhan, C. N., and Petasis, N. A. (2011) Resolvins and protectins in inflammation resolution, *Chem Rev 111*, 5922-5943.

77. Belch, J. J., and Hill, A. (2000) Evening primrose oil and borage oil in rheumatologic conditions, *Am J Clin Nutr 71*, 352S-356S.

78. Strasser, T., Fischer, S., and Weber, P. C. (1985) Leukotriene B5 is formed in human neutrophils after dietary supplementation with icosapentaenoic acid, *Proc Natl Acad Sci U S A 82*, 1540-1543.

79. Serhan, C. N. (2010) Novel lipid mediators and resolution mechanisms in acute inflammation: to resolve or not?, *Am J Pathol 177*, 1576-1591.

80. Im, D. S. (2012) Omega-3 fatty acids in anti-inflammation (pro-resolution) and GPCRs, *Prog Lipid Res 51*, 232-237.

81. Hirasawa, A., Tsumaya, K., Awaji, T., Katsuma, S., Adachi, T., Yamada, M., Sugimoto, Y., Miyazaki, S., and Tsujimoto, G. (2005) Free fatty acids regulate gut incretin glucagon-like peptide-1 secretion through GPR120, *Nat Med 11*, 90-94.

82. Miyauchi, S., Hirasawa, A., Iga, T., Liu, N., Itsubo, C., Sadakane, K., Hara, T., and Tsujimoto, G. (2009) Distribution and regulation of protein expression of the free fatty acid receptor GPR120, *Naunyn Schmiedebergs Arch Pharmacol 379*, 427-434.

83. Oh, D. Y., Talukdar, S., Bae, E. J., Imamura, T., Morinaga, H., Fan, W., Li, P., Lu, W. J., Watkins, S. M., and Olefsky, J. M. (2010) GPR120 is an omega-3 fatty acid receptor mediating potent anti-inflammatory and insulin-sensitizing effects, *Cell 142*, 687-698.

84. Briscoe, C. P., Tadayyon, M., Andrews, J. L., Benson, W. G., Chambers, J. K., Eilert, M. M., Ellis, C., Elshourbagy, N. A., Goetz, A. S., Minnick, D. T., Murdock, P. R., Sauls, H. R., Jr., Shabon, U., Spinage, L. D., Strum, J. C., Szekeres, P. G., Tan, K. B., Way, J. M., Ignar, D. M., Wilson, S., and Muir, A. I. (2003) The orphan G protein-coupled receptor GPR40 is activated by medium and long chain fatty acids, *J Biol Chem 278*, 11303-11311.

85. Yan, Y., Jiang, W., Spinetti, T., Tardivel, A., Castillo, R., Bourquin, C., Guarda, G., Tian, Z., Tschopp, J., and Zhou, R. (2013) Omega-3 fatty acids prevent inflammation and metabolic disorder through inhibition of NLRP3 inflammasome activation, *Immunity 38*, 1154-1163.

86. Moraes, L. A., Piqueras, L., and Bishop-Bailey, D. (2006) Peroxisome proliferator-activated receptors and inflammation, *Pharmacol Ther 110*, 371-385.

87. Bonilla, D. L., Ly, L. H., Fan, Y. Y., Chapkin, R. S., and McMurray, D. N. (2010) Incorporation of a dietary omega 3 fatty acid impairs murine macrophage responses to Mycobacterium tuberculosis, *PLoS One 5*, e10878.

88. Chiu, C. Y., Gomolka, B., Dierkes, C., Huang, N. R., Schroeder, M., Purschke, M., Manstein, D., Dangi, B., and Weylandt, K. H. (2012) Omega-6 docosapentaenoic acid-derived resolvins and 17-hydroxydocosahexaenoic acid modulate macrophage function and alleviate experimental colitis, *Inflamm Res 61*, 967-976.

89. Moghaddami, N., Irvine, J., Gao, X., Grover, P. K., Costabile, M., Hii, C. S., and Ferrante, A. (2007) Novel action of n-3 polyunsaturated fatty acids: inhibition of arachidonic acid-induced increase in tumor necrosis factor receptor expression on neutrophils and a role for proteases, *Arthritis Rheum 56*, 799-808.

90. Sperling, R. I. (1998) The effects of dietary n-3 polyunsaturated fatty acids on neutrophils, *Proc Nutr Soc 57*, 527-534.

91. Gorjao, R., Verlengia, R., Lima, T. M., Soriano, F. G., Boaventura, M. F., Kanunfre, C. C., Peres, C. M., Sampaio, S. C., Otton, R., Folador, A., Martins, E. F., Curi, T. C., Portiolli, E. P., Newsholme, P., and Curi, R. (2006) Effect of docosahexaenoic acid-rich fish oil supplementation on human leukocyte function, *Clin Nutr 25*, 923-938.

92. Saini, A., Harjai, K., and Chhibber, S. (2013) Inhibitory effect of polyunsaturated fatty acids on apoptosis induced by Streptococcus pneumoniae in alveolar macrophages, *Indian J Med Res 137*, 1193-1198.

93. Mauri, C., and Bosma, A. (2012) Immune regulatory function of B cells, *Annu Rev Immunol 30*, 221-241.

94. Pillai, S., and Cariappa, A. (2009) The follicular versus marginal zone B lymphocyte cell fate decision, *Nat Rev Immunol 9*, 767-777.

95. Clark, M. R., Mandal, M., Ochiai, K., and Singh, H. (2014) Orchestrating B cell lymphopoiesis through interplay of IL-7 receptor and pre-B cell receptor signalling, *Nat Rev Immunol 14*, 69-80.

96. Clark, M. R., Cooper, A. B., Wang, L. D., and Aifantis, I. (2005) The pre-B cell receptor in B cell development: recent advances, persistent questions and conserved mechanisms, *Curr Top Microbiol Immunol 290*, 87-103.

97. Herzog, S., Reth, M., and Jumaa, H. (2009) Regulation of B-cell proliferation and differentiation by pre-B-cell receptor signalling, *Nat Rev Immunol 9*, 195-205.

98. Allman, D., Lindsley, R. C., DeMuth, W., Rudd, K., Shinton, S. A., and Hardy, R. R. (2001) Resolution of three nonproliferative immature splenic B cell subsets reveals multiple selection points during peripheral B cell maturation, *J Immunol 167*, 6834-6840.

99. Baumgarth, N. (2011) The double life of a B-1 cell: self-reactivity selects for protective effector functions, *Nat Rev Immunol 11*, 34-46.

100. Cerutti, A., Cols, M., and Puga, I. (2013) Marginal zone B cells: virtues of innate-like antibody-producing lymphocytes, *Nat Rev Immunol 13*, 118-132.

101. Treml, L. S., Carlesso, G., Hoek, K. L., Stadanlick, J. E., Kambayashi, T., Bram, R. J., Cancro, M. P., and Khan, W. N. (2007) TLR stimulation modifies BLyS receptor expression in follicular and marginal zone B cells, *J Immunol 178*, 7531-7539.

102. He, B., Santamaria, R., Xu, W., Cols, M., Chen, K., Puga, I., Shan, M., Xiong, H., Bussel, J. B., Chiu, A., Puel, A., Reichenbach, J., Marodi, L., Doffinger, R., Vasconcelos, J., Issekutz, A., Krause, J., Davies, G., Li, X., Grimbacher, B., Plebani, A., Meffre, E., Picard, C., Cunningham-Rundles, C., Casanova, J. L., and Cerutti, A. (2010) The transmembrane activator TACI triggers immunoglobulin class switching by activating B cells through the adaptor MyD88, *Nat Immunol 11*, 836-845.

103. Janeway, C. A., Jr., and Medzhitov, R. (2002) Innate immune recognition, *Annu Rev Immunol 20*, 197-216.

104. Martin, F., Oliver, A. M., and Kearney, J. F. (2001) Marginal zone and B1 B cells unite in the early response against T-independent blood-borne particulate antigens, *Immunity 14*, 617-629.

105. Bos, N. A., Kimura, H., Meeuwsen, C. G., De Visser, H., Hazenberg, M. P., Wostmann, B. S., Pleasants, J. R., Benner, R., and Marcus, D. M. (1989) Serum immunoglobulin levels and naturally occurring antibodies against carbohydrate antigens in germ-free BALB/c mice fed chemically defined ultrafiltered diet, *Eur J Immunol 19*, 2335-2339.

106. Haury, M., Sundblad, A., Grandien, A., Barreau, C., Coutinho, A., and Nobrega, A. (1997) The repertoire of serum IgM in normal mice is largely independent of external antigenic contact, *Eur J Immunol 27*, 1557-1563.

107. Hooijkaas, H., Benner, R., Pleasants, J. R., and Wostmann, B. S. (1984) Isotypes and specificities of immunoglobulins produced by germ-free mice fed chemically defined ultrafiltered "antigen-free" diet, *Eur J Immunol 14*, 1127-1130.

108. Baumgarth, N., Herman, O. C., Jager, G. C., Brown, L. E., Herzenberg, L. A., and Chen, J. (2000) B-1 and B-2 cell-derived immunoglobulin M antibodies are nonredundant components of the protective response to influenza virus infection, *J Exp Med 192*, 271-280.

109. Boes, M., Prodeus, A. P., Schmidt, T., Carroll, M. C., and Chen, J. (1998) A critical role of natural immunoglobulin M in immediate defense against systemic bacterial infection, *J Exp Med 188*, 2381-2386.

110. Ochsenbein, A. F., Fehr, T., Lutz, C., Suter, M., Brombacher, F., Hengartner, H., and Zinkernagel, R. M. (1999) Control of early viral and bacterial distribution and disease by natural antibodies, *Science 286*, 2156-2159.

111. Zhou, Z. H., Zhang, Y., Hu, Y. F., Wahl, L. M., Cisar, J. O., and Notkins, A. L. (2007) The broad antibacterial activity of the natural antibody repertoire is due to polyreactive antibodies, *Cell Host Microbe 1*, 51-61.

112. Kaminski, D. A., and Stavnezer, J. (2006) Enhanced IgA class switching in marginal zone and B1 B cells relative to follicular/B2 B cells, *J Immunol 177*, 6025-6029.

113. Tarlinton, D. M., McLean, M., and Nossal, G. J. (1995) B1 and B2 cells differ in their potential to switch immunoglobulin isotype, *Eur J Immunol 25*, 3388-3393.

114. Mizoguchi, A., Mizoguchi, E., Takedatsu, H., Blumberg, R. S., and Bhan, A. K. (2002) Chronic intestinal inflammatory condition generates IL-10-producing regulatory B cell subset characterized by CD1d upregulation, *Immunity 16*, 219-230.

115. Yanaba, K., Bouaziz, J. D., Haas, K. M., Poe, J. C., Fujimoto, M., and Tedder, T. F. (2008) A regulatory B cell subset with a unique CD1dhiCD5+ phenotype controls T cell-dependent inflammatory responses, *Immunity 28*, 639-650.

116. Fillatreau, S., Sweenie, C. H., McGeachy, M. J., Gray, D., and Anderton, S. M. (2002) B cells regulate autoimmunity by provision of IL-10, *Nat Immunol 3*, 944-950.

117. Carter, N. A., Vasconcellos, R., Rosser, E. C., Tulone, C., Munoz-Suano, A., Kamanaka, M., Ehrenstein, M. R., Flavell, R. A., and Mauri, C. (2011) Mice lacking endogenous IL-10-producing regulatory B cells develop exacerbated disease and present with an increased frequency of Th1/Th17 but a decrease in regulatory T cells, *J Immunol 186*, 5569-5579.

118. Shen, P., Roch, T., Lampropoulou, V., O'Connor, R. A., Stervbo, U., Hilgenberg, E., Ries, S., Dang, V. D., Jaimes, Y., Daridon, C., Li, R., Jouneau, L., Boudinot, P., Wilantri, S., Sakwa, I., Miyazaki, Y., Leech, M. D., McPherson, R. C., Wirtz, S., Neurath, M., Hoehlig, K., Meinl, E., Grutzkau, A., Grun, J. R., Horn, K., Kuhl, A. A., Dorner, T., Bar-Or, A., Kaufmann, S. H., Anderton, S. M., and Fillatreau, S. (2014) IL-35-producing B cells are critical regulators of immunity during autoimmune and infectious diseases, *Nature 507*, 366-370.

119. Klein, U., and Dalla-Favera, R. (2008) Germinal centres: role in B-cell physiology and malignancy, *Nat Rev Immunol 8*, 22-33.

120. Gururajan, M., Jacob, J., and Pulendran, B. (2007) Toll-like receptor expression and responsiveness of distinct murine splenic and mucosal B-cell subsets, *PLoS One 2*, e863.

121. Genestier, L., Taillardet, M., Mondiere, P., Gheit, H., Bella, C., and Defrance, T. (2007) TLR agonists selectively promote terminal plasma cell differentiation of B cell subsets specialized in thymus-independent responses, *J Immunol 178*, 7779-7786.

122. Sindhava, V., Woodman, M. E., Stevenson, B., and Bondada, S. (2010) Interleukin-10 mediated autoregulation of murine B-1 B-cells and its role in Borrelia hermsii infection, *PLoS One 5*, e11445.

123. Rawlings, D. J., Schwartz, M. A., Jackson, S. W., and Meyer-Bahlburg, A. (2012) Integration of B cell responses through Toll-like receptors and antigen receptors, *Nat Rev Immunol 12*, 282-294.

124. Shaikh, S. R., Jolly, C. A., and Chapkin, R. S. (2012) n-3 Polyunsaturated fatty acids exert immunomodulatory effects on lymphocytes by targeting plasma membrane molecular organization, *Mol Aspects Med 33*, 46-54.

125. Weise, C., Hilt, K., Milovanovic, M., Ernst, D., Ruhl, R., and Worm, M. (2011) Inhibition of IgE production by docosahexaenoic acid is mediated by direct interference with STAT6 and NFkappaB pathway in human B cells, *J Nutr Biochem 22*, 269-275.

126. Selvaraj, R. K., and Cherian, G. (2004) Dietary n-3 fatty acids reduce the delayed hypersensitivity reaction and antibody production more than n-6 fatty acids in broiler birds, *European Journal of Lipid Science and Technology 106*, 3-10.

127. Beli, E., Li, M., Cuff, C., and Pestka, J. J. (2008) Docosahexaenoic acid-enriched fish oil consumption modulates immunoglobulin responses to and clearance of enteric reovirus infection in mice, *J Nutr 138*, 813-819.

128. Banchereau, J., Briere, F., Caux, C., Davoust, J., Lebecque, S., Liu, Y. J., Pulendran, B., and Palucka, K. (2000) Immunobiology of dendritic cells, *Annu Rev Immunol 18*, 767-811.

129. Hackstein, H., and Thomson, A. W. (2004) Dendritic cells: emerging pharmacological targets of immunosuppressive drugs, *Nat Rev Immunol 4*, 24-34.

130. Kong, W., Yen, J. H., and Ganea, D. (2011) Docosahexaenoic acid prevents dendritic cell maturation, inhibits antigen-specific Th1/Th17 differentiation and suppresses experimental autoimmune encephalomyelitis, *Brain Behav Immun 25*, 872-882.

131. Draper, E., Reynolds, C. M., Canavan, M., Mills, K. H., Loscher, C. E., and Roche, H. M. (2011) Omega-3 fatty acids attenuate dendritic cell function via NF-kappaB independent of PPARgamma, *J Nutr Biochem 22*, 784-790.

132. Kong, W., Yen, J. H., Vassiliou, E., Adhikary, S., Toscano, M. G., and Ganea, D. (2010) Docosahexaenoic acid prevents dendritic cell maturation and in vitro and in vivo expression of the IL-12 cytokine family, *Lipids Health Dis 9*, 12.

133. Wang, H., Hao, Q., Li, Q. R., Yan, X. W., Ye, S., Li, Y. S., Li, N., and Li, J. S. (2007) Omega-3 polyunsaturated fatty acids affect lipopolysaccharide-induced maturation of dendritic cells through mitogen-activated protein kinases p38, *Nutrition 23*, 474-482.

134. Karlsson, E. A., and Beck, M. A. (2010) The burden of obesity on infectious disease, *Exp Biol Med (Maywood) 235*, 1412-1424.

135. Huttunen, R., and Syrjanen, J. (2010) Obesity and the outcome of infection, *Lancet Infect Dis 10*, 442-443.

136. Nave, H., Beutel, G., and Kielstein, J. T. (2011) Obesity-related immunodeficiency in patients with pandemic influenza H1N1, *Lancet Infect Dis 11*, 14-15.

137. Louie, J. K., Acosta, M., Samuel, M. C., Schechter, R., Vugia, D. J., Harriman, K., and Matyas, B. T. (2011) A novel risk factor for a novel virus: obesity and 2009 pandemic influenza A (H1N1), *Clin Infect Dis 52*, 301-312.

138. Jain, S., Kamimoto, L., Bramley, A. M., Schmitz, A. M., Benoit, S. R., Louie, J., Sugerman, D. E., Druckenmiller, J. K., Ritger, K. A., Chugh, R., Jasuja, S., Deutscher, M., Chen, S., Walker, J. D., Duchin, J. S., Lett, S., Soliva, S., Wells, E. V., Swerdlow, D., Uyeki, T. M., Fiore, A. E., Olsen, S. J., Fry, A. M., Bridges, C. B., and Finelli, L. (2009) Hospitalized patients with 2009 H1N1 influenza in the United States, April-June 2009, *N Engl J Med 361*, 1935-1944.

139. Sheridan, P. A., Paich, H. A., Handy, J., Karlsson, E. A., Hudgens, M. G., Sammon, A. B., Holland, L. A., Weir, S., Noah, T. L., and Beck, M. A. (2012) Obesity is associated with impaired immune response to influenza vaccination in humans, *Int J Obes (Lond) 36*, 1072-1077.

140. Chapkin, R. S., McMurray, D. N., Davidson, L. A., Patil, B. S., Fan, Y. Y., and Lupton, J. R. (2008) Bioactive dietary long-chain fatty acids: emerging mechanisms of action, *Br J Nutr 100*, 1152-1157.

141. Stillwell, W., and Wassall, S. R. (2003) Docosahexaenoic acid: membrane properties of a unique fatty acid, *Chem Phys Lipids 126*, 1-27.

142. Shaikh, S. R., Jolly, C. A., and Chapkin, R. S. (2011) n-3 Polyunsaturated fatty acids exert immunomodulatory effects on lymphocytes by targeting plasma membrane molecular organization, *Mol Aspects Med*.

143. Shaikh, S. R. (2012) Biophysical and biochemical mechanisms by which dietary N-3 polyunsaturated fatty acids from fish oil disrupt membrane lipid rafts, *J Nutr Biochem 23*, 101-105.

144. Rockett, B. D., Teague, H., Harris, M., Melton, M., Williams, J., Wassall, S. R., and Shaikh, S. R. (2012) Fish oil increases raft size and membrane order of B cells accompanied by differential effects on function, *J Lipid Res 53*, 674-685.

145. Stillwell, W., Jenski, L. J., Zerouga, M., and Dumaual, A. C. (2000) Detection of lipid domains in docasahexaenoic acid-rich bilayers by acyl chain-specific FRET probes, *Chem Phys Lipids 104*, 113-132.

146. McIntosh, A. L., Huang, H., Atshaves, B. P., Wellberg, E., Kuklev, D. V., Smith, W. L., Kier, A. B., and Schroeder, F. (2010) Fluorescent n-3 and n-6 very long chain polyunsaturated fatty acids: three-photon imaging in living cells expressing liver fatty acid-binding protein, *J Biol Chem 285*, 18693-18708.

147. Lin, Q., Ruuska, S. E., Shaw, N. S., Dong, D., and Noy, N. (1999) Ligand selectivity of the peroxisome proliferator-activated receptor alpha, *Biochemistry 38*, 185-190.

148. Shaikh, S. R., Rockett, B. D., Salameh, M., and Carraway, K. (2009) Docosahexaenoic acid modifies the clustering and size of lipid rafts and the lateral organization and surface expression of MHC class I of EL4 cells, *J Nutr 139*, 1632-1639.

149. Rockett, B. D., Franklin, A., Harris, M., Teague, H., Rockett, A., and Shaikh, S. R. (2011) Membrane raft organization is more sensitive to disruption by (n-3) PUFA than nonraft organization in EL4 and B cells, *J Nutr 141*, 1041-1048.

150. Bolte, S., and Cordelieres, F. P. (2006) A guided tour into subcellular colocalization analysis in light microscopy, *J Microsc 224*, 213-232.

151. Heyn, M. P., Cherry, R. J., and Dencher, N. A. (1981) Lipid--protein interactions in bacteriorhodopsin--dimyristoylphosphatidylcholine vesicles, *Biochemistry 20*, 840-849.

152. Thumser, A. E., and Storch, J. (2007) Characterization of a BODIPY-labeled fluorescent fatty acid analogue. Binding to fatty acid-binding proteins, intracellular localization, and metabolism, *Mol Cell Biochem 299*, 67-73.

153. Karsenty, J., Helal, O., de la Porte, P. L., Beauclair-Deprez, P., Martin-Elyazidi, C., Planells, R., Storch, J., and Gastaldi, M. (2009) I-FABP expression alters the intracellular distribution of the BODIPY C16 fatty acid analog, *Mol Cell Biochem 326*, 97-104.

154. Shaikh, S. R., Brzustowicz, M. R., Stillwell, W., and Wassall, S. R. (2001) Formation of inverted hexagonal phase in SDPE as observed by solid-state (31)P NMR, *Biochem Biophys Res Commun 286*, 758-763.

155. Reyes Mateo, C., Ulises Acuna, A., and Brochon, J. C. (1995) Liquid-crystalline phases of cholesterol/lipid bilayers as revealed by the fluorescence of trans-parinaric acid, *Biophys J 68*, 978-987.

156. Kim, W., Khan, N. A., McMurray, D. N., Prior, I. A., Wang, N., and Chapkin, R. S. (2010) Regulatory activity of polyunsaturated fatty acids in T-cell signaling, *Prog Lipid Res 49*, 250-261.

157. Shaikh, S. R., Mitchell, D., Carroll, E., Li, M., Schneck, J., and Edidin, M. (2008) Differential effects of a saturated and a monounsaturated fatty acid on MHC class I antigen presentation, *Scand J Immunol 68*, 30-42.

158. Raza Shaikh, S., and Brown, D. A. (2012) Models of plasma membrane organization can be applied to mitochondrial membranes to target human health and disease with polyunsaturated fatty acids, *Prostaglandins Leukot Essent Fatty Acids*.

159. Stillwell, W., Jenski, L. J., Crump, F. T., and Ehringer, W. (1997) Effect of docosahexaenoic acid on mouse mitochondrial membrane properties, *Lipids 32*, 497-506.

160. Hamilton, J. A. (1999) Transport of fatty acids across membranes by the diffusion mechanism, *Prostaglandins Leukot Essent Fatty Acids 60*, 291-297.

161. Hamilton, J. A. (2007) New insights into the roles of proteins and lipids in membrane transport of fatty acids, *Prostaglandins Leukot Essent Fatty Acids 77*, 355-361.

162. Chapkin, R. S., Wang, N., Fan, Y. Y., Lupton, J. R., and Prior, I. A. (2008) Docosahexaenoic acid alters the size and distribution of cell surface microdomains, *Biochim Biophys Acta 1778*, 466-471.

163. Schley, P. D., Brindley, D. N., and Field, C. J. (2007) (n-3) PUFA alter raft lipid composition and decrease epidermal growth factor receptor levels in lipid rafts of human breast cancer cells, *J Nutr 137*, 548-553.

164. Mihailescu, M., Soubias, O., Worcester, D., White, S. H., and Gawrisch, K. (2011) Structure and dynamics of cholesterol-containing polyunsaturated lipid membranes studied by neutron diffraction and NMR, *J Membr Biol 239*, 63-71.

165. Kim, W., Fan, Y. Y., Barhoumi, R., Smith, R., McMurray, D. N., and Chapkin, R. S. (2008) n-3 polyunsaturated fatty acids suppress the localization and activation of signaling proteins at the immunological synapse in murine CD4+ T cells by affecting lipid raft formation, *J Immunol 181*, 6236-6243.

166. Pare, C., and Lafleur, M. (1998) Polymorphism of POPE/cholesterol system: a 2H nuclear magnetic resonance and infrared spectroscopic investigation, *Biophys J 74*, 899-909.

167. de Almeida, R. F., Loura, L. M., Fedorov, A., and Prieto, M. (2005) Lipid rafts have different sizes depending on membrane composition: a time-resolved fluorescence resonance energy transfer study, *J Mol Biol 346*, 1109-1120.

168. Koseki, M., Hirano, K., Masuda, D., Ikegami, C., Tanaka, M., Ota, A., Sandoval, J. C., Nakagawa-Toyama, Y., Sato, S. B., Kobayashi, T., Shimada, Y., Ohno-Iwashita, Y., Matsuura, F., Shimomura, I., and Yamashita, S. (2007) Increased lipid rafts and accelerated lipopolysaccharide-induced tumor necrosis factor-alpha secretion in Abca1-deficient macrophages, *J Lipid Res 48*, 299-306.

169. Fessler, M. B., and Parks, J. S. (2011) Intracellular lipid flux and membrane microdomains as organizing principles in inflammatory cell signaling, *J Immunol 187*, 1529-1535.

170. Duda, M. K., O'Shea, K. M., Tintinu, A., Xu, W., Khairallah, R. J., Barrows, B. R., Chess, D. J., Azimzadeh, A. M., Harris, W. S., Sharov, V. G., Sabbah, H. N., and Stanley, W. C. (2009) Fish oil, but not flaxseed oil, decreases inflammation and prevents pressure overload-induced cardiac dysfunction, *Cardiovasc Res 81*, 319-327.

171. Han, Y. Y., Lai, S. L., Ko, W. J., Chou, C. H., and Lai, H. S. (2012) Effects of fish oil on inflammatory modulation in surgical intensive care unit patients, *Nutr Clin Pract 27*, 91-98.

172. Luu, N. T., Madden, J., Calder, P. C., Grimble, R. F., Shearman, C. P., Chan, T., Dastur, N., Howell, W. M., Rainger, G. E., and Nash, G. B. (2007) Dietary supplementation with fish oil modifies the ability of human monocytes to induce an inflammatory response, *J Nutr 137*, 2769-2774.

173. Trebble, T. M., Stroud, M. A., Wootton, S. A., Calder, P. C., Fine, D. R., Mullee, M. A., Moniz, C., and Arden, N. K. (2005) High-dose fish oil and antioxidants in Crohn's

disease and the response of bone turnover: a randomised controlled trial, *Br J Nutr 94*, 253-261.

174. McMurray, D. N., Jolly, C. A., and Chapkin, R. S. (2000) Effects of dietary n-3 fatty acids on T cell activation and T cell receptor-mediated signaling in a murine model, *J Infect Dis 182 Suppl 1*, S103-107.

175. Guermouche, B., Yessoufou, A., Soulimane, N., Merzouk, H., Moutairou, K., Hichami, A., and Khan, N. A. (2004) n-3 fatty acids modulate T-cell calcium signaling in obese macrosomic rats, *Obes Res 12*, 1744-1753.

176. Chapkin, R. S., Arrington, J. L., Apanasovich, T. V., Carroll, R. J., and McMurray, D. N. (2002) Dietary n-3 PUFA affect TcR-mediated activation of purified murine T cells and accessory cell function in co-cultures, *Clin Exp Immunol 130*, 12-18.

177. Monk, J. M., Jia, Q., Callaway, E., Weeks, B., Alaniz, R. C., McMurray, D. N., and Chapkin, R. S. (2012) Th17 cell accumulation is decreased during chronic experimental colitis by (n-3) PUFA in Fat-1 mice, *J Nutr 142*, 117-124.

178. Yog, R., Barhoumi, R., McMurray, D. N., and Chapkin, R. S. (2010) n-3 polyunsaturated fatty acids suppress mitochondrial translocation to the immunologic synapse and modulate calcium signaling in T cells, *J Immunol 184*, 5865-5873.

179. Brix, S., Lund, P., Kjaer, T. M., Straarup, E. M., Hellgren, L. I., and Frokiaer, H. (2010) CD4(+) T-cell activation is differentially modulated by bacteria-primed dendritic cells, but is generally down-regulated by n-3 polyunsaturated fatty acids, *Immunology 129*, 338-350.

180. Zhang, P., Smith, R., Chapkin, R. S., and McMurray, D. N. (2005) Dietary (n-3) polyunsaturated fatty acids modulate murine Th1/Th2 balance toward the Th2 pole by suppression of Th1 development, *J Nutr 135*, 1745-1751.

181. Rockett, B. D., Salameh, M., Carraway, K., Morrison, K., and Shaikh, S. R. (2010) n-3 PUFA improves fatty acid composition, prevents palmitate-induced apoptosis, and differentially modifies B cell cytokine secretion in vitro and ex vivo, *J Lipid Res 51*, 1284-1297.

182. Steinman, R. M. (2012) Decisions about dendritic cells: past, present, and future, *Annu Rev Immunol 30*, 1-22.

183. Zeyda, M., Saemann, M. D., Stuhlmeier, K. M., Mascher, D. G., Nowotny, P. N., Zlabinger, G. J., Waldhausl, W., and Stulnig, T. M. (2005) Polyunsaturated fatty acids

block dendritic cell activation and function independently of NF-kappaB activation, *J Biol Chem 280*, 14293-14301.

184. Geyeregger, R., Zeyda, M., Zlabinger, G. J., Waldhausl, W., and Stulnig, T. M. (2005) Polyunsaturated fatty acids interfere with formation of the immunological synapse, *J Leukoc Biol 77*, 680-688.

185. Zech, T., Ejsing, C. S., Gaus, K., de Wet, B., Shevchenko, A., Simons, K., and Harder, T. (2009) Accumulation of raft lipids in T-cell plasma membrane domains engaged in TCR signalling, *Embo J 28*, 466-476.

186. Kim, W., McMurray, D. N., and Chapkin, R. S. (2010) n-3 polyunsaturated fatty acids--physiological relevance of dose, *Prostaglandins Leukot Essent Fatty Acids 82*, 155-158.

187. Bays, H. (2008) Rationale for prescription omega-3-acid ethyl ester therapy for hypertriglyceridemia: a primer for clinicians, *Drugs Today (Barc) 44*, 205-246.

188. Miles, E. A., and Calder, P. C. (2012) Influence of marine n-3 polyunsaturated fatty acids on immune function and a systematic review of their effects on clinical outcomes in rheumatoid arthritis, *Br J Nutr 107 Suppl 2*, S171-184.

189. Chen, L., Arora, M., Yarlagadda, M., Oriss, T. B., Krishnamoorthy, N., Ray, A., and Ray, P. (2006) Distinct responses of lung and spleen dendritic cells to the TLR9 agonist CpG oligodeoxynucleotide, *J Immunol 177*, 2373-2383.

190. Hofmann, J., Mair, F., Greter, M., Schmidt-Supprian, M., and Becher, B. (2011) NIK signaling in dendritic cells but not in T cells is required for the development of effector T cells and cell-mediated immune responses, *J Exp Med 208*, 1917-1929.

191. Tan, J. K., Periasamy, P., and O'Neill, H. C. (2010) Delineation of precursors in murine spleen that develop in contact with splenic endothelium to give novel dendritic-like cells, *Blood 115*, 3678-3685.

192. Loike, J. D., and Silverstein, S. C. (1983) A fluorescence quenching technique using trypan blue to differentiate between attached and ingested glutaraldehyde-fixed red blood cells in phagocytosing murine macrophages, *J Immunol Methods 57*, 373-379.

193. Owen, D. M., Rentero, C., Magenau, A., Abu-Siniyeh, A., and Gaus, K. (2012) Quantitative imaging of membrane lipid order in cells and organisms, *Nat Protoc 7*, 24-35.

194. Folch, J., Lees, M., and Sloane Stanley, G. H. (1957) A simple method for the isolation and purification of total lipides from animal tissues, *J Biol Chem 226*, 497-509.

195. Malhotra, V., Hogg, N., and Sim, R. B. (1986) Ligand binding by the p150,95 antigen of U937 monocytic cells: properties in common with complement receptor type 3 (CR3), *Eur J Immunol 16*, 1117-1123.

196. Keizer, G. D., Te Velde, A. A., Schwarting, R., Figdor, C. G., and De Vries, J. E. (1987) Role of p150,95 in adhesion, migration, chemotaxis and phagocytosis of human monocytes, *Eur J Immunol 17*, 1317-1322.

197. Nakajima, K., Yamashita, T., Kita, T., Takeda, M., Sasaki, N., Kasahara, K., Shinohara, M., Rikitake, Y., Ishida, T., Yokoyama, M., and Hirata, K. (2011) Orally administered eicosapentaenoic acid induces rapid regression of atherosclerosis via modulating the phenotype of dendritic cells in LDL receptor-deficient mice, *Arterioscler Thromb Vasc Biol 31*, 1963-1972.

198. Zapata-Gonzalez, F., Rueda, F., Petriz, J., Domingo, P., Villarroya, F., Diaz-Delfin, J., de Madariaga, M. A., and Domingo, J. C. (2008) Human dendritic cell activities are modulated by the omega-3 fatty acid, docosahexaenoic acid, mainly through PPAR(gamma):RXR heterodimers: comparison with other polyunsaturated fatty acids, *J Leukoc Biol 84*, 1172-1182.

199. Schwerbrock, N. M., Karlsson, E. A., Shi, Q., Sheridan, P. A., and Beck, M. A. (2009) Fish oil-fed mice have impaired resistance to influenza infection, *J Nutr 139*, 1588-1594.

200. Myones, B. L., Dalzell, J. G., Hogg, N., and Ross, G. D. (1988) Neutrophil and monocyte cell surface p150,95 has iC3b-receptor (CR4) activity resembling CR3, *J Clin Invest 82*, 640-651.

201. Ihanus, E., Uotila, L. M., Toivanen, A., Varis, M., and Gahmberg, C. G. (2007) Red-cell ICAM-4 is a ligand for the monocyte/macrophage integrin CD11c/CD18: characterization of the binding sites on ICAM-4, *Blood 109*, 802-810.

202. Dilioglou, S., Cruse, J. M., and Lewis, R. E. (2003) Function of CD80 and CD86 on monocyte- and stem cell-derived dendritic cells, *Exp Mol Pathol 75*, 217-227.

203. Sanderson, P., MacPherson, G. G., Jenkins, C. H., and Calder, P. C. (1997) Dietary fish oil diminishes the antigen presentation activity of rat dendritic cells, *J Leukoc Biol 62*, 771-777.

204. Kew, S., Mesa, M. D., Tricon, S., Buckley, R., Minihane, A. M., and Yaqoob, P. (2004) Effects of oils rich in eicosapentaenoic and docosahexaenoic acids on immune cell composition and function in healthy humans, *Am J Clin Nutr 79*, 674-681.

205. Wong, S. W., Kwon, M. J., Choi, A. M., Kim, H. P., Nakahira, K., and Hwang, D. H. (2009) Fatty acids modulate Toll-like receptor 4 activation through regulation of receptor dimerization and recruitment into lipid rafts in a reactive oxygen species-dependent manner, *J Biol Chem 284*, 27384-27392.

206. Calder, P. C. (2012) Omega-3 polyunsaturated fatty acids and inflammatory processes: Nutrition or pharmacology?, *Br J Clin Pharmacol*, n/a-n/a.

207. Serhan, C. N., Chiang, N., and Van Dyke, T. E. (2008) Resolving inflammation: dual anti-inflammatory and pro-resolution lipid mediators, *Nat Rev Immunol 8*, 349-361.

208. Kalupahana, N. S., Claycombe, K. J., and Moustaid-Moussa, N. (2011) (n-3) Fatty Acids Alleviate Adipose Tissue Inflammation and Insulin Resistance: Mechanistic Insights, *Advances in Nutrition: An International Review Journal 2*, 304-316.

209. Miles, E. A., and Calder, P. C. (2012) Influence of marine n-3 polyunsaturated fatty acids on immune function and a systematic review of their effects on clinical outcomes in rheumatoid arthritis, *The British journal of nutrition 107 Suppl 2*, S171-184.

210. Shaikh, S. R., Jolly, C. A., and Chapkin, R. S. (2012) n-3 Polyunsaturated fatty acids exert immunomodulatory effects on lymphocytes by targeting plasma membrane molecular organization, *Molecular aspects of medicine 33*, 46-54.

211. Rivera, A., Chen, C.-C., Ron, N., Dougherty, J. P., and Ron, Y. (2001) Role of B cells as antigen-presenting cells in vivo revisited: antigen-specific B cells are essential for T cell expansion in lymph nodes and for systemic T cell responses to low antigen concentrations, *Int Immunol 13*, 1583-1593.

212. Rauch, P. J., Chudnovskiy, A., Robbins, C. S., Weber, G. F., Etzrodt, M., Hilgendorf, I., Tiglao, E., Figueiredo, J.-L., Iwamoto, Y., Theurl, I., Gorbatov, R., Waring, M. T., Chicoine, A. T., Mouded, M., Pittet, M. J., Nahrendorf, M., Weissleder, R., and Swirski, F. K. (2012) Innate Response Activator B Cells Protect Against Microbial Sepsis, *Science 335*, 597-601.

213. Allman, D., and Pillai, S. (2008) Peripheral B cell subsets, *Curr Opin Immunol 20*, 149-157.

214. Yang, M., Rui, K., Wang, S., and Lu, L. (2013) Regulatory B cells in autoimmune diseases, *Cell Mol Immunol 10*, 122-132.

215. Rockett, B. D., Salameh, M., Carraway, K., Morrison, K., and Shaikh, S. R. (2010) n-3 PUFA improves fatty acid composition, prevents palmitate-induced apoptosis, and differentially modifies B cell cytokine secretion in vitro and ex vivo, *Journal of lipid research 51*, 1284-1297.

216. Drew Rockett, B., Harris, M., and Raza Shaikh, S. (2012) High dose of an n-3 polyunsaturated fatty acid diet lowers activity of C57BL/6 mice, *Prostaglandins, Leukotrienes and Essential Fatty Acids 86*, 137-140.

217. Rockett, B. D., Teague, H., Harris, M., Melton, M., Williams, J., Wassall, S. R., and Shaikh, S. R. (2012) Fish oil increases raft size and membrane order of B cells accompanied by differential effects on function, *Journal of lipid research 53*, 674-685.

218. Gurzell, E. A., Teague, H., Harris, M., Clinthorne, J., Shaikh, S. R., and Fenton, J. I. (2013) DHA-enriched fish oil targets B cell lipid microdomains and enhances ex vivo and in vivo B cell function, *J Leukoc Biol 93*, 463-470.

219. Sheridan, P. A., Paich, H. A., Handy, J., Karlsson, E. A., Hudgens, M. G., Sammon, A. B., Holland, L. A., Weir, S., Noah, T. L., and Beck, M. A. (2012) Obesity is associated with impaired immune response to influenza vaccination in humans, *Int J Obes (Lond) 36*, 1072-1077.

220. Weber Dj, R. W. A. S. G. P. S. J. E. L. S. M. (1985) OBesity as a predictor of poor antibody response to hepatitis b plasma vaccine, *JAMA: The Journal of the American Medical Association 254*, 3187-3189.

221. Eliakim, A., Swindt, C., Zaldivar, F., Casali, P., and Cooper, D. M. (2006) Reduced tetanus antibody titers in overweight children, *Autoimmunity 39*, 137-141.

222. Karlsson, E. A., and Beck, M. A. (2010) The burden of obesity on infectious disease, *Experimental Biology and Medicine 235*, 1412-1424.

223. Milner, J. J., Sheridan, P. A., Karlsson, E. A., Schultz-Cherry, S., Shi, Q., and Beck, M. A. (2013) Diet-Induced Obese Mice Exhibit Altered Heterologous Immunity during a Secondary 2009 Pandemic H1N1 Infection, *The Journal of Immunology 191*, 2474-2485.

224. Rockett, B. D., Melton, M., Harris, M., Bridges, L. C., and Shaikh, S. R. (2013) Fish oil disrupts MHC class II lateral organization on the B-cell side of the immunological synapse independent of B-T cell adhesion, *J Nutr Biochem 24*, 1810-1816.

225. Teague, H., Rockett, B. D., Harris, M., Brown, D. A., and Shaikh, S. R. (2013) Dendritic cell activation, phagocytosis and CD69 expression on cognate T cells are suppressed by n-3 long-chain polyunsaturated fatty acids, *Immunology 139*, 386-394.

226. Maki, K. C., Lawless, A. L., Kelley, K. M., Dicklin, M. R., Kaden, V. N., Schild, A. L., Rains, T. M., and Marshall, J. W. (2011) Effects of Prescription Omega-3-Acid Ethyl Esters on Fasting Lipid Profile in Subjects With Primary Hypercholesterolemia, *J Cardiovasc Pharmacol 57*, 489-494 410.1097/FJC.1090b1013e318210fca318215.

227. Sacks, F. M., Bray, G. A., Carey, V. J., Smith, S. R., Ryan, D. H., Anton, S. D., McManus, K., Champagne, C. M., Bishop, L. M., Laranjo, N., Leboff, M. S., Rood, J. C., de Jonge, L., Greenway, F. L., Loria, C. M., Obarzanek, E., and Williamson, D. A. (2009) Comparison of Weight-Loss Diets with Different Compositions of Fat, Protein, and Carbohydrates, *New England Journal of Medicine 360*, 859-873.

228. Fhaner, C. J., Liu, S., Ji, H., Simpson, R. J., Reid, G. E. (2012) Comprehensive Lipidome Profiling of Isogenic Primary and Metastatic Colon Adenocarcinoma Cell Lines, *Anal. Chem. 84*, 8917-8926.

229. Fhaner, C. J., Liu, S., Zhou, X., Reid, G. E. (2013) Functional Group Selective Derivatization and Gas-Phase Fragmentation Reactions of Plasmalogen Glycerophospholipids, *Mass Spectrom. 2*, S0015.

230. Haimi, P., Uphoff, A., Hermansson, M., Somerharju, P. (2006) Software tools for analysis of mass spectrometric lipidome data, *Anal. Chem. 78*, 8324-8331.

231. Jacobs, D. M. (1975) Structural and Genetic Basis of the in Vivo Immune Response to TNP-LPS, *The Journal of Immunology 115*, 988-992.

232. Fidler, J. M. (1976) The Induction of Hapten-Specific Immunologic Tolerance and Immunity in B Lymphocytes: I. The Effect of Delayed Immunization on the Adoptive Response to TNP-LPS, *The Journal of Immunology 116*, 1188-1193.

233. Pellegrini, A., Guinazu, N., Aoki, M. P., Calero, I. C., Carrera-Silva, E. A., Girones, N., Fresno, M., and Gea, S. (2007) Spleen B cells from BALB/c are more prone to activation than spleen B cells from C57BL/6 mice during a secondary immune response to cruzipain, *Int Immunol 19*, 1395-1402.

234. Haas, K. M., Hasegawa, M., Steeber, D. A., Poe, J. C., Zabel, M. D., Bock, C. B., Karp, D. R., Briles, D. E., Weis, J. H., and Tedder, T. F. (2002) Complement Receptors CD21/35 Link Innate and Protective Immunity during Streptococcus pneumoniae Infection by Regulating IgG3 Antibody Responses, *Immunity 17*, 713-723.

235. Watanabe, C., Shu, G. L., Zheng, T. S., Flavell, R. A., and Clark, E. A. (2008) Caspase 6 regulates B cell activation and differentiation into plasma cells, *J Immunol 181*, 6810-6819.

236. DeFuria, J., Belkina, A. C., Jagannathan-Bogdan, M., Snyder-Cappione, J., Carr, J. D., Nersesova, Y. R., Markham, D., Strissel, K. J., Watkins, A. A., Zhu, M., Allen, J., Bouchard, J., Toraldo, G., Jasuja, R., Obin, M. S., McDonnell, M. E., Apovian, C., Denis, G. V., and Nikolajczyk, B. S. (2013) B cells promote inflammation in obesity and type 2 diabetes through regulation of T-cell function and an inflammatory cytokine profile, *Proceedings of the National Academy of Sciences 110*, 5133-5138.

237. Winer, D., Winer, S., Shen, L., Wadia, P., Yantha, J., Paltser, G., Tsui, H., Wu, P., Davidson, M., Alonso, M., Leong, H., Glassford, A., Caimol, M., Kenkel, J., Tedder, T., McLaughlin, T., Miklos, D., Dosch, H. M., and Engleman, E. (2011) B cells promote insulin resistance through modulation of T cells and production of pathogenic IgG antibodies, *Nat Med 17*, 610-617.

238. Chung, J. B., Silverman, M., and Monroe, J. G. (2003) Transitional B cells: step by step towards immune competence, *Trends Immunol 24*, 342-348.

239. Vossenkämper, A., Lutalo, P. M. K., and Spencer, J. (2012) Translational Mini-Review Series on B cell subsets in disease. Transitional B cells in systemic lupus erythematosus and Sjögren's syndrome: clinical implications and effects of B cell-targeted therapies, *Clinical & Experimental Immunology 167*, 7-14.

240. Rubtsov, A. V., Swanson, C. L., Troy, S., Strauch, P., Pelanda, R., and Torres, R. M. (2008) TLR Agonists Promote Marginal Zone B Cell Activation and Facilitate T-Dependent IgM Responses, *The Journal of Immunology 180*, 3882-3888.

241. Nashi, E., Wang, Y., and Diamond, B. (2010) The role of B cells in lupus pathogenesis, *The International Journal of Biochemistry & Cell Biology 42*, 543-550.

242. Wong, F. S., Hu, C., Xiang, Y., and Wen, L. (2010) To B or not to B — pathogenic and regulatory B cells in autoimmune diabetes, *Curr Opin Immunol 22*, 723-731.

243. Yang, M., Sun, L., Wang, S., Ko, K.-H., Xu, H., Zheng, B.-J., Cao, X., and Lu, L. (2010) Cutting Edge: Novel Function of B Cell-Activating Factor in the Induction of IL-10–Producing Regulatory B Cells, *The Journal of Immunology 184*, 3321-3325.

244. DiLillo, D. J., Matsushita, T., and Tedder, T. F. (2010) B10 cells and regulatory B cells balance immune responses during inflammation, autoimmunity, and cancer, *Ann N Y Acad Sci 1183*, 38-57.

245. Weise, C., Hilt, K., Milovanovic, M., Ernst, D., Rühl, R., and Worm, M. (2011) Inhibition of IgE production by docosahexaenoic acid is mediated by direct interference with STAT6 and NFκB pathway in human B cells, *J Nutr Biochem 22*, 269-275.

246. Lauritzen, L., Kjaer, T. M., Porsgaard, T., Fruekilde, M. B., Mu, H., and Frokiaer, H. (2011) Maternal intake of fish oil but not of linseed oil reduces the antibody response in neonatal mice, *Lipids 46*, 171-178.

247. Ramon, S., Gao, F., Serhan, C. N., and Phipps, R. P. (2012) Specialized Proresolving Mediators Enhance Human B Cell Differentiation to Antibody-Secreting Cells, *The Journal of Immunology 189*, 1036-1042.

248. Wang, C.-Y., and Liao, J. (2012) A Mouse Model of Diet-Induced Obesity and Insulin Resistance, In *mTOR* (Weichhart, T., Ed.), pp 421-433, Humana Press.

249. Carsetti, R. (2000) The development of B cells in the bone marrow is controlled by the balance between cell-autonomous mechanisms and signals from the microenvironment, *J Exp Med 191*, 5-8.

250. Del Nagro, C. J., Otero, D. C., Anzelon, A. N., Omori, S. A., Kolla, R. V., and Rickert, R. C. (2005) CD19 function in central and peripheral B-cell development, *Immunol Res 31*, 119-131.

251. Tsitsikov, E. N., Gutierrez-Ramos, J. C., and Geha, R. S. (1997) Impaired CD19 expression and signaling, enhanced antibody response to type II T independent antigen and reduction of B-1 cells in CD81-deficient mice, *Proc Natl Acad Sci U S A 94*, 10844-10849.

252. Lewis, M. J., Malik, T. H., Ehrenstein, M. R., Boyle, J. J., Botto, M., and Haskard, D. O. (2009) Immunoglobulin M is required for protection against atherosclerosis in low-density lipoprotein receptor-deficient mice, *Circulation 120*, 417-426.

253. Kyaw, T., Tay, C., Krishnamurthi, S., Kanellakis, P., Agrotis, A., Tipping, P., Bobik, A., and Toh, B. H. (2011) B1a B lymphocytes are atheroprotective by secreting natural IgM that increases IgM deposits and reduces necrotic cores in atherosclerotic lesions, *Circ Res 109*, 830-840.

254. Kiecolt-Glaser, J. K., Belury, M. A., Andridge, R., Malarkey, W. B., Hwang, B. S., and Glaser, R. (2012) Omega-3 supplementation lowers inflammation in healthy middle-aged and older adults: a randomized controlled trial, *Brain Behav Immun 26*, 988-995.

255. Itariu, B. K., Zeyda, M., Hochbrugger, E. E., Neuhofer, A., Prager, G., Schindler, K., Bohdjalian, A., Mascher, D., Vangala, S., Schranz, M., Krebs, M., Bischof, M. G., and Stulnig, T. M. (2012) Long-chain n-3 PUFAs reduce adipose tissue and systemic inflammation in severely obese nondiabetic patients: a randomized controlled trial, *Am J Clin Nutr 96*, 1137-1149.

256. Spencer, M., Finlin, B. S., Unal, R., Zhu, B., Morris, A. J., Shipp, L. R., Lee, J., Walton, R. G., Adu, A., Erfani, R., Campbell, M., McGehee, R. E., Jr., Peterson, C. A., and Kern, P. A. (2013) Omega-3 fatty acids reduce adipose tissue macrophages in human subjects with insulin resistance, *Diabetes 62*, 1709-1717.

257. Dayspring, T. D. (2011) Understanding hypertriglyceridemia in women: clinical impact and management with prescription omega-3-acid ethyl esters, *Int J Womens Health 3*, 87-97.

258. Monk, J. M., Hou, T. Y., Turk, H. F., Weeks, B., Wu, C., McMurray, D. N., and Chapkin, R. S. (2012) Dietary n-3 polyunsaturated fatty acids (PUFA) decrease obesity-associated Th17 cell-mediated inflammation during colitis, *PLoS One 7*, e49739.

259. Teague, H., Fhaner, C. J., Harris, M., Duriancik, D. M., Reid, G. E., and Shaikh, S. R. (2013) n-3 PUFAs enhance the frequency of murine B-cell subsets and restore the impairment of antibody production to a T-independent antigen in obesity, *J Lipid Res 54*, 3130-3138.

260. Gurzell, E. A., Teague, H., Harris, M., Clinthorne, J., Shaikh, S. R., and Fenton, J. I. (2013) DHA-enriched fish oil targets B cell lipid microdomains and enhances ex vivo and in vivo B cell function, *J Leukoc Biol 93*, 463-470.

261. Tomasdottir, V., Thorleifsdottir, S., Vikingsson, A., Hardardottir, I., and Freysdottir, J. (2014) Dietary omega-3 fatty acids enhance the B1 but not the B2 cell immune response in mice with antigen-induced peritonitis, *J Nutr Biochem 25*, 111-117.

262. Strobel, C., Jahreis, G., and Kuhnt, K. (2012) Survey of n-3 and n-6 polyunsaturated fatty acids in fish and fish products, *Lipids Health Dis 11*, 144.

263. Kalupahana, N. S., Claycombe, K. J., and Moustaid-Moussa, N. (2011) (n-3) Fatty acids alleviate adipose tissue inflammation and insulin resistance: mechanistic insights, *Adv Nutr 2*, 304-316.

264. Pellegrini, A., Guinazu, N., Aoki, M. P., Calero, I. C., Carrera-Silva, E. A., Girones, N., Fresno, M., and Gea, S. (2007) Spleen B cells from BALB/c are more prone to activation than spleen B cells from C57BL/6 mice during a secondary immune response to cruzipain, *Int Immunol 19*, 1395-1402.

265. Gaus, K., Zech, T., and Harder, T. (2006) Visualizing membrane microdomains by Laurdan 2-photon microscopy, *Mol Membr Biol 23*, 41-48.

266. Shaikh, S. R., and Edidin, M. (2007) Immunosuppressive effects of polyunsaturated fatty acids on antigen presentation by human leukocyte antigen class I molecules, *J Lipid Res 48*, 127-138.

267. Kwik, J., Boyle, S., Fooksman, D., Margolis, L., Sheetz, M. P., and Edidin, M. (2003) Membrane cholesterol, lateral mobility, and the phosphatidylinositol 4,5-bisphosphate-dependent organization of cell actin, *Proc Natl Acad Sci U S A 100*, 13964-13969.

268. Gronwall, C., Vas, J., and Silverman, G. J. (2012) Protective Roles of Natural IgM Antibodies, *Front Immunol 3*, 66.

269. Kratz, M., Kuzma, J. N., Hagman, D. K., van Yserloo, B., Matthys, C. C., Callahan, H. S., and Weigle, D. S. (2013) n3 PUFAs do not affect adipose tissue inflammation in overweight to moderately obese men and women, *J Nutr 143*, 1340-1347.

270. Hou, T. Y., Monk, J. M., Fan, Y. Y., Barhoumi, R., Chen, Y. Q., Rivera, G. M., McMurray, D. N., and Chapkin, R. S. (2012) n-3 polyunsaturated fatty acids suppress phosphatidylinositol 4,5-bisphosphate-dependent actin remodelling during CD4+ T-cell activation, *Biochem J 443*, 27-37.

271. Hao, W., Wong, O. Y., Liu, X., Lee, P., Chen, Y., and Wong, K. K. (2010) omega-3 fatty acids suppress inflammatory cytokine production by macrophages and hepatocytes, *J Pediatr Surg 45*, 2412-2418.

272. Nelson, S. D., and Munger, M. A. (2013) Icosapent ethyl for treatment of elevated triglyceride levels, *Ann Pharmacother 47*, 1517-1523.

273. Olson, M. V., Liu, Y. C., Dangi, B., Paul Zimmer, J., Salem, N., Jr., and Nauroth, J. M. (2013) Docosahexaenoic acid reduces inflammation and joint destruction in mice with collagen-induced arthritis, *Inflamm Res 62*, 1003-1013.

274. Notley, C. A., Brown, M. A., Wright, G. P., and Ehrenstein, M. R. (2011) Natural IgM is required for suppression of inflammatory arthritis by apoptotic cells, *J Immunol 186*, 4967-4972.

275. Nishimura, S., Manabe, I., Takaki, S., Nagasaki, M., Otsu, M., Yamashita, H., Sugita, J., Yoshimura, K., Eto, K., Komuro, I., Kadowaki, T., and Nagai, R. (2013) Adipose Natural Regulatory B Cells Negatively Control Adipose Tissue Inflammation, *Cell Metab*.

276. Ulven, S. M., Kirkhus, B., Lamglait, A., Basu, S., Elind, E., Haider, T., Berge, K., Vik, H., and Pedersen, J. I. (2011) Metabolic effects of krill oil are essentially similar to those of fish oil but at lower dose of EPA and DHA, in healthy volunteers, *Lipids 46*, 37-46.

277. Xin, W., Wei, W., and Li, X. (2012) Effects of fish oil supplementation on inflammatory markers in chronic heart failure: a meta-analysis of randomized controlled trials, *BMC Cardiovasc Disord 12*, 77.

278. Johansen, O., Seljeflot, I., Hostmark, A. T., and Arnesen, H. (1999) The effect of supplementation with omega-3 fatty acids on soluble markers of endothelial function in patients with coronary heart disease, *Arterioscler Thromb Vasc Biol 19*, 1681-1686.

279. Itariu, B. K., Zeyda, M., Leitner, L., Marculescu, R., and Stulnig, T. M. (2013) Treatment with n-3 polyunsaturated fatty acids overcomes the inverse association of vitamin D deficiency with inflammation in severely obese patients: a randomized controlled trial, *PLoS One 8*, e54634.

280. Kawasaki, K., Abe, M., Tada, F., Tokumoto, Y., Chen, S., Miyake, T., Furukawa, S., Matsuura, B., Hiasa, Y., and Onji, M. (2013) Blockade of B-cell-activating factor signaling enhances hepatic steatosis induced by a high-fat diet and improves insulin sensitivity, *Lab Invest 93*, 311-321.

281. Winer, D. A., Winer, S., Shen, L., Wadia, P. P., Yantha, J., Paltser, G., Tsui, H., Wu, P., Davidson, M. G., Alonso, M. N., Leong, H. X., Glassford, A., Caimol, M., Kenkel, J. A., Tedder, T. F., McLaughlin, T., Miklos, D. B., Dosch, H. M., and Engleman, E. G. (2011) B cells promote insulin resistance through modulation of T cells and production of pathogenic IgG antibodies, *Nat Med 17*, 610-617.

282. DeFuria, J., Belkina, A. C., Jagannathan-Bogdan, M., Snyder-Cappione, J., Carr, J. D., Nersesova, Y. R., Markham, D., Strissel, K. J., Watkins, A. A., Zhu, M., Allen, J., Bouchard, J., Toraldo, G., Jasuja, R., Obin, M. S., McDonnell, M. E., Apovian, C., Denis, G. V., and Nikolajczyk, B. S. (2013) B cells promote inflammation in obesity and type 2 diabetes through regulation of T-cell function and an inflammatory cytokine profile, *Proc Natl Acad Sci U S A 110*, 5133-5138.

283. Sacks, F. M., Bray, G. A., Carey, V. J., Smith, S. R., Ryan, D. H., Anton, S. D., McManus, K., Champagne, C. M., Bishop, L. M., Laranjo, N., Leboff, M. S., Rood, J. C., de Jonge, L., Greenway, F. L., Loria, C. M., Obarzanek, E., and Williamson, D. A. (2009) Comparison of weight-loss diets with different compositions of fat, protein, and carbohydrates, *N Engl J Med 360*, 859-873.

284. Turchini, G. M., Nichols, P. D., Barrow, C., and Sinclair, A. J. (2012) Jumping on the omega-3 bandwagon: distinguishing the role of long-chain and short-chain omega-3 fatty acids, *Crit Rev Food Sci Nutr 52*, 795-803.

285. Yanaba, K., Bouaziz, J. D., Matsushita, T., Magro, C. M., St Clair, E. W., and Tedder, T. F. (2008) B-lymphocyte contributions to human autoimmune disease, *Immunol Rev 223*, 284-299.

286. Marino, E., and Grey, S. T. (2012) B cells as effectors and regulators of autoimmunity, *Autoimmunity 45*, 377-387.

287. Baumgarth, N., Herman, O. C., Jager, G. C., Brown, L., and Herzenberg, L. A. (1999) Innate and acquired humoral immunities to influenza virus are mediated by distinct arms of the immune system, *Proc Natl Acad Sci U S A 96*, 2250-2255.

288. Cesena, F. H., Dimayuga, P. C., Yano, J., Zhao, X., Kirzner, J., Zhou, J., Chan, L. F., Lio, W. M., Cercek, B., Shah, P. K., and Chyu, K. Y. (2012) Immune-modulation by polyclonal IgM treatment reduces atherosclerosis in hypercholesterolemic apoE-/- mice, *Atherosclerosis 220*, 59-65.

289. Werwitzke, S., Trick, D., Kamino, K., Matthias, T., Kniesch, K., Schlegelberger, B., Schmidt, R. E., and Witte, T. (2005) Inhibition of lupus disease by anti-double-stranded DNA antibodies of the IgM isotype in the (NZB x NZW)F1 mouse, *Arthritis Rheum 52*, 3629-3638.

290. de Faire, U., and Frostegard, J. (2009) Natural antibodies against phosphorylcholine in cardiovascular disease, *Ann N Y Acad Sci 1173*, 292-300.

291. Kroese, F. G., Butcher, E. C., Stall, A. M., Lalor, P. A., Adams, S., and Herzenberg, L. A. (1989) Many of the IgA producing plasma cells in murine gut are derived from self-replenishing precursors in the peritoneal cavity, *International immunology 1*, 75-84.

292. Williams, J. A., Batten, S. E., Harris, M., Rockett, B. D., Shaikh, S. R., Stillwell, W., and Wassall, S. R. (2012) Docosahexaenoic and eicosapentaenoic acids segregate differently between raft and nonraft domains, *Biophys J 103*, 228-237.

293. Shaikh, S. R., and Teague, H. (2012) N-3 fatty acids and membrane microdomains: from model membranes to lymphocyte function, *Prostaglandins Leukot Essent Fatty Acids 87*, 205-208.

294. Teague, H., Ross, R., Harris, M., Mitchell, D. C., and Shaikh, S. R. (2013) DHA-fluorescent probe is sensitive to membrane order and reveals molecular adaptation of DHA in ordered lipid microdomains, *J Nutr Biochem 24*, 188-195.

295. Rajamoorthi, K., Petrache, H. I., McIntosh, T. J., and Brown, M. F. (2005) Packing and viscoelasticity of polyunsaturated omega-3 and omega-6 lipid bilayers as seen by (2)H NMR and X-ray diffraction, *J Am Chem Soc 127*, 1576-1588.

296. Mills, K. H. (2011) TLR-dependent T cell activation in autoimmunity, *Nat Rev Immunol 11*, 807-822.

297. Calder, P. C. (2008) The relationship between the fatty acid composition of immune cells and their function, *Prostaglandins Leukot Essent Fatty Acids 79*, 101-108.

298. Shen, W., Wang, C., Xia, L., Fan, C., Dong, H., Deckelbaum, R. J., and Qi, K. (2014) Epigenetic modification of the leptin promoter in diet-induced obese mice and the effects of N-3 polyunsaturated Fatty acids, *Sci Rep 4*, 5282.

299. Oh, D. Y., and Olefsky, J. M. (2012) Omega 3 fatty acids and GPR120, *Cell Metab 15*, 564-565.

300. Fan, Y. Y., McMurray, D. N., Ly, L. H., and Chapkin, R. S. (2003) Dietary (n-3) polyunsaturated fatty acids remodel mouse T-cell lipid rafts, *J Nutr 133*, 1913-1920.

301. Shaikh, S. R., Kinnun, J. J., Leng, X., Williams, J. A., and Wassall, S. R. (2014) How polyunsaturated fatty acids modify molecular organization in membranes: Insight from NMR studies of model systems, *Biochim Biophys Acta*.

302. Ruth, M. R., Proctor, S. D., and Field, C. J. (2009) Feeding long-chain n-3 polyunsaturated fatty acids to obese leptin receptor-deficient JCR:LA- cp rats modifies immune function and lipid-raft fatty acid composition, *Br J Nutr 101*, 1341-1350.

303. Calder, P. C. (2010) Lipid-laden dendritic cells fail to function, *Cell Res 20*, 1089-1091.

304. Weatherill, A. R., Lee, J. Y., Zhao, L., Lemay, D. G., Youn, H. S., and Hwang, D. H. (2005) Saturated and polyunsaturated fatty acids reciprocally modulate dendritic cell functions mediated through TLR4, *J Immunol 174*, 5390-5397.

305. Cortese, M., Sinclair, C., and Pulendran, B. (2014) Translating glycolytic metabolism to innate immunity in dendritic cells, *Cell Metab 19*, 737-739.

306. Everts, B., Amiel, E., Huang, S. C., Smith, A. M., Chang, C. H., Lam, W. Y., Redmann, V., Freitas, T. C., Blagih, J., van der Windt, G. J., Artyomov, M. N., Jones, R. G., Pearce, E. L., and Pearce, E. J. (2014) TLR-driven early glycolytic reprogramming via the

kinases TBK1-IKKvarepsilon supports the anabolic demands of dendritic cell activation, *Nat Immunol 15*, 323-332.

307. Jump, D. B., Botolin, D., Wang, Y., Xu, J., Demeure, O., and Christian, B. (2008) Docosahexaenoic acid (DHA) and hepatic gene transcription, *Chem Phys Lipids 153*, 3-13.

308. Baumgarth, N., Tung, J. W., and Herzenberg, L. A. (2005) Inherent specificities in natural antibodies: a key to immune defense against pathogen invasion, *Springer Semin Immunopathol 26*, 347-362.

309. Ogden, C. A., Kowalewski, R., Peng, Y., Montenegro, V., and Elkon, K. B. (2005) IGM is required for efficient complement mediated phagocytosis of apoptotic cells in vivo, *Autoimmunity 38*, 259-264.

310. Quartier, P., Potter, P. K., Ehrenstein, M. R., Walport, M. J., and Botto, M. (2005) Predominant role of IgM-dependent activation of the classical pathway in the clearance of dying cells by murine bone marrow-derived macrophages in vitro, *Eur J Immunol 35*, 252-260.

311. Chen, Y., Khanna, S., Goodyear, C. S., Park, Y. B., Raz, E., Thiel, S., Gronwall, C., Vas, J., Boyle, D. L., Corr, M., Kono, D. H., and Silverman, G. J. (2009) Regulation of dendritic cells and macrophages by an anti-apoptotic cell natural antibody that suppresses TLR responses and inhibits inflammatory arthritis, *J Immunol 183*, 1346-1359.

312. Chen, Y., Park, Y. B., Patel, E., and Silverman, G. J. (2009) IgM antibodies to apoptosis-associated determinants recruit C1q and enhance dendritic cell phagocytosis of apoptotic cells, *J Immunol 182*, 6031-6043.

313. Justel, M., Socias, L., Almansa, R., Ramirez, P., Gallegos, M. C., Fernandez, V., Gordon, M., Andaluz-Ojeda, D., Nogales, L., Rojo, S., Valles, J., Estella, A., Loza, A., Leon, C., Lopez-Mestanza, C., Blanco, J., Berezo, J. A., Rosich, S., Cilloniz, C., Torres, A., de Lejarazu, R. O., Martin-Loeches, I., and Bermejo-Martin, J. F. (2013) IgM levels in plasma predict outcome in severe pandemic influenza, *J Clin Virol 58*, 564-567.

314. Ehrenstein, M. R., Cook, H. T., and Neuberger, M. S. (2000) Deficiency in serum immunoglobulin (Ig)M predisposes to development of IgG autoantibodies, *J Exp Med 191*, 1253-1258.

315. Kamada, N., Seo, S. U., Chen, G. Y., and Nunez, G. (2013) Role of the gut microbiota in immunity and inflammatory disease, *Nat Rev Immunol 13*, 321-335.

316. Fagarasan, S., Kawamoto, S., Kanagawa, O., and Suzuki, K. (2010) Adaptive immune regulation in the gut: T cell-dependent and T cell-independent IgA synthesis, *Annu Rev Immunol 28*, 243-273.

317. Ochoa-Reparaz, J., Mielcarz, D. W., Ditrio, L. E., Burroughs, A. R., Foureau, D. M., Haque-Begum, S., and Kasper, L. H. (2009) Role of gut commensal microflora in the development of experimental autoimmune encephalomyelitis, *J Immunol 183*, 6041-6050.

318. Lee, Y. K., Menezes, J. S., Umesaki, Y., and Mazmanian, S. K. (2011) Proinflammatory T-cell responses to gut microbiota promote experimental autoimmune encephalomyelitis, *Proc Natl Acad Sci U S A 108 Suppl 1*, 4615-4622.

319. Berer, K., Mues, M., Koutrolos, M., Rasbi, Z. A., Boziki, M., Johner, C., Wekerle, H., and Krishnamoorthy, G. (2011) Commensal microbiota and myelin autoantigen cooperate to trigger autoimmune demyelination, *Nature 479*, 538-541.

320. Wu, H. J., Ivanov, II, Darce, J., Hattori, K., Shima, T., Umesaki, Y., Littman, D. R., Benoist, C., and Mathis, D. (2010) Gut-residing segmented filamentous bacteria drive autoimmune arthritis via T helper 17 cells, *Immunity 32*, 815-827.

321. Wen, L., Ley, R. E., Volchkov, P. Y., Stranges, P. B., Avanesyan, L., Stonebraker, A. C., Hu, C., Wong, F. S., Szot, G. L., Bluestone, J. A., Gordon, J. I., and Chervonsky, A. V. (2008) Innate immunity and intestinal microbiota in the development of Type 1 diabetes, *Nature 455*, 1109-1113.

322. Ramon, S., Gao, F., Serhan, C. N., and Phipps, R. P. (2012) Specialized proresolving mediators enhance human B cell differentiation to antibody-secreting cells, *J Immunol 189*, 1036-1042.

323. Bird, L. (2014) Immunometabolism: regulatory B cells weigh in, *Nat Rev Immunol 14*, 6-7.

324. Nagasawa, T. (2006) Microenvironmental niches in the bone marrow required for B-cell development, *Nat Rev Immunol 6*, 107-116.

325. Allman, D., Li, J., and Hardy, R. R. (1999) Commitment to the B lymphoid lineage occurs before DH-JH recombination, *J Exp Med 189*, 735-740.

326. King, L. B., and Monroe, J. G. (2000) Immunobiology of the immature B cell: plasticity in the B-cell antigen receptor-induced response fine tunes negative selection, *Immunol Rev 176*, 86-104.

327. Pillai, S., Cariappa, A., and Moran, S. T. (2005) Marginal zone B cells, *Annu Rev Immunol 23*, 161-196.

328. Shapiro-Shelef, M., and Calame, K. (2005) Regulation of plasma-cell development, *Nat Rev Immunol 5*, 230-242.

329. Tarlinton, D. (2006) B-cell memory: are subsets necessary?, *Nat Rev Immunol 6*, 785-790.

330. Minton, K. (2011) B cells: Short- and long-term memory, *Nat Rev Immunol 11*, 160.

331. Weber, G. F., Chousterman, B. G., Hilgendorf, I., Robbins, C. S., Theurl, I., Gerhardt, L. M., Iwamoto, Y., Quach, T. D., Ali, M., Chen, J. W., Rothstein, T. L., Nahrendorf, M., Weissleder, R., and Swirski, F. K. (2014) Pleural innate response activator B cells protect against pneumonia via a GM-CSF-IgM axis, *J Exp Med 211*, 1243-1256.

332. Rauch, P. J., Chudnovskiy, A., Robbins, C. S., Weber, G. F., Etzrodt, M., Hilgendorf, I., Tiglao, E., Figueiredo, J. L., Iwamoto, Y., Theurl, I., Gorbatov, R., Waring, M. T., Chicoine, A. T., Mouded, M., Pittet, M. J., Nahrendorf, M., Weissleder, R., and Swirski, F. K. (2012) Innate response activator B cells protect against microbial sepsis, *Science 335*, 597-601.

333. Soehnlein, O. (2012) Multiple roles for neutrophils in atherosclerosis, *Circ Res 110*, 875-888.

334. Spite, M., Claria, J., and Serhan, C. N. (2014) Resolvins, specialized proresolving lipid mediators, and their potential roles in metabolic diseases, *Cell Metab 19*, 21-36.

335. Morgan, O. W., Bramley, A., Fowlkes, A., Freedman, D. S., Taylor, T. H., Gargiullo, P., Belay, B., Jain, S., Cox, C., Kamimoto, L., Fiore, A., Finelli, L., Olsen, S. J., and Fry, A. M. (2010) Morbid obesity as a risk factor for hospitalization and death due to 2009 pandemic influenza A(H1N1) disease, *PLoS One 5*, e9694.

336. Morita, M., Kuba, K., Ichikawa, A., Nakayama, M., Katahira, J., Iwamoto, R., Watanebe, T., Sakabe, S., Daidoji, T., Nakamura, S., Kadowaki, A., Ohto, T., Nakanishi, H., Taguchi, R., Nakaya, T., Murakami, M., Yoneda, Y., Arai, H., Kawaoka, Y., Penninger, J. M., Arita, M., and Imai, Y. (2013) The lipid mediator protectin D1 inhibits influenza virus replication and improves severe influenza, *Cell 153*, 112-125.

337. Ramon, S., Serhan, C. N., Topham, D., and Phipps, R. P. (2013) Endogenous specialized proreslving mediators enhance antigen-specific antibody response against

influena virus: A new class of adjuvant (P4285), In *AAI Annual Meeting*, The Journal of Immunology, Honolulu, Hawaii.

338. Jost, S. A., Tseng, L. C., Matthews, L. A., Vasquez, R., Zhang, S., Yancey, K. B., and Chong, B. F. (2014) IgG, IgM, and IgA antinuclear antibodies in discoid and systemic lupus erythematosus patients, *ScientificWorldJournal 2014*, 171028.

339. Ichimura, A., Hirasawa, A., Poulain-Godefroy, O., Bonnefond, A., Hara, T., Yengo, L., Kimura, I., Leloire, A., Liu, N., Iida, K., Choquet, H., Besnard, P., Lecoeur, C., Vivequin, S., Ayukawa, K., Takeuchi, M., Ozawa, K., Tauber, M., Maffeis, C., Morandi, A., Buzzetti, R., Elliott, P., Pouta, A., Jarvelin, M. R., Korner, A., Kiess, W., Pigeyre, M., Caiazzo, R., Van Hul, W., Van Gaal, L., Horber, F., Balkau, B., Levy-Marchal, C., Rouskas, K., Kouvatsi, A., Hebebrand, J., Hinney, A., Scherag, A., Pattou, F., Meyre, D., Koshimizu, T. A., Wolowczuk, I., Tsujimoto, G., and Froguel, P. (2012) Dysfunction of lipid sensor GPR120 leads to obesity in both mouse and human, *Nature 483*, 350-354.

APPENDIX A: ANIMAL USE PROTOCOLS

EAST CAROLINA UNIVERSITY
ANIMAL USE PROTOCOL (AUP) FORM
LATEST REVISION NOVEMBER, 2013

Project Title:
High Fat Diets Modulate Adaptive Immune Responses

	Principal Investigator	**Secondary Contact**
Name	S. Raza Shaikh	Jarrett Whelan
Dept.	Biochemistry & Molecular Biology	Click here to enter text.
Office Ph #	744-2585	744-2119
Cell Ph #	317-409-9565	252-414-8700
Pager #	Click here to enter text.	Click here to enter text.
Home Ph #	Click here to enter text.	Click here to enter text.
Email	shaikhsa@ecu.edu	whelanj@ecu.edu

For IACUC Use Only

AUP #			
New/Renewal			
Full Review/Date	DR/Date		
Approval Date			
Study Type			
Pain/Distress Category			
Surgery	Survival	Multiple	
Prolonged Restraint			
Food/Fluid Regulation			
Other			
Hazard Approval/Dates	Rad	IBC	EHS
OHP Enrollment			
Mandatory Training			
Amendments Approved			

I. Personnel

A. Principal Investigator(s):
S. Raza Shaikh

B. Department(s):
Biochemistry & Molecular Biology

C. List all personnel (PI's, co-investigators, technicians, students) that will be working with live animals and describe their qualifications and experience with these specific procedures. If people are to be trained, indicate by whom:

Name/Degree/ Certification	Position/Role(s)/ Responsibilities in this Project	Required Online IACUC Training (Yes/No)	Relevant Animal Experience/Training (include species, procedures, number of years, etc.)
Heather Teague (Ph.D. student)	Feeding mice special diets, conducting experiments (i.e. infecting mice with antigens or influenza, Echo-MRI, euthanizing mice)	Yes	Yes, 4 years of working with C57BL/6 mice, OT-II transgenics, IL-5 knockouts, bleeding mice for insulin/glucose tests, feeding special diets. Training is by the PI for insulin/glucose tests.
Perrine Lallemand (technician)	Feeding mice special diets, infecting with influenza, euthanizing mice	Yes	Yes, working with C57BL/6 mice, IL-5 knockouts, bleeding mice, feeding special diets for the past 3 months. Training is by the PI.
Jarrett Whelan, Ph.D.	Feeding mice special diets, conducting experiments (i.e. infecting mice with antigens or influenza, Echo-MRI, euthanizing mice)	Yes	September 2009-September 2011 and recently since January 2014. His experience is with C57BL/6 and IL-5 knockout mice. Training is by the PI.
Madison Sullivan (Ph.D. student)	Feeding mice special diets, conducting experiments (i.e. infecting mice with antigens or influenza, Echo-MRI, euthanizing mice)	Yes	Since September 2013. She has worked with C57BL/6 mice. Training is by the PI.
Tyler Hayden (undergraduate	Feeding mice special diets	Yes	Since Fall 2013 September, Tyler has

)			worked with C57BL/6 mice. Training is by the PI.
S. Raza Shaikh	Feeding mice special diets, conducting experiments (i.e. infecting mice with antigens or influenza, Echo-MRI, euthanizing mice)	Yes	Since 2006 working with Balb/c, C57BL/6, OT transgenics, IL-5 knockouts
Click here to enter text.	Click here to enter text.	Choose an item.	Click here to enter text.
Click here to enter text.	Click here to enter text.	Choose an item.	Click here to enter text.
Click here to enter text.	Click here to enter text.	Choose an item.	Click here to enter text.
Click here to enter text.	Click here to enter text.	Choose an item.	Click here to enter text.

II. Regulatory Compliance

A. Non-Technical Summary

Using language a non-scientist would understand, please provide a clear, concise, and sequential description of animal use. Additionally, explain the overall study objectives and benefits of proposed research or teaching activity to the advancement of knowledge, human or animal health, or good of society. (More detailed procedures are requested later in the AUP.)
Do not cut and paste the grant abstract.

Obesity is as an epidemic on a worldwide scale, a consequence of nutritional and genetic factors. High fat diets are major factors that promote the development of obesity, which results in disorders including diabetes mellitus, cardiovascular disease, hypertension, and immune dysfunction with increased susceptibility to infection. One major factor that predisposes obese individuals to infection is nutritional status. Our laboratory's focus is on identifying the targets and mechanisms by which dietary fatty acids modify the adaptive immune system. The rationale for focusing on fatty acids is that very little is known about how different types of fats consuming in the diet impact the immune system. We are currently studying how fatty acids ranging from saturated fats to unsaturated fats affect the adaptive immune system of mice. Using a combination of techniques, we are studying how different fatty acids affect the function of immune cells of the spleen, which play a vital role in combating infection and inflammation. Overall, animals are fed varying diets with different fat compositions and sacrificed for specific tissues. In some studies, we will induce inflammation by injecting the animals with an inflammatory agent and then sacrifice or infect mice with influenza virus and then sacrifice.

B. Ethics and Animal Use

B.1. Duplication

Does this study duplicate existing research? No

If yes, why is it necessary? (note: teaching by definition is duplicative)

Click here to enter text.

B.2. Alternatives to the Use of Live Animals

Are there less invasive procedures, other less sentient species, isolated organ preparation, cell or tissue culture, or computer simulation that can be used in place of the live vertebrate species proposed here? No

If yes, please explain why you cannot use these alternatives.

Click here to enter text.

B.3. Consideration of Alternatives to Painful/Distressful Procedures

a. Include a literature search to ensure that alternatives to all procedures that may cause more than momentary or slight pain or distress to the animals have been considered.

1. Please list all of the potentially painful or distressful procedures in the protocol:

Injecting with antigen, LPS injection, influenza infection.

2. For the procedures listed above, provide the following information (please do not submit search results but retain them for your records):

Date Search was performed:	February 4, 2014
Database(s) searched:	Pubmed, Google scholar
Time period covered by the search (i.e. 1975-2013):	All
Search strategy (including scientifically relevant terminology):	Obesity, infection, saturated fatty acids, monounsaturated fatty acids, n-3 and n-6 polyunsaturated fatty acids, antigen presentation, T cell proliferation, high fat diets, mechanisms, alternatives, immunological synapse, B-T cell synapse, lipid rafts, lipopolysaccharide (LPS), lymphocyte activation, membrane microviscosity, cell culture, refinement strategies for murine pain, strategies for murine distress, influenza, B cell activation, LPS stimulation, B cell subsets, PR8 methods, pain control, distress and influenza
Other sources consulted:	Google

3. In a few sentences, please provide a brief narrative indicating the results of the search(es) to determine the availability of alternatives and explain why these alternatives were not chosen. Also, please address the 3 Rs of

refinement, reduction, and replacement in your response. Refinement refers to modification of husbandry or experimental procedures to enhance animal well-being and minimize or eliminate pain and distress. Replacement refers to absolute (i.e. replacing animals with an inanimate system) or relative (i.e. using less sentient species) replacement. Reduction involves strategies such as experimental design analysis, application of newer technologies, use of appropriate statistical methods, etc., to use the fewest animals or maximize information without increasing animal pain or distress.

When searching for the effects of high fat diets on the targets and mechanisms of adaptive immunity, the only alternative possibility is to use fatty acids in cell culture (i.e. replacement). However, this method does not depict the in vivo condition of consuming a high fat diet, and results from cell culture can lead to artifacts. In order to avoid these artifacts, feeding mice high fat diets and then isolating specific cell types for experiments is the closest to the in vivo condition. However, to address fundamental mechanisms, we implement the use of cell culture experiments to minimize the use of animals.

We also investigated the possibility of using heat-inactivated influenza in our studies in order to conduct cell culture studies on how influenza modulates B cell mediated immunity (again, replacement strategy). However, the mechanisms by which heat-inactivated influenza activated B cells is not the same as the in vivo condition, where select cytokines from T cells aid in the development of antibody directed against influenza.

We have also investigated how distress and pain management will be addressed with the LPS and influenza studies (i.e. refinement). Distress will be minimized by providing a long sipper tube and/or Hydrogel for hydration, as needed. We anticipate no major changes with animal husbandry. We also employ humane endpoints to minimize pain and distress.

C. Hazardous Agents

1. Protocol related hazards (chemical, biological, or radiological):
Please indicate if any of the following are used in animals and the status of review/approval by the referenced committees:

HAZARDS	Oversight Committee	Status (Approved, Pending, Submitted)/Date	AUP Appendix I Completed?
Radioisotopes	**Radiation**	Click here to enter text.	Choose an item.
Ionizing radiation	**Radiation**	Click here to enter text.	Choose an item.

Infectious agents (bacteria, viruses, rickettsia, prions, etc.)	**IBC**	Influenza, approved on 8/7/13	Choose an item.
Toxins of biological origins (venoms, plant toxins, etc.)	**IBC**	LPS, approved on 5/24/11 (re-approved 3/25/14)	Choose an item.
Transgenic, Knock In, Knock Out Animals--- breeding, cross breeding or any use of live animals or tissues	**IBC**	IL-5 knockouts, approved on 4/24/13	Choose an item.
Human tissues, cells, body fluids, cell lines	**IBC**	Click here to enter text.	Choose an item.
Viral/Plasmid Vectors/Recombinant DNA or recombinant techniques	**IBC**	Click here to enter text.	Choose an item.
Oncogenic/toxic/mutagenic chemical agents	**EH&S**	Click here to enter text.	Choose an item.
Nanoparticles	**EH&S**	Click here to enter text.	Choose an item.
Cell lines, tissues or other biological products injected or implanted in animals	**DCM**	Click here to enter text.	Choose an item.
Other agents	**DNP-KLH**	Approved 7/18/13	Choose an item.

2. Incidental hazards

Will personnel be exposed to any incidental zoonotic diseases or hazards during the study (field studies, primate work, etc)? If so, please identify each and explain steps taken to mitigate risk:

No

III. Animals and Housing

Species and strains:

C57BL/6, BALB/c, TCR transgenics (OT-I and OT-II), and IL-5 knockouts.

The OT mice and IL-5 knockouts are on a C57BL/6 background. The OT-II are C57BL/6-Tg(TcraTcrb)425Cbn/J and OT-I are C57BL/6-Tg(TcraTcrb)1100Mjb/J. OT-II and OT-I are transgenic for the T cell receptor (TCR) on the surface of helper T cells. The IL-5 knockout mice are designated as C57BL/6-Il5^{tm1Kopf}/J.

A. Weight, sex and/or age:

Males, 4-6 weeks of age, occasional females, also 4-6 weeks of age. Generally studies start off with a weight of 14-18g.

C. Animal numbers:

1. Please complete the following table:

Total number of animals in treatment and control groups	**Additional animals (Breeders, substitute animals)**	**Total number of animals used for this project**
2400	+150	=2550

2. Justify the species and number (use statistical justification when possible) of animals requested:

Statistical justification. Based on the F test in the ANOVA and conservative effect, we need 8-9 mice per diet, depending on the functional and mechanistic outcome. To be safe, we will rely on 10 mice per diet.

Treatment groups	# of mice/study	# of studies over 3 years	# animals/group
C57BL/6 on 10 diets	10 mice/time point x 2 time points x 3 doses for each study	a. Study #1 with LPS b. Study #2 with KLH c. Study #3 with influenza	10 mice per diet x 10 diets x 2 time points x 3 doses x 3 studies = 1800
IL-5 knockouts on 10 diets	10 mice/time point x 2 time points	a. Study #1 with LPS	10 mice per diet x 10 diets x 2 time points x 1 study = 200
OT-II (TCR transgenic)	10 mice	a. MHC class II activation b. Immune synapse	10 mice per diet x 10 diets x 2 studies = 200
OT-I (TCR transgenic)	10mice	a. MHC class I activation b. Immune synapse	10 mice per diet x 10 diets x 2 studies = 200
OT-II for breeding	N/A	5 males and 5 females/year	10 x 3 years = 30
OT-I for breeding	N/A	5 males and 5 females/year	10 x 3 years = 30
C57BL/6 for breeding	N/A	10 males and 10 females/year	20 x 3 years = 60

IL-5 knockout for breeding	N/A	5 males and 5 females/year	10 x 3 years = 30

Total: 2550. Note that the time points represent different periods of administering the diet. We have recently discovered that the effects of n-3 polyunsaturated fatty acids are highly time dependent. Thus, the time points will likely be short (3 weeks) and long-term (14 weeks) of dietary intervention.

3. Justify the number and use of any additional animals needed for this study:
An additional 150 mice are needed for breeding.

a. **For unforeseen outcomes/complications:**
Click here to enter text.

b. For refining techniques:
Click here to enter text.

c. For breeding situations, briefly justify breeding configurations and offspring expected:
Click here to enter text.

d. Indicate if following IACUC tail snip guidelines: Yes
(if no, describe and justify)
Click here to enter text.

4. Will the phenotype of mutant, transgenic or knockout animals predispose them to any health, behavioral, physical abnormalities, or cause debilitating effects in experimental manipulations? Yes **(if yes, describe)**

The TCR transgenic can be a bit more prone to infection. However, in the past few years, we have not experienced any problems. We handle the mice carefully and avoid handling excessively. The IL-5 knockout mice are generally devoid of defects even though they lack some subsets of B cells. Thus, we anticipate no major problems with these mice either.

5. Are there any deviations from standard husbandry practices?
Yes, we will rely on single housing upon dietary intervention (i.e. when conducting our studies with various experimental diets). Thus, one male mouse is placed in one cage (i.e. we are not housing multiple mice in a given mouse cage). For the influenza studies, mice will be moved to the appropriate biosafety level upon infection. Mice will need to be kept one per microisolater cage.

If yes, then describe conditions and justify the exceptions to standard housing (temperature, light cycles, sterile cages, special feed, prolonged weaning times, wire-bottom cages, etc.):
The rationale is that our lab is studying the immune response at the whole animal and cellular levels. By placing several male mice in one cage, we risk the possibility of fighting. This can lead to changes in the immune response, which will make it difficult for us to determine if a measured change is due to the diet (our variable of interest) or due to social interactions between the mice. Therefore, it is critical for us to single house the mice for our studies. For the influenza studies, the microisolater cages are needed to ensure that virus is not exposed to other mice.

6. The default housing method for social species is pair or group housing (including mice, rats, guinea pigs, rabbits, dogs, pigs, monkeys). Is it necessary for animals to be singly housed at any time during the study? Yes, after we initiate the special diets **(If yes, describe housing and justify the need to singly house social species):**
The explanation is provided above in point #5.

7. Are there experimental or scientific reasons why routine environmental enrichment should not be provided? No
(If yes, describe and justify the need to withhold enrichment)
Click here to enter text.
8. If wild animals will be captured or used, provide permissions (collection permit # or other required information):
N/A.
9. List all laboratories or locations outside the animal facility where animals will be used. Note that animals may not stay in areas outside the animal facilities for more than 12 hours without prior IACUC approval. For field studies, list location of work/study site.
N/A.

IV. Animal Procedures

A. Outline the Experimental Design including all treatment and control groups and the number of animals in each. Tables or flow charts are particularly useful to communicate your design. Briefly state surgical plans in this section. Surgical procedures can be described in detail in IV.S.

Breeding
For all of the proposed studies, mice are set up in pairs and we maintain a given set for a few months.

Diets. For all the proposed studies, mice will be given one of ten experimental diets, which were developed with a nutritionist from Harlan-Teklad: (i) Normal diet (5% fat by weight) which is a standard purified diet. This diet serves as the primary control (ii) N-3 polyunsaturated fatty acid (PUFA) diet (5% fat by weight) made up of flaxseed and/or fish oil (1/1). (iii) Saturated fatty acid-rich (SFA) high fat diet (20% fat by weight) made up of coconut oil and/or milk fat. (iv) Monounsaturated fatty acid-rich (MUFA) high fat diet (20% fat by weight) made up of olive oil. (v) PUFA-rich high fat diet (20% fat by weight) made up of fish oil and flaxseed oil (1/1). (vi) Hydrogenated high fat diet (20% fat by weight) made up of hydrogenated vegetable oils. (vii) n-6 PUFA high fat diet (20% fat by weight) made up of soybean oil. (viii-x) will be either fish oil, flaxseed oil, or a specific ratio of fish to flaxseed (all at 5-10% fat by weight) depending on some data that we are currently analyzing. All of the high fat diets correspond to ~40% total kcal of energy from fat. For select studies, we will compare our 40% of total kcal of energy from

fat with 60% (which is the typical high fat diet that is commercially available). All of the fatty acids in the diets are in the form of either triglycerides or ethyl esters, which models human oil intake from differing food and supplement sources. Furthermore, diets are stored under nitrogen gas and changed every other day to further minimize oxidation. We will verify the lipid composition of the diets for the mice using gas chromatography.

Based on existing studies, we will conduct studies with different levels of fatty acids in the diet (~5-60% fat by weight) for different periods of feeding (time points fall within the 3-14 week range) to assess the effects of dose and time. Our diets have been tested with C57BL/6, OT-II and AND TCR transgenic mice. We have not observed any adverse effects. We will provide fresh food every other day and monitor food intake and body weights. Food intake is monitored every other day and body weights are taken at least once a week.

Cardiac puncture and submandibular bleeding. We will obtain blood via cardiac puncture on the day we are going to euthanize a set of mice fed different high fat diets. The mice will be placed in the CO_2 chamber and prior to death we will insert a syringe with a ~22g needle to draw blood. The mouse will be immediately euthanized after taking the blood. For some studies, we will rely on submandibular bleeding. For these studies, blood will be collected from the submandibular vein and blood will be placed into a capiject tube (Fisher) coated with serum separator. Mice will be immediately euthanized after submandibular bleeding.

STUDY #1 – MEASURE THE EFFECT OF DIET UPON STIIMULATION WITH LPS

The objective of this study is to determine how the diet impacts the immune response to lipopolysaccharide (LPS).

LPS PROTOCOL. As described in extensive detail above, mice will be fed the differing diets. We will then inject the mice i.p. with ~0.5ml of sterile PBS containing E. Coli serotype 0111:B4 LPS (purchased from Sigma). The dose that we anticipate injecting will be 100μg LPS/20g body weight. Control mice will receive PBS alone. The mice will then be exposed to CO_2 inhalation and blood will be obtained via cardiac puncture. We will ensure the mice are dead using cervical dislocation. For these studies, we will first have to measure the kinetic response to the LPS. We anticipate euthanizing mice within 60 minutes after injection up to 3 days after injection. Once we establish the impact of the LPS on the cytokine profile from the isolated blood, then we will pursue experiments at select time points within 60 minutes up to 3 days.

Our protocol is based on a well-established method from the Philip Calder laboratory (UK Southampton), one of the leading experts in nutritional immunology. Their lab published their original protocol in Immunology 1999, vol 96, pgs. 404-410, entitled "Dietary lipids modify the cytokine response to bacterial lipopolysaccharide in mice". Should any of the mice fail to groom, become unresponsive, or display body loss greater than 20% of their body weight, the mice will be immediately euthanized. Those

mice that are surviving greater than 60 minutes are checked at least daily for the aforementioned clinical signs. Overall, the goal of these studies is to induce inflammation (i.e. inflammatory cytokine release from activated lymphocytes) and study the impact of diet on inflammation ex vivo; therefore, we are not modeling sepsis.

It is anticipated that 600 mice will be used for this study. The mice will consume select diets at differing doses for two time points (likely 3 weeks and 14 weeks).

STUDY #2 – MEASURE THE EFFECT OF DIET UPON STIMULATION WITH KLH

The objective of this study is to determine how the diet impacts the immune response to another antigen, known as KLH.

KLH PROTOCOL. After providing specific diets for a given time frame, mice will be injected i.p. with 4 micrograms of 2,4-dinitrophenylated keyhole limpet protein (DNP-KLH), purchased from Calbiochem and 4 milligrams of aluminum hydroxide, purchased from Sigma. Mice will be subjected to injection 3-10 weeks after feeding the mice the experimental diets. A booster injection will be given 21 days after the primary injection in order to generate a secondary immune response.
C57BL/6 mice will be immunized with DNP-KLH.

It is anticipated that 600 mice will be used for this study. The mice will consume select diets at differing doses for two time points (likely 3 weeks and 14 weeks).

STUDY #3 – MEASURE THE EFFECT OF DIET UPON STIMULATION WITH INFLUENZA

The objective of this study is to determine how the diet impacts the immune response to influenza infection.

INFLUENZA PROTOCOL. After completion of a given time of feeding (e.g. after 3 weeks of feeding), the mice will be anesthetized with isoflurane. Isoflurane will be administered in a bell jar under a hard-ducted biosafety cabinet. A small amount of isoflurane will be placed on a cotton ball, which will not be in contact with the mouse. Mice will be removed from the container under anesthesia in order to infect with the PR8 virus. Upon completion, the cotton ball will be bagged in an appropriate disposal bag and the container will be disinfected inside and outside with Clidox for 10 minutes (for those materials that are not autoclavable) or autoclaved.

Subsequently, mice will be exposed to intranasal infection with 2.5 plaque-forming units (30μl) of mouse-adapted PR8 live virus (influenza virus A/Puerto Rico/8/34/H1N1; Mount Sinai strain). This dose is sub-lethal (Wolf et al., JCI 2011 vol 121 pgs. 3954-3964) given that it is less than 0.1 LD50. Blood will be collected from tail veins on days 7, 21, and 30 post infection in order to measure antibody levels. Control mice will receive saline only injections. Note that the same mice will not be used for each time

point for measuring immune responses at day 7, 21, and 30. To measure B cell class switching, we will conduct secondary immunization with influenza, 30 to 60 days after the first immunization. The second immunization will entail the exact same procedure as the first immunization. Again, blood will be collected 7, 21, and 30 days post infection.

The key clinical sign that we will monitor will be body weight and failure to groom. Weight loss of greater than 20% or lack of grooming will constitute humane endpoints. Upon infection, the mice will be monitored 3 times per day up to four days post-infection. After this time frame, mice will monitored once per day until the termination of the study. With the dose that is being used, immobility, major weight loss, and other signs of distress are not anticipated. Finally, distress will be minimized by providing a long sipper tube and/or Hydrogel for hydration.

Note, the majority of rodent influenza virus research in the field relies on C57BL/6 mice using the lab adapted A/Puerto Rico/8/1934 (H1N1) [PR8] virus. Most inbred mouse strains including C57BL/6 are highly susceptible to death upon PR8 infection. The LD_{50} for PR8 is 100 PFU (we will be using a dose well below this level). Mice infected with PR8 will not transmit the virus to humans. However, infected mice will infect naïve mice by aerosol and contact methods. Peak viral replication in the lungs of mice occurs 2-4 days post infection, after which infectivity of naïve mice is greatly diminished. Antibodies are detectable by day 7 and persist until day 28. To be safe, we will define infectivity as up to 4 days or 96 hours post infection.

It is anticipated that 600 mice will be used for this study. The mice will consume select diets at differing doses for two time points (likely 3 weeks and 14 weeks).

STUDY #4: INVESTIGATE THE ROLE OF IL-5 ON IMMUNE RESPONSES IN RESPONSE TO DIETARY INTERVENTION

The objective of this study is to determine if the effects of some diet types are driven by the cytokine IL-5.

IL-5 STUDY PRTOCOL. The IL-5 knockout mice will be fed the differing diets and then injected with LPS as described above for Study #1. Should the need arise for additional antigens, we will seek an amendment to the AUP. In addition, we will require tail snips for PCR to verify the genotype. Tail snips will be conducted in agreement with the IACUC approved tail snip policy. To minimize pain and distress, mice for tail snips will be between 10-21 days old. This time frame (based on the literature searches) is selected since tail tissue is soft and the tail vertebrae have not calcified. The mouse will be manually restrained and we will apply ice-cold ethyl alcohol (applied until the tail is blanched) prior to conducting the tail snip. A sterile razor blade will be used on the mouse and a maximum of 2mm of the tail will be obtained. The mouse will be observed upon returning the animal to the cage (to ensure there is no major blood loss). Any bleeding will be controlled with pressure using sterile gauze followed by the use of 1% lidocaine. All instruments will be sterile between animals. Not all mice will be tail

snipped given that the mice are homozygous. We will randomly conduct tail snips on any new mice that are born in order to ensure we are maintaining the knockout phenotype. It is anticipated that 200 mice will be used for this study based on two times points of feeding (3 weeks and 14 weeks).

In sections IV.B-IV.S below, please respond to all items relating to your proposed animal procedures. If a section does not apply to your experimental plans, please leave it blank.

Please refer to DCM and IACUC websites for relevant guidelines and SOPs.

B. Anesthesia/Analgesia/Tranquilization/Pain/Distress Management For Procedures Other than Surgery:

Adequate records describing anesthetic monitoring and recovery must be maintained for all species.
If anesthesia/analgesia must be withheld for scientific reasons, please provide compelling scientific justification as to why this is necessary:
Click here to enter text.

1. **Describe the pre-procedural preparation of the animals:**
   a. **Food restricted for** Click here to enter text. **hours**
   b. **Food restriction is not recommended for rodents and rabbits and must be justified:**
   Click here to enter text.
   c. **Water restricted for** Click here to enter text. **hours**
   d. **Water restriction is not recommended in any species for routine pre-op prep and must be justified:**
   Click here to enter text.

2. Anesthesia/Analgesia *for Procedures Other than Surgery*

	Agent	**Concentration**	**Dose (mg/kg)**	**Max Volume**	**Route**	**Frequency**	**Number of days administered**
Pre-procedure analgesic	Click here to enter text.	Click here to enter text.	Click here to enter text.	Click here to enter text.	Click here to enter text.	Click here to enter text.	Click here to enter text.
Pre-anesthetic	Click here to enter text.	Click here to enter text.	Click here to enter text.	Click here to enter text.	Click here to enter	Click here to enter text.	Click here to enter text.

					text.		
Anesthetic	isoflurane	1mL on a cottonball	N/A.	1mL	I.N.	Once after the mice have consumed the experimental diet	Once
Post procedure analgesic	Lidocaine	1%	1% w/v	300ul	Applied to tail	Once	Once
Other	Click here to enter text.	Click here to enter text.	Click here to enter text.	Click here to enter text.	Click here to enter text.	Click here to enter text.	Click here to enter text.

3. Reason for administering agent(s):
The isoflurane is to infect mice with influenza. The 1% lidocaine is to minimize pain based on a tail snip.
4. For which procedure(s):
Study #3 described above. The 1% lidocaine is for genotyping of IL-5 mice.
5. Methods for monitoring anesthetic depth:
Toe pinch for isoflurane.
6. Methods of physiologic support during anesthesia and recovery:
N/A.
7. Duration of recovery:
5 minutes
8. Frequency of recovering monitoring:
Continuous for 10-15 minutes after removal of the mouse from the bell jar.
9. Specifically what will be monitored?
Breathing, locomotor activity
10. When will animals be returned to their home environment?
10-15 minutes after the administration of isoflurane
11. Describe any behavioral or husbandry manipulations that will be used to alleviate pain, distress, and/or discomfort:
As described in our protocol, tail vein blood will be collected to obtain the minimal amount of blood for measuring an antibody response. Providing a long sipper tube and/or Hydrogel for hydration will minimize distress. If the mice lose more than 20% of their body weight or fail to groom, they will be euthanized.

C. Use of Paralytics

1. Will paralyzing drugs be used? No
2. For what purpose:
Click here to enter text.
3. Please provide scientific justification for paralytic use:
Click here to enter text.
4. Paralytic drug:
Click here to enter text.
5. Dose:
Click here to enter text.
6. Method of ensuring appropriate analgesia during paralysis:
Click here to enter text.

D. Blood or Body Fluid Collection

1. Please fill out appropriate sections of the chart below:

	Location on animal	Needle/catheter size	Volume collected	Frequency of procedure	Time interval between collections
Blood Collection	tail	Nick	A small nick should provide 5 microliters, which is adequate for antibody measurements. A new sterile needle will be used for each mouse.	For influenza, twice (either day 7, 21, or 30 after first immunization with influenza and then 30 additional days after secondary immunization For KLH, twice, 7 days after the first immunization and 7 days after the second immunization. Note the second immunization	30 days for influenza, 21 days for KLH

				is 21 days after the first one.	
Body Fluid Collection		Click here to enter text.	Click here to enter text.	Click here to enter text.	Click here to enter text.
Other	Tail snip (from IL-5 knockout mice)	Razor blade	2mm snip should provide 5-20ul	Once at the age of 10-21 days old	None

E. Injections, Gavage, & Other Substance Administration

1. Please fill out appropriate sections of the chart below:

	Compound	**Location & Route of admin**	**Needle/ catheter/gavage size**	**Max volume admin**	**Freq of admin (ie two times per day)**	**Number of days admin (ie for 5 days)**	**Max dosages (mg/kg)**
Injection/ Infusion	LPS	Intraperitoneal	25g	100μg LPS/20g body weight. The volume will be 0.5ml or less. PBS (control) will be added, also at 0.5ml	Once	Once	0.1mg /.02kg
Injection/ Infusion	DNP-KLH + aluminum hydroxide	Intraperitoneal	26 3/8	0.2 ml saline	Once after 3-10 weeks of feeding mice experimental diets. Then one more injection 21 days later.	Once in a given day	4ug per mouse of DNP-KLH and 4mg of aluminum hydro

							xide. The amount injected is not dependent on the body weight. We will give this to mice greater than 20g.
Gavage	Click here to enter text.	Click here to enter text.	Click here to enter text.	Click here to enter text.	Click here to enter text.	Click here to enter text.	Click here to enter text.
Other	Influenza virus	Intranasal	N/A	N/A	Once	Once	2.5 plaque-forming units

3. **Pharmaceutical grade drugs, biologics, reagents, and compounds are defined as agents approved by the Food and Drug Administration (FDA) or for which a chemical purity standard has been written/established by any recognized pharmacopeia such as USP, NF, BP, etc. These standards are used by manufacturers to help ensure that the products are of the appropriate chemical purity and quality, in the appropriate solution or compound, to ensure stability, safety, and efficacy. For all injections and infusions for CLINICAL USE, PHARMACEUTICAL GRADE compounds must be used whenever possible. Pharmaceutical grade injections and infusions for research test articles are preferred when available. If pharmaceutical grade compounds are not available and non-pharmaceutical grade agents must be used, then the following information is necessary:**

a. **Please provide a scientific justification for the use of ALL non-pharmaceutical grade compounds. This may include pharmaceutical-grade**

compound(s) that are not available in the appropriate concentration or formulation, or the appropriate vehicle control is unavailable.

b. Indicate the method of preparation, addressing items such as purity, sterility, pH, osmolality, pyrogenicity, adverse reactions, etc. (please refer to ECU IACUC guidelines for non-pharmaceutical grade compound use), labeling (i.e. preparation and use-by dates), administration and storage of each formulation that maintains stability and quality/sterility of the compound(s).

For all of the proposed studies, we will rely on pharmaceutical grade compounds except KLH. The KLH reagents are not classified by the companies as pharmaceutical grade. In communication with the companies, they will provide certificate of analyses ensuring that the materials are safe for animals use (including issues related to pH, osmolality, sterility, as required by IACUC) only after purchase. Thus, we can purchase the materials and provide the certificates to the animal use committee. Stock solutions will be made with sterile PBS (sterilized by autoclaving) and stored in sterile Eppendorf tubes at 4C. A certificate of analysis is provided by Calbiochem. We will use KLH which is highly purified (>95%) and collected under sterile conditions, endotoxin and pyrogen-free, and has a pH of 6.5. The lyophilized powder will be aseptically reconstituted and stored as described above.

F. <u>Prolonged restraint with mechanical devices</u>

Prolonged restraint in this context means *beyond routine care and use procedures* for rodent and rabbit restrainers, and large animal stocks. Prolonged restraint also includes *any* use of slings, tethers, metabolic crates, inhalation chambers, primate chairs and radiation exposure restraint devices.

N/A

1. For what procedure(s):

Click here to enter text.

2. Explain why non-restraint alternatives cannot be utilized:

Click here to enter text.

3. Restraint device(s):

Click here to enter text.

4. Duration of restraint:

Click here to enter text.

5. Frequency of observations during restraint/person responsible:

Click here to enter text.

6. Frequency and total number of restraints:

Click here to enter text.

7. Conditioning procedures:

Click here to enter text.

8. Steps to assure comfort and well-being:

Click here to enter text.

9. Describe potential adverse effects of prolonged restraint and provide humane endpoints (criteria for either humanely euthanizing or otherwise removing from study):
Click here to enter text.

G. Tumor Studies, Disease Models, Toxicity Testing, Vaccine Studies, Trauma Studies, Pain Studies, Organ or System Failure Studies, Shock Models, etc.

1. Describe methodology:
INFLUENZA PROTOCOL. After completion of a given time of feeding, the mice will be anesthetized with isoflurane, and expose to intranasal infection with 2.5 plaque-forming units (30μl) of mouse-adapted PR8 live virus (influenza virus A/Puerto Rico/8/34/H1N1; Mount Sinai strain). This dose is sub-lethal (Wolf et al., JCI 2011 vol 121 pgs. 3954-3964) given that it is less than 0.1 LD50. Blood will be collected from tail veins on days 7, 21, and 30 post infection in order to measure antibody levels. Control mice will receive saline only injections. To measure B cell class switching, we will conduct secondary immunization with influenza, 30 to 60 days after the first immunization. The second immunization will entail the exact same procedure as the first immunization. Again, blood will be collected 7, 21, and 30 days post infection.

2. Expected model and/or clinical/pathological manifestations:
The key clinical sign that we will monitor will be body weight and failure to groom. Weight loss of greater than 20% or lack of grooming will constitute humane endpoints. The second dose of influenza will not make the mice sicker and in fact, the mice are expected to be much healthier.

3. Signs of pain/discomfort:
With the dose that is being used, immobility, major weight loss, and other signs of distress are not anticipated. Distress will be minimized by providing a long sipper tube and/or Hydrogel for hydration.

4. Frequency of observations:
Upon infection, the mice will be monitored 3 times per day up to four days post-infection. After this time frame, mice will monitored once per day until the termination of the study.

5. Describe potential adverse side effects of procedures and provide humane endpoints (criteria for either humanely euthanizing or otherwise removing from study): No major adverse side effects are anticipated. However, more than 20% weight loss and failure to groom will result in euthanasia.

H. Treadmills/Swimming/Forced Exercise

1. Describe aversive stimulus (if used):
Click here to enter text.

2. Conditioning:

Click here to enter text.

3. Safeguards to protect animal:

Click here to enter text.

4. Duration:

Click here to enter text.

5. Frequency:

Click here to enter text.

6. Total number of sessions:

Click here to enter text.

7. Describe potential adverse effects of procedures and provide humane endpoints (criteria for either humanely euthanizing or otherwise removing from study):

Click here to enter text.

I. <u>Projects Involving Food and Water Regulation or Dietary Manipulation</u>
(*Routine pre-surgical fasting not relevant for this section)*

1. Food Regulation

a. Amount regulated and rationale:

Click here to enter text.

b. Frequency and duration of regulation (hours for short term/weeks or months for long term):

Click here to enter text.

c. Frequency of observation/parameters documented (i.e. recording body weight, body condition, etc.):

Click here to enter text.

d. Describe potential adverse effects of procedures and provide humane endpoints (criteria for either humanely euthanizing or otherwise removing from study):

Click here to enter text.

2. Fluid Regulation

a. Amount regulated and rationale:

Click here to enter text.

b. Frequency and duration of regulation (hours for short term/weeks or months for long term):

Click here to enter text.

c. Frequency of observation/parameters documented (body weight, hydration status, etc.):

Click here to enter text.

d. Describe potential adverse effects of procedures and provide humane endpoints (criteria for either humanely euthanizing or otherwise removing from study):

Click here to enter text.

3. Dietary Manipulations

a. Compound supplemented/deleted and amount:

Experimental lean and high fat diets supplemented with various fat types. As Mice will be given one of ten experimental diets, which were developed with a nutritionist from Harlan-Teklad: (i) Control diet, which is a standard purified diet. (ii) N-3 polyunsaturated fatty acid (PUFA) diet made up of flaxseed and/or fish oil components. (iii) Saturated fatty acid-rich (SFA) high fat diet made up of coconut oil and/or milk fat. (iv) Monounsaturated fatty acid-rich (MUFA) high fat diet made up of olive oil. (v) PUFA-rich high fat diet made up of fish oil and/or flaxseed oil. (vi) Hydrogenated high fat diet made up of hydrogenated vegetable oils. (vii) n-6 PUFA high fat diet made up of soybean oil. (viii-x) will be high fat diets ranging from 45-60% of total kcal from fat of which fatty acids are supplied as triglycerides or ethyl esters. The control diet provides 13% of total kcal from fat.

b. Frequency and duration (hours for short term/week or month for long term):

Anywhere from 3 to 14 weeks of feeding depending on the functional endpoint.

c. Frequency of observation/parameters documented:

Observations on body weight, especially of a new diet, are made on a weekly basis and food is administered every other day, which includes weighing the food and general health of the animal.

d. Describe potential adverse effects of procedures and provide humane endpoints (criteria for either humanely euthanizing or otherwise removing from study):

We do not anticipate any adverse effects of the diets since our fat levels are below those that would induce insulin resistance. However, with any intervention, failure to groom and/or loss of >~20% body weight will result in euthanasia. Mice will be weighed weekly to check for body weight.

J. Endoscopy, Fluoroscopy, X-Ray, Ultrasound, MRI, CT, PET, Other Imaging

1. Describe animal methodology:

Click here to enter text.

2. Duration of procedure:

Click here to enter text.

3. Frequency of observations during procedure:

Click here to enter text.

4. Frequency/total number of procedures:

Click here to enter text.

5. Method of transport to/from procedure area:

Click here to enter text.

6. Describe potential adverse side effects of procedures and provide humane endpoints (criteria for either humanely euthanizing or otherwise removing from study):
Click here to enter text.

7. Please provide or attach appropriate permissions/procedures for animal use on human equipment:
Click here to enter text.

K. Polyclonal Antibody Production

1. **Antigen/adjuvant used and justification for adjuvant choice:**
   Click here to enter text.
2. **Needle size:**
   Click here to enter text.
3. **Route of injection:**
   Click here to enter text.
4. **Site of injection:**
   Click here to enter text.
5. **Volume of injection:**
   Click here to enter text.
6. **Total number of injection sites:**
   Click here to enter text.
7. **Frequency and total number of boosts:**
   Click here to enter text.
8. **What will be done to minimize pain/distress:**
   Click here to enter text.
9. **Describe potential adverse effects of procedures and provide humane endpoints (criteria for either humanely euthanizing or otherwise removing from study):**
   Click here to enter text.

L. Monoclonal Antibody Production

1. Describe methodology:
Click here to enter text.

2. Is pristane used: Choose an item.
Volume of pristane:
Click here to enter text.

3. Will ascites be generated: Choose an item.

i. **Criteria/signs that will dictate ascites harvest:**
   Click here to enter text.
ii. **Size of needle for taps:**
   Click here to enter text.
iii. **Total number of taps:**
   Click here to enter text.
iv. **How will animals be monitored/cared for following taps:**
   Click here to enter text.

4. What will be done to minimize pain/distress:
Click here to enter text.

5. Describe potential adverse effects of procedures and provide humane endpoints (criteria for either humanely euthanizing or otherwise removing from study):
Click here to enter text.

M. Temperature/Light/Environmental Manipulations

1. Describe manipulation(s):
Click here to enter text.
2. Duration:
Click here to enter text.
3. Intensity:
Click here to enter text.
4. Frequency:
Click here to enter text.
5. Frequency of observations/parameters documented:
Click here to enter text.
6. Describe potential adverse effects of procedures and provide humane endpoints (criteria for either humanely euthanizing or otherwise removing from study):
Click here to enter text.

N. Behavioral Studies

1. Describe methodology/test(s) used:
Click here to enter text.
2. Will conditioning occur? If so, describe:
Click here to enter text.
3. If aversive stimulus used, frequency, intensity and duration:
Click here to enter text.
4. Length of time in test apparatus/test situation: *(i.e., each test is ~10 mins)*
Click here to enter text.
5. Frequency of testing and duration of study: *(i.e., 5 tests/week for 6 months)*
Click here to enter text.
6. Frequency of observation/monitoring during test:
Click here to enter text.
7. Describe potential adverse effects of procedures and provide humane endpoints (criteria for either humanely euthanizing or otherwise removing from study):
Click here to enter text.

O. Capture with Mechanical Devices/Traps/Nets

1. Description of capture device/method:
Click here to enter text.
2. Maximum time animal will be in capture device:
Click here to enter text.
3. Frequency of checking capture device:

Click here to enter text.

4. Methods to ensure well-being of animals in capture device:
Click here to enter text.

5. Methods to avoid non-target species capture:
Click here to enter text.

6. Method of transport to laboratory/field station/processing site and duration of transport:
Click here to enter text.

7. Methods to ensure animal well-being during transport:
Click here to enter text.

8. Expected mortality rates:
Click here to enter text.

9. Describe potential adverse effects of procedures and provide humane endpoints (criteria for either humanely euthanizing or otherwise removing from study):
Click here to enter text.

P. Manipulation of Wild-Caught Animals in the Field or Laboratory

1. Parameters to be measured/collected:
Click here to enter text.

2. Approximate time required for data collection per animal:
Click here to enter text.

3. Method of restraint for data collection:
Click here to enter text.

4. Methods to ensure animal well-being during processing:
Click here to enter text.

5. Disposition of animals post-processing:
Click here to enter text.

6. Describe potential adverse effects of procedures and provide humane endpoints (criteria for either humanely euthanizing or otherwise removing from study):
Click here to enter text.

Q. Wildlife Telemetry/Other Marking Methods

1. Describe methodology (including description of device):
Click here to enter text.

2. Will telemetry device/tags/etc. be removed? Choose an item. **If so, describe:**
Click here to enter text.

3. Describe potential adverse effects of procedures and provide humane endpoints (criteria for either humanely euthanizing or otherwise removing from study):
Click here to enter text.

R. Other Animal Manipulations

1. Describe methodology:
Click here to enter text.

2. Describe methods to ensure animal comfort and well-being:
Click here to enter text.
3. Describe potential adverse effects of procedures and provide humane endpoints (criteria for either humanely euthanizing or otherwise removing from study):
Click here to enter text.

S. Surgical Procedures

All survival surgical procedures must be done aseptically, regardless of species or location of surgery. Adequate records describing surgical procedures, anesthetic monitoring and postoperative care must be maintained for all species.

1. Location of Surgery (Building & Room #):
Click here to enter text.

2. Type of Surgery (check all that are appropriate):
Click here to enter text.

☐ **Non-survival surgery (animals euthanized without regaining consciousness)**
☐ **Major survival surgery (major surgery penetrates and exposes a body cavity or produces substantial impairment of physical or physiologic function)**
☐ **Minor survival surgery**
☐ **Multiple survival surgery**
If yes, provide scientific justification for multiple survival surgical procedures:
Click here to enter text.

3. Describe the pre-op preparation of the animals:

a. **Food restricted for** Click here to enter text. **hours**
b. **Food restricted is not recommended for rodents and rabbits and must be justified:**
Click here to enter text.
c. Water restricted for Click here to enter text. **hours**
d. Water restriction is not recommended in any species for routine pre-op prep and be justified:
Click here to enter text.

4. Minimal sterile techniques will include (check all that apply):
Please refer to DCM Guidelines for Aseptic Surgery for specific information on what is required for each species and type of surgery (survival vs. non-survival).

☐ **Sterile instruments**
How will instruments be sterilized?
Click here to enter text.

If serial surgeries are done, how will instruments be sterilized between surgeries:
Click here to enter text.

☐ **Sterile gloves**
☐ **Mask**
☐ **Cap**
☐ **Sterile gown**
☐ **Sanitized operating area**
☐ **Clipping or plucking of hair or feathers**
☐ **Skin preparation with a sterilant such as betadine**
☐ **Practices to maintain sterility of instruments during surgery**
☐ **Non-survival (clean gloves, clean instruments, etc.)**

5. **Describe all surgical procedures:**
   a. Skin incision size and site on the animal:
   Click here to enter text.
   b. Describe surgery in detail (include size of implant if applicable):
   Click here to enter text.
   c. Method of wound closure:
   Click here to enter text.
   i. Number of layers
   Click here to enter text.
   ii. Type of wound closure and suture pattern:
   Click here to enter text.
   iii. Suture type/size/wound clips/tissue glue:
   Click here to enter text.
   iv. Plan for removing of skin sutures/wound clip/etc:
   Click here to enter text.

6. **Anesthetic Protocol:**
   a. If anesthesia/analgesia must be withheld for scientific reasons, please provide compelling scientific justification as to why this is necessary:
   Click here to enter text.

b. Anesthesia/Analgesia For Surgical Procedures

	Agent	Dose (mg/kg or %)	Volume	Route	Frequency	Number of days administered
Pre-operative analgesic	Click here to enter text.	Click here to enter text.	Click here to enter text.	Click here to enter text.	Click here to enter text.	Click here to enter text.
Pre-anesthetic	Click here to enter text.	Click here to enter text.	Click here to enter text.	Click here to enter text.	Click here to enter text.	Click here to enter

						text.
Anesthetic	Click here to enter text.	Click here to enter text.	Click here to enter text.	Click here to enter text.	Click here to enter text.	Click here to enter text.
Post-operative Analgesic	Click here to enter text.	Click here to enter text.	Click here to enter text.	Click here to enter text.	Click here to enter text.	Click here to enter text.
Other	Click here to enter text.	Click here to enter text.	Click here to enter text.	Click here to enter text.	Click here to enter text.	Click here to enter text.

c. Methods that will be used to monitor anesthetic depth (include extra measures employed when paralyzing agents are used):
Click here to enter text.

d. Methods of physiologic support during anesthesia and immediate post-op period (fluids, warming, etc.):
Click here to enter text.

e. List what parameters are monitored during immediate post-op period. Provide the frequency and duration:
Click here to enter text.

f. Describe any other manipulations that will be used to alleviate pain, distress, and/or discomfort during the immediate post-op period (soft bedding, long sipper tubes, food on floor, dough diet, etc.):
Click here to enter text.

g. List criteria used to determine when animals are adequately recovered from anesthesia and when the animals can be returned to their home environment:
Click here to enter text.

7. Recovery from Surgical Manipulations (after animal regains consciousness and is returned to its home environment)
Click here to enter text.

a. What parameters (behavior, appetite, mobility, wound healing, etc.) will be monitored:
Click here to enter text.

b. How frequently (times per day) will animals be monitored:
Click here to enter text.

c. How long post-operatively (days) will animals be monitored:
Click here to enter text.

8. Surgical Manipulations Affecting Animals

a. Describe any signs of pain/discomfort/functional deficits resulting from the surgical procedure:
Click here to enter text.

b. What will be done to manage any signs of pain or discomfort (include pharmacologic and non-pharmacologic interventions):
Click here to enter text.
c. Describe potential adverse effects of procedures and provide humane endpoints (criteria for either humanely euthanizing or otherwise removing from study):
Click here to enter text.

V. Euthanasia

Please refer to the AVMA Guidelines for the Euthanasia of Animals: 2013 Edition and DCM Guidelines to determine appropriate euthanasia methods.

A. Euthanasia Procedure*. All investigators, even those conducting non-terminal studies, must complete this section in case euthanasia is required for humane reasons.*

1. Physical Method- If a physical method is used, the animal should be first sedated/anesthetized with CO_2 or other anesthetic agent. If prior sedation is not possible, a scientific justification must be provided:
Mice infected with influenza will be euthanized by isoflurane overdose followed by cervical dislocation.

2. Inhalant Method- CO2
(if other, describe the agent and delivery method)
Click here to enter text.

3. Non-Inhalant Pharmaceutical Method (injectables, MS-222, etc.)- Please provide the following:

a. Agent:
Click here to enter text.
b. Dose or concentration:
Click here to enter text.
c. Route:
Click here to enter text.

B. Method of ensuring death (can be physical method, such as pneumothorax or decapitation for small species and assessment method such as auscultation for large animals):
Absence of heartbeat. All mice will be cervically dislocated as a means of ensuring death.

C. Describe disposition of carcass following euthanasia:
Numerous tissues are removed from the mice after euthanasia. All carcasses are disposed of in the DCM cooler after tissue removal.

I acknowledge that humane care and use of animals in research, teaching and testing is of paramount importance, and agree to conduct animal studies with professionalism, using ethical principles of sound animal stewardship. I further acknowledge that I will perform only those procedures that are described in this AUP and that my use of animals must conform to the standards described in the Animal Welfare Act, the Public Health Service Policy, The Guide For the Care and Use of Laboratory Animals, the Association for the Assessment and Accreditation of Laboratory Animal Care, and East Carolina University.

Please submit the completed animal use protocol form via e-mail attachment to iacuc@ecu.edu. You must also carbon copy your Department Chair.

PI Signature: _____ 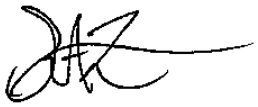 **____ Date__4/5/14_____**

Veterinarian:_____ Date:_____

IACUC Chair: _____Date:_____

APPENDIX 1-HAZARDOUS AGENTS			
Principal Investigator: S. Raza Shaikh	Campus Phone: 744-2585		Home Phone: (317)409-9565
IACUC Protocol Number: AUP CO59a	Department: Biochemistry & Molecular Biology		E-Mail: shaikhsa@ecu.edu
Secondary Contact: Jarrett Whelan Department: Biochemistry	Campus Phone: 744-2119	Home Phone (252) 414-8700	E-Mail: WHELANJ@ecu.edu
Chemical Agents used:N/A		Radioisotopes used:N/A	
Biohazardous Agents used: Influenza PR8, LPS	Animal Biosafety Level: 2	Infectious to humans? No	
PERSONAL PROTECTIVE EQUIPMENT REQUIRED:			
Route of Excretion: Feces, urine, exhalation			
Precautions for Handling Live or Dead Animals: For influenza: With live animals, the major concern is getting bit; thus, we will double glove (even though the mice will be anesthetized). With dead animals, mice will be placed in a biohazard bag and labeled appropriately to indicate infection. For LPS: there are no precautions required.			
Animal Disposal: For influenza: Mice will be disposed in the standard freezers. Infectivity is not an issue since the virus clears in about 48 hours and will not exist in the dead animals. To be safe, we will define infectivity as 96 hours post infection. For LPS: mice will be disposed in the standard freezers.			
Bedding/Waste Disposal: For influenza: During the 48 hours in which the mice can spread infection, proper clothing and precautions with bedding will be required. Bedding should be autoclaved if changed during the 48 hours after infection. Disinfectant should also be used during handling. For LPS: there is no need for special bedding or waste disposal.			
Cage Decontamination: For influenza: During the 48 hours in which the mice can spread infection, the cages should be autoclaved. In addition, disinfectant should also be used during handling. For LPS: no need for special cage decontamination.			
Additional Precautions to Protect Personnel, Adjacent Research Projects including Animals and the Environment: For influenza: Mice will be in an isolated area that are infected, personnel will be double gloved, and appropriate work will be done in a biosafety cabinet. For LPS: there are no special precautions.			
Initial Approval Safety/Subject Matter Expert Signature & Date Approved 8/17/13 _____			

NOTE: THIS FORM WAS APPROVED BY EDDIE JOHNSON ON 3/25/1

APPENDIX B: SUPPLEMENTAL FIGURES

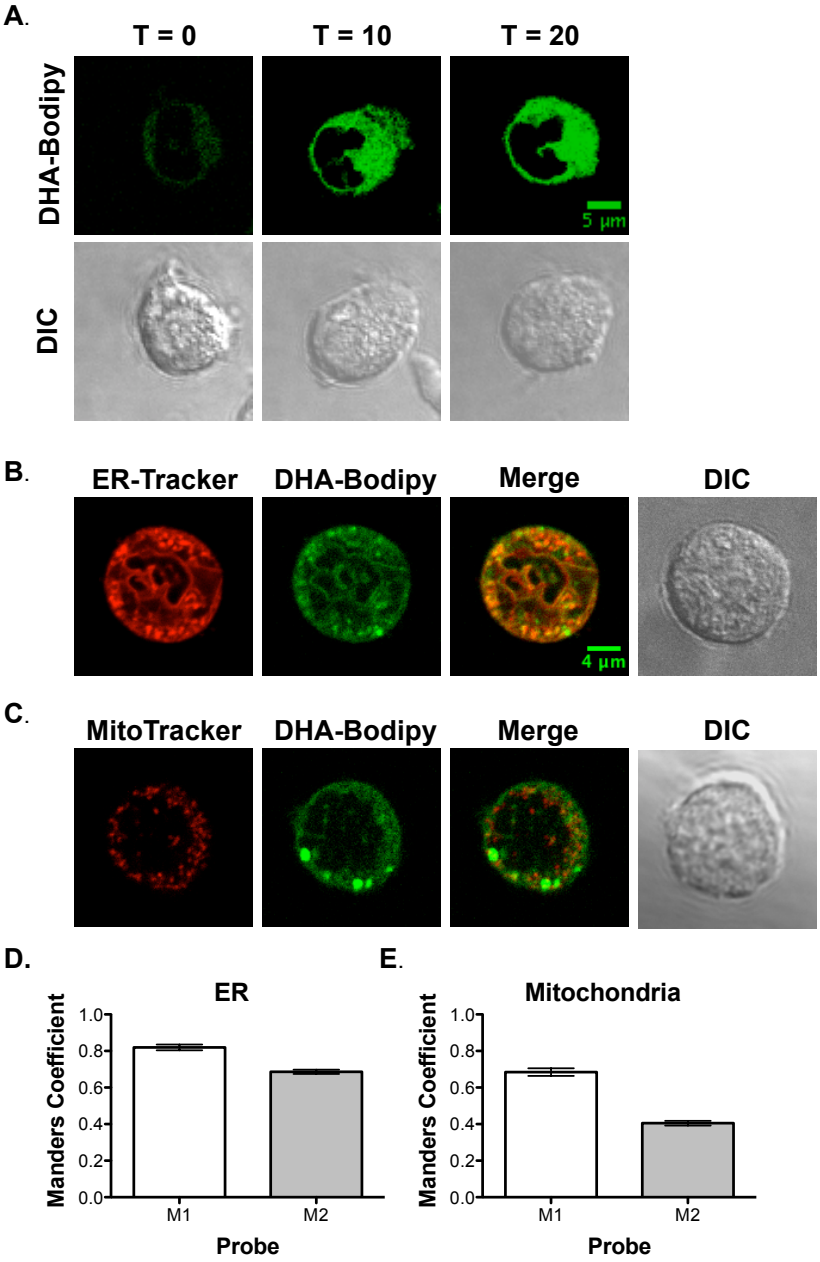

Supplemental Figure 1: DHA-Bodipy shows uptake of the probe into the ER and mitochondria of EL4 cells.

(A) Sample fluorescent and DIC images of DHA-Bodipy in EL4 cells as a function of short-term treatment. Images of DHA-Bodipy, upon long-term treatment, co-localizing with the (B) ER and (C) mitochondria of EL4 cells. Corresponding quantification of fluorescence co-localization between the Bodipy probe and the (D) ER or (E) mitochondria in terms of Manders correlation coefficients M1 and M2. EL4 cells were stained at 37°C. Data are average ± S.E. from 3-4 independent experiments.

A.

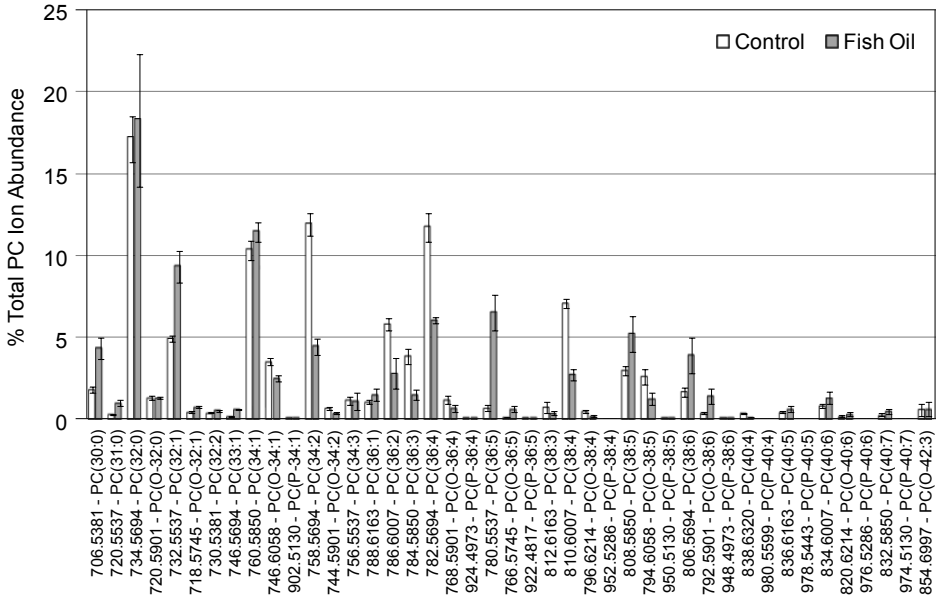
% Total PC Ion Abundance
Control
Fish Oil
706.5381 - PC(30:0)
720.5537 - PC(31:0)
734.5694 - PC(32:0)
720.5901 - PC(O-32:0)
732.5537 - PC(32:1)
718.5745 - PC(O-32:1)
730.5381 - PC(32:2)
746.5694 - PC(33:1)
760.5850 - PC(34:1)
746.6058 - PC(O-34:1)
902.5130 - PC(P-34:1)
758.5694 - PC(34:2)
744.5901 - PC(O-34:2)
756.5537 - PC(34:3)
788.6163 - PC(36:1)
786.6007 - PC(36:2)
784.5850 - PC(36:3)
782.5694 - PC(36:4)
768.5901 - PC(O-36:4)
924.4973 - PC(P-36:4)
780.5537 - PC(36:5)
766.5745 - PC(O-36:5)
922.4817 - PC(P-36:5)
812.6163 - PC(38:3)
810.6007 - PC(38:4)
796.6214 - PC(O-38:4)
952.5286 - PC(P-38:4)
808.5850 - PC(38:5)
794.6058 - PC(O-38:5)
950.5130 - PC(P-38:5)
806.5694 - PC(38:6)
792.5901 - PC(O-38:6)
948.4973 - PC(P-38:6)
838.6320 - PC(40:4)
980.5599 - PC(P-40:4)
836.6163 - PC(40:5)
978.5443 - PC(P-40:5)
834.6007 - PC(40:6)
820.6214 - PC(O-40:6)
976.5286 - PC(P-40:6)
832.5850 - PC(40:7)
974.5130 - PC(P-40:7)
854.6997 - PC(O-42:3)

B.

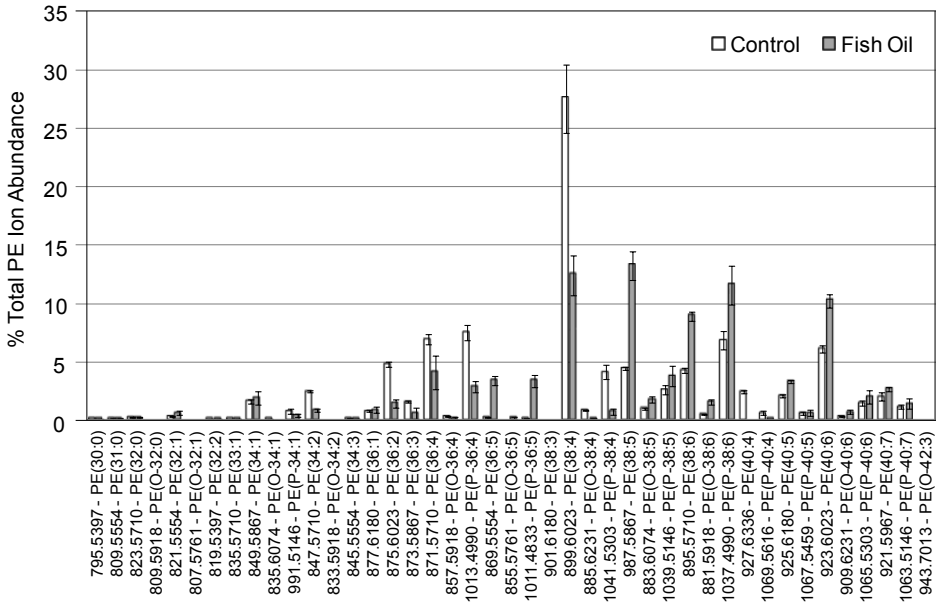
% Total PE Ion Abundance
Control
Fish Oil
795.5397 - PE(30:0)
809.5554 - PE(31:0)
823.5710 - PE(32:0)
809.5918 - PE(O-32:0)
821.5554 - PE(32:1)
807.5761 - PE(O-32:1)
819.5397 - PE(32:2)
835.5710 - PE(33:1)
849.5867 - PE(34:1)
835.6074 - PE(O-34:1)
991.5146 - PE(P-34:1)
847.5710 - PE(34:2)
833.5918 - PE(O-34:2)
845.5554 - PE(34:3)
877.6180 - PE(36:1)
875.6023 - PE(36:2)
873.5867 - PE(36:3)
871.5710 - PE(36:4)
857.5918 - PE(O-36:4)
1013.4990 - PE(P-36:4)
869.5554 - PE(36:5)
855.5761 - PE(O-36:5)
1011.4833 - PE(P-36:5)
901.6180 - PE(38:3)
899.6023 - PE(38:4)
885.6231 - PE(O-38:4)
1041.5303 - PE(P-38:4)
987.5867 - PE(38:5)
883.6074 - PE(O-38:5)
1039.5146 - PE(P-38:5)
895.5710 - PE(38:6)
881.5918 - PE(O-38:6)
1037.4990 - PE(P-38:6)
927.6336 - PE(40:4)
1069.5616 - PE(P-40:4)
925.6180 - PE(40:5)
1067.5459 - PE(P-40:5)
923.6023 - PE(40:6)
909.6231 - PE(O-40:6)
1065.5303 - PE(P-40:6)
921.5967 - PE(40:7)
1063.5146 - PE(P-40:7)
943.7013 - PE(O-42:3)

C.

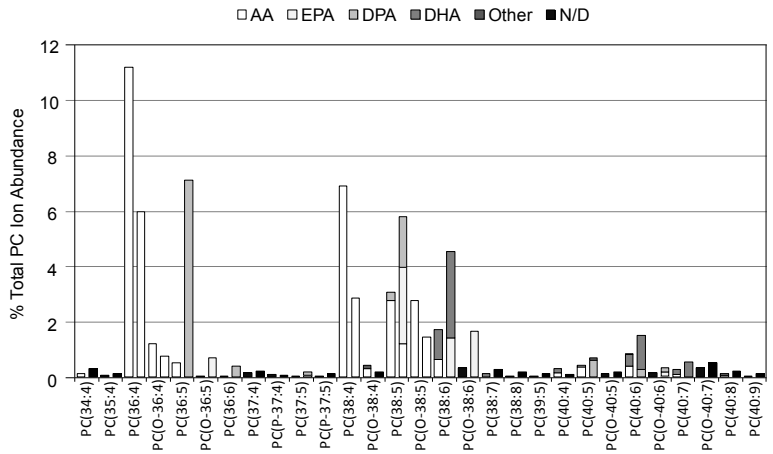
AA EPA DPA DHA Other N/D
% Total PC Ion Abundance
0
2
4
6
8
10
12
PC(34:4)
PC(35:4)
PC(36:4)
PC(O-36:4)
PC(36:5)
PC(O-36:5)
PC(36:6)
PC(37:4)
PC(P-37:4)
PC(37:5)
PC(P-37:5)
PC(38:4)
PC(O-38:4)
PC(38:5)
PC(O-38:5)
PC(38:6)
PC(O-38:6)
PC(38:7)
PC(38:8)
PC(39:5)
PC(40:4)
PC(40:5)
PC(O-40:5)
PC(40:6)
PC(O-40:6)
PC(40:7)
PC(O-40:7)
PC(40:8)
PC(40:9)

D.

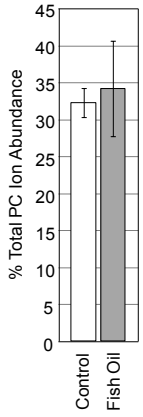
% Total PC Ion Abundance
0
5
10
15
20
25
30
35
40
45
Control
Fish Oil

E.

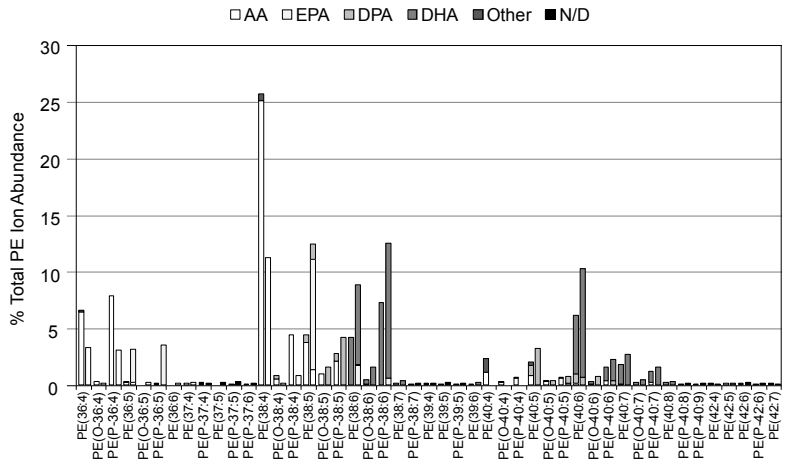
AA EPA DPA DHA Other N/D
% Total PE Ion Abundance
0
5
10
15
20
25
30
PE(36:4)
PE(O-36:4)
PE(P-36:4)
PE(36:5)
PE(O-36:5)
PE(P-36:5)
PE(36:6)
PE(37:4)
PE(P-37:4)
PE(37:5)
PE(P-37:5)
PE(P-37:6)
PE(38:4)
PE(O-38:4)
PE(P-38:4)
PE(38:5)
PE(O-38:5)
PE(P-38:5)
PE(38:6)
PE(O-38:6)
PE(P-38:6)
PE(38:7)
PE(P-38:7)
PE(39:4)
PE(39:5)
PE(P-39:5)
PE(39:6)
PE(40:4)
PE(O-40:4)
PE(P-40:4)
PE(40:5)
PE(O-40:5)
PE(P-40:5)
PE(40:6)
PE(O-40:6)
PE(P-40:6)
PE(40:7)
PE(O-40:7)
PE(P-40:7)
PE(40:8)
PE(P-40:8)
PE(P-40:9)
PE(42:4)
PE(42:5)
PE(42:6)
PE(P-42:6)
PE(42:7)

F.

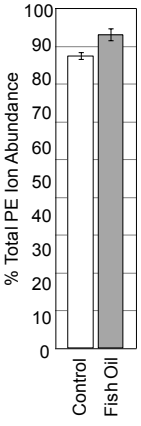
% Total PE Ion Abundance
0
10
20
30
40
50
60
70
80
90
100
Control
Fish Oil

G.

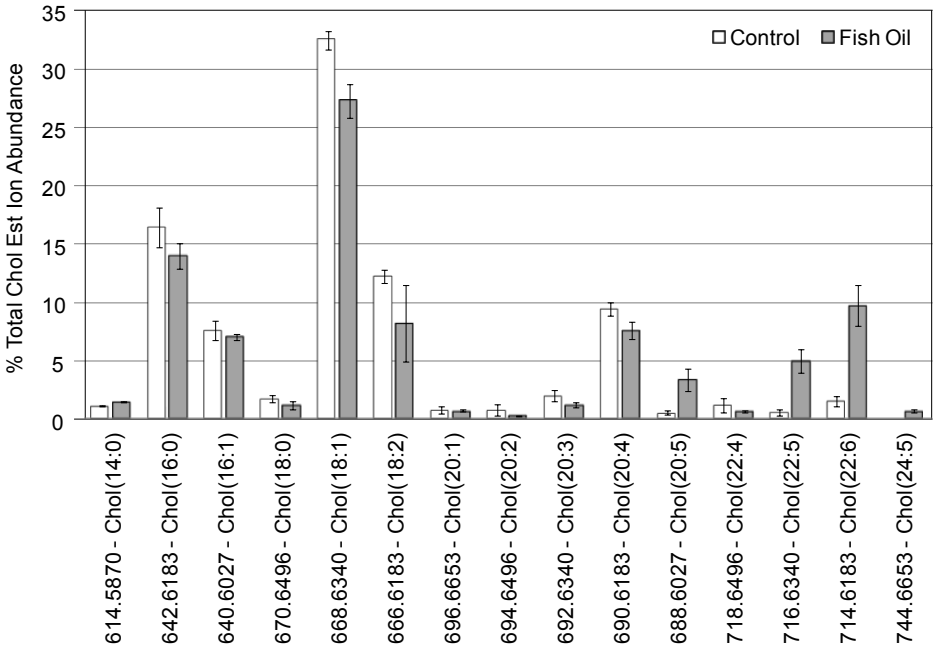

Supplemental Figure 2: B-cell lipidome analysis of mice fed control and n-3 PUFA diets.

(A) Percent individual PC lipid ion abundances compared to the total PC lipid ion abundance, (B) percent individual PE lipid ion abundances compared to the total PE lipid ion abundance (only lipids with ion abundances >0.5% total PC or PE ion abundance are shown in A and B). (C) Distribution of AA, EPA, DPA and DHA among polyunsaturated PC lipid ions containing at least 4 degrees of unsaturation. (D) Distribution of AA, EPA, DPA and DHA among polyunsaturated PE lipid ions containing at least 4 degrees of unsaturation (control – left, n-3 PUFA – right). (E) Percent total PC lipid ion abundance attributed to polyunsaturated PC species, (F) percent total PE lipid ion abundance attributed to polyunsaturated PE species, (G) percent individual cholesterol ester lipid ion abundances compared to the total cholesterol ester lipid ion abundance.

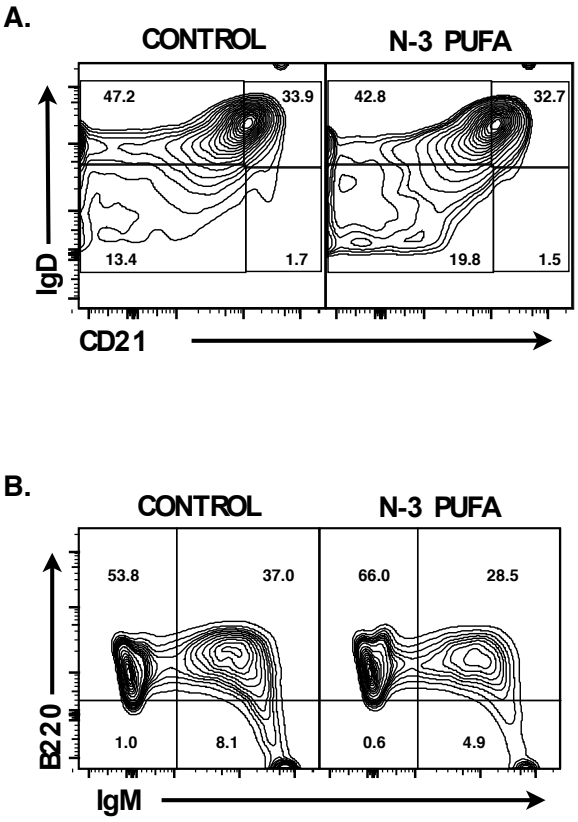

Supplemental Figure 3: Sample contour plots of splenic B cells and bone marrow from control and n-3 PUFA fed mice.
(A) Gating strategy for $B220^{+}IgM^{+}$ splenic B cells and (B) $CD19^{+}$ bone marrow cells.

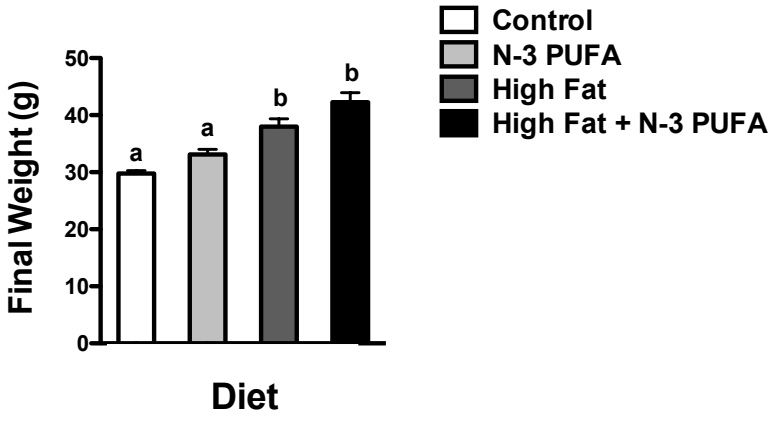

Supplemental Figure 4: High fat and high fat + n-3 PUFA diets increased body weight.
Final weight of mice consuming control, n-3 PUFA, high fat or high fat + n-3 PUFA for 10 weeks. Initial body weights of all mice were equivalent. Letters that do not match indicate statistical significance ($p<0.05$).

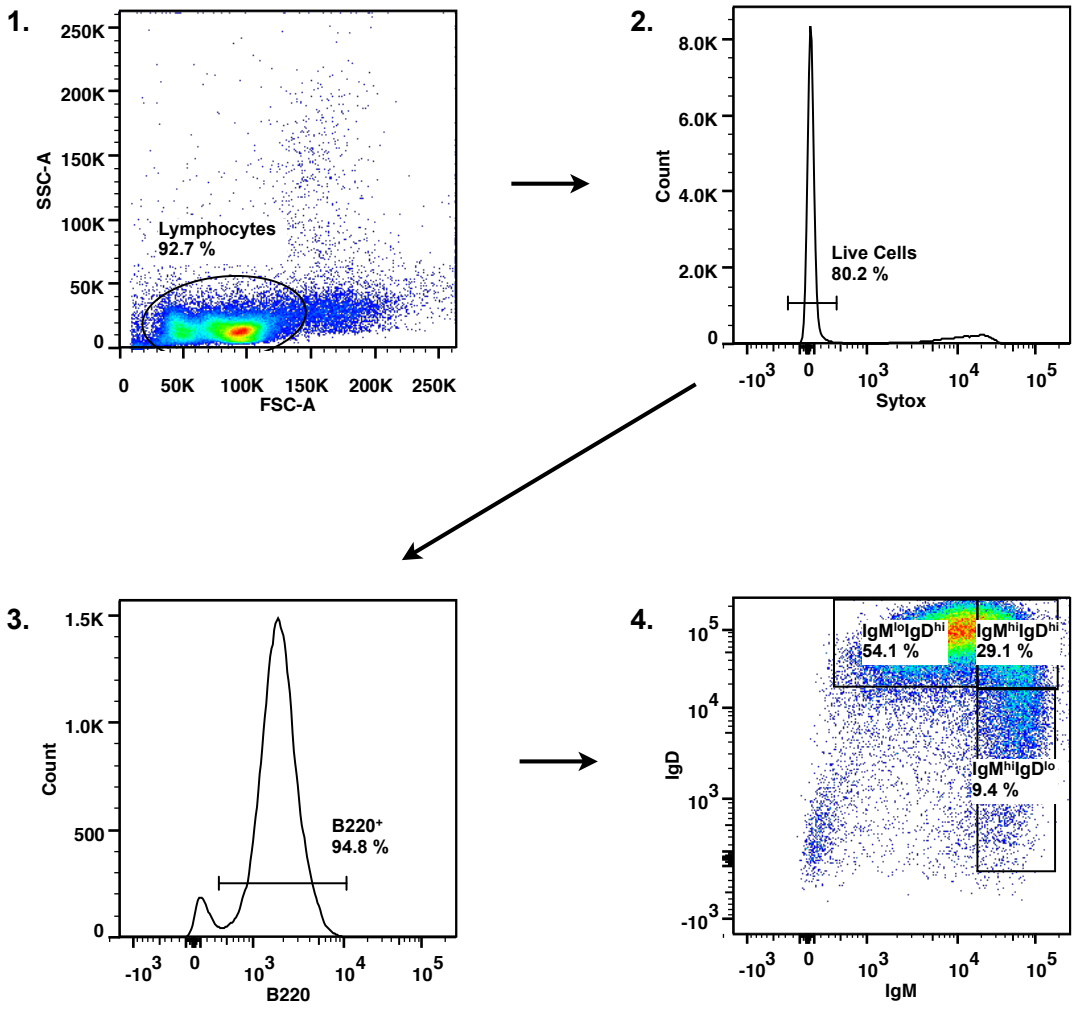
1.
SSC-A
FSC-A
Lymphocytes
92.7 %
2.
Count
Sytox
Live Cells
80.2 %
3.
Count
B220
B220+
94.8 %
4.
IgD
IgM
IgMloIgDhi
54.1 %
IgMhiIgDhi
29.1 %
IgMhiIgDlo
9.4 %

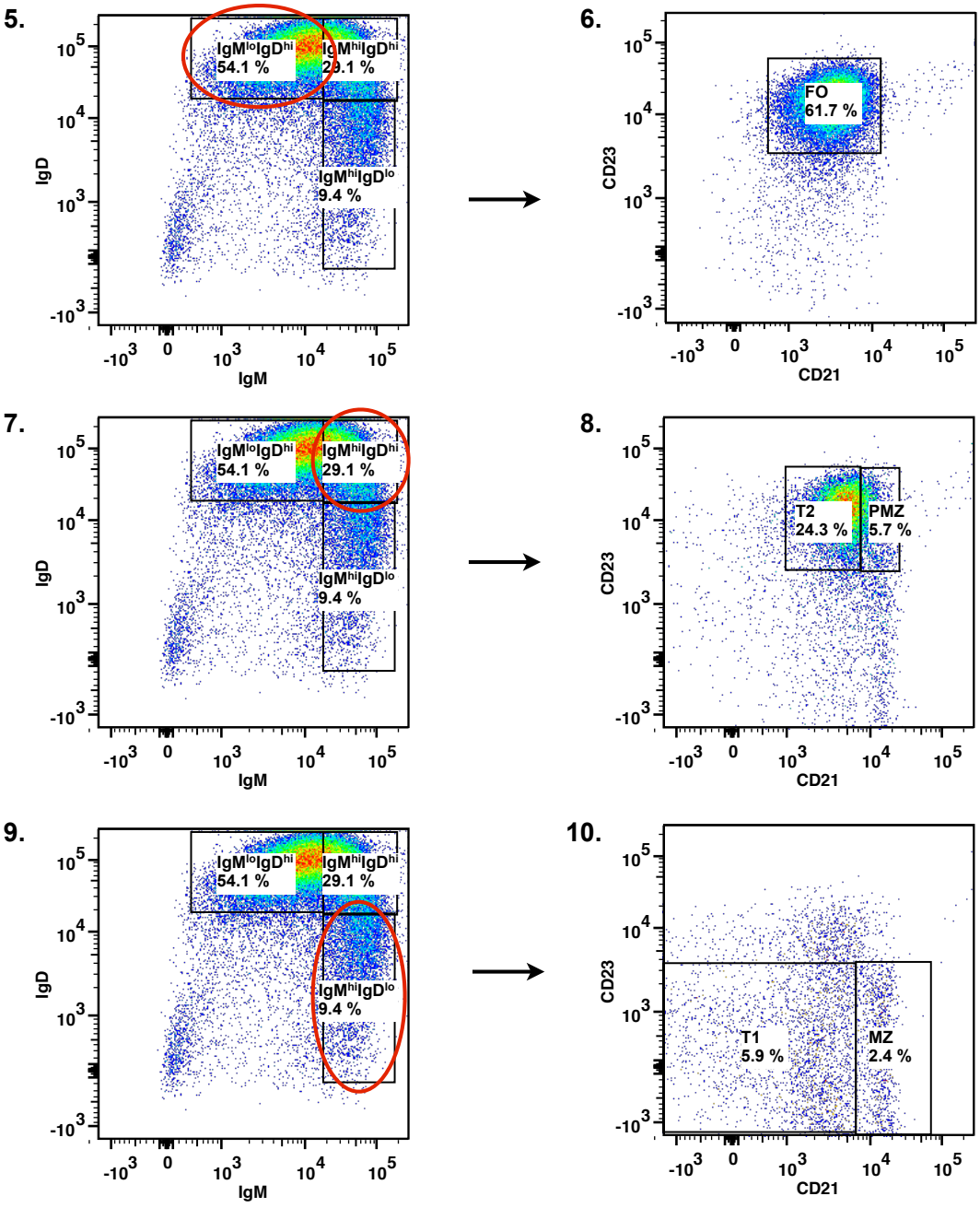

Supplemental Figure 5: Splenic B220$^+$ B-cell subset gating strategy.
The gating strategy utilized to determine the percentage of IgM$^+$IgD$^-$ CD21^{low}CD23$^-$ (transitional 1), IgM$^+$IgD$^+$CD21^{mid}CD23$^+$ (transitional 2), IgM$^+$IgD$^+$CD21^{hi}CD23$^+$ (pre-marginal zone), IgM$^+$IgD$^-$CD21^{hi}CD23$^-$ (marginal zone) and IgD$^+$IgM$^-$CD21^{mid}CD23$^+$ (follicular) B-cell subsets.

APPENDIX C: SUPPLEMENTAL TABLES

Supplemental Table 1: Composition of diets.[a]

Ingredients	Control	N-3 PUFA	High Fat	High Fat + N-3 PUFA
Casein	185.0	185.0	205.0	205.0
L-cystine	2.5	2.5	3.0	3.0
Corn starch	369.98	369.98	98.94	98.94
Maltodextrin	140.0	140.0	140.0	140.0
Sucrose	150.0	150.0	225.0	225.0
Cellulose (fiber)	50.0	50.0	24.0	24.0
Soybean oil	50.0	0.0	15.0	15.0
Anhydrous milk fat	0.0	0.0	223.0	160.0
Fish Oil	0.0	50.0	0.0	63.0
Mineral mix, AIN-93M-MX	35.0	35.0	44.0	44.0
Vitamin mix, AIN-93-VX	15.0	15.0	19.0	19.0
Choline bitartrate	2.5	2.5	3.0	3.0
TBHQ antioxidant	0.02	0.02	0.06	0.06

[a]Values are grams per kilogram.

Supplemental Table 2: Composition of diets.[b]

Ingredients	Control	HF	HF-OA	HF-EPA	HF-DHA
Casein	185.0	205.0	205.0	205.0	205.0
L-cystine	2.5	3.0	3.0	3.0	3.0
Corn starch	369.98	98.94	98.94	98.94	98.94
Maltodextrin	140.0	140.0	140.0	140.0	140.0
Sucrose	150.0	225.0	225.0	225.0	225.0
Cellulose (fiber)	50.0	24.0	24.0	24.0	24.0
Soybean oil	50.0	15.0	15.0	15.0	15.0
Anhydrous milk fat	0.0	223.0	204.6	204.6	204.6
OA ethyl ester	0.0	0.0	18.4	0.0	0.0
EPA ethyl ester	0.0	0.0	0.0	18.4	0.0
DHA ethyl ester	0.0	0.0	0.0	0.0	18.4
Mineral mix, AIN-93M-MX	35.0	44.0	44.0	44.0	44.0
Vitamin mix, AIN-93-VX	15.0	19.0	19.0	19.0	19.0
Choline bitartrate	2.5	3.0	3.0	3.0	3.0
TBHQ antioxidant	0.02	0.06	0.06	0.06	0.06

[b]Values are grams per kilogram.

APPENDIX D: PROTOCOLS

SUBMANDIBULAR BLOOD WITHDRAW AND PROCESSING

Materials and Reagents

- 5 mm Lancet (Braintree Scientific, Inc., 5mm Goldenrod, Item GR 5MM)
- Capiject Capillary Blood Collection System (Therumo, Item 3T-MG)
- Remington Electric Razor

Method

1) Get a good grip on the mouse, stretching the skin around the neck with the thumb and first finger while holding his feet and tail between the pinky and ring finger.
2) Shave the side of the face of the mouse with a Remington Electric Razor.
3) Feel around for the soft spot on the side of the face and pierce with a Lancet, aiming to hit the vein that connects coming from the eye and the mouth. Try not to pierce to high causing the mouse to bleed out its ear.
4) Collect the blood in Capiject tubes.
5) Let the blood sit at room temp for 20-30 mins allowing the blood to clot.
6) Spin for 15 mins at 1300 g at room temperature.
7) Collect serum and store in -20°C for future analysis.

Note: The rule of thumb for rodents is total blood volume is ~ 10% of body weight (in kg). Hence, only 1% of body weight can be drawn every 14 days without needing supplemental fluids etc. So a 30 g mouse can only really give ~ 0.3 ml or 300 µl every 2 weeks (this is all for survival). If you want to get more than that or increase the frequency, subcutaneous saline is recommended, although physiological changes may be induced (i.e. decreases in cardiac output and blood pressure).

LYOPHILIZATION

Materials and Reagents

- 15 ml falcon tube
- 1X phosphate buffered saline (PBS)
- Acetone/dry ice bath
- GC vial with Teflon top
- Teflon tape

Method

1) Transfer 10 x 10^6 cells to a 15 mL Falcon tube.
2) Wash cells once with 1 ml of 1X PBS.
3) Dump the supernatant and mix the sample with the liquid that collects in the bottom of the conical tube.
4) Transfer to a GC vial with a P200 pipette.
5) Prepare an acetone/dry ice bath.
6) Freeze the samples in an acetone/dry ice bath while spinning rapidly.
7) Place the frozen samples on the lyophilizer and run for about 2 hours.
8) Remove samples once they are completely dry and all liquid has been removed.
9) Place the Teflon top on the GC vial and seal with Teflon tape. Store samples at -20ºC for further analysis.

PHENOTYPING BONE MARROW

Materials and Reagents

- FcR Block (Miltenyi Biotec, Cat # 130-092-575)
- B220-FITC (Miltenyi Biotec, Cat # 130-091-829)
- IgM-PE (Southern Biotech, Cat # 1021-09)
- CD19-PerCP/Cy5.5 (Biolegend, Cat # 115534)
- IgD-APC (Biolegend, Cat # 405714)
- 1X phosphate buffered solution with 0.1% bovine serum albumin (PBS + BSA)
- 96-well flat bottom plate
- Sytox Blue

Method

1) Re-suspend bone marrow at a concentration of 2.0×10^6 cells /ml.
2) Transfer 0.5×10^6 cells by adding 250 ul of cells to a 96-well flat bottom plate.
3) Wash once with 100 ul of 1X PBS + 0.1% BSA.
4) Prep a solution of FcR Receptor Block by adding 10 ul of FcR Block to 990 ul of 1X PBS + 0.1% BSA.
5) Add 100 ul of the FcR Block solution to each well and stain on ice in the dark for 10 mins.
6) Wash the plate twice with 100 ul of 1X PBS + 0.1% BSA.
7) Prep an antibody cocktail by adding 2 ul of antibody per 100 ul of stain to 1X PBS + 0.1% BSA. For example, if preparing 800 ul of antibody cocktial then add 16 ul of each antibody to 736 ul of 1X PBS + 0.1% BSA.
8) Add 75 ul of the antibody cocktail to each well and stain on ice for 20 minutes in the dark.
9) Wash the plate three times with 100 ul of cold 1X PBS.
10) Prepare a fresh sytox solution each time as follows:
    a. Add 2 uL of the sytox stock solution to 38 ul of DMSO for the working solution (50 uM).
    b. Add 20 ul of the sytox working solution to 1980 ul of 1X PBS for a final solution.
11) Add 200 ul of the final sytox solution to each well.
12) Run the plate on the LSR II flow cytometer.

PHENOTYPING SPLENICS

Materials and Reagents

- FcR Block (Miltenyi Biotec, Cat # 130-092-575)
- B220-FITC (Miltenyi Biotec, Cat # 130-091-829)
- IgM-PE (Southern Biotech, Cat # 1021-09)
- CD19-PerCP/Cy5.5 (Biolegend, Cat # 115534)
- IgD-APC (Biolegend, Cat # 405714)
- CD21-PerCp/Cy5.5 (Biolegend, Cat # 123416)
- 1X phosphate buffered solution with 0.1% bovine serum albumin (PBS + BSA)
- 96-well flat bottom plate
- Sytox Blue

Method

1) Re-suspend bone marrow at a concentration of 2.0 x 10^6 cells /ml.
2) Transfer 0.5 x 10^6 cells by adding 250 ul of cells to a 96-well flat bottom plate.
3) Wash once with 100 ul of 1X PBS + 0.1% BSA.
4) Prep a solution of FcR Receptor Block by adding 10 ul of FcR Block to 990 ul of 1X PBS + 0.1% BSA.
5) Add 100 ul of the FcR Block solution to each well and stain on ice in the dark for 10 mins.
6) Wash the plate twice with 100 ul of 1X PBS + 0.1% BSA.
7) Prep an antibody cocktail by adding 2 ul of antibody per 100 ul of stain to 1X PBS + 0.1% BSA. For example, if preparing 800 ul of antibody cocktial then add 16 ul of each antibody to 736 ul of 1X PBS + 0.1% BSA.
8) Add 75 ul of the antibody cocktail to each well and stain on ice for 20 minutes in the dark.
9) Wash the plate three times with 100 ul of cold 1X PBS.
10) Prepare a fresh sytox solution each time as follows:
    a. Add 2 uL of the sytox stock solution to 38 ul of DMSO for the working solution (50 uM).
    b. Add 20 ul of the sytox working solution to 1980 ul of 1X PBS for a final solution.
11) Add 200 ul of the final sytox solution to each well.
12) Run the plate on the LSR II flow cytometer.

TNP-LPS MOUSE INJECTION

Materials and Reagents

- TNP-Lipopolysaccharide (Biosearch Technologies, Catalog # T-5065, 5 mg)
- 0.9% Sterile Saline Solution
- 2 ml Empty Sterile Bottle (Greer, Cat # SE2508020)
- FACS tube
- 1 ml Syringe (BDm REF 309659)
- 25 Gauge Needle (BD Worldwide, Precision Glide, Cat # 305122)

Method

1) Dilute the TNP-LPS to 5 mg/ml in 0.9% sterile saline and aliquot out into 25 µl aliquots. Store in the -20ºC freezer.
2) Prepare a 0.005 or 0.25 µg/ul working solution of TNP-LPS in 0.9% sterile saline in a sterile FACS tube.
3) Transfer the solution to an empty 2 ml sterile bottle.
4) Withdraw the TNP-LPS solution into the syringe in excess and remove all bubbles from syringe to 200 µL. NOTE: Make sure to prep the syringe before removing mouse from the cage.
5) Insert needle in the mouse in lower right abdomen (the left side if the mouse is stomach-up) and aspirate the syringe to ensure no fluid is withdrawn into the syringe.
6) Inject mouse, return to cage and incubate for 5-7 days.

TNP-LPS MOUSE ANTIBODY PRODUCTION

Materials and Reagents

- TNP-BSA (Biosearch Technologies, Catalog # T-5050)
- HRP-conjugated goat-anti-mouse IgM, µ-chain specific (SouthernBiotech, Catalog # 1021-05)
- TMB SureBlue (KPL, Catalog # 52-00-01)
- TMB Stop Solution (KPL, Catalog # 50-85-05)
- 96-well flat bottom plate
- Biolegend Sticky Plate Cover (Biolegend, Cat # 78101)
- 1X phosphate buffered saline (PBS)
- 5% milk in 1X PBS
- 1% milk in 1X PBS

Method

1) Prep TNP(30)-BSA by diluting in 1X PBS to 1 mg/ml.
2) Prepare an ELISA plate 2 days before the experiment by coating a 96-well flat bottom plate with 100 µL of 5 µg/ml of TNP(30)-BSA in 1X PBS overnight at 4ºC.
3) Snap the plate to remove the coating antigen.
4) Wash the plate 3 times with 100 µl of 1X PBS per well.
5) Add 200 µl of 5% milk in 1X PBS per well.
6) Cover plate and incubate overnight at 4ºC.
7) Thaw serum and prepare serum dilutions according to the table below in 1 mL eppendorf tubes in 1% milk in 1X PBS.
8) Transfer 150 µl of each sample to a non-antigen coated 96 well plate. NOTE: By transferring sample to a clean 96-well plate, sample loading onto the antigen coated plate can be completed with a multichannel pipette, minimizing the exposure time differences to the capture antigen between samples.
9) Wash the antigen coated plate 3 times with 200 µl of 1X PBS per well.
10) Transfer 100 µl of sample from the non-antigen coated plate to the antigen coated plate.
11) Wrap or cover the plate and incubate for exactly 1 hour at 37ºC.
12) Wash plate 6 times with 100 µl 1X PBS + 0.05% Tween-20.
13) Prepare a 1:5000 dilution of HRP-conjugated goat-anti-mouse IgM in 1% milk in 1X PBS. For example, add 2 µl of HRP-conjugated goat-anti-mouse IgM to 10 mL of 1% milk in 1X PBS.
14) Add 100 µl of 1% milk in 1X PBS containing HRP-conjugated goat-anti-mouse IgM diluted 1:5000 to each well.
15) Cover plate and incubate for exactly 1 hour at 37ºC.
16) Wash plate 6 times with 100 µl of 1X PBS + 0.05% Tween-20 allowing a 1 minute incubation during each wash to minimize background.
17) Following the last wash adding 100 µl of room temperature TMB SureBlue reagent per well to develop the plate.
18) Incubate for 2 minutes and 30 seconds at room temperature.
19) Stop the reaction by adding 100 µl of TMB Stop Solution per well.
20) Read absorbance at 450 nm.

PHAGOCYTOSIS ASSAY

Materials and Reagents

- BioParticles Fluorescent Particles and Opsonizing Reagent (Molecular Probes, Cat # E-2861, E-2870)
- 1X HBSS, plus calcicum and magnesium
- sodium azide
- tissue-grade H_20
- trypan blue

Method (Keep Cells at 4°C until assay)

RECONSTITUTING *E. coli* BIOPARTICLES AN OPSONIZING REAGENT

1) Reconstitute (~ 300 x 10^6 particles/mg, 6 x 10^6 bioparticles/µL) *E. coli* bioparticles in 1X HBSS (plus calcium and magnesium) to a final conc. of 20 mg/ml.
2) Add 0.5 ml 1X HBSS to bottle containing 10 mg *E. coli* bioparticles
3) Cap the tube and gently swirl the particles into suspension.
4) Vigorously vortex the particles (3 times for 15 seconds on high)
5) Add sodium azide to a final conc. of 2 mM. and store at 4C for several weeks
6) Add 0.065 g sodium azide for final conc. of 2 mM
7) To achieve homogeneity of the solution sonicate.
8) Count particles in hemocytometer. Most experiments should use between 1 and 100 particles per leukocyte.
9) Reconstitute the vial of bioparticles opsonizing reagent with 0.5 mL of tissue-culture grade water.
10) For opsonizing bioparticles mix equal volumes of the opsonizing reagent and with E. coli suspension.
11) Vortex the suspension and incubate at 37 C for one hour.
12) Wash 2-3 times with PBS using low speed centrifugation (800-15-- g, 15-20 mins, to form loosely packed pellets.
13) Ressuspend at 3.0 x 10^6 bioparticles/µL. Take out desired aliquot and place remaining in 4°C.

TRYPAN BLUE QUENCHING SOLUTION

1) Prep a 1 mg/ml solution of trypan blue in 1X PBS
    a. Example: Trypan blue is 0.4% solution (g/100ml) in 1X PBS which equals 4mg/ml. To prep 5 mls combine 3.75 ml of 1X PBS and 1.25 ml of trypan blue.
2) Vortex until mixed well.

PHAGOCYTOSIS ASSAY

1) Count leukocytes and aliquot into FACS tubes 0.5 x 10^6 cells per sample.
2) Wash 3 times in 1ml 1X HBSS buffer with calcium and magnesium.
3) Add 100 µL *E. coli* bioparticles at a 1:10 ratio leukocytes to bioparticles and incubate in water bath for allotted time.
    a. NOTE: Positive control is measuring phagocytosis at 37C. Negative

controls are no bioparticles at 37C and the addition of bioparticles at 4C. At 4C no phagocytosis should be observed.

4) To stop phagocytosis remove samples from water bath and add to ice.
5) Wash 1 time with 1ml of 1X PBS.
6) Decant and add 200 µL of 1mg/ml trypan blue for 2 min on ice to quench extracellular fluorescence, mix vigorously.
7) Wash 2 times with 1 ml of 1X PBS and fully decant.
8) Re-suspend in 198 µL of 1X PBS, add 2 µL of 50 µM sytox blue and run on flow.

$CD11c^+$ SPLENIC DENDRITIC CELL ISOLATION

Materials and Reagents

- Collagenase D (Cat # C5138)
- Collagenase D Solution
    - HEPES
    - NaCl
    - KCl
    - $MgCl_2$
    - $CaCl_2$
- MACs CD11c Positive Selection Isolation Kit (Miltenyi Biotec, Cat # 130-052-001)
- Splenocyte Media (l-glut, 5% FBS, penn/strep, β-me)
- MACS Buffer (Bovine Serum Albumin, EDTA, degassed)
- LS Columns (Miltenyi Biotec, Cat # 130-042-401)
- 15 ml Falcon tube (BD)
- 50 ml Falcon tube (BD)
- 40 µm cell strainer (BD, Cat # 352340)
- 70 µm cell strainer (BD, Cat # 352350)
- 25G Needles (Cat # 305125)
- Small petri dish

Method

COLLAGENASE D SOLUTION PREP

HEPES:

$(0.5\ L)(10 \times 10^{-3}\ mol\ HEPES/L)(238.30\ g/mol\ HEPES) = 1.19\ g\ HEPES$

NaCl:

$(0.5\ L)(150 \times 10^{-3}\ mol\ NaCl/L)(58.44\ g\ NaCl/mol) = 4.38\ g\ NaCl$

KCl:

$(0.5\ L)(5 \times 10^{-3}\ mol\ KCl/L)(74.55\ g\ KCl/mol) = 0.19\ g\ KCl$

$MgCl_2$:

$(0.5\ L)(1 \times 10^{-3}\ mol\ MgCl_2/L)(95.211\ g\ MgCl_2/mol) = 0.05\ g\ MgCl_2$

$CaCl_2$:

$(0.5L)(1.8 \times 10^{-3}\ mol\ CaCl_2/L)\ (110.98\ g\ CaCl_2/mol) = 0.10\ g\ CaCl2$

Note: $MgCl_2$ was actually a 1M solution, have to calculated volume added

1) Prepped 0.5 L buffer solution before adding collagenase D (type IV)
2) Add salts to DI water while mixing on a stir plate
3) Adjust the pH with NaOH to ~7.40
4) Mixed well and refrigerated buffer solution
5) Prepped a 10mL aliquot morning of sample prep by taking out 10mL of buffer solution and adding 0.02g collagenase IV to solution.

6) Heated in a water bath at 37˚C to allow collagenase to get into solution
7) Store remaining collagenase at –20˚C for future use.

NOTE: For optimal results, store buffer in fridge and prep collagenase D fresh on day of experiment

SPLEEN PREP/SPLENOCYTE ISOLATION: (Protocol derived from MACS CD11c Isolation protocol)

1) Place isolated spleen in a 6 cm petri-dish with sufficient Collagenase D soln. to completely cover the bottom of the dish (5 mL/ spleen)
2) Inject mouse spleen with 500 µL of collegnase D solution per spleen using a 1 mL syringe and a 25G needle.
3) Cut the tissue in smaller pieces using sharp scissors.
4) Incubate the spleen pieces in collagenase D soln for 30 mins at 37°C
5) Pass the whole material, including collagenase D in plate, through a 70 µm cell strainer mashing remaining spleen tissue with a plunger
6) Add 6.5 mL of MACS buffer to wash. Make sure to rinse the plunger to ensure maximum recovery of splenocytes
7) Spin cells at 300g for 5 mins at 4˚C, decant in hood
8) Strain through a 40 µm cell strainer into 50 mL conical tube. Add 14 mL of MACS buffer and spin again. Decant in the hood.
9) Lyse red blood cells by adding 2 mL of lysing buffer for 2 mins. Then add 18 mL of splenocyte media and centrifuge at 300g, 4°C for 5 mins
10) Re-suspend cells in 20 mL of splenocyte media.
11) Strain through a 40 µm cell strainer into 50 mL conical tube
12) Count Cells
13) Spin Cells at 300g for 5mins, 4°C while counting

MAGNETIC LABELLING:

1) Prep FcR Receptor block, 90 µL + 10 µL FcR Blocking Reagent + MACS buffer, per 10^7 cells
2) Mix gently with pipette and refrigerate 10 mins
    a. NOTE: FcR Blocking Reagent is light sensitive, perform step in the dark, make sure to mix while in fridge
3) Add 400 µL of MACS buffer per 10^8 total cells, or splenocytes
4) Add 100 µL of CD11c microbeads per 10^8 total cells or splenocytes
    a. NOTE: Add MACS buffer and CD11c beads directly to cells, no need to dump or wash FcR Blocking reagent out of conical tube
5) Mix gently with pipette and incubate 15 mins in the fridge at 4°C
6) Wash cells 3X with 10 mL of MACS buffer at 300 for 5 mins at 4°C
7) Dump supernatant
8) Resuspend cell in 2 mL of MACS buffer

MAGNETIC SEPARATION:

1) Place LS column in magnetic field
2) Rinse column with 3 mL of MACS buffer

3) Apply cell suspension to the column 0.5 mL at a time
4) Add 8 mL of MACS buffer to conical tube previously containing cell suspension
5) Add 3 mL of buffer at a time to minimize pressure until buffer is completely gone.
6) Remove column from magnetic field and place over a suitable collection tube (50 mL conical). Add 5 mL of MACS buffer to the column and use plunger to push buffer through. This portion contains the dendritic cells.
    a. NOTE: for optimum purity repeat steps 1-5. If using a second column elute cells directly into second column instead of in a collection tube.
7) Count Cells

T-CELL ACTIVATION PROTOCOL

Materials and Reagents

- 96-well flat bottom plates
- OVA Peptide
- CD4-PE
- CD25-APC
- CD69-FITC
- Sytox Blue
- Splenocyte Media (l-glut, 5% FBS, penn/strep, β-me)
- dH_2O
- 1X Phosphate Buffered Solution (PBS)

Method

T-CELL ACTIVATION -PLATE SET-UP AND OVA TREATMENT

1) Once dendritic cells are isolated wash 2X with splenocyte media, resuspend in ~1 mL and do a final count
2) Bring up to volume to 2.0 x 10^6 cells/mL and then add 50 µL to wells containing dendritic cells
3) Wash T cells 2X with splenocyte media and re-suspend in about 2 mLs and do a final count.
4) Bring cells up to volume to 6.0 x 10^6 cells/mL then add 50 µL to wells containing T cells
5) Add 50 µL splenocyte media to final volume of 100µL to wells containing a single cell type
6) Add 1 µL 10^{-3} peptide to wells for final conc. 10^{-5} M OVA
    a. Add 1 µL 10^{-5} peptide to wells for final conc. 10^{-7} M OVA
    b. Add 1 µL 10^{-11} peptide to wells for final conc. 10^{-13} M OVA
    c. Add 1 µL dH_2O to wells for final conc. 0 M OVA
7) Incubated plates for 1 hour at 37°C
8) Wash cells 2X with splenocyte media to remove OVA peptide
9) Re-suspended in 200 µL of splenocyte media and incubate 24 hours

STAINING PLATES:

1) Analyze plates under microscope to visualize extent of clumping
2) Centrifuge 4°C, 300* for 5 mins
3) Remove 50 µL of supes and place in -20°C for future analysis
4) Wash 2X with 100 µL of 1X PBS per well
5) Prep antibody cocktail as follows:
    a. Add 1/4 µL CD4-PE per 100 µL of 1X PBS
    b. Add 1/4 µL CD69-FITC per 100 µL 1X PBS
    c. Add 1/4 µL CD25-APC per 100 µL 1X PBS
6) Add 100 µL of antibody cocktail to each well
7) Stain in refrigerator for 15 mins in dark
8) Wash 2X with 1X PBS
9) Prep sytox blue solution as follows:

a. Add 1 µL sytox blue per 200 µL of 1X PBS
b. Add 200 µL of sytox blue solution to each well

10) Run on LSR II flow cytometer using the following setting:
a. Sample Flow Rate (µl/s) = 3.0
b. Sample Volume (µl) = 150
c. Mixing Volume (µl) = 100
d. Mixing Speed (µl/s) = 100
e. Number of Mixes = 2
f. Wash Volume = 400
g. NOTE**:** Flow cytometer settings were optimized to minimize air bubble accumulation in lines

TIRF STAINING FOR DCs

Materials and Reagents

- Poly-d-lysine
- 6-well plate
- Coverslips
- Vacuum Pump
- dH_20
- 1X phosphate buffered solution (PBS)
- 1X PBS + 2% Bovine Serum Albumin (BSA)
- 4% paraformaldehyde (PFA)
- Whatman filter paper

Method

1) Place coverslip in a 6 well plate and add 2 ml of 0.1 mg/ml Poly-d-lysine for 30 mins at room temp
2) Wash 3 times by aspirating off soln. with a vacuum pump then add 2 ml of DI water and repeat, letting the coverslip sit for 2 mins each time. On the last wash completely dry coverslip and dish.
3) Aliquot 2.0 x 106 cells into FACS tubes, spin down at 24°C, 300g for 5 mins and resuspend in 400 µL of media.
4) Add 125 µL to each coverslip (625,000 cells) and incubate for 30 mins at 37°C.
5) Wash cells 1 time with 2 ml cold 1X PBS and aspirate without touching the cover slip.
6) Add 2 ml of 4% PFA to each coverslip for 30 mins at room temp in the dark.
7) Prep antibody stain at desired conc. in 1X PBS + 2% BSA. This will vary depending on protein expression and cell type.
8) After fixation gently wash cells 3X with 3 ml of 1X PBS, allowing wash to sit for 4 mins each time. On the last wash use 1X PBS + 2% BSA.
9) Add 1 ml of stain to well. Allow to stain for 1 hour.
10) Wash 3X with 2 ml of 1X PBS. Let each wash sit for 4 mins.
11) Add 100 µL of 1X PBS to microscope slide. Place coverslip on slide and use Whatman filter paper to absorb excess liquid.
12) Seal onto slide with nail polish. Polish sides as even as possible. Uneven polish will effect the quality of the images.
13) Store samples in the fridge at 4°C.

GLUCOSE TOLERANCE TESTING

Materials and Reagents

- Dextrose (Hospira, Inc.)
- 25G Needles (BD, Cat # 305125)
- 1 ml syringe
- glucometer
- glucometer strips

Method

1) 2 days before performing GTT, measure lean mass utilizing an EchoMRI instrument
2) Calculate the amount of dextrose to inject (2.5 g dextrose/kg lean mass)
3) Remove food from mouse cage 6 hours prior to glucose measurements.
4) Move mice to room where measurements will be taken to allow them to acclimate to the surroundings. Keep as quiet as possible to avoid causing any stress to the mice.
5) Measure fasting glucose through tail vein.
6) I.p. inject mouse with dextrose. Acquire glucose measurements through tail vein at 5, 10 15, 30 45, 60 and 120 mins post injection.